Reconfiguring mine cooling auxiliaries for optimal operation

KJ Oberholzer

22087567

Dissertation submitted in fulfilment of the requirements for the degree *Magister* in Mechanical Engineering at the Potchefstroom Campus of the North-West University

Supervisor: Prof M Kleingeld

May 2016

It all starts here ™

NORTH-WEST UNIVERSITY
YUNIBESITI YA BOKONE-BOPHIRIMA
NOORDWES-UNIVERSITEIT

ABSTRACT

Title: Reconfiguring mine cooling auxiliaries for optimal operation
Author: Kasper Jakobus Oberholzer
Supervisor: Prof M. Kleingeld

Deep level gold mines utilise energy intensive cooling systems to maintain an acceptable underground working environment. The majority of these cooling systems are old as they were installed a few years after the mines' inception. The outdated cooling equipment and inadequate maintenance thereof resulted in reduced efficiencies. Identifying the inefficient cooling subsystems and reconfiguring them for optimal operation will be beneficial for mines. The optimised system will ensure the cooling systems' service delivery is improved, allowing electricity and cost savings during certain periods of the day.

Through investigation, mine A's cooling system was identified as inefficient and required reconfiguration to ensure optimal operation. A universal methodology was developed to obtain the optimal operation for the mine's cooling subsystem. Theoretical simulations were developed to predict the effect the subsystem reconfiguration will have on the cooling system's performance.

The simulation proved that improved service delivery is possible by reconfiguring the mine's cooling system. The reconfigurations were suggested to mine A. Implementation thereof was done on some of the cooling subsystems. The implemented reconfigurations were used to validate the simulation model, from where the effect of the other reconfigurations could be predicted. For each of the new desired chilled water temperatures a baseline simulation was done to determine the savings that could be realised when compared to the original chill dam temperature.

Implementing the suggested reconfigurations on mine A's cooling subsystem will realise a power saving of 10.4% on the mine's total power usage (close to 9 MW) whilst delivering a chilled water temperature of 5°C. With a chilled water setpoint of 4°C the baseline total power usage will increase with 4.8%. The cooling system will be able to maintain a chilled outlet water temperature of 4°C whilst obtaining a power saving of 11% on the new baseline.

When the chilled water setpoint is set to 3°C the baseline simulation power usage will increase with 9%. The chilled water will have an average outlet water temperature of 3.2°C

whilst realising in a power saving of 7.8% on the baseline power usage. Due to the successful implementation of some of the reconfiguration initiative strategies and validation of the simulation model, it is safe to state that the mines' cooling systems can be optimised through reconfiguration of their cooling sub systems.

Keywords: Cooling System, Cooling subsystem, chilled water, baseline, underground, working environment, improved efficiencies, service delivery, power savings

ACKNOWLEDGEMENTS

The research presented in this dissertation is my own work. Credit was given to the external sources referenced in the document. Any omissions or errors brought to my attention will be amended.

First and foremost, my Lord and Saviour for blessing me with adequate knowledge, ability and opportunity to complete my dissertation. Without Him it would not be possible for me to complete this study.

The following institutions and people are also acknowledged:

1. I would like to thank the authorities of TEMM International (Pty) Ltd for funding the research and providing the opportunity to complete my master's degree.
2. A special thanks to Dr Hendrik Brand and Mr Johan Bredenkamp for your valuable guidance, inputs and continuous help throughout the course of this study. Your inputs were immeasurable and are sincerely appreciated.
3. Prof Marius Kleingeld, thank you for your advice and guidance during the study.
4. To my colleagues, thank you for all your support and suggestions throughout this study.
5. To Mr Piet, thank you for your valuable recommendations and technical feedback.
6. Thank you to all the relevant mine personnel who provided me with sufficient information and data during the study.
7. A special thanks to my parents, Mr Kobus Oberholzer and Mrs Barbara Oberholzer, for raising me the way they did and providing me with the opportunity to complete my mechanical engineering degree.
8. Lastly I want to thank the love of my life, Mrs Carnia Piater for motivation and support throughout this study.

TABLE OF CONTENTS

LIST OF FIGURES

LIST OF TABLES

ABBREVIATIONS

BAC	Bulk Air Cooler
CA	Cooling Auxiliaries
COP	Coefficient of Performance
DSM	Demand-Side Management
ESCo	Energy Service Company
IDM	Integrated Demand Management
NPSH	Net Positive Suction Head
OEM	Original Equipment Manufacturer
PCD	Pre-cool Dam
PID	Proportional Integral Derivative
PLC	Programmable Logic Controller
PTB	Process Toolbox
RAW	Return Air Way
SCADA	Supervisory Control and Data Acquisition
VRT	Virgin Rock Temperature
VSD	Variable Speed Drive
WB	Wet-Bulb

SYMBOLS AND UNITS

Symbol	Description	Unit
C_p (kJ/kg.K)	Specific Heat Constant	
COP	Coefficient of Performance	(-)
D	Diameter	(m)
EC	Energy Consumption	(kJ)
ES	Energy Saving	(kJ)
ESP	Energy Saving Percentage	(%)
h	Enthalpy	(kJ/kg)
H	Head	(m)
Hz	Hertz	(Hz)
kPa	Kilo Pascal	(kPa)
kW	Kilowatt	(kW)
ℓ	Litre	(ℓ)
ℓ/s	Flow Rate	(ℓ/s)
LF	Load Factor	(-)
$\dot{m}$	Mass Flow	(kg/s)
MW	Megawatt	(MW)
N	Rotational Speed	(RPM)
η	Efficiency	(%)
OH	Running Hours	(hours)
P	Electrical Power	(kW)
Q	Thermal Energy	(kJ/kg)
RH	Relative Humidity	(%)
T, Temp, temp.	Temperature	(℃)
W	Watt	(W)
$\dot{W}$	Sum of all Components Power	(kW)
℃	Degrees Celsius	(℃)
%	Percentage	(%)

GLOSSARY

Term		Description
Bush-man	-	An underground mining railway pneumatic back actor used to load rock into the hopper cars.
Condenser, Cond	-	Refers to the fridge plants condenser circuit
Convention	-	Heat transfer where a gas absorbs the heat.
December holidays	-	The period during which the mines usually close over the festive season.
Dynamic solution	-	A solution that will continuously adapt the control philosophy according to the system's current operations.
Eskom	-	Power supplier of South Africa.
Eskom peak periods	-	Period during which Eskom increases the electricity to encourage users to use less power during these periods. Low demand: 07:00-10:00 and 18:00-20:00. High demand season 06:00-09:00 and 17:00-19:00.
Evaporator, Evap	-	Refers to the fridge plants evaporator circuit.
Feedback loop	-	System output is used to determine the adjustment of the new input.
Fissure water	-	Water from underground rivers and boreholes that gathers at shaft bottom and needs to be pumped to surface through the mine's cascade system.
Hopper cars	-	Railway cars that transport the rock to the stations.
Latent heat transfer	-	The heat being transferred when the body's phase changes at a constant temperature.
Psychrometric conditions	-	Denotes the ambient physical and thermodynamics of a gas.
Run to failure	-	The machine is running until it fails, only then is the machine replaced.
Scraper winches	-	Mechanical winches used to move mining ore and waste to the hopper cars.
Sensible cooling	-	Heat is transferred between two mediums and the temperature changes and their phase remain the same.
Steady state solution	-	A solution that will provide one set of answers for the specific inputs and cannot adapt as the actual conditions change.

Stopes	-	An incline or vertical set of steps consisting of mining ore close to the mineral containing ore.
Temperature, Temp		Refers to the described temperature.
Virgin Rock temperatures	-	The rock face temperature after blasting.

Chapter 1. INTRODUCTION

"Your destiny is to fulfil those things upon which you focus most intently. So choose to keep your focus on that which is truly magnificent, beautiful, uplifting and joyful. Your life is always moving toward something." - Ralph Marston

1.1. GOLD MINING IN SOUTH AFRICA

History

The first discovery of gold in South Africa was during June 1884 on a farm known as Vogelstruisfontein. This was considered an insignificant discovery as the gold reef did not contain significant gold. During July 1886 George Harrison made the first discovery of the famous 400km South African gold reef, stretching from Mpumalanga to Virginia in the Free State on a farm known as Langlaagte [1], [2].

Open pit mining was the primary technique used by the first era of gold mining companies to exploit the shallow gold reefs in South Africa [2]. South African gold mining companies were unaware of the deep level gold mining techniques, as the reefs were shallow and did not require deep level mining. The first deep-level gold mine in South Africa was sunk in 1906 to a depth of 800m [2]. At that time it was the world's deepest gold producing mine [2].

The South African mining industry was limited to these depths for 54 years due to high underground temperatures [3]. The mines had to be ventilated to lower the underground temperatures and remove toxic gasses like methane [4]. Surface ventilation is suitable for mines up to a depth of 900 m below surface with virgin rock temperature (VRT) as high as 32℃ [3], [5], [6]. High underground temperatures cause the mineworkers to suffer from heat stroke [7].

In 1996, the South African Government established laws for the South African gold mining industry preventing mining activities above wet bulb temperatures of 32.5 ˚C at the stopes and 27.5℃ at the station [8]. The act forced mining companies to install or upgrade their cooling systems if underground temperatures were not within the temperatures prescribed by the Mine Health and Safety Act 1996 [9]. The Mine Health and Safety Act 29 of 1996 was revised in 2013, but the underground temperature restrictions did not change [9].

All mining companies within the South African border had to comply with the act in order to continue mining. The act ensures safe working conditions for mineworkers and lowers their risk to suffer from heat stroke.

The developing mines encountered increased VRT as they reached greater depths [5], [6]. Figure 1 depicts different types of cooling equipment available and their cooling capabilities to cool the underground working environment sufficiently up to certain depths [3], [5], [6].

Installation of new cooling equipment is mandatory when the underground environment temperatures rise above the crucial temperature. The cooling equipment is upgraded when the mine's installed cooling equipment is not capable of handling the heat load. Equipment upgrades are expensive and gold mining companies tend to postpone the upgrade for as long as possible [10], [11], [12].

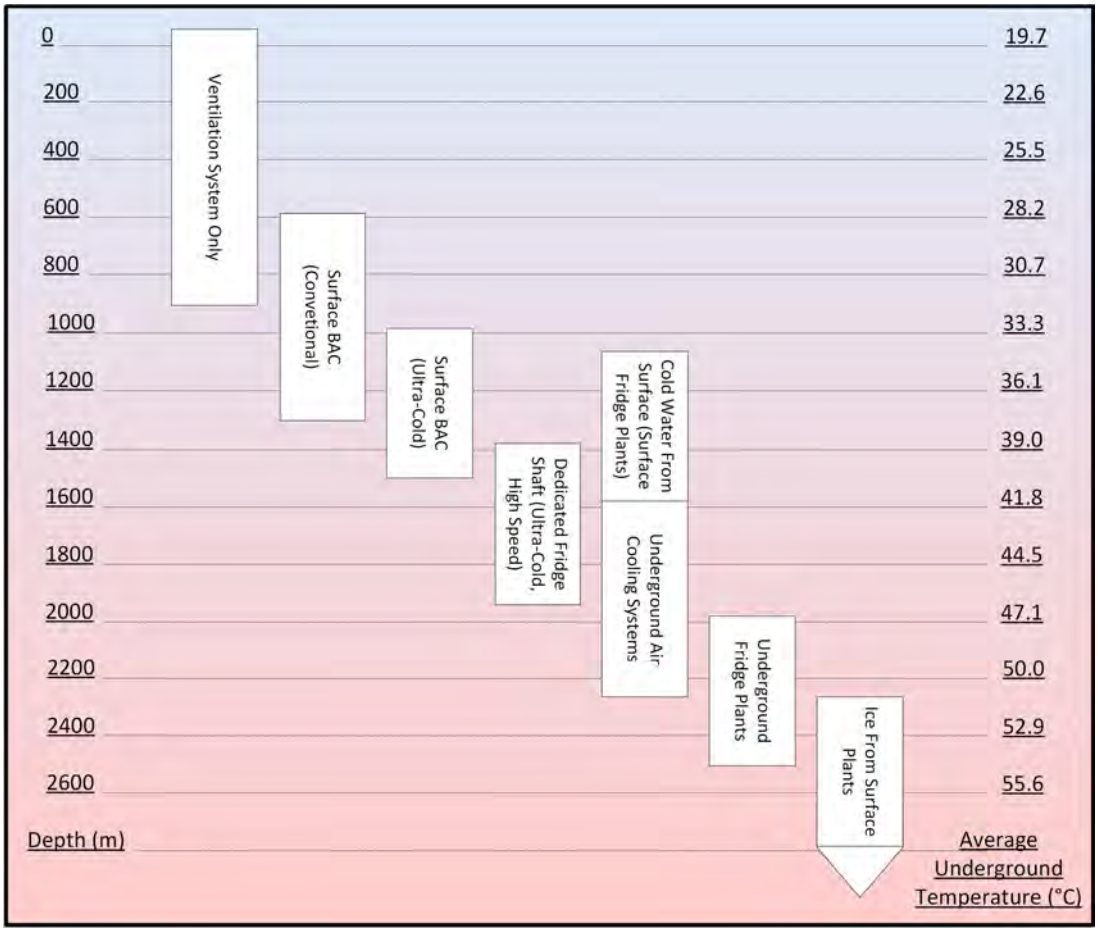

Figure 1: Cooling required at certain depths [3], [5], [6]

The first installations of mine cooling and ventilation as we know it today was on a Brazilian gold mine and British coal mine during the 1920s [4].The equipment and technologies available to the South African mine industry to cool the rock face and reduce environmental temperatures were limited [4]. Cooling systems were introduced to the South African mining industry during the 1930s. However, it was only during the 1960s when the gold on the shallow mines in South Africa deteriorated leading to the increased demand for deep-level gold mining and cooling systems [4].

Artificial cooling is added as soon as the average dry-bulb temperature at the working areas exceeds 32℃ [13]. Mines reaching a depth of 1 300 m below surface can expect

underground temperatures as high as 38℃ [5], [6]. Surface ventilation and bulk air coolers (BACs) are utilised to maintain acceptable underground working conditions at these depths [3]. Surface BACs with dedicated FPs can be sufficient up to a depth of 1 900 m where VRT of 45℃ can be expected [3], [5], [6].

Surface fridge plants (FPs) are installed to supply the surface BACs with chilled water for improved service delivery and to provide chilled water to mining levels. The chilled water is utilised underground to cool mining equipment and the VRT of 35℃ at a depth of 1 100 m below surface. Surface FPs and BACs are sufficient up to a depth of 1 570 m. Mining activities beyond this depth requires underground air cooling systems [3], [5], [6]. The surface FPs provide the underground BACs with chilled water to cool the underground environment.

Typically surface FPs lower the water temperature from 18℃ to 3℃ [14]. The temperature difference over the FPs is dependent on the FP type, layout and efficiency. The chilled water temperature increases at a rate of 1℃ per 250 m as it travels vertically down the shaft and horizontally into the mining levels. This is due to auto compression down the shaft and heat absorption from the underground environment [15]. Therefore, surface FPs are only effective up to a depth of 2 000 m.

Mining activities beyond 2 000 m require underground FPs [3]. Underground FPs are less effective than surface FPs as the FPs' heat discharge is limited to the underground environment. This reduces the COP from approximately 5.4 to 3.6. Surface FPs discharge their heat into the atmosphere whilst underground FPs discharge the heat into the return airway (RAW) or hot water at some shafts. Extraction fans on the surface extract the discharged heat to the surface.

VRTs of 51℃ have been reported at 2 300 m below surface [3], [5], [6]. The mining environment at these depths is cooled with ice from a surface ice plant. The ice from the surface is sent to an underground ice dam. The ice melts as it absorbs heat from the warmer water inside the ice dam. Ice dam outlet water temperature can be as low as 1℃ at 2 300 m below surface [16]. The outlet ice water is utilised for the same application as the chilled water.

Mining in South Africa has developed to a depth of 3 900 m where VRTs of 78℃ have been reported [5], [6], [17], [18]. These mines also utilise surface ice plants, underground and surface FPs and BACs to cool the mining environment. The cooling plants are added to

counteract the increased heat load from the mines' increased depth. The importance of the mine's cooling systems is therefore crucial to develop a safe working environment and comply with the mining laws of South Africa.

1.2. RELEVANCE OF COOLING

Modern day cooling equipment

Depending on the grade of the gold inside the ore deposits, a gold mine's average life expectancy is between ten to thirty-five years [19]. Gold mines are decommissioned when the richest gold containing ore has been excavated, when the overheads increase or when a natural disaster causes the mine to collapse [20].

From the inception of cooling equipment the design has not changed significantly [21].Cooling equipment has a life expectancy of one to nine years [22]. Therefore, it is fair to assume that cooling equipment older than ten years has passed their operational lifetime. During the mine's lifetime several equipment breakdowns will be encountered. Maintenance intervals and -mentality have an enormous effect on the cooling system's service delivery. These maintenance solutions are not always properly recorded, resulting in future uninformed maintenance decisions.

The majority of gold mines in South Africa's maintenance is based on a run-to-failure mind-set. Mine personnel are required to ensure equipment failure and breakdown periods are kept to a minimum irrespective of the effect it has on the system's service delivery [23]. With this type of maintenance mentality, the optimal solution is often overlooked.

A compressor's date of installation is a fairly accurate estimation when determining the age of a mine [19]. This assumption relies on the fact that a compressor has a fairly long life expectancy and the compressor was installed when shaft sinking commenced. A mine older than twenty-five years can be considered old [19].

Mine cooling equipment installation dates are not the same as the compressor installation date. Cooling equipment was only added to mines as they reached greater depths and encountered increased VRT [3], [5], [6]. The added equipment was designed to provide suitable cooling for the mine's heat load at that time to ensure acceptable working conditions are maintained for mineworkers [24]. The work load is calculated with a safety factor to maintain a working environment below the crucial temperatures and allow future

development. Unfortunately the predicted heat load did not compensate for reduced service delivery and extreme mining development.

Unforeseen equipment failure and incorrect maintenance thereof cause the systems' cooling capacity to decrease [11], [23]. The aging of cooling equipment and poor maintenance thereof reduces the equipment's efficiency over time. The inefficient cooling equipment causes increased underground environmental temperatures just below the crucial boundary temperatures. Identifying these inefficient components and reconfiguring them for optimal operation will lower the mine's risk of losing lives or being closed due to high underground temperatures.

Historically mine cooling design did not predict the mining techniques to develop as they did and therefore did not compensate for the increased heat load from mining at these record breaking depths [18]. The distance between the stopes and the stations has increased due to improved mining technologies [25]. The changes caused the mine's heat load to increase and the initial cooling equipment design did not compensate for the extreme heat load increase. Presently the cooling equipment maintains underground temperatures just below the crucial temperatures. Mining companies have the tendency to install new expensive equipment without conducting a proper feasibility study to improve their current installed equipment service delivery [16]. Table 1 represents the mine's FP information on different gold mines in the Goldfields.

Table 1: FP installation information on different shafts

Fridge Plant Installation Information for Different Shafts							
Mines	**Location**	**Amount**	**Year of Installation**	**Type**	**Brand**	**Winter**	**Summer**
Mine A	Surface	2	1992	High Pressure	York	2	2
	Surface	1	1992	High Pressure	York	0.5	1
	Surface	1	2013	High Pressure	York	0	1
Mine B	Surface	2	1980	High Pressure	Carrier	0	1
	58L	4	1982	High Pressure	Carrier	3	3
Mine C	Surface	3	2013	Low Pressure	Trane	0	2
Mine D	Surface	2	1985	High Pressure	Hitachi	0	2
	Surface	1	1987	High Pressure	Hitachi		

From Table 1 the majority mines in the Goldfields region are older than twenty-five years and can be consider as old. Table 1 depicts the majority of the cooling equipment older than 10 years and can be considered as old and outdated equipment. During 2013 mine A

installed entirely new FPs without considering reconfiguration of the installed equipment for improved efficiencies.

During 2013, the cooling equipment at mine D was decommissioned as their efficiencies were too low. New state-of-the-art cooling equipment was installed at mine C to cool the underground environment. Even though it is state-of-the-art cooling equipment, minor reconfiguration to the system can be implemented to ensure optimal operation.

The research proved mines would rather add a new plant instead of reconfiguring their installed equipment for improved service delivery. Reconfiguring of installed equipment can maximise the service delivery and postpone new installation. In cases where new installations are mandatory, the reconfiguration will ensure optimal operation of the old equipment. This will allow the old and new equipment to be synchronised. The mining industry will benefit from the reconfiguring of their equipment for optimal operation.

The historically low Eskom electricity tariffs caused mining industries to consume recklessly high amounts of electricity. Mining personnel only became aware of energy efficiency during the late 1990s, but they chose not to pursue energy saving measures [21]. Recent electricity tariff increases forced mine management to implement energy efficient initiatives. Mine personnel are under the impression that a power reduction will reduce the system's service delivery [15]. It is important to persuade mine personnel to be more aware of energy efficiency and the importance and benefits thereof.

In the past, mine personnel were responsible for maintaining the cooling equipment to ensure sufficient water- and ventilation outputs, irrespective of the power consumption and cost. These mine personnel are reluctant to accept behavioural changes for power savings [23]. Sometimes it requires many tests and reports to reassure mine personnel of the project's feasibility before implementation can commence.

Energy saving projects have never been part of a mine's budget. Mining companies do not have the funds available to upgrade their equipment for improved efficiency. Fortunately, with the South African energy crises, Eskom has allocated funds for demand-side management (DSM) projects [26]. Energy saving companies (ESCos) identify the power saving opportunities and implement the projects with funds from Eskom's Integrated

Demand Management (IDM). The projects focus on reducing the energy consumption during the Eskom peak periods without affecting the service delivery.

Mine cooling equipment requires reconfiguration for optimal operation, as the presently installed equipment is old and energy inefficient. Mine employees used to resist power saving initiatives. The South African mining industry is moving towards a mind-set where power saving is a priority. Mine management imposing power saving initiatives realises that these initiatives will ultimately lead to improved viability of efficiency and power saving projects.

1.3. MARKET RESEARCH

Cooling and ventilation in the mining sector are well-documented topics. Most of the research include ad hoc research of the mines' cooling or ventilation components. Available research is either aimed at DSM load shift projects or improving the systems' efficiencies. Most of the research proposals are implemented by ESCos enabling the researcher to validate his research.

The following section summarises previous research conducted in the mine cooling auxiliary field. The research authors are listed in Table 2 with a summary of where their research was focused on.

Bluhm, SJ [27] – did substantial research on both the cooling and ventilation of the mining sector. In one of his articles (*Practical aspects of the ventilation of high-speed developing tunnels in hot working environments*) he aimed to improve the ventilation at high speed developing tunnels. Bluhm improved the distribution of the cooled air. It can be more cost effective to first optimise the cooled air producing system. The effect of an optimised cooling system will be seen throughout the entire mine while ventilation in developing areas only improves the cooling at that specific area.

Buys, JL [28] – implemented a DSM energy efficiency project on the cooling system of a platinum mine. His research included the installation of variable speed drives (VSDs) on some of the cooling auxiliaries and BAC pumps for improved efficiency. The addition of new equipment for improved control lead to power saving on the cooling equipment. The study did not consider any reconfiguring of the cooling auxiliaries.

Du Plessis, GE [21] - developed an energy efficient cooling auxiliary's model and implemented it as a DSM project on gold mines. The model entails controlling the cooling auxiliaries with VSDs, meeting the mine's prescribed temperature- and water demands, whilst consuming less power. Du Plessis's research included replacing the mine's pre-cooling towers and adding equipment to improve the cooling auxiliaries' control. His research realised a power saving of 35.4%. Du Plessis work have been cited in excess of 280 times.

Du Plessis, JJL [29] – conducted a study to improve a gold mine's ventilation system efficiency as a DSM project by adjusting the inlet guide vanes of the main surface fans. The saving was obtained and the underground air flow was reduced by 6.36%. Du Plessis's research focused on reconfiguring the main surface fan guide vanes and did not consider reconfiguring of the mine's other cooling equipment. However, a reduction in the underground air flow reduces the BAC's thermal load and in return improves the utilisation of the BAC's output cold air.

Els, R [30] – research was based on determining the viability of load shifting a mine's surface and underground cooling equipment. His theory was tested through a simulation. The simulation utilised a building HVAC simulation software packaged called QUICKcontrol. This software's accuracy has been reported to be within 10% of the actual values [31]. His research was validated by successfully implementing the project on a gold mine.

Greyling, J [17] – research focused on determining the optimal location of cooling equipment for deep level gold mining. The research was simulation based. Estimated level temperatures were retrieved from VUMA simulation while Flownex software was utilised to simulate the dam capacities, pumps and pipe sizes. His studies concluded that optimal cooling for mines mining 4 000 m below surface is ice plants located on surface and underground closed loop chillers and BACs.

Holman, AM [11] – investigated the benefits of advanced monitoring of the mine's cooling auxiliaries. His theory was tested by implementing it as a DSM project on a gold mine. Holman's study focused on quantifying the effect certain maintenance decisions and the maintenance periods have on the machine's efficiency and life expectancy. Holman proved that regular equipment maintenance can increase the savings potential of cooling equipment. The research utilised the PTB simulation software, and validated the software accuracy to identify energy savings opportunities.

Kukard, WC [32] – proved that energy efficient and load shifting projects are feasible on a gold mine's underground auxiliary- and main surface fans. A possible load shift saving of 3.5 MW and 2.25 MW can be realised by load shifting the fans at two of South Africa's most advanced mines. Kukard's research only focused on the fans and did not include the other cooling auxiliary's components. His research did not include any reconfiguring.

Lambrechts, JV [33] – research focused on deriving an empirical formula to predict the underground station and stopes temperatures. The formula was subject to different variables. Lambrechts's research did not include any physical changes to the mine's cooling equipment but contributes to the field of study when the underground environmental temperatures have to be predicted during a BAC load shift.

Maré, P [23] – conducted a study to improve the sustainability of energy efficient DSM project implementation strategies. The strategy was validated on two different gold mines; firstly on a new project and secondly on an old project where the energy savings were neglected. Both of these projects' power savings were sustained for 7 months and 17 months respectively.

Maré's research did not include reconfiguring of the cooling auxiliaries as the case study on the new project only consisted of adding new equipment to improve the mine's control capabilities. Maré's research utilised the PTB simulation software validating its accuracy when comparing it to the case studies.

Schutte, AJ [15] – research mainly focused on the feasibility of load shifting the surface BACs and the effect it has on the underground temperatures. It also included improving the cooling system's efficiency; both these improvements were implemented as a DSM project on gold mines. Schutte's thesis indicated that the mine cooling and ventilation is a complex system and a two hour load shift of the surface BAC does not have an effect on the underground temperature.

New equipment was added to the mine's cooling to improve the systems' control and he adjusted the systems' control philosophy. The chilled water demand was decreased as the chilled water flow through the BAC was more than the design flow rate. Schutte's research did not include reconfiguring of the cooling equipment. However, his research proved a BAC load shift is viable. The study exposed the energy savings realised by reducing the BAC water flow to its design specifications.

Swart, C [24] – designed a simulation model to determine the optimal control philosophy. The simulation model was validated on a mine and proved a significant portion of the cooling was lost by over cooling the air. Altering the control philosophies to provide sufficient cooling will reduce the mine's ventilation and FP power consumption by 15%.

Uys, DC [16] – the study focused on converting a surface ice plant to an FP. The study included reconfiguration of a component within the mine's cooling equipment. The conversion reduced the power consumption with 2.6 MW as the ice plant was stopped and the converted FP acts as a backup plant. The conversion increased the mine's chill water storage capacity, enabling the mine to implement a morning and evening load shift. The load shift realised a power saving of 3.4 MW and 2.2 MW respectively. The study did not consider the reconfiguration of other components.

Although the concept of mining cooling and ventilation is a well-researched topic, the majority of these researchers recommend further research on the mine cooling system. The recommendation includes the following:

- Further studies to implement more DSM projects on mines' cooling system [15].
- Investigation of the mine's BAC to control the air and water flow for optimal operation and possibly include LS of the BAC during peak periods [28], [21] & [15].
- Investigate the reconfiguration of a mine's pre-cooling towers for optimal operation [28].
- Investigate the reconfiguration of inefficient subsystems within a large mine cooling system by replacing old equipment with modern equipment [21].

It is evident from the preceding market research that the reconfiguring of cooling auxiliaries for optimal operation has not been investigated sufficiently. Du Plessis, JJL [29] reconfigured a mine's ventilation fan blades for improved energy efficiency. The only form of reconfiguring on cooling auxiliaries was done by Uys, DC [16]. However, his study did not consider the reconfiguration of existing equipment for optimal operation. It focused on converting the ice plant to an FP for improved energy efficiency. Table 2 summarises all the market research applicable to the cooling and ventilation field of study.

.

Table 2: Summary of market research

Author	Investigated	Simulated			Implemented		Cooling							Ventilation							Project Type		
							Surface				Underground			Surface			Underground					DSM Project		
		PTB Software	Other Software	Modelling	New Equipment	Control Philosophy Update/Change	Refrigeration	Pump Flow Control	Pre-Cooling Towers	Reconfiguring	Refrigeration	Pump Flow Control	Reconfiguring	Fans	BACs	Reconfiguring	Fans	BACs	Mobile Units	Development Cooling	Reconfiguring	Load Shift	Energy Efficient	Service Delivery
Arndt, D	✓			✓		✓		✓							✓									✓
Bluhm, SJ	✓													✓						✓				✓
Buys, JL	✓				✓			✓							✓								✓	
Du Plessis, GE	✓				✓	✓		✓	✓						✓								✓	
Du Plessis, JJL	✓													✓		✓							✓	
Els, R	✓		✓			✓	✓	✓			✓	✓		✓								✓		
Greyling, J	✓		✓	✓							✓								✓	✓				✓
Holman, AM	✓	✓				✓	✓	✓	✓														✓	
Jonker, AJ	✓																							
Kukard, WC	✓													✓			✓					✓	✓	
Lambechts JV	✓																			✓				✓
Maré, P	✓	✓			✓		✓	✓	✓														✓	
Schutte, AJ	✓				✓		✓	✓							✓							✓	✓	
Swart, C	✓			✓		✓					✓	✓		✓										✓
Uys, DC	✓	✓					✓	✓		✓												✓	✓	
Van Eldik, M	✓				✓														✓					✓
Vosloo, J	✓			✓				✓				✓										✓	✓	✓
Whillier, A	✓						✓											✓	✓					✓

.

1.4. PROBLEM STATEMENT AND NEED

Energy saving projects are implemented ad hoc on mining equipment by ESCos. These projects mainly focus on improving a component's efficiency. Table 2 indicates that insufficient research has been done on reconfiguring a mine's cooling system components for optimal operation. The implemented projects have proved to reduce the component's power consumption or improved service delivery. The opportunity realised from reconfiguring old equipment in order to ensure that all the components are optimised for optimal operation, are often overlooked. System optimisation is neglected as a result of insufficient funding. ESCos also neglect the optimising as they are not rewarded financially for project over performance [34].

The only research found to have a slight correlation was done by Bredenkamp, JIG [20]. His study focused on reconfiguring a mine's compressed air network for cost savings. The study identified the system to be inefficient due to the systems design being based on old operations. The compressed air network was reconfigured to ensure optimal operation whilst fulfilling the systems requirements. Bredenkamp utilised simulation software called KYPipe and validated his simulation by implementing the project as an Eskom DSM energy efficient project. The project realised in average power saving of 1.7 MW.

Mine cooling systems is a well-researched topic and the room for new improvements is small. However, reconfiguring the old equipment to ensure all of the new installations are optimised has not been researched sufficiently. Reconfiguring the mine's cooling system will ensure that it operates at its optimal efficiency and can possibly result in cost savings.

It is evident from the information above that the equipment installed on mines are old. In the past, mining companies did not realise the benefits of energy saving initiatives. Mining companies generally only focus on maintaining their cooling equipment. Outdated and incorrectly maintained equipment results in inefficiencies.

Mining companies do not always have the funding available to properly maintain their equipment. External companies (ESCos) and researchers have identified the opportunity of investigating the retrofit of inefficient equipment to improve the mine's equipment efficiency. ESCos have identified the inefficient equipment and, together with Eskom DSM funding, helped to improve mining equipment efficiencies. DSM projects are implemented ad hoc on the gold mines' equipment.

The ad hoc implemented projects do not always ensure optimal service delivery as they only focus on certain aspects of the mines' cooling equipment. The ESCo do not always ensure the integration of new equipment with the old equipment. Minor changes to the cooling equipment layout and control philosophies will ensure all the equipment is integrated for optimal operations.

Therefore, this study will focus on the feasibility of reconfiguring of a mine's cooling system for optimal operation and possible cost savings. Reconfiguration will be investigated to ensure optimal operation through the integration of the old and new equipment. Equipment not operating at their original equipment manufacturing (OEM) design specification, will be reconfigured for optimal operations. Power saving can be realised from the improved system efficiencies.

1.5. CONCLUSION

This dissertation will fill the gaps of previous researches by reconfiguring the cooling system for optimal operation. The optimal operation of the cooling system for the highest service delivery will be determined with Process Toolbox (PTB) simulation software. The simulated results will be validated with a case study.

The reconfiguring will include the following:

- minor changes to the mine's cooling layout;
- changes to the control philosophies for optimal operation;
- upgrade or replacement of the outdated and inefficient equipment; and
- adding of equipment for improved control.

The reconfiguration will focus on improving the cooling system's energy efficiency to its maximum capabilities. Currently the majority of mine cooling equipment operate at full capacity to maintain allowable underground working conditions. An optimised system will allow the mine to lower the underground working temperatures to create improved underground working conditions. In return it can improve the mine's gold production but increase the cooling equipment operating costs. Maintaining the underground environment below the crucial temperature will not improve the mines productivity but will reduce the mine's cooling equipment-running cost.

The reconfiguring of mining cooling systems for optimal operation will benefit the mine, whether it is for improved underground working conditions to increase production, for cost savings or a balance between the two.

1.6. OVERVIEW

Chapter 1: Provides a historical overview of gold mining development and mines' cooling equipment in South Africa. Identifies the mine's age and classifies its installed equipment as old and inefficient. The crucial underground temperatures at which mines are forced to stop all mining procedures are identified. Market research was conducted to determine existing cooling auxiliary improvement technologies. Finally, the research objective is formulated.

Chapter 2: All of the components forming part of the cooling system are identified and discussed. Fundamental formulas utilised to characterise and evaluate mines' cooling systems are researched. The different layouts of cooling systems and their different applications are discussed. Lastly, the application of the cooling system outputs are identified.

The different simulation software packages are identified and the benefits of utilising a simulation model are discussed.

Chapter 3: A strategy is develop to identify and analyse the inefficient components within a mine's cooling systems. The different control philosophies are discussed. The information gathered in chapter 1 and 2 is utilised as guidance to develop the optimal strategy.

Chapter 4: The strategy is implemented on a mine. Inefficient components are identified and the required reconfigurations are simulated. The simulation is validated through a case study. The optimal control philosophy is determined.

Chapter 5: Concludes the study in stating whether the research was successful or not, and summarises the results. Recommendations are made for possible future research.

Chapter 2. LITERATURE REVIEW OF DEEP LEVEL GOLD MINE COOLING SYSTEMS

KJ Oberholzer

"You have to learn the rules of the game. And then you have to play better than anyone else." - Albert Einstein

2.1. INTRODUCTION

A mine's cooling system can be considered as the heart of a deep level gold mine. Without cooling, deep level gold mining will be impossible. From chapter one it is evident that the underground temperature increases as greater depths are reached. South African deep level gold mines are prohibited by the Mine Health and Safety Act 29 of 1996 to mine above wet bulb temperatures of 32.5 ˚C at the stopes and 27.5℃ at the station [8].

The mine's cooling system maintains the underground working environment temperatures below the crucial temperatures to ensure productivity and worker safety, but also to ensure adequate environment temperature for mining equipment to function without breakdowns caused by heat [35]. Lower ambient working temperatures result in increased gold production [36]. Cooling systems consist of multiple subsystems to provide the cooling required. Figure 2 represents a cooling system's configuration and the subsystems commonly found on a deep level gold mine.

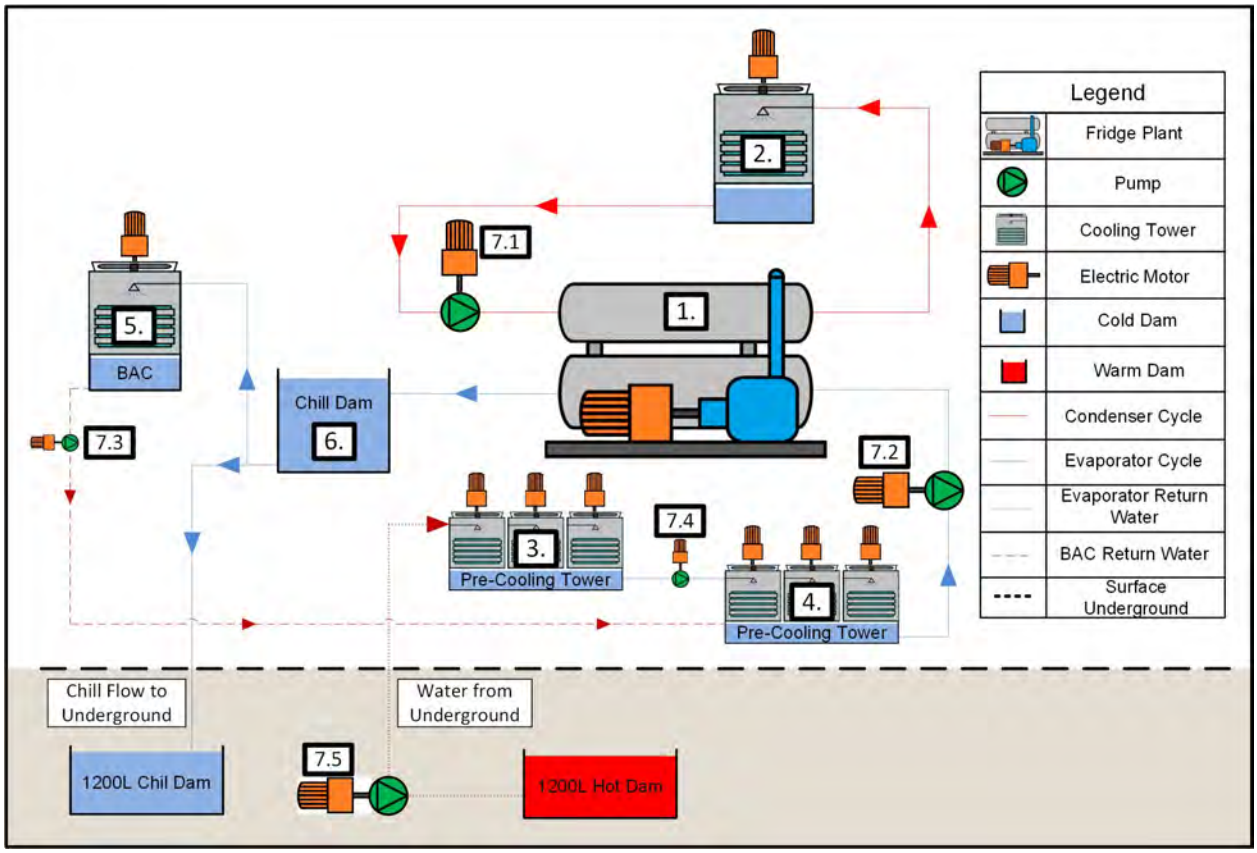

Figure 2: Typical deep level gold mine cooling system and its components

The components are listed below and their numbers correspond with the components' numbers in Figure 2 [37]:

1. Fridge plant.
2. Condenser cooling tower.
3. First stage pre-cooling towers.
4. Second stage pre-cooling towers.
5. BAC
6. Chill dams
7. Pumps
   7.1 Condenser Pump
   7.2 Evaporator pump
   7.3 BAC sump pump
   7.4 Pre-cooling pump
   7.5 Underground pumps

Surface refrigeration can consist of two water loops; one closed water loop providing the BACs with chilled water and another loop providing chilled water for mining purposes. Two loops are utilised when the required mining chilled water temperature is less than the required BAC water temperature. Cooling will be lost unnecessarily if the BAC inlet water temperature is lower than the BAC's OEM design inlet water temperature specifications.

2.2. MINE REFRIGERATION COMPONENTS

Preamble

The section that follows, elaborates on the different cooling subsystems' functions, responsibilities and the different layouts available within a mine's cooling system. It is important to understand the components' fundamental operation principles, performance considerations, design strategies and specifications before a cooling system can be analysed.

Fridge plants

The largest energy consumers within a cooling system are refrigeration machines; they utilise up to 66% of the cooling system's total power [21]. The FPs use a vapour-compression or ammonia absorption refrigeration cycle to lower the water temperature [38].

The vapour-compression cycle is in principle the same as the majority of cooling systems found in air conditioners fitted in vehicles, households and malls as HVAC systems [4].

Figure 3 depicts an FP which consists of three cycles: Refrigerant gas cycle to extract heat from the evaporator water cycle which discharges heat to the condenser water cycle; evaporator water cycle to distribute the chilled water throughout the mine; and the condenser water loop to absorb the heat from the gas. Figure 3 also shows which components form part of the condenser and evaporator water cycles.

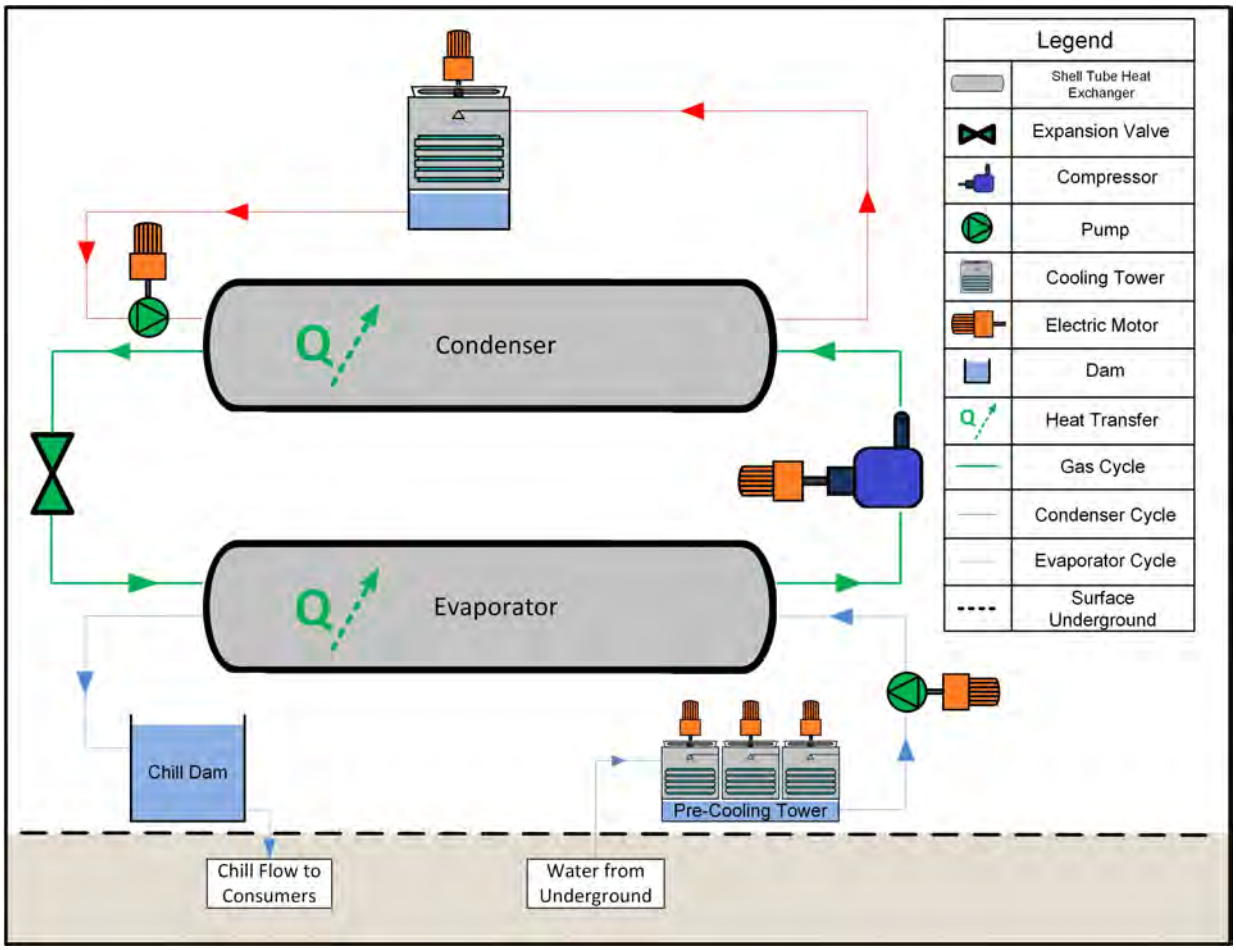

Figure 3: FP's vapour, condenser water and evaporator water cycles

There are many different models, suppliers, and designs of FPs available. Most of the FPs utilise the same vapour-compression cycle principles [4]. The vapour-compressed cycle is utilised by the mining industry due to its simplicity and relative low operating costs when compared to the other cycles available. The gas is also preferred by mines as it is not toxic, unlike ammonia gas [39].

FPs utilise different refrigerant gases, each being the most efficient for the specific application. The correct refrigerant gas for a vapour-compression cycle is selected by ensuring the gas properties, pressure and temperature, adhere to the cycle's requirements. Ammonia and R134a are the most common refrigerant gases utilised in the mining industry due to their relatively low cost. Figure 4 is a schematic representation of a vapour-compression cycle.

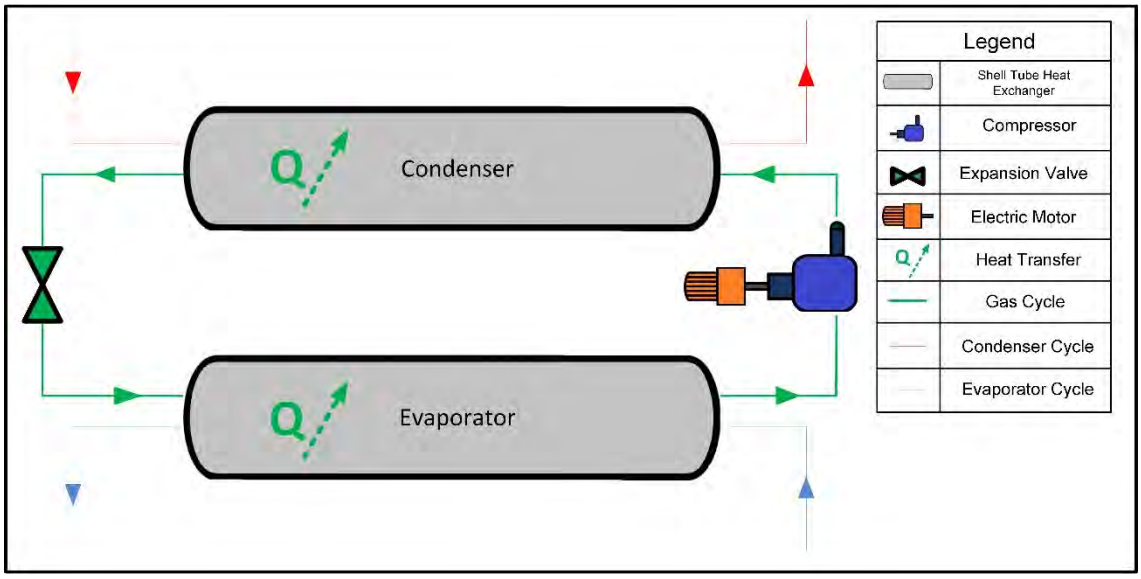

Figure 4: Vapour compression cycle

Figure 4 depicts a vapour-compression cycle that consists of a compressor, two shell tube heat exchanging pressure vessels and an expansion valve. The compressor in the cycle can be considered as the pump which is responsible for circulating the gas. Figure 5 represents the refrigerant gas pressure and enthalpy properties for a vapour compression cycle.

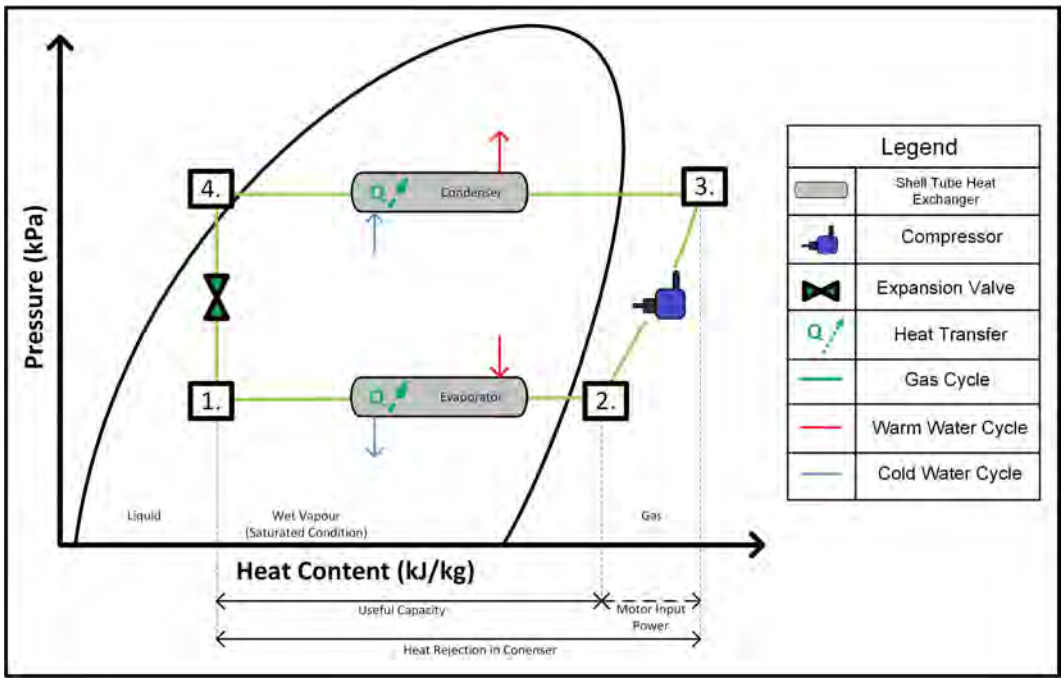

Figure 5: Refrigerant gas pressure against enthalpy diagram

Referring to Figure 5, the superheated refrigerant gas enters the compressor to increase the gas's pressure and temperature from point 2 to 3. The heat generated from the compression and the heat from the evaporator pressure vessel are rejected in the condenser shell tube heat exchanger. The superheated gas condenses at a constant pressure causing the gas to be subcooled. The gas pressure stays constant and the temperature decreases from point 3 to 4, allowing latent heat transfer. The heat is absorbed by the condenser water cycle, increasing the condenser water temperature [38].

The gas then passes from point 4 to point 1 through an expansion valve to throttle the vapour to lower the pressure and to change the gas phase to wet vapour, before entering the evaporator vessel. The liquid gas passes through the evaporator pressure vessel from point 1 to 2 and extracts latent heat from the evaporator water causing the gas to boil at a constant pressure, increasing the gas's temperature, while reducing the water temperature [38].

The compressor can either be a screw- or a centrifugal compressor depending on the system's required volume and pressure [40]. The cooling load is controlled by the inlet guide vanes of the centrifugal compressor and sliding valves for a screw compressor [41], [40]. The vanes control the amount of cooling the compressor does by using a feedback loop. The vanes are 100% open until the desired output chilled water temperature is achieved. The compressor vanes will cut back as soon as the desired outlet chilled water temperature is met [21]. The guide vanes throttle the refrigerant gas to maintain the required evaporator

water outlet temperature [21]. The guide vanes reduce the electricity consumption of the compressor and act as a safety measure to prevent the pressure vessel's tubes from freezing. Figure 6 represents a simplified illustration of a shell tube heat exchanger.

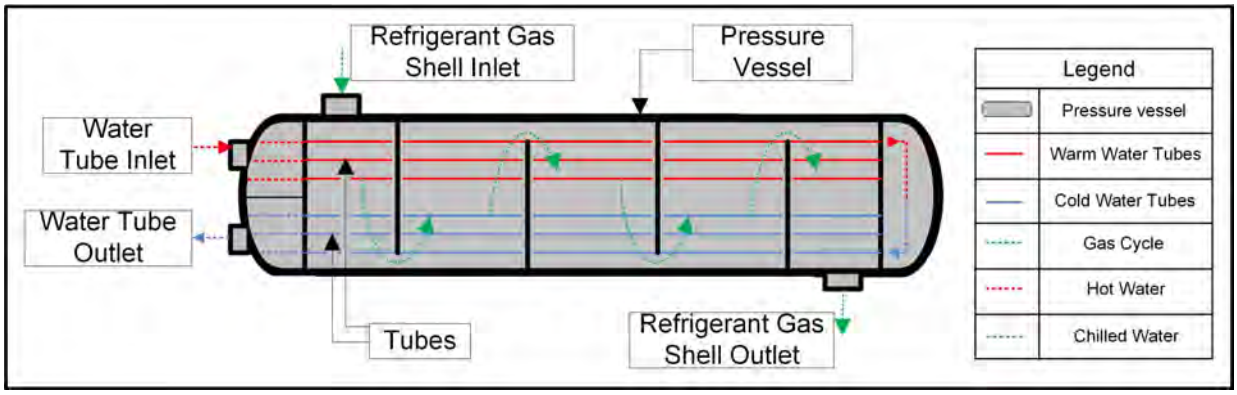

Figure 6: Schematic representation of a shell tube heat exchanger

Figure 6 depicts a shell tube heat exchanger that consists of a pressure vessel (the shell) with tubes inside the vessel (the tubes). The water from the evaporator and condenser flows through the tubes inside the pressure vessels, while the refrigerant gas passes over the tubes inside the vessel. A shell tube heat exchanger allows heat exchange between two mediums. In certain instances, where space is one of the design constraints, a plate heat exchanger is utilised, as it is more compact [40].

It is important to do regular maintenance on the tubes to prevent them from blocking. Blocked tubes will reduce the plant efficiency and will decrease the plant's overall performance. The compressor's coefficient of performance ($COP_{compressor}$) is a representation of the compressor's efficiency and is given by Equation 1 [39]. COP indicates the amount of thermal cooling that is done by the FP compared to the electrical input of the FP compressor. A higher refrigeration machine COP indicates that the refrigeration machine is more efficient than the same refrigeration machine with a lower COP. Smaller chillers usually have a COP of three while larger chillers COP can be as high as six [38].

$$COP_{Machine} = \frac{Q_{Evap}}{P_{Ref}} \quad (1)$$

$COP_{Machine}$ = Refrigeration Machine Coefficient of Performance
Q_{Evap} = Evaporator Heat Transfer (kW)
P_{Ref} = Electric Motor Power (kW)

The plant's coefficient of performance (COP_{plant}) is given by Equation 2 [39]. The equation indicates the amount of thermal cooling that is done for the total amount of electricity units utilised by the entire cooling system to cool the evaporator water.

$$COP_{Plant} = \frac{Q_{Evap}}{P_{Ref} + P_{Aux}} \quad (2)$$

COP_{Plant} = FP Coefficient of Performance
Q_{Evap} = Evaporator Cycle Heat Transfer (kW)
P_{Ref} = Electric Motor Power (kW)
P_{Aux} = Sum of Auxiliaries Power (Pumps, Fans, etc.)

The refrigeration machine's efficiency is given by Equation 3 [39]

$$\eta_{Machine} = \frac{Q_{Evap} + P_{Ref}}{Q_{Cond}} \quad (3)$$

$\eta_{Machine}$ = Refrigeration Machine efficiency
Q_{Evap} = Evaporator Cycle Heat Transfer (kW)
P_{Ref} = Electric Motor Power (kW)
Q_{Cond} = Condenser Cycle Heat Transfer(kW)

Water condenser cycle

Figure 7 represents the closed loop condenser water cycle. The cycle consists of the condenser shell tube heat exchanger, condenser cooling towers, condenser pumps and in some scenarios a launder dam. The condenser water cycle absorbs heat from the refrigerant gas as it passes through the condenser shell tube heat exchanger. The warm condenser water is pumped through the condenser heat exchanger and condenser cooling towers.

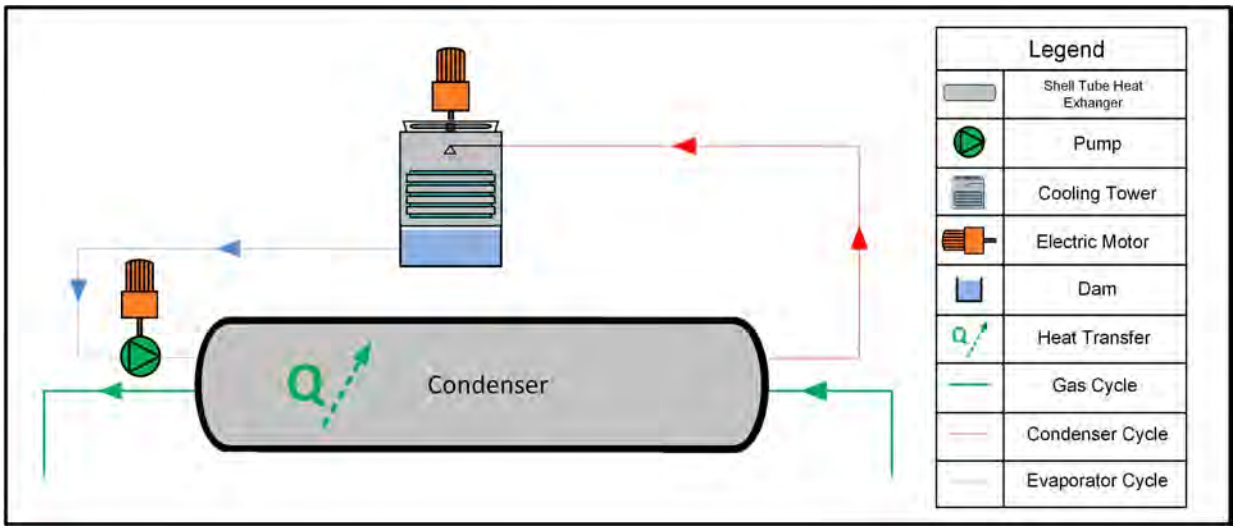

Figure 7: Condenser water cycle

The condenser cooling fans and the condenser pumps are the only power consumers on the condenser water cycle loop. The condenser cooling towers absorb the heat from the water and reduce the water temperature with approximately 5℃, before the water enters the condenser heat exchanger again. The water enters the condenser heat exchanger and absorbs the heat that the refrigerant gas rejects. This causes the refrigerant gas to condensate. The water leaves the condenser vessel approximately 5ºC warmer.

The water heat transfer is known as heat rejection process. The condenser pumps are usually larger than the evaporator pumps as the condenser loop requires a much higher flow rate than the evaporator loop. A detailed analysis of the cooling towers and pumps will follow later in this chapter. Equation 4 below is used to calculate the heat dissipated by the condenser into the atmosphere [39]:

$$Q_{Cond} = \dot{m}_{Water}.C_{p\,Water}.(T_{In} - T_{Out}) \quad (4)$$

Q_{Cond} = Condenser Cycle Heat Transfer (kW)

$\dot{m}_{Water}$ = Water Mass Flow(kg/s)

$C_{p\,Water}$ = Specific Heat of Water $(KJ/kg.K)$

T_{Out} = Water Temperature Out (K)

T_{In} = Water Temperature In (K)

Launder dams

Figure 8 represents a condenser loop that utilises a launder dam. The launder dam acts as a temperature control measurement. During the transition months the condenser cooling tower outlet water temperature could decrease to be lower than the FP's condenser design inlet temperature range. Water below the inlet design temperature range causes the condenser to absorb too much heat from the gas, causing the gas to have a low evaporator pressure. This can cause the FP to trip. If the mine switches off a condenser cooling tower, the condenser cooling tower's outlet water temperature could increase above the condenser inlet temperature design range. This will lead to the condenser water not being able to absorb sufficient heat from the gas, causing the FP to trip on high evaporator pressure[1]. Consequently, a launder dam is utilised.

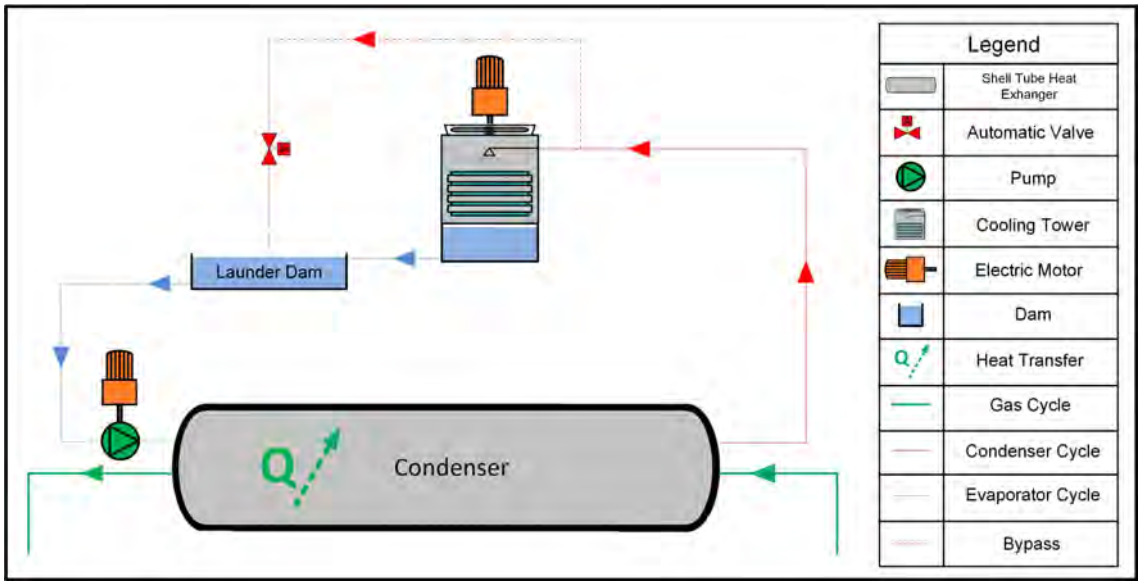

Figure 8: Condenser cycle with launder dam included

Launder dams are situated between the FP condenser inlet and the condenser cooling tower outlet. Mines use launder dams to regulate the FP condenser water inlet temperature at a certain setpoint. Launder dams are not a necessity for FPs. There are different methods for controlling the FP condenser water inlet temperatures. A launder dam is one of the older methods to control the FP condenser inlet temperatures. The temperature is controlled by mixing the cold condenser inlet water with the warmer condenser outlet water to achieve the setpoint temperature. The launder dam ensures sufficient mixing of the hot and cold water before it enters the FP condenser vessel. The FP will have the best efficiency if the launder dams supply the FP condenser with the design inlet water temperature.

[1] Nico Pienaar Mechanical Foreman

Water evaporator cycle

Figure 9 represents the semi closed loop evaporator water cycle which is responsible for producing cold water for mining purposes. The cold water is also known as chilled water and is utilised for various mining applications that will be discussed later in this chapter. The cycle can be considered as a semi closed loop as the amount of chilled water that is sent underground is not necessarily equal to the water pumped to surface. The volume of water can decrease due to evaporation into the atmosphere, or increase due to fissure water entering the shaft. The underground water enters the water evaporator cycle on surface at a temperature in the vicinity of 26℃. The evaporator cycle lowers the water to a temperature in the vicinity of 3-5℃, depending on the cycle's load and the mine's requirements.

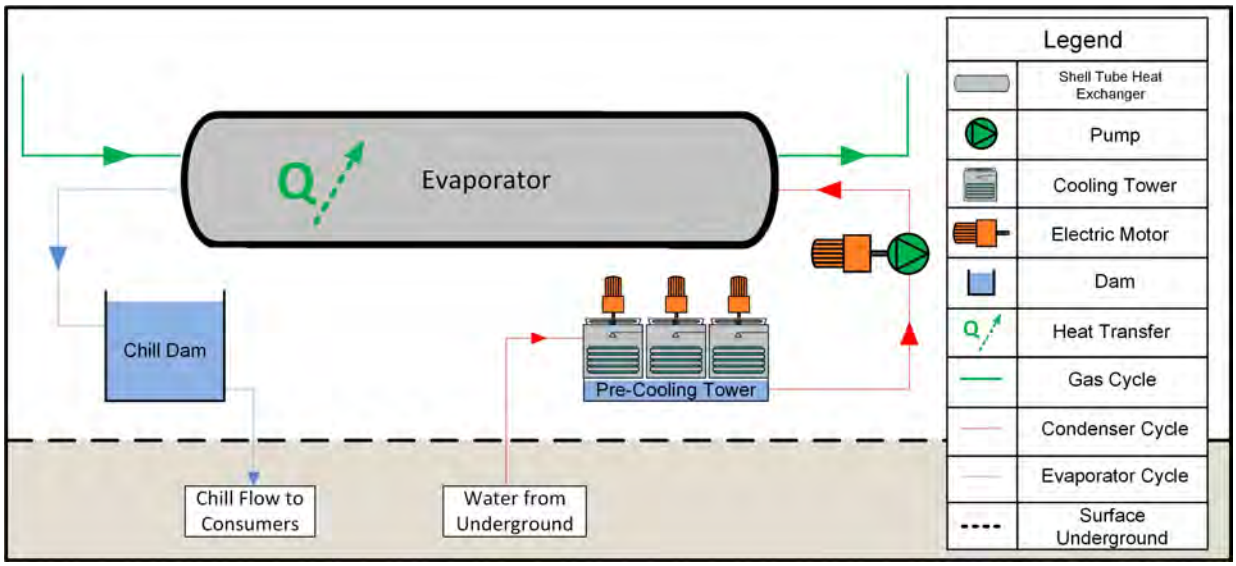

Figure 9: Water evaporator cycle

The warm water from underground is pumped into a hot water storage dam or directly through pre-cooling towers on surface. The warm water passes through single- or two stage pre-cooling towers. The single stage pre-cooling towers can lower the 26℃ mining water to a minimum of 2℃ above ambient WB temperature, depending on the cooling tower's efficiency[2].

Two stage pre-cooling requires relatively small pumps to transfer the pumps from the first to the second stage. Instances where the evaporator output water temperature does not

[2] Deon Arndt Partner of Enoveer Engineering Innovation

meet the preferred output temperature, chilled water is recycled as presented by Figure 10. If the pre-cooling stages are well maintained, they have the capability to decrease the evaporator cycle's cooling load at relatively low power consumption.

The evaporator water requires longer contact time with the refrigerant gas for maximum heat transfer. Therefore, the evaporator pumps are smaller than the condenser pumps as a reduced water flow increases the contact time between the water and gas. From Equation 5 it is evident that if the energy absorption stays constant, a low flow rate will result in a bigger temperature decrease with the same COP [39].

$$Q_{Evap} = \dot{m}_{Water}.C_{p\,Water}.(T_{Out} - T_{In}) \quad (5)$$

Q_{Evap} = Evaporator Cycle Heat Transfer (kW)

$\dot{m}_{Water}$ = Water Mass Flow(kg/s)

$C_{p\,Water}$ = Specific Heat of Water $(KJ/kg.K)$

T_{Out} = Water Temperature Out (K)

T_{In} = Water Temperature In (K)

The evaporator heat exchanger utilises the latent heat from the phase transition of the refrigerant gas to accommodate the heat transfer from the water to the refrigerant gas [21]. The warm water enters the evaporator heat exchanger in the vicinity of 13℃ and exits the heat exchanger as chilled water in the vicinity of 5℃. The chilled water is temporarily stored in the chill dams from where it is distributed to the various chilled water consumers. Chill dams are situated on surface and underground, and they can consist of one large dam or several smaller dams.

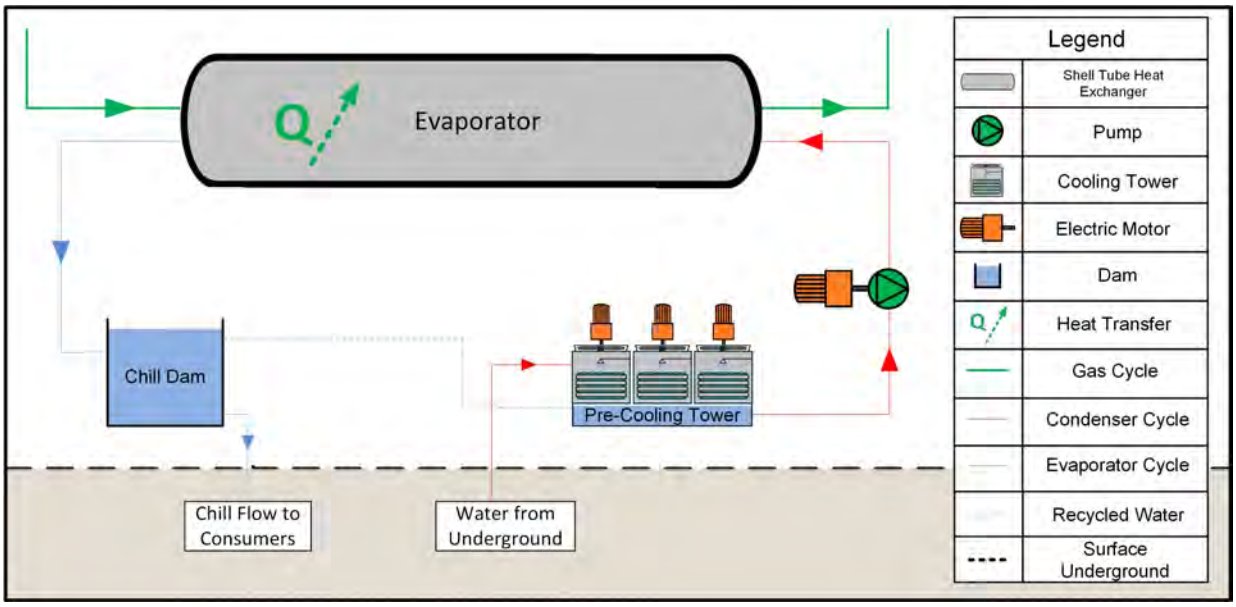

Figure 10: Water evaporator cycle with re-cycled water

Figure 10 represents the evaporator water cycle with recycled water from the chill dam to the precooling towers. Recycled water can reduce the pre-cooling dam temperature from 18 ° to 12℃ [42]. As soon as the chill dam level is above a certain level the water flows from the chill dam to the pre-cooling towers. The chilled water is dumped in the pre-cooling dams, as close to the evaporator suction as possible to prevent cooling loss. The recycled chilled water will reduce the evaporator inlet water temperature.

Cooling towers

Cooling towers utilise mechanical force draft towers, consisting of a steel or concrete structure with a mechanical suction fan mounted on top of the structure [43]. The hot water is sprayed in the cooling towers to create a water mist. The suction fan forces ambient air through the water mist. The water's heat is absorbed by the air via conventional heat transfer into the atmosphere [21]. The cooling towers lower the water temperature drastically utilising a relatively small amount of power. A cooling tower's performance is dependent on the water temperature and the ambient psychrometric conditions [44].The coefficient of performance of a cooling tower water cycle is in the vicinity of 30 and can be calculated using Equation 6 and Equation 7 [11].

$$COP_{Cooling\ Towers} = \frac{Q_{Cooling\ Towers}}{P_{Ref}\ CT} \tag{6}$$

$$Q_{Cooling\ Towers} = \dot{m}_{Water}.C_{p\ Water}.(T_{Out} - T_{In}) \tag{7}$$

$COP_{Cooling\ Towers}$	=	Refrigeration Machine Coefficient of Performance
$Q_{Cooling\ Towers}$	=	Evaporator Cycle Heat Transfer (kW)
$P_{Ref\ CT}$	=	Electric Fan Motor Power (kW)
$\dot{m}_{Water}$	=	Water Mass Flow (kg/s)
$C_{p\ Water}$	=	Specific Heat of Water $(KJ/kg.K)$
T_{Out}	=	Water Temperature Out (K)
T_{In}	=	Water Temperature In (K)

The COP is dependent on the following: water mass flow, inlet-, outlet water temperatures and the installed cooling tower's capacity [4]. A cooling tower's cooling capabilities also depend on the environmental inlet psychometric conditions and the quality and duration of the water air contact period [4]. Water can only be cooled to 2℃ above the ambient wet-bulb temperature [45].

The cooling tower's COP is dependent on the ambient psychrometric conditions. Thus, the cooling tower COP is only an accurate representation of a cooling tower's performance if the COPs are calculated for two days with similar ambient psychrometric conditions. The efficiency of the cooling tower air-side is difficult to determine as the outlet air temperature is seldom recorded. A cooling tower's water side efficiency is a more accurate representation of a cooling tower's performance as it incorporates the ambient psychrometric conditions. Equation 8 up to Equation 10 are utilised to calculate the water side efficiency of a cooling tower [23], [21]. These equations can be applied to the majority of mines as all the variables are recorded.

$$\eta_W = \frac{\dot{Q}_{Actual}}{\dot{Q}_{Ideal}} = \frac{Range}{Aproach} \tag{8}$$

$$Range = T_{Wo} - T_{Wi} \tag{9}$$

$$Approach = T_{Ai(WB)} - T_{Wi} \tag{10}$$

η_W	=	Water Side Efficiency (%)
T_{Wo}	=	Water Outlet Temperature $(°C)$
T_{Wi}	=	Water Inlet Temperature $(°C)$
$T_{Ai(WB)}$	=	Air Inlet Wet-bulb Temperature $(°C)$

A cooling tower with a fairly low approach value can be considered as an efficient cooling tower with an efficient water-side. The range only quantifies the temperature drop over the cooling tower's water side and should be considered relative to the approach [21]. Figure 11 is a schematic representation of a cooling tower.

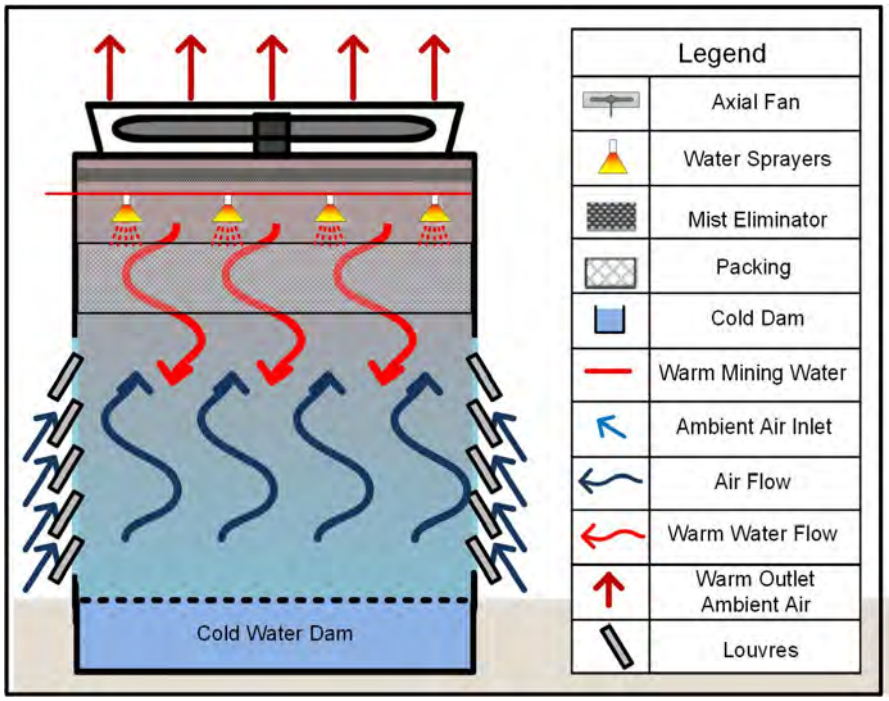

Figure 11: Schematic representation of a cooling tower

Water sprayers located at the top of the cooling towers spray the warm water in the vertical cooling towers. The mechanically driven suction fan at the top of the cooling tower creates a vertical air draft in the opposite direction of the water movement. The air velocities in the cooling towers usually range between 1.5 m/s and 3.6 m/s [11]. Water mist is often blown into the atmosphere by the condenser cooling towers, the water loss is reduced by mist eliminator lining between the fan and the water sprayers [46].

The water sprayers spray the water onto a splash fill to increase the water and air contact time and area in the cooling towers. The fill ensures the water- and air flows are evenly spread throughout the cooling tower [21]. The fills are manufactured in various shapes and utilise different materials like PVC, polypropylene and galvanised steel bars. Damaged cooling tower fills or blocked fills will cause the condenser cooling tower efficiencies to decrease [47].

The decrease in water temperature is realised from a combination of sensible and latent cooling. The sensible cooling occurs via conventional heat transfer (water and air temperature difference) and latent cooling occurs via evaporative heat transfer (from water phase change) [21]. The cooled water is collected in the pre-cooling tower dam at the bottom of the pre-cooling tower from where it is pumped by the evaporator pumps through the FPs.

Pumps

Water pumps are utilised to distribute water to the different chilled water consumers within the cooling system. Centrifugal pumps operate at fixed speed, delivering a constant flow. The water flow will decrease as the efficiency of the pump decreases over time. Pumps' motors vary between 30 kW to 400 kW. Pump configurations vary depending on flow and pressure requirements. Figure 12 depicts the location of water pumps within a deep level gold mine. Pumps are usually found at the following locations: FP condenser water cycle, FP evaporator water cycle, BAC sump dams, two stage pre-cooling and underground at the dewatering cascade system.

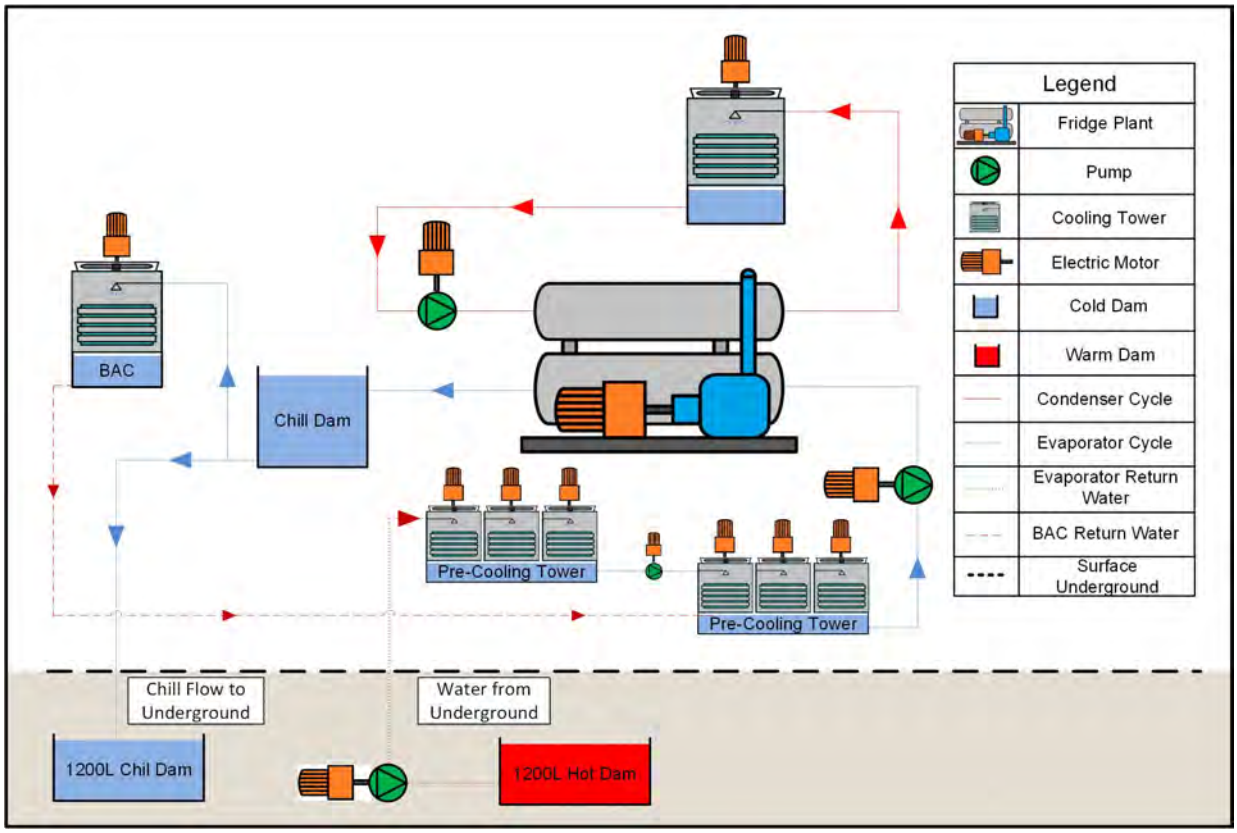

Figure 12: Pumps location in the mining industry

An electric motor propels the centrifugal pump impeller and causes the water to accelerate in order to move the water [48]. The water's high velocity causes a pressure increase. The correct pump for a specific application is determined by the required flowrate and pressure head. These characteristics are determined by the pump impeller blades and shape of the pump's casing. Figure 13 is a representation of a specific centrifugal pump design performance characteristics [48]. The point of optimal pumping is determined by plotting the head, efficiency, power and net positive suction head (NPSH) required against the flow rate for a specific pump. The required flow rate determines the point from the pump characteristics curves [49].

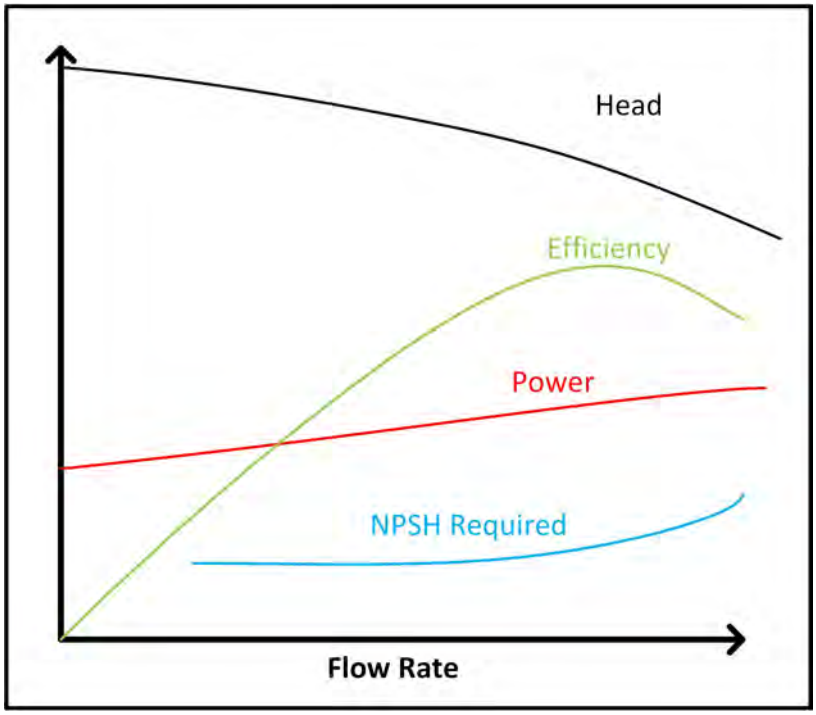

Figure 13: Centrifugal pump typical characteristic curves [48]

Altering the pump impeller speed and diameter will change the pump characteristic curves. This is proven by the centrifugal pump affinity laws. The flow rate is proportional to the impeller diameter, rotational speed, pressure head and pump power [49]. Changes to the valve opening in the water flow pipeline result in a pressure difference and reduce the water flow. The affinity formulae are as follows [28]:

$$\frac{Q_1}{Q_2} = \frac{D_1}{D_2} \tag{11}$$

$$\frac{\dot{Q}_1}{\dot{Q}_2} = \frac{N_1}{N_2} \tag{12}$$

$$\frac{H_1}{H_2} = \left(\frac{\dot{Q}_1}{\dot{Q}_2}\right)^2 \tag{13}$$

$$\frac{P_1}{P_2} = \left(\frac{N_1}{N_2}\right)^3 \tag{14}$$

$\dot{Q}$ = Water-flow Rate (l/s)
D = Impeller Diameter (m)
N = Rotational Speed (rpm)
H = Pressure Head (m)
P = Pump Input Power (kW)

From the affinity formulae, it is evident that the required flow rate can be achieved by manipulating any of the following: impeller diameter, rotational speed, pressure head and pump input power. Depending on the system requirements, adjustments can be made to ensure the desired flow rate is achieved. If the system requires permanent changes, the following physical alteration can be considered: reducing the impeller diameter if flow is too high, or installing an impeller with the pump design diameter to increase the flow.

The pressure head can be altered by increasing or decreasing the pipe diameters. The power can be adjusted by altering the number of poles on the motor or replacing the pump motor with the correct size motor [50]. However, it has been shown that almost half of all industrial motors are loaded below 40% rated capacity, resulting in reduced operating efficiencies [51].

In order to achieve a more controllable alteration a valve can be throttled to decrease the water flow to the pump. A more accurate control alteration will be to install a VSD on the pump motor. The VSD will adjust the pump's power frequency to reduce the pump's power and rotational speed to achieve the desired flow rate. VSD indicatives lower the motor's current that will result in a power saving [52].

Variable speed drives (VSD)

The increased demand for energy-saving initiatives led to the development of variable speed drive applications [53]. VSDs are installed on the power supply of the motor [54]. The VSD modulates the motor speed by changing the supply frequency whilst controlling the speed continuously. VSDs have great power saving potential and can be implemented on conveyors, compressors, fans, pumps and winders [55], [56]. Significant energy saving potential exists by installing VSDs to control the cooling system's electrical motors [57]. The power savings are realised when the VSD reduces the electricity's frequency and the motor operate at part load [58].

VSDs do not only ensure power savings, but also:

- extend the life expectancy of the pumps and electric motors [59];
- reduce the maintenance on the motors, as the VSD has the capability to soft start and stop the motors [56];
- improve the reliability and system performance [60];
- improve the control process [61] and;
- improve the correction power factor [62].

The power saving that is realised from VSD installation can be calculated from Equation 15 and Equation 16 [21]:

$$ES_{Chiller} = EC_{Chiller} - EC_{Chiller,VSD} \quad (15)$$

$ES_{Chiller}$ = Chiller's Energy Saving Realised from VSD Installation (kJ)
$EC_{Chiller}$ = Chiller's Energy Consumption (kJ)
$EC_{Chiller,VSD}$ = Chiller's Energy Consumption after VSD installation (kJ)

Equation 16 is used to determine the power saving realised by an FP with VSDs controlling the chiller pumps. A VSD improves the FP's efficiency and if an increased service delivery is required the energy consumption could increase. Therefore, it is important when calculating the energy saving that the chiller's load is kept the same [58].

$$ES_{Pump,Fan} = OH \,.\, \dot{P}_{Rated} \,.\, ESP \quad (16)$$

$ES_{Pump,Fan}$ = Pump or Fan Energy Saving (kJ)
OH = Running Hours $(hours)$

$\dot{P}_{Rated}$ = Motor Rated Power (kW)

ESP = Energy Savings Percentage $(\%)$

Equation 16 is used to estimate the power impact saving realised by controlling a fan or pump with a VSD [21]. Instances where the electricity power consumption is not logged but the statuses and system parameters are, the energy consumption can be calculated using Equation 17 and Equation 18 [21]:

$$EC_{Chiller} = OH \,.\, \dot{Q}_C \,.\, LF_C \,.\, COP^{-1} \tag{17}$$

$$EC_{Pump,Fan} = OH \,.\, \dot{P}_{Rated} \,.\, LF_P \tag{18}$$

$EC_{Chiller}$ = Chiller's Energy Consumption (kJ)

OH = Running Hours $(hours)$

$\dot{Q}_C$ = Chiller's Heat Transfer Rate (W)

LF_C = Cooling Loading Factor

COP = Coefficient of Performance

$EC_{Pump,Fan}$ = Pump or Fan Energy Consumption (kJ)

$\dot{P}_{Rated}$ = Motor Rated Power (kW)

LF_P = Pump or Fan Loading Factor

Figure 14 is a diagram of the essential VSD components and how they interact with each other.

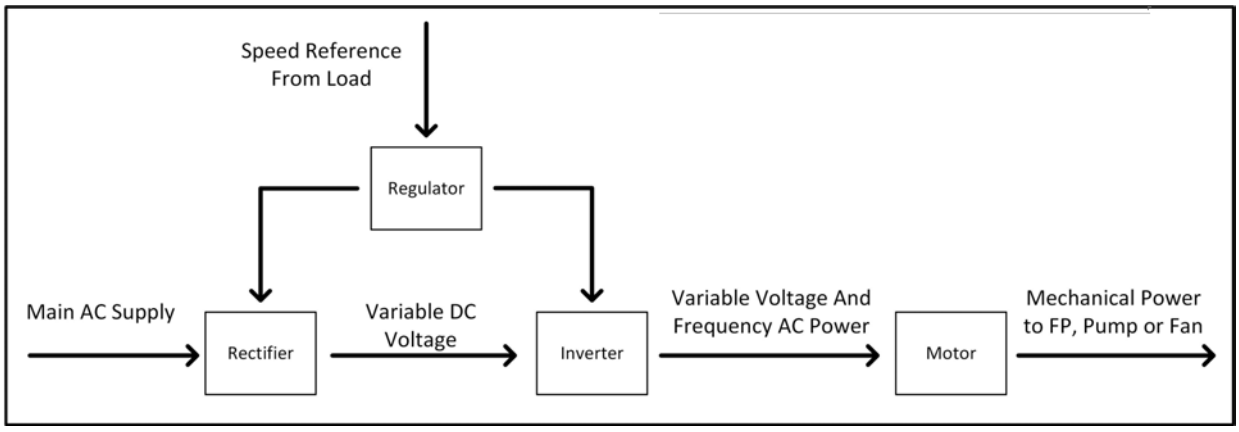

Figure 14: Variable speed drive components diagram [54]

As depicted by Figure 14 a VSD consists of an inverter, rectifier and regulator. The supplied three phase alternative current (AC) is converted to direct current (DC) by the rectifier [63].

The regulator regulates the rectifier and the inverter to get the power output as close to the setpoint as possible. An internal or external control unit regulates the power setpoint according to the system outputs. The inverter changes the DC voltages to an AC voltage with a certain frequency (HZ) value by rapidly switching the DC voltage in the positive and negative directions [21]. The more rapid the inverter switches the DC voltage the higher frequency is produced.

Noise is generated when the VSD switches the power from AC to DC and back to AC [64]. A VSD could cause the power usage to be non-linear, which can lead to current distortion and harmonic voltage to occur on the main power supply [21]. Equipment susceptible to radio frequency may experience interference. The following complications can occur: circuit breaker trips, errors with the network communication, equipment overheating, motors failing prematurely, reduced motor efficiencies and power wastage [65].

Studies on VSD installations have proved to be successful in the following industries: boiler houses, cement plants, conveyor systems, gold mining cooling and ventilation systems, petroleum plants, platinum mining cooling and ventilation systems and refineries [50] [66] [67] [68] [28] [21].

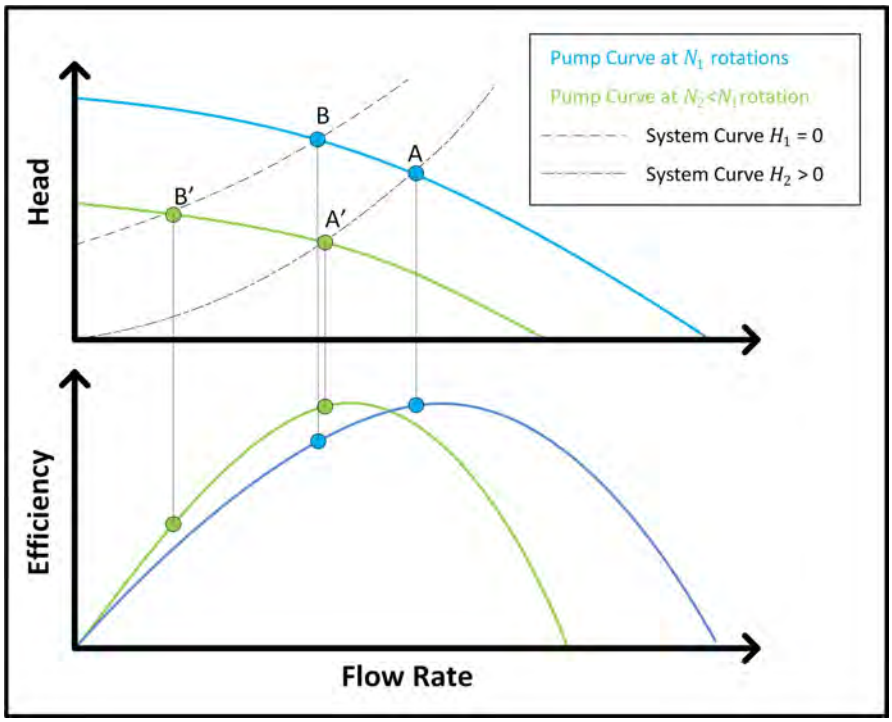

Figure 15: Characteristic curves of a VSD controlled pump [23]

Figure 15 represents two sets of pumps' head and efficiency characteristic curves, plotted against the water flow. The first set of characteristic curves represents a pump at full load while the translated characteristics curves represent the characteristics of a pump controlled by a VSD at reduced speed. Point A represents a point where the static head is zero at a rotation speed N_1. Point A is translated to A' at a reduced speed. It is evident from the efficiency curve that points A and A' operate at the same efficiency (ISO-efficiency). It is evident that, at a zero static head, the reduction in speed has no effect on the pump efficiencies. Point B represents a system with a static head. Point B translates to B' at a lower rotational speed, producing a lowered static head. The pump efficiency and water flow are reduced as a result of the lowered rotational speed [69]. Although the pump efficiencies are reduced, it is important to consider the overall improvement a VSD has on the global system COP. It has been reported that reduced condenser and evaporator water flow rate increase the chillers' COP [70], [71]. The global COP is given by Equation 19, Equation 20 and Equation 21 [38]:

$$Global\ COP = \frac{\dot{Q}_{Cooling\ System}}{\dot{W}_{Cooling\ System}} \tag{19}$$

$$\dot{Q}_{Cooling\ System} = \dot{m}_{W,Daily\ Avg}.C_{p\ Water}.(T_{From\ UG} - T_{Chill\ Dam}) \tag{20}$$

$$\dot{W}_{Cooling\ System} = \sum \dot{W}_{In\ Cooling\ System} \tag{21}$$

$Global\ COP$ = FP and Cooling Auxiliaries Coefficient of Performance
$\dot{Q}_{Cooling\ System}$ = Heat Transfer through the FP and CA's (kW)
$\dot{m}_{W,Daily\ Avg}$ = Daily Average Water Mass Flow (kg/s)
$C_{p\ Water}$ = Specific Heat of Water $(KJ/kg.K)$
$T_{From\ UG}$ = Warm Water Temperature from Underground (K)
$T_{Chill\ Dam}$ = Cold Water Temperature inside the Chill Dam (K)
$\dot{W}_{Cooling\ System}$ = Sum of the FP and Cooling Auxiliaries Power input (kW)

If the average electricity consumed by an FP is reduced and the cooling load remains constant the global COP will increase. Therefore, the global COP can be considered as an accurate parameter to evaluate the energy efficient strategy [21].

However, the trade-off between the changed pump efficiencies and the reduced flow rate for power savings needs to be carefully evaluated. Reduced pump efficiencies may increase the maintenance cost or reduce the pump's life expectancy. It is important to ensure that the minimum frequency that the VSD can cut back still provides the pump with its minimum NPSH required to prevent the pump from cavitation. Cavitation will cause unnecessary wear on the pump impellers. A control philosophy that requires regular start and stop of electric motors should be adjusted so that the VSD start and stop pump gradually (soft starter). This will reduce the mechanical stresses generated on the bearings and rotating parts from starting the pump [48].

Ice plants

Ice plants is a relatively new initiative to deep level mining cooling systems [3]. Ice plants are considered when a mine reaches depths beyond 2 200 m below surface. There are different types of ice plants, some form solid ice, whilst others form ice in the snow crystals form. Ice plants are situated on surface and send ice down the shaft in an ice shoot to the underground chill dam. The ice melts and lowers the chill dam temperature from where the mine's chilled water is supplied.

2.3. MINE COOLING SYSTEMS

Preamble

Deep level gold mines require chilled water to cool the underground environment. South African mines are forced by the government under the regulations of the Mine Health and Safety Act 29 of 1996 to maintain a station wet-bulb temperature below 27.5℃ [72]. A mineworker's productivity decreases immensely when the stopes wet-bulb temperatures rise above 28℃ [73]. Furthermore, the environmental dry bulb temperature should be kept below 37℃ as the human body starts absorbing heat above this temperature [22]. Table 3 represent the effect wet-bulb temperature increases have on a mineworker's effectiveness.

Table 3: Effect of WB temperature on work efficiency [15]

WB temperature range	Effect on worker efficiency
T_{wb} < 27℃	100% Worker efficiency
27℃ < T_{wb} < 29℃	Worker acclimatised, work effectiveness still economic
29℃ < T_{wb} < 33℃	Safety factor range corrective action required
33℃ < T_{wb}	Worker can work for short periods with adequate breaks

Cooling systems are utilised to cool the mining water. Deep level gold mines utilise FPs and their auxiliaries with different sizes and configurations to accommodate the specific gold mine's requirements. The FPs' outlet water temperature varies between 3℃ and 6℃ [21], [44].

Fridge plant configurations

Different refrigerant configurations are found on deep level gold mines. The depth of the mine determines the amount of cooling that is required. This also relates to the FP's and auxiliaries' installed capacity and layout. Figure 16 represents a schematic illustration of the three different configurations found in mines.

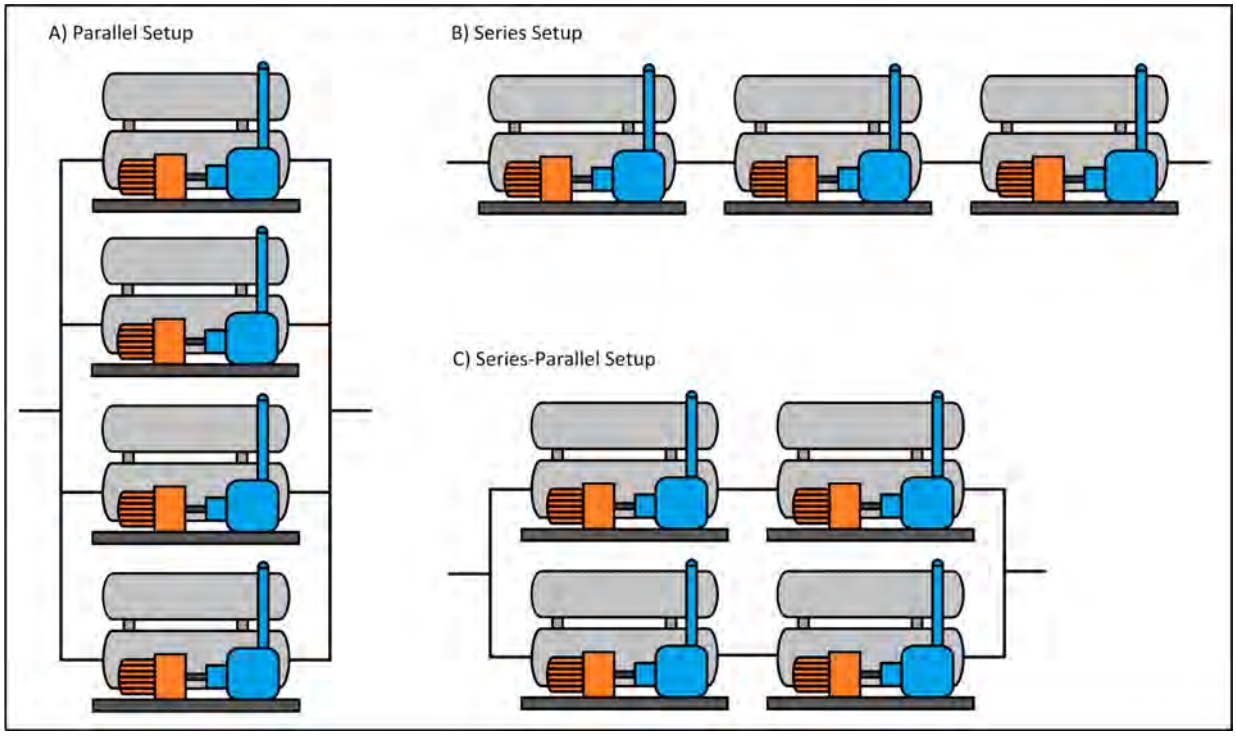

Figure 16: FP configurations

Figure 16 a - Parallel configuration is utilised if the cooling load remains the same and the water flow is controlled. The temperature difference over the plants stays constant while the water flow could be varied by isolating one of the plants with valves [74].

Figure 16 b - Series configuration is utilised when a constant water flow is required and the amount of cooling being done needs to be controlled. The cooling load increases during the

summer months, thus with a series FP configuration some of the FPs can be switched off when the cooling load reduces as the ambient conditions change [74].

Figure 16 c – Series-parallel configuration is utilised if the water flow and the cooling load are controlled. If the cooling load is reduced due to ambient conditions that change, one of the FPs in series can be switched off. The FP in one of the parallel loops can easily be isolated if the required water flow is reduced [74].

Pump configurations

The pumps that provide the FPs with water can be configured in parallel or series with a FP. Figure 17 represents the two different pump layouts:

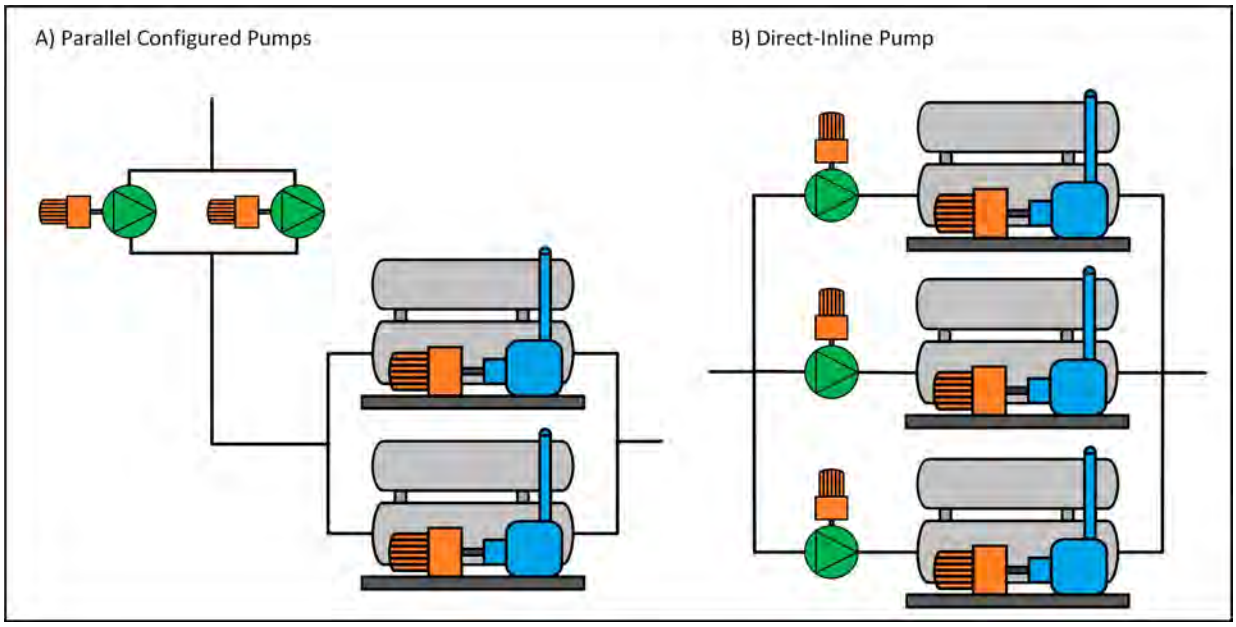

Figure 17: FP pump configuration

Figure 17 a - depicts parallel-configured pumps that pump water into a common manifold. The manifold distributes the water to a single FP or multiple FPs. It can be difficult to detect the inefficient pump within a parallel-configured pump network as it is common practice to install only one flow meter after the common manifold before the FP. Due to a pressure drop caused by the common manifold it is advised that valves are installed at the inlet of each FP to control the pressure and water flow entering each plant [11].

A parallel configuration of pumps is usually found on an FP with a series or parallel-series configuration. This configuration of pumps can simplify maintenance or replacement as that

line can easily be isolated with minimal effect on the plant operation. If parallel configured pumps have a spare isolated pump, maintenance can be conducted without affecting the plant's water flow.

Figure 17 b - depicts a direct-inline pump or a series configuration where the pump is configured in line with the FP. A single pump provides a plant with the correct water flow. Series configurations ease the fault detection process as the decreased water flow can easily be related to the pump in line with FP experiencing low water flow.

However, the FP needs to be stopped if the pump requires maintenance or replacement. This can be difficult if there is only one FP or the chilled water demand is high. This configuration is usually found on parallel configured plants. With this configuration, the plant and pump can easily be isolated for maintenance or power savings. Pumps that are configured directly in line with the plant are more suitable for speed reduction control, as the VSD only affects the plant in line with the pump [75].

2.4. CHILLED WATER CONSUMERS

Preamble

The main purpose of FP is to provide chilled water to the chill water consumers in order to lower the water temperature to cool the mine's underground working environment. The average VRT at 2 000 m below surface can be as high as 76 ˚C [76].

The mine's heat stress is defined by the working environment air velocity, humidity radiant energy and temperature. Heat strain is the physiological response to heat stress. The underground air is rejected between a wet-bulb temperature of 25.5 ˚C and 29.0 ˚C [15]. The rejected warm air is removed from the underground environment to be exhausted into the atmosphere on surface.

The adiabatic compression, fissure water, electromechanical equipment, heat from broken rock, wall rock heat flow and other causes are some of the factors that increase the underground heat load. Fissure water temperature is almost as high as the VRT. The fissure water continuously releases heat into the environment until it is pumped to surface [15]. Figure 18 represents the VRT at different gold mines in South Africa at certain depths.

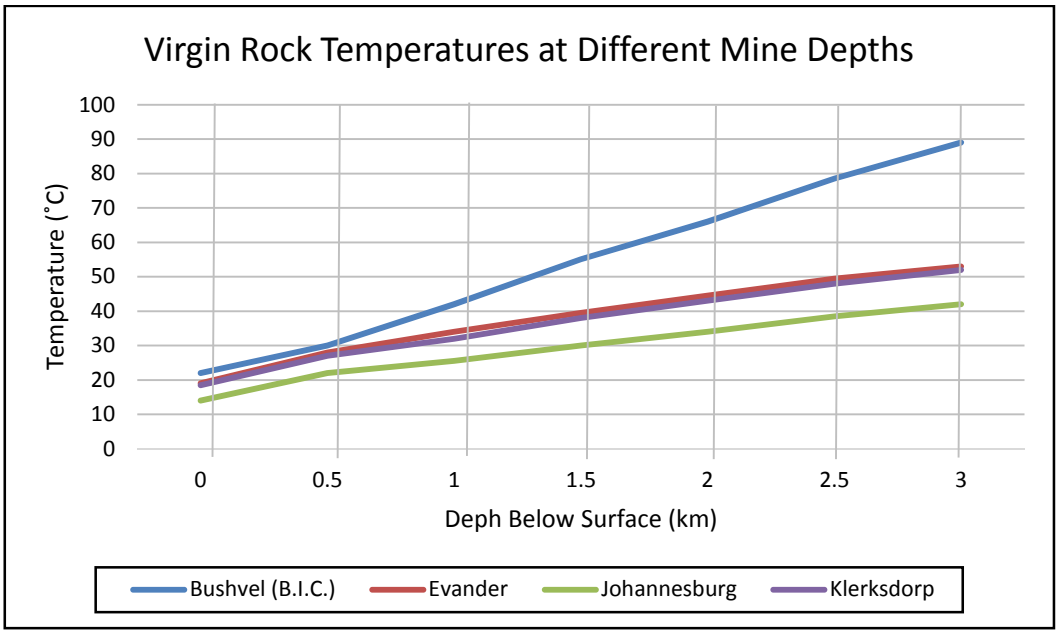

Figure 18: Virgin rock face temperatures [76]

Chilled water temperature increases as it is sent underground. Heat exchange between the surrounding rock, and pressure increase due to gravity, cause the water temperatures to increase at a rate of 1℃ for every 250 m down the shaft [15]. No cooling is lost when the chilled water temperature increases as it is sent to underground. The chilled water absorbs the heat from the underground environment and in effect reduces the underground environment temperature. The chilled water consumers of a deep level gold mine can be divided into three groups: convection -, conduction -, and unintended chilled water consumers.

Convection chilled water consumers

Convection chilled water consumers are BACs and Cooling Cars (CC). Convection chilled water induces cooling without contact to the underground area being cooled. The cold air is used as a medium and blown past the rock face to cool the underground environment.

Bulk Air Cooler

BACs are located on surface and underground, depending on the mine's layout. BACs utilise approximately 7% of the mine's cooling system total power consumption. Underground BACs are vital at mines where the shaft ventilation is acceptable but the mining areas and haulage are above the regulated mining temperature [46]. BACs utilise chilled water from the FPs to cool the underground air. The cold air is forced down the shaft

to cool the underground environment. Figure 19 represents a typical deep level mine's air reticulation system.

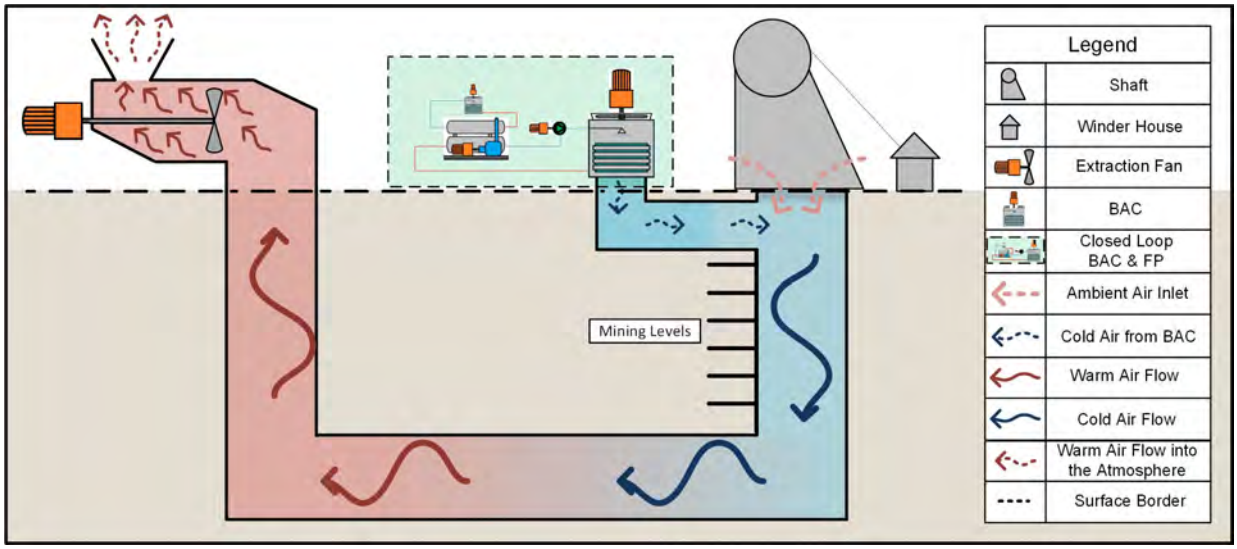

Figure 19: BAC air reticulation

Extraction fans are located on surface on the RAW next to the main shaft. The extraction fans extract hot air from underground, creating a negative air pressure below the main shaft [15]. The BACs cool and dehumidify the ambient air. The cooled air from the BAC mixes with a small amount of ambient air that enters from the main shaft opening. The negative pressure draws the mixed air down the main shaft preventing the air from escaping into the atmosphere. Equation 22 below is used to determine the amount of cooling done by the BAC [38]:

$$Q_{BAC} = \dot{m}_{air}(h_{out} - h_{in}) \quad (22)$$

Q_{BAC} = BAC's Heat Transfer (kW)
$\dot{m}_{air}$ = Air Mass Flow (kg/s)
h_{out} = Air's Enthalpy out of the BAC (KJ/kg)
h_{in} = Air's Enthalpy into the BAC (KJ/kg)

The BAC's performance improves as the ambient relative humidity decreases [28]. During the winter months the BAC is switched off when the difference between ambient wet bulb air temperature and the chilled water temperature is low. This allows the mine to conduct maintenance on the standing BACs and FPs [15]. Figure 20 represents the water reticulation of a surface BAC.

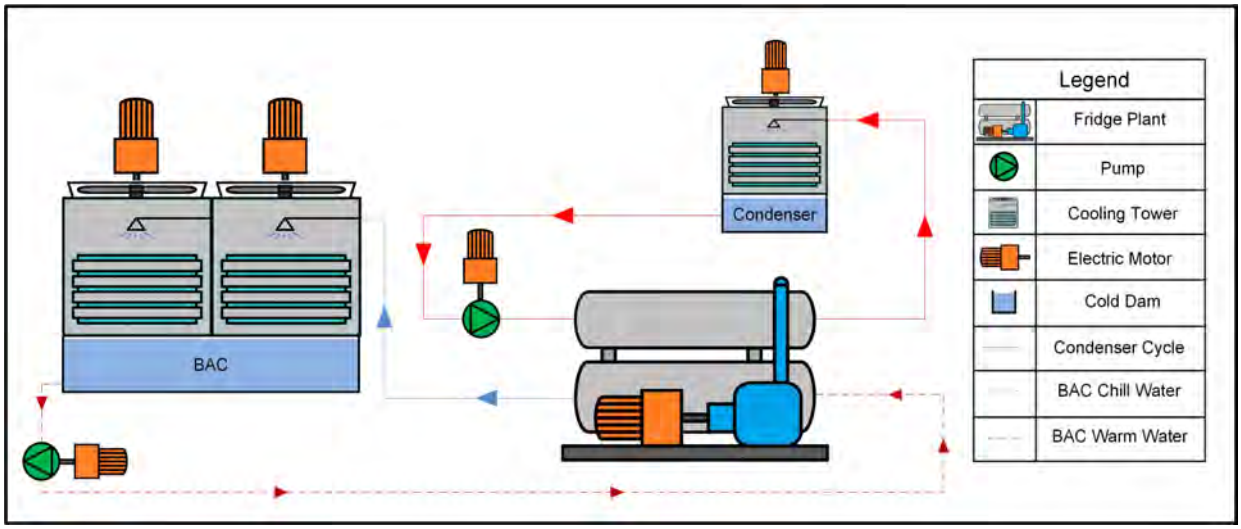

Figure 20: Surface BAC water reticulation

Surface BACs utilise chilled water either form the chill dam or directly from the FPs. The chilled water enters the BAC at 4℃ and exits the BAC at 12℃. The BAC sump dam water is pumped into the FP inlet dam (pre-cool dam). The BAC return-water reduces the FPs' inlet water as the BAC outlet water temperature is lower than the water from underground. This enables the FPs to reduce the chilled water temperature even further.

The BAC is in principal similar to the cooling tower as they both utilise evaporative spray chambers to accommodate sensible and conventional heat transfer. The difference between the two is that a cooling tower (condenser- and pre-cooling towers) cools the water with ambient air, while the BACs utilise chilled water to cool the ambient air. This causes chilled water temperature through the BACs to increase. The BACs maintain an outlet air WB temperature as cold as possible to ensure the underground cooling requirements are met [77].

The average ambient air enters the BAC at 22.1℃ with a relative humidity (RH) of 67.6% during the summer months. The air undergoes sensible cooling until the air is fully saturated (RH 100%). The saturated air is then further cooled beneath the dew point to dehumidify the air. Dehumidification occurs when the water condenses through latent and sensible cooling [15]. The air exits the BAC with an absolute humidity ratio ($g_{moisture}/kg_{dry\ air}$) of 100%. The dehumidification rate is defined by the water removal Equation 23 [78]:

$$X_{H_2O} = \dot{m}_{Air}(W_1 - W_2) \quad (23)$$

X_{H_2O} = Water Removal Rate (kg/s)

$\dot{m}_{Air}$ = Air Mass Flow (kg/s)

W_1 = Humidity Ratio (kg/kg)

W_2 = Humidity Ratio (kg/kg)

There are two types of BACs; vertical and horizontal forced draft BACs [79]. Figure 21 represents a schematic illustration of a vertical forced draft BAC tower.

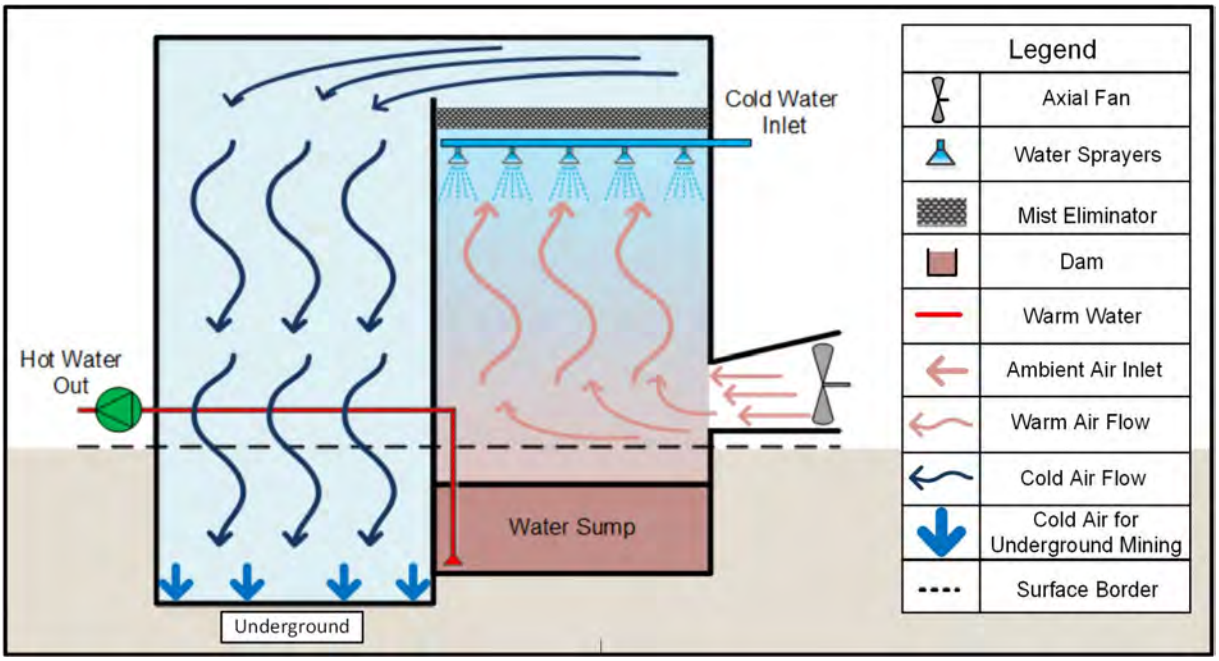

Figure 21: Schematic illustration of a vertical forced draft BAC

Vertical forced draft BACs are located on surface of a deep level gold mine. The mechanically driven fans force ambient air into the BAC. Water sprayers located at the top of the BAC spray chilled water mist into the BAC. Gravity forces the water mist down the BAC and into the BAC sump dam from where the warm water is pumped to the pre-cool dam. The ambient air enters the BAC at the bottom and follows the air path through the BAC. The air flow is in the opposite direction of the chilled water for maximum heat transfer. The air's heat is transferred to the chilled water. The cooled air passes through a mist eliminator mesh before it is sent underground.

Vertical draft BACs are the least expensive cooling method to cool the underground air temperature [74]. Vertical draft BACs have a greater cooling capacity than a horizontal BAC [11]. Figure 22 represents a schematic illustration of a horizontal forced draft BAC.

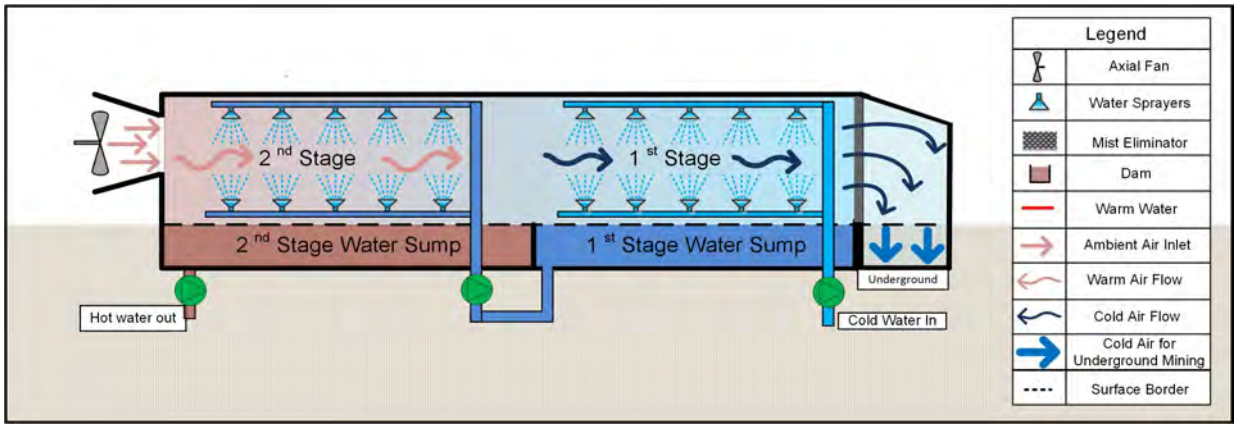

Figure 22: Schematic illustration of a horizontal multistage forced draft BAC

Horizontal multi stage draft forced BACs are located on surface and underground; however, they are more often installed underground as less excavation is required [4]. The mechanical driven fans force ambient air into the BAC. The air first passes through the second stage and then through the first stage's water mist to allow maximum heat transfer. The cooled air is forced down the shaft. The water sprayers are located at the top and the bottom of the horizontal BAC. The water mist cools the air, after which the water accumulates at the BAC sump dam. Chilled water flows through the first stage of the BAC, while the water from the first stage is pumped through the second stage to pre-cool the ambient air.

BACs that are located underground operate in a closed loop with underground FP, or in an open loop system utilising water from the underground chill dams. The underground closed loop BAC system is more efficient than the open loop BAC system, since the open loop BAC system utilises more power as the BAC outlet water has to be pumped to the FPs on surface for cooling. The open loop BAC's outlet water can be utilised for conductional cooling or dumped into the underground hot dam.

Cooling Cars

Mines with inadequate ventilation and high underground temperatures add underground cooling cars positioned at the working areas [80]. Cooling cars are also located at the stopes and developing working areas. Cooling cars are also known as spot coolers, as they only cool a specific area. Cooling cars can be permanently installed at a section or be mobile,

depending on the period during which cooling is required at a specific section. The mobile cooling cars are utilised at the stopes, as they can easily be directed to the section where more cooling is required. Figure 23 is a schematic representation of a cooling car.

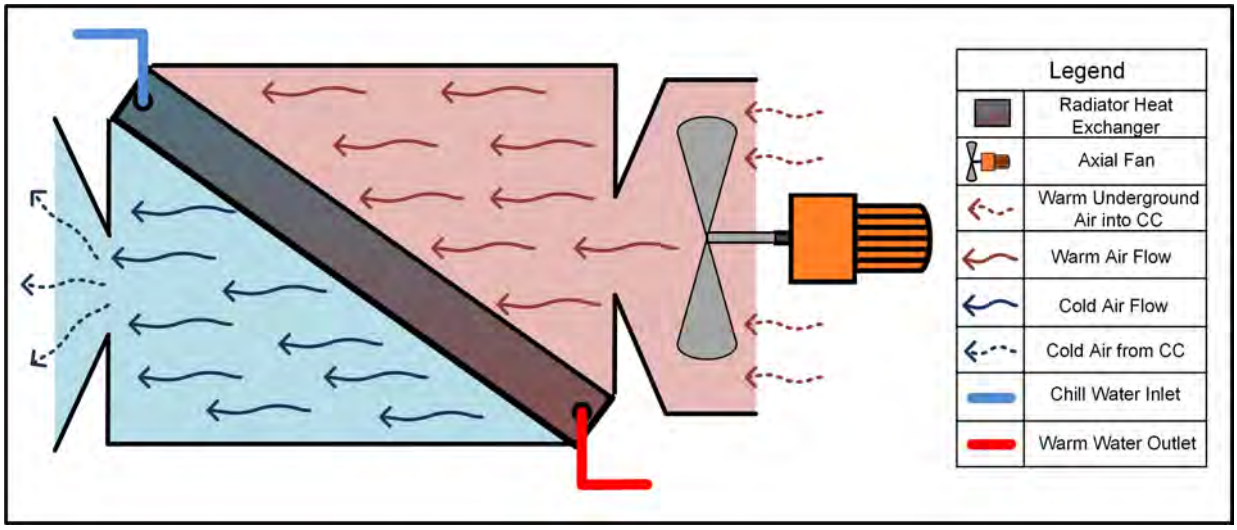

Figure 23: Schematic representation of a cooling car

Figure 23 depicts a cooling car comprising of a fan, cooling coil, and metal construction. The chilled water is sent to the stopes through the chilled water pipe network for cooling. The chilled water is drained from the underground pipe network. The water passes through the cooling coil of the cooling car. A fan forces underground air over the coil to induce convection heat transfer through sensible cooling [76]. The warm water is dumped in the mine to form part of the warm water cascade system making the cooling car an open water cycle loop.

At the specific working area where a cooling car is utilised, it could feel as if the cooling car has a great impact on the underground environmental temperatures. However, if the effects of the cooling car's outlet water are taken into consideration, the cooling cars' efficiency is only 21.25% [22]. This is due to the warm water evaporating and increasing the underground humidity downstream from the working area. The efficiency of a cooling car can be improved by changing the water cycle into a closed loop water cycle. Figure 24 shows an image of a cooling car on surface.

Figure 24: Cooling car

Conduction chilled water consumers

Chilled water is utilised underground to cool the virgin rock after blasting. Contact between the rock face and the chilled water induces conductional heat transfer through sensible cooling. Conductional heat transfer is a highly efficient thermal heat transfer process, but requires a significant amount of pumping [28]. An underground closed loop cooling system reduces the amount of pumping, but has a lower thermal heat transfer efficiency [3]. Pneumatic drills, water sprayers, and high-pressure water cannons utilise chilled water to induce heat transfer [81]. These consumers are found at the stopes and development areas.

Drills

In order for blasting to commence, mine personnel drill holes in the rock face to plant the explosives. Although some mines use hydro powered drills [82], the majority of mines make use of pneumatic drills [20]. Pneumatic drills require chilled water to cool the drill bit and the virgin rock, the chilled water also acts as a dust suppressor [82]. Figure 25 displays underground drilling of the rock face.

Figure 25: Deep level drilling [82]

Water Sprayers

Blasting produces significant dust, which can infect a human being's lungs and cause gold worker's pneumoconiosis (GWP) and chronic obstructive pulmonary (COP) disease [83]. Mines use chilled water sprayers to suppress the dust and cool the environment in order to allow mine employees to re-enter the section after blasting [84]. Chilled water is sprayed against the rock face to cool the virgin rock as seen in Figure 26.

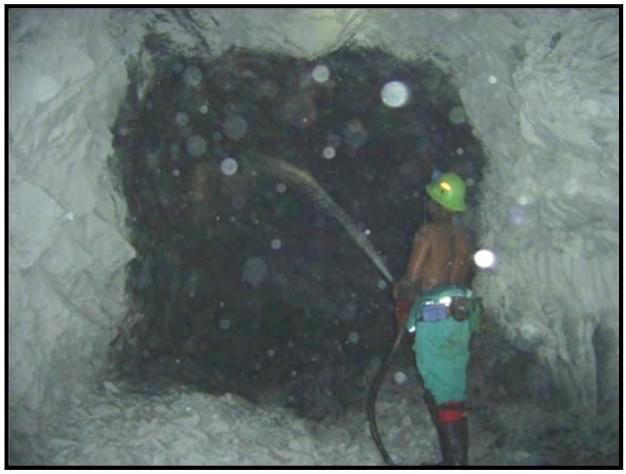

Figure 26: Deep level water spraying [82]

Water Canons

Blasting causes the rock face to deteriorate in different sizes of rock. The larger sized rocks are moved by hand or with a "bush-man". The smaller sized rocks are moved with the water cannons or water jets [82]. The water cannons use high-pressure chilled water to move the rock, whilst at the same time cooling the virgin rock face. Water cannons substituted the scraper winches [85], [86].

Figure 27: High pressure water cannons [87], [82]

Unintended chilled water consumers

The mine loses cooling through unintended chilled water consumers. Unintended water consumers can be identified as chilled water wastage and illegal miners using water. The unintended water consumers also increase the amount of water that needs to be pumped to surface.

Chilled water wastage can be summarised as negligent water wastage and water leaks. Negligent water wastage is when mine employees use chilled water for unintended purposes, and/or when the mine personnel neglect to close a chilled water valve.

Leaks are located on chilled and warm water pipe lines with faulty installation or corrosion. These leaks should be reported and repaired to prevent unnecessary water wastage. Deep level gold mines can reduce the amount of chilled water sent to underground by improving their water wastage management [72].

Illegal miners utilise the same mining method as the mine personnel between mine shifts or during December holidays. The chilled water is utilised for the same applications as the mine personnel, mining and cooling, only on a smaller scale.

Interpretation of chilled water consumers

Chilled water is one of the essential components of deep level gold mining. Without a cooling system, producing gold from deep level mines would be impossible. It is vital for mine management to emphasise the importance of reducing water wastage. A decrease in water wastage will have a direct impact on the mine's power consumption.

2.5. SIMULATION AND CONTROLLERS' BACKGROUND

A gold mine cooling and ventilation system is a complex system [15]. Maintaining the underground conditions below the crucial temperatures is a great challenge for the mining industry [88]. Utilising dynamic simulation software packages to analyse, evaluate and improve a mine's cooling and ventilation system will be beneficial to the mining when determining their optimal operation [30]. The simulation software has the capability to solve problems and enhance the performance of current installed cooling equipment. Properly validated simulation software can avoid occasional, dangerous and costly physical testing [30].

The simulation model has to include different equipment inputs and outputs to accurately simulate a dynamic cooling and ventilation system. The simulation has to include various equipment's physiological and physical properties, like; input and output temperature, mass flow rate, installed capacities, thermal flow, dam capacities, pipe sizes and equipment efficiencies [24]. The simulation software has to analyse all the different variables to predict what effect reconfiguring would have on a mine's cooling equipment's thermal performance and the mine's electricity consumption [23].

Simulation software is required to accurately simulate a mine's cooling and ventilation system [23]. An accurate simulation model will enable the researcher to determine the optimal reconfigured model through multiple iterations. The simulation software model should be able to adapt to various mine cooling and ventilation scenarios from the available data [23]. The majority of the South African mine's historical data storage capabilities are limited, therefore, the simulation model inputs should be kept to a minimum [21]. Complex simulation software will not appeal to the mining industry.

There is a whole range of simulation software packages available, capable of controlling or simulating either a component or the entire heating and ventilation system within different industries. A list of the software follows: ACSL, APROS, ARTIFEX, ARENA, AutoMod, C++SIM, ENVIRON, FLOWNEX, FluidFLow, Gepassi, GPSS, JavaSim, JavSim, KYPipe, MJX, MedModel, Multiverse, Network, OPNET Modeler, POSES++, POWERDOE, PowerSim, PTB, Quest, QUICKcontrol, REAL, REMS Fridge Plants, RTP ControlTM , SA Patent No. 2004/1172 by Temm International (Pty) Ltd, SCADA, SCFD, SHIFT, SIMAN, SimBank, SIMPLE++, SimPlusPlus, Simlat8, SMPL, SPICE, TIERRA, TRNSYS, U.S. Patents No 6366889 by Zalloom et al, 6178362 by Woolard et al and 5963458 by Cascia et

al, VUMA and Witness [17], [30], [31], [24], [89], [90], [91], [92], [93], [94], [95], [96], [97], [98], [99].

Historically the software available to simulate and control mine cooling and ventilation systems was limited. Therefore, researchers utilised building heating and ventilation software combined with other software to simulate mine ventilation and cooling [17], [30], [24]. Fortunately, the void has been filled and multiple software packages for controlling and simulating mines' cooling and ventilation systems have been developed. In this section, some of the available controlling and simulation software's applications will be discussed. The software's pros and cons will also be highlighted:

KYPipe

KYPipe is a steady state simulation software package. The software is a powerful hydraulic simulator, focusing on the distribution systems of air, chemicals, water, petroleum, refined products, refrigerant and more. The software is ideal to determine the system's optimal pipe configuration. The software is not capable of simulating a system in real time or implementing automatic control. The software is a steady state simulation, meaning it only simulates ideal situations and cannot determine how a system will react to certain errors or breakdowns.

Process Toolbox (PTB) SA Patent No. 2014/08034 by Temm International (Pty) Ltd. [100]

PTB is a dynamic simulation model based on mining components. PTB is coded in Visual Basic and utilises its own interface to simulate a mine system. PTB software has the capabilities to simulate a mine's cooling equipment, dewatering system and compressed air networks to determine optimal operation and predict possible power savings. The software is designed to balance mass flow and energy over certain intervals. Since the simulation is a dynamic solution, the system's reaction to certain changes or errors can be simulated within a certain time frame.

The simulation software requires the minimum input values to accurately simulate a mine's system. The required inputs are the variables commonly logged by mine SCADA systems, making it user-friendly. The software's accuracy has been validated by P. Maré and A.M. Holman [11], [23]. The simulation is ideal for simulating reconfiguration for optimal operation and to predict power consumption. The software does not allow real-time analysis or to stop and start equipment, but to optimise.

Real-time Energy Management System (REMS) Cooling Auxiliaries [97]

REMS was developed by Temm International (Pty) Ltd. There are different REMS packages that control different mine systems. REMS Cooling Auxiliaries (CA) is responsible for controlling a mine's cooling equipment. REMS is mainly utilised to control and monitor mine installed equipment at real time. REMS is installed on a server with large storage capacity enabling storing of important historical data of the equipment for future use. REMS can also be used to simulate a certain model system. It has been validated by successful implementation of load shift and energy efficient projects.

Supervisory control an data acquisition (SCADA) packages

A SCADA is the mine's centralised monitor and control system enabling the mine to control the entire mine's equipment via a remote connection in the mine's control room on surface. Fibre optic cable establishes the communication between the SCADA and the remote terminal units (RTUs) or PLCs. The RTUs and PLCs are near the controlled equipment. The SCADA can send a command to the RTUs and PLCs to start and stop a pump or to control a valve to alter the water flow or air pressure, whereas the RTUs and PLCs can send the following information to the mine's SCADA: pump warnings, pump status, dam temperature and dam level. The SCADA is able to save the information on a database.

The SCADA controls the PLCs through algorithms designed by the user. The user will be able to code a list of checks that the system should run through before a command can be sent out. SCADA can be used to control pump and refrigeration systems. The SCADA is not a user friendly program for new users and requires experienced and highly skilled personnel to do the coding for a mine's SCADA. There are only a few mine personnel capable of altering the SCADA's code. SCADA development is generally done by externally contracted companies.

SCADA software cannot optimize the system as it does not have the capability to solve complex calculations or perform simulations. This means determining the feasibility of a load shifting project by means of a SCADA program is impossible. Implementing such a project without proper simulations can lead to injuries, damage and high cost. Wonderware InTouch, Adroid and WinCC are all different developers of SCADA software.

U.S. Patent No. 5963458 by Cascia et al [95]

The US patent No 5963458 controls a component within a cooling, ventilation or hoisting system. It utilises a digital controller to calculate in real time the component's ideal setpoint for optimal energy consumption. This patent cannot be implemented on an integrated system. The patent also only focuses on energy efficiency and does not consider the possibility of a load shift [93].

U.S. Patent No. 6178362 by Woolard and U.S. Patent No.6366889 by Zalloom et al [96]**.**

U.S. patents No. 6178362 and No. 6366889 utilise internet-based communication to analyse the user's energy consumption trends in real time. This patents claim the patent will be able to identify costing and operational errors within a system. The patent can be applied to HVAC systems in buildings, mines and industries. The patent is not automated as the simulation results and answers are once-off from where the applicable changes have to be implemented [93].

Ventilation of Underground Mine Atmospheres VUMA [36]

VUMA is a mine modelling tool for water network and is a subdivision of the registered name Coolflow®. The software is able to simulate a complex water-cooling and ventilation system. The software is able to simulate the effect changes to the chilled water temperature and mass flow have on the production zone, it includes the chilled water dam and predicts the system losses through a mine network quantified per component. The system was utilised in the design of Mponeng mine, the world's deepest mine [18].

Coolflow® is only a simulation tool with the ability to accurately optimize the system. The software cannot automatically control the mine's system. The software is extremely complex and requires substantial information, as well as properly trained and qualified personnel to obtain accurate results.

Interpretation of Simulation Software

There are many different simulating and controlling software packages available on the market, each of them being ideal for its specific application. Choosing the correct simulation software and utilising it to its maximum capabilities will ensure the optimal results. It is not necessarily the best solution to have a simulating and controlling software in one package.

Combining two different software packages to simulate and control the system will end in optimal results.

2.6. CONCLUSION

It is evident from the research that there is significant power consuming equipment on a mine's cooling system responsible to maintain acceptable underground mining conditions and ensure maximum productivity from mineworkers. Most of the equipment forms part of a subsystem within the cooling system. These systems are outdated and maintenance is mandatory. The equipment is often maintained without considering the effect the maintenance procedure has on the plant's efficiency.

An overview of all the equipment and their layouts that form part of a cooling system was discussed. The equations used to determine the components' efficiencies were identified. The chilled water consumers were discussed and the minimum underground working conditions were identified.

It is concluded that it is necessary to investigate the reconfiguration of mine cooling auxiliaries for optimal operation and possible cost savings. It is important to identify the specific mine's minimum allowable outputs. The study will focus on providing the maximum required service delivery from the installed equipment from minor reconfigurations. The control will then be adjusted to provide the minimum required service delivery and lastly the most efficient control philosophy will be determined.

Chapter 3. METHODOLOGY

KJ Oberholzer

"Our greatest weakness lies in giving up. The most certain way to succeed is always to try just one more time." – Thomas A. Edison

3.1. INTRODUCTION

The mine's main focus and priority is to maintain their maximum productivity whilst ensuring the safety of their employees [15]. This should not be affected when reconfiguring the mine's cooling system for optimal operation. The current service delivery of the cooling systems should not be degraded by the reconfiguration interventions [101].

Cooling equipment on gold mines is old and maintenance thereof is compulsory [23]. However, the maintenance solution often neglects to consider what effect the specific solution will have on the entire cooling system's performance. These maintenance solutions are often implemented and not properly recorded, causing the new employees to be uninformed. Identifying these components will create an opportunity for reconfiguration. The most elegant and robust solutions for mine cooling systems are often obtained from simplifying the operations [21]. Figure 28 represents a universal methodology for investigating the possibility of reconfiguring a mine's cooling auxiliaries for optimal operations.

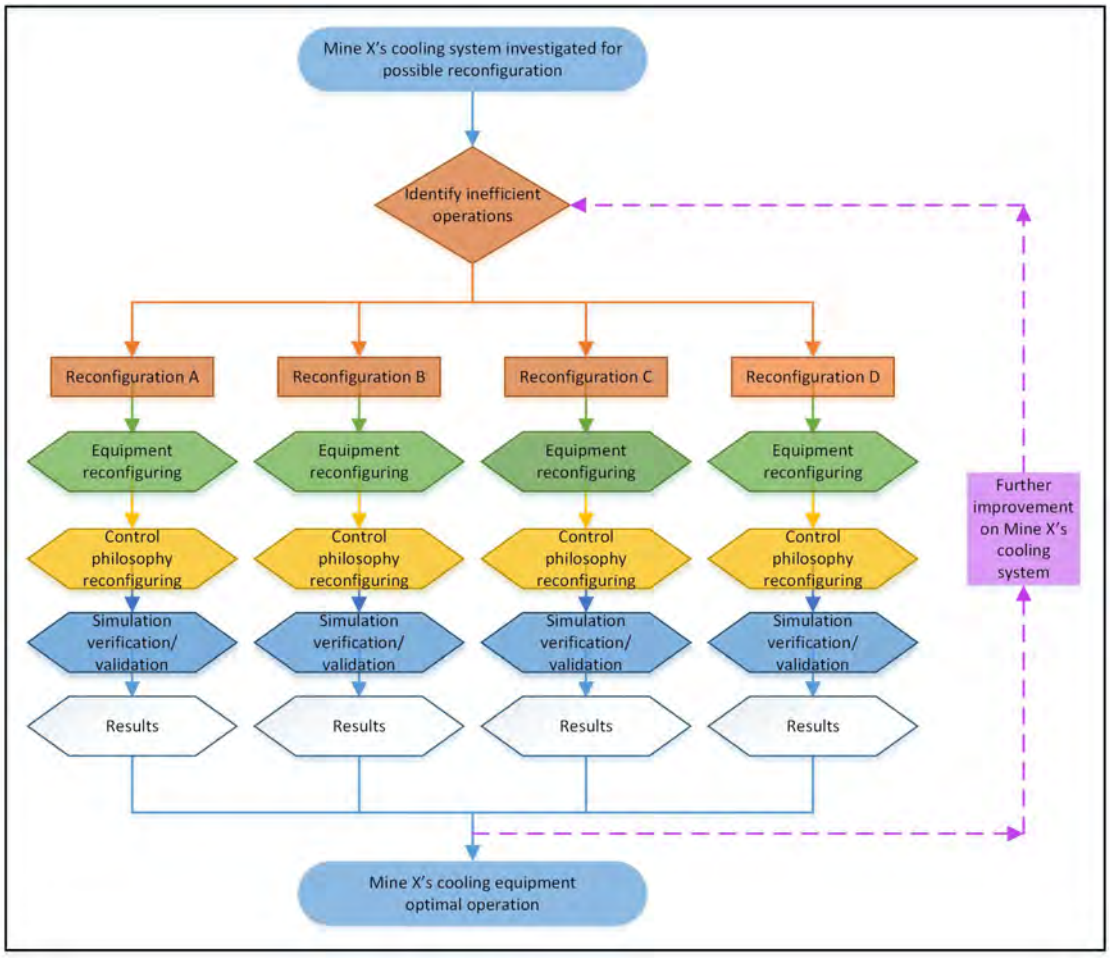

Figure 28: Universal approach for reconfiguring a mine's cooling auxiliaries for optimal operations

The universal approach is applicable to a mine's entire cooling system to help identify the inefficient subsystems. The identified inefficient subsystem can be optimised by following the progressive guide lines. Each of these guidelines will be explained in the following section.

3.2. UNIVERSAL RECONFIGURATION STRATEGY

Identifying Inefficient Operations

The reconfiguration will focus on reconfiguring the identified inefficient cooling subsystems to improve the cooling system efficiency. Figure 29 depicts the procedure to identify the inefficient equipment.

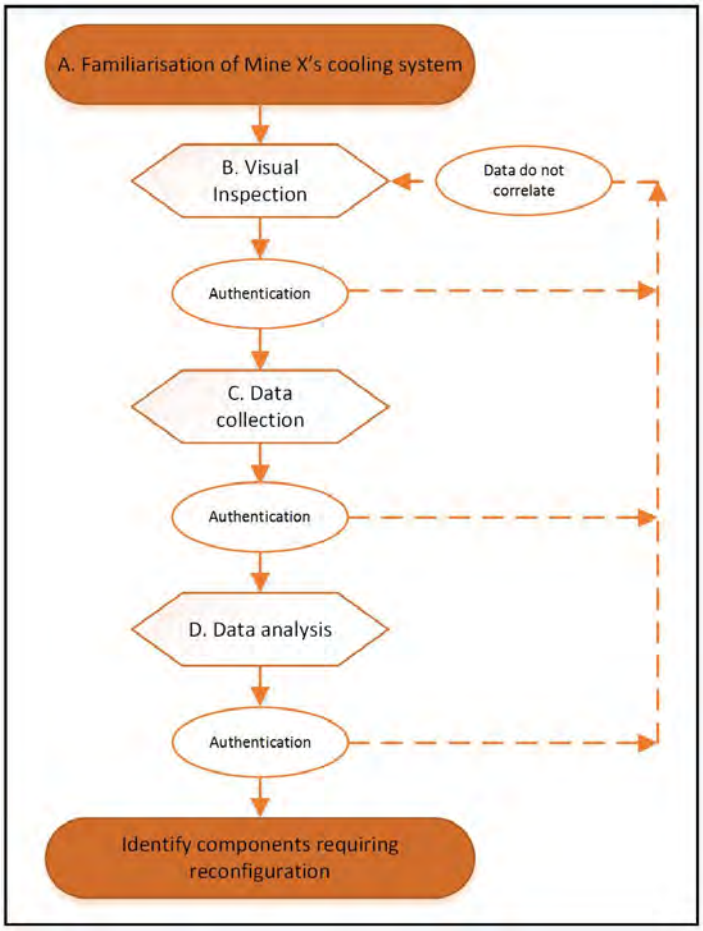

Figure 29: Identification of inefficient equipment process

From Figure 29 it is evident the process to identify the inefficient cooling subsystems is divided into three steps. After each step the data is authenticated. If the new data does not correlate with the previous collected data, the process should be repeated until the correct

data is obtained and the data correlates with one another. Each of the steps will be discussed below.

A. Familiarisation of mine's the cooling system:

It is important when investigating cooling systems for possible reconfiguration to be familiar with the site. This can be done through a site visit where one will walk through the plants, have verbal discussion with experienced mine personnel or scrutinise a cooling auxiliary layout drawing. Experienced mine personnel will be able to describe the system's OEM design specifications. Each mine's cooling system is unique and differs to suit the mine's requirements. When familiarising oneself with the mine's cooling system it is important to establish which components are installed at the mine and the installed capacity, quantity and layout thereof.

If the mass flow or temperatures are not electronically logged, a manual measurement will be able to provide an estimated value or expected value. It is important to ensure that the mine is satisfied with their current operating conditions. If the mine is not satisfied with their current operation, the reconfiguration could possibly include the improvement of the cooling system. An example of a data sheet that is utilised to gather the required data from a mine to do a proper simulation can be found in Appendix A.

B. Visual Inspection:

The site visit will allow visual inspection of the cooling auxiliary components. The old and poorly maintained components can easily be identified. The cooling system's technicians will be able to provide the components' breakdown intervals and maintenance mind-sets. Components experiencing regular breakdown can easily be identified as inefficient components that require reconfiguration.

C. Data Collection:

The cooling system's information is often logged. Mines with state of the art upgrades will be able to provide data logged in 2 minute intervals. Mines with older technology might have hourly log book data available. These data items are processed into a 24 hour profile. If temperature data is missing, temporary temperature probes can be installed.

D. Data Analysis:

The collected data is used to analyse the cooling subsystem. Inefficient subsystems are identified as systems utilising too much power for the output service delivery, or subsystems utilising too much chilled water for the cooling produced. The inefficient subsystem is analysed to determine the cause of the inefficiency.

Cooling equipment physical reconfiguration

The cooling components that require reconfiguration were identified in the preceding section. There are many different improvements available. Ensuring the optimal reconfiguration is selected will be done by following the process diagram displayed in Figure 30. After each step the solution is analysed to determine the feasibility thereof. If the solution is impractical the process is repeated until the optimal solution is obtained.

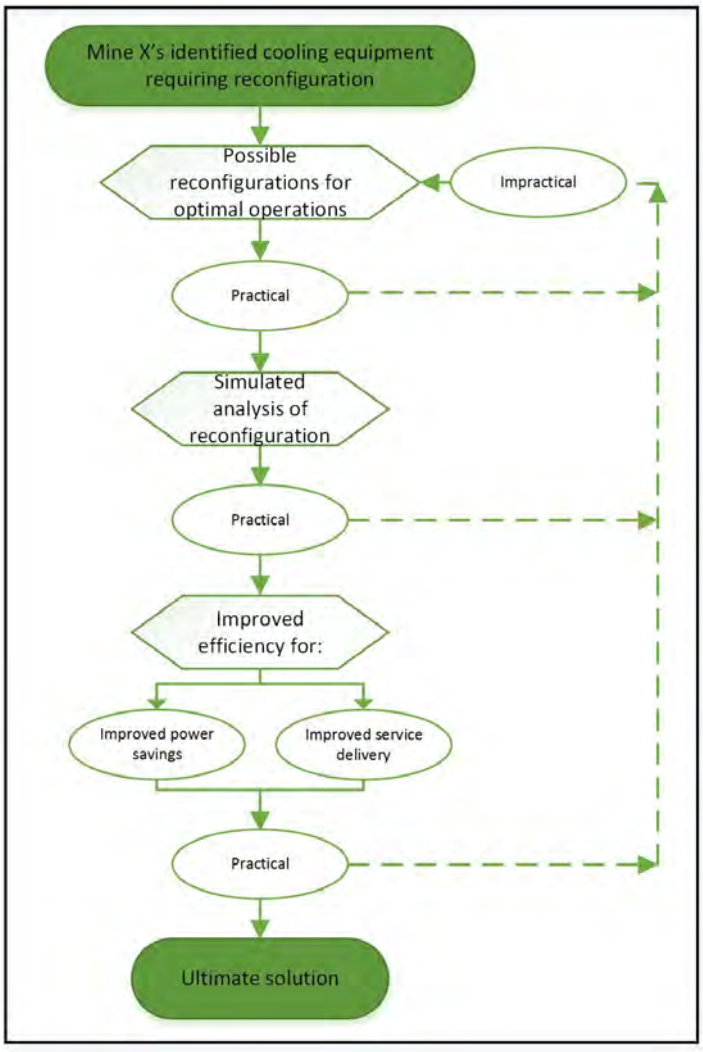

Figure 30: Determining the optimal physical reconfiguration process

Figure 30 depicts the improved reconfigured initiatives that will be simulated to determine the effect the reconfiguration will have on the entire system. It will be redundant to reconfigure a cooling subsystem and in return negatively affect the service delivery of the entire cooling system. The reconfiguration with an improved efficiency will either realise in an increased power saving or improved service delivery. It is all dependent on the selected control philosophy and the desired setpoint temperatures.

Control philosophy reconfiguration

The reconfigured cooling components will require a control philosophy update. The updated control philosophy should remain within the component OEM design specification to prevent the component's efficiency from degrading over time. The control philosophy update will not only include the reconfigured components but will consider the entire cooling system's control philosophy. The updated control philosophy will ensure that the new and old equipment is synchronised with one another for optimal operations. Figure 31 represents the procedure followed to determine the optimal control philosophy for the cooling system with the newly reconfigured equipment.

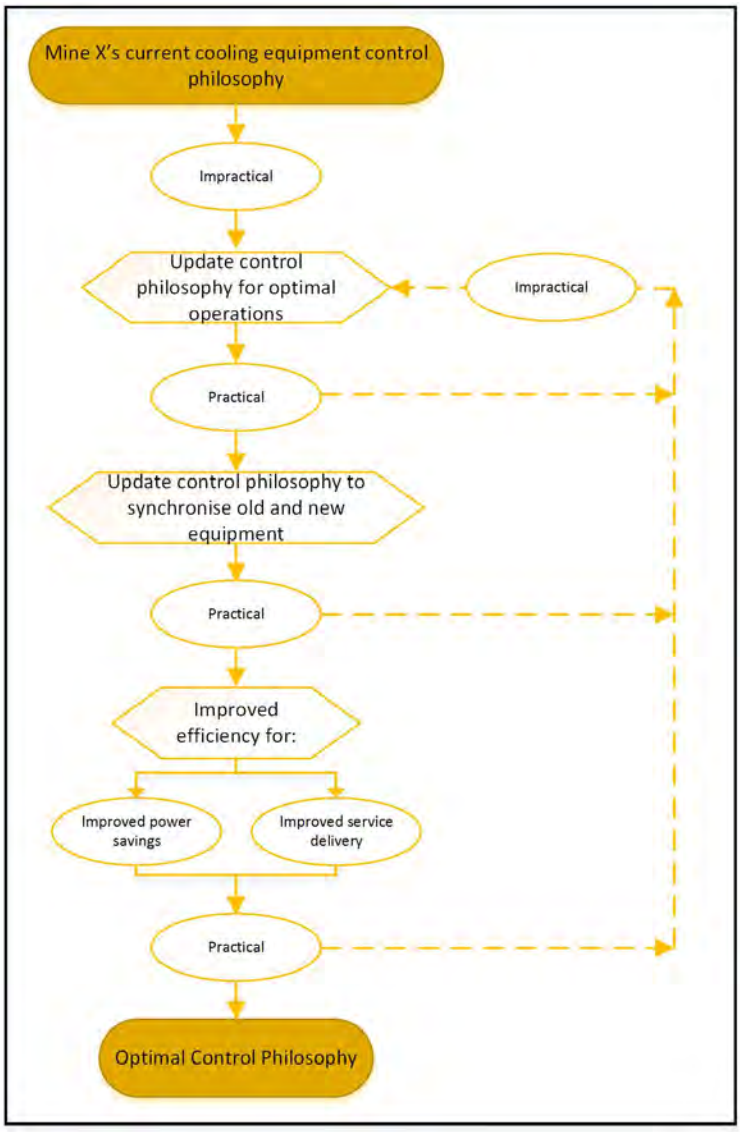

Figure 31: Determining the optimal control philosophy process

From Figure 31 it is evident that, firstly the optimal control philosophy will be determined for the reconfigured subsystem. Multiple iterations will be simulated until the optimal control philosophy is determined. Secondly, the simulation will then include the entire cooling system to ensure the new equipment is synchronised with the old equipment until the optimal control philosophy for the entire cooling system is obtained. The control philosophy will ensure optimal operation from the cooling system. Depending on the mine's required setpoint temperature, the reconfiguration will either result in reduced power consumption or improved service delivery of the cooling system.

As soon as the optimal reconfiguration is obtained with the most suitable control philosophy, the reconfiguration will be implemented. Each reconfiguration will be simulated and implemented individually to determine the individual effect of the reconfiguration.

Simulation Validation

A simulation model has to be developed to determine the feasibility of component reconfiguration on the cooling systems and the maximum service delivery thereof. Different simulation software packages have been identified and their capabilities have been investigated in section 2.5. Process Toolbox (PTB) has been identified as the most appropriate simulation software for this study. PTB is capable of accurately simulating a mine's cooling system and is able to predict the power utilised by the cooling equipment. PTB software has been utilised and validated on mines' cooling systems by preceding researchers Maré and Holman [11], [23]. Figure 32 represents the simulation process to develop an accurate simulation model and accurately determine the realised power savings.

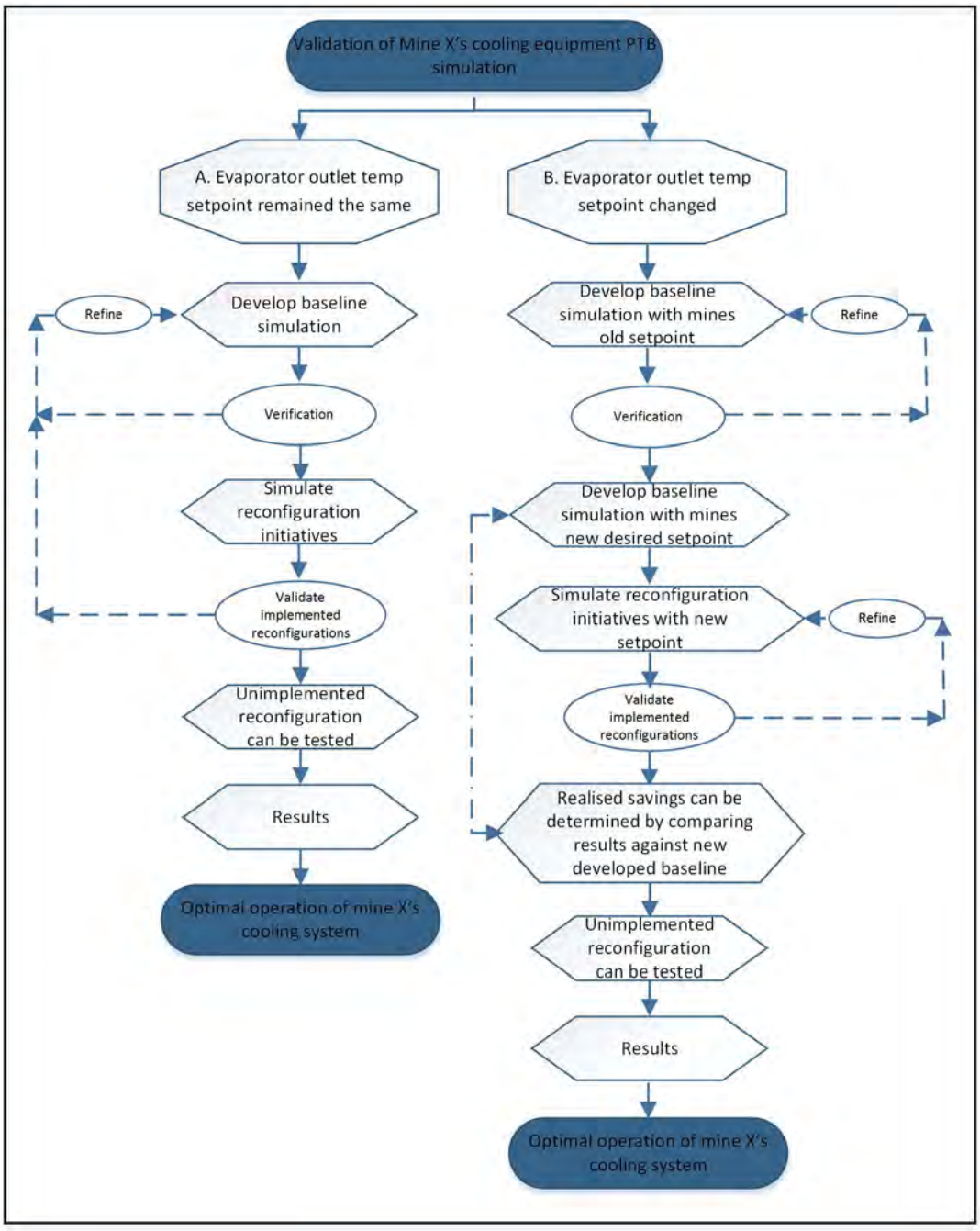

Figure 32: Simulation validation process

Figure 32 indicates that there are two scenarios for developing an accurate simulation model. The first scenario is when the mine's evaporator outlet water temperature remained unchanged. The second scenario is for when the mine changed their desired evaporator outlet water temperature. The realised power savings cannot be determined accurately if a mine changes their desired evaporator outlet water temperature to deliver an improved service delivery. The mine's cooling equipment will utilise more power to meet the increased

chilled water demand. Therefore, a new baseline has to be developed to accurately determine the power saving that will be realised.

A. Evaporator outlet water temperature setpoint remained unchanged

Should the mine be satisfied with their evaporator outlet water temperature, their current operation before implementing reconfiguration will be considered as the baseline. The cooling system will be simulated on the PTB software package and validated against actual data. The simulation development will be iterated until the simulation is as close to the actual results as possible.

The physical reconfigurations will be simulated to obtain the cooling system's ideal operation with the optimal control philosophy. The reconfiguration will be implemented on a case study to obtain the actual results. The reconfigured simulation will then be validated to determine the simulation accuracy. The simulation should prove an acceptable accuracy. If the validation proves that the simulation is not accurate, the simulation will be iterated with the additional data until the baseline and implemented simulation correlate with one another. All the cooling subsystems should be validated. With a validated simulation, additional reconfigurations can be tested on the simulation. The simulation results of the additional reconfigurations can then be considered as accurate as the simulation will be validated with actual data.

B. Evaporator outlet water temperature setpoint changed

If the mine changes the required evaporator outlet temperature, a new baseline simulation has to be develop. An improved service delivery cannot be claimed if the evaporator setpoint was reduced. Furthermore, inaccurate power savings will be claimed if the improved system is compared against a baseline with a different evaporator outlet setpoint. If possible, the mine should change their evaporator outlet water temperature setpoint to the new desired setpoint for at least three months during the summer period before the project is implemented. This will ensure that the mine's cooling system's performance is accurately determined under the new evaporator outlet water temperature setpoint to develop an accurate baseline. This will allow the researcher to use the prescribed method of simulation.

If it is not possible to change the evaporator setpoint due to the fact that installation of the new equipment has commenced, or it is during an unfavourable season, the following method will be applied. A baseline simulation will be developed from the available data. The simulation will be validated with the mine's current available evaporator outlet water

temperature setpoint. The simulation will be refined through an iterative process until an accurate simulation model has been developed.

A new baseline will be developed with the evaporator outlet temperature set to the new desired setpoint. This will ensure the correct improved service delivery and power savings are accounted for. The proposed initiatives will be simulated to determine the optimal reconfiguration and control philosophy. The proposed solution will be implemented on a case study. The reconfigured simulation will be validated on a case study to determine the simulation's accuracy. If the simulation proves to be inaccurate, the baseline simulation will be updated with the new complete data until the simulation is sufficiently validated. All the various subsystems have to be validated in order to test additional reconfigurations on the simulation model. If the mine does not implement the suggested reconfigurations, the simulation values can be considered as accurate as the simulation was validated with the implemented reconfiguration.

3.3. SIMULATION

Mine A's cooling system setup

Mine A is situated in the Free State and can be considered as a large mine. The installed cooling capacity of mine A's cooling system is 12 MW. The mine was established in 1985 and can be considered as an old mine. Figure 33 is a schematic representation of mine A's refrigeration and mining level layout.

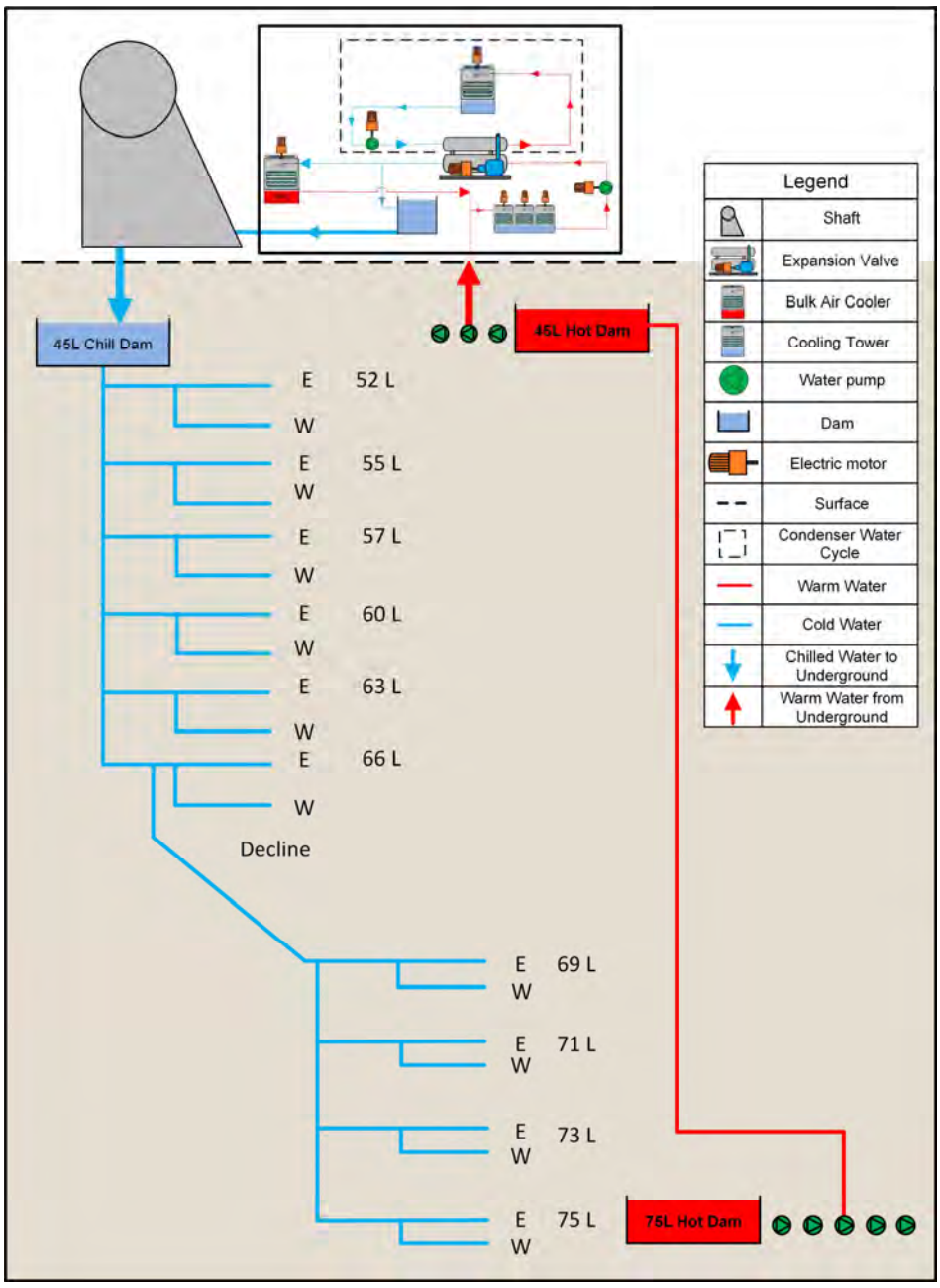

Figure 33: Mine A's refrigerant location and mining levels layout

FPs are utilised to cool the warm mining water from underground [23]. Mine A utilises four surface FPs in parallel as it is the most cost effective method to cool their water for underground mining applications. Figure 33 represents mine A's mining levels and illustrates that the levels stretch from 52 L at 1 585 m up to 75 L at 2 286 m underground, with the decline starting after level 66 L at a depth of 2 012 m. Figure 34 is a visual representation of mine A's cooling layout situated on surface.

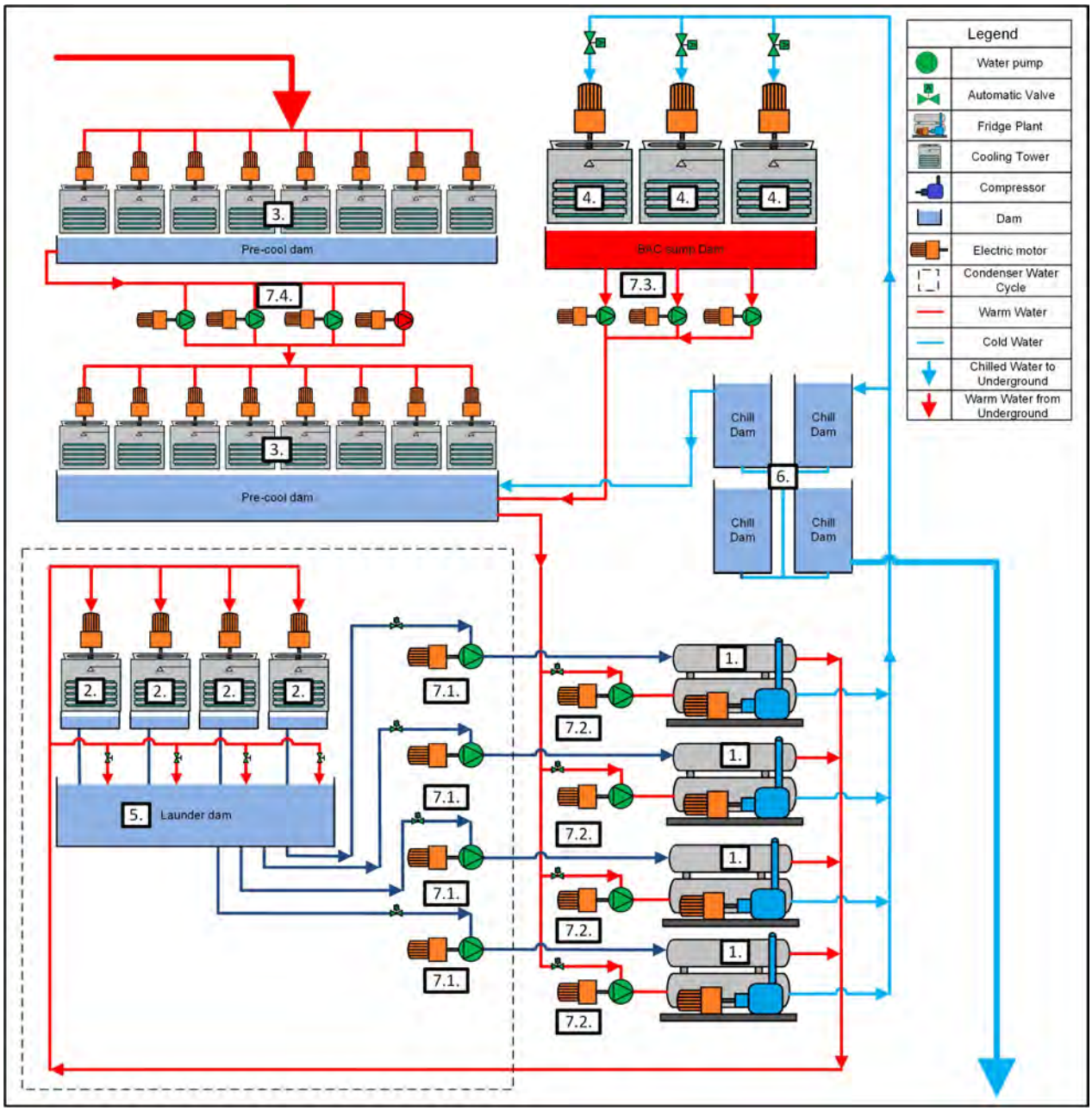

Figure 34: Mine A's refrigeration system's layout

Figure 34 depicts that mine A's cooling system consists of the following components:

1. Four surface FPs in parallel;
2. Four condenser cooling towers;
3. Two stage evaporator cooling towers each consisting of eight cooling towers;
4. Three BAC's;
5. Launder dam;
6. Four chill dams;
7. Pumps;
   7.1 Four condenser pumps each in series with a FP;
   7.2 Four evaporator pumps each in series with a FP;
   7.3 Three BAC sump pumps;
   7.4 Four pre-cooling pumps;

The FPs' chilled water is stored in the chill dams. From the chill dams the chilled water is distributed to the different users; underground, BACs and recycled chilled water. The recycled chilled water and BAC return water is dumped in the pre-cooling tower second stage dam in front of the FP inlet. This is to reduce FPs' inlet water temperature as the BAC return water is colder than the water from the second stage pre-cooling towers.

Simulation assumptions

Certain variables have to be defined in order to develop an accurate simulation model. The water flowing from underground into the cooling system and the water flowing to underground from the cooling system is assumed constant at the average water flow of 370 ℓ/s.

The pre-cooling towers and condenser cooling towers utilise atmospheric air to reduce the cooling system's water temperature. The BACs cool the ambient air before the air is sent to cool the underground mining environment. Since there is unlimited air in the atmosphere, mines do not measure the amount of air-flow through the towers. The ambient air temperature is however recorded at the majority of the mines. The simulation software requires an airflow in order to solve the simulation; therefore, the assumption will be made that the air-flow through the pre-cooling towers and the BAC is equal to the water flow

through the respective towers and the condenser cooling towers' air-flow is 70% of the water flow through the condenser cooling tower [3].

The simulation will be verified by using the daily average ambient psychrometric condition for three summer months in the simulation. These conditions will be used throughout the verification process up to a point where the simulation can be validated. The simulation will then be validated by changing the simulation ambient psychrometric conditions and component statuses to correspond with the properties of one specific day. This will ensure the simulation is validated under the same conditions.

Simulation inputs and layout

The simulation software has different components available to the user. The different components for a system are added to the simulation worksheet and connected with different pipe-node configurations to form the simulation model. The simulation software allows the user to simulate an entire cooling system, part or section of the cooling system. This enables the user to conduct a study on a specific sub-system to optimise the operation. The optimised sub-system can then be added to the cooling system simulation to determine what effect the optimisation had on the other components.

The simulation can also be simplified for a "quick" simulation to obtain results with acceptable accuracy. The user can replace four FPs with a single FP with the installed capacity of all four FPs added together. The simulation will use average or manifold water temperatures and total flow values for the simulation. For the purpose of this dissertation a full simulation model will be developed to evaluate the components individually and ensure best simulation accuracy as far as possible.

The cooling system's simulation will be developed by partially simulating all the component in the different cooling subsystems. The simulation will be iterated until the simulated subsystem reacts to the ambient variables as the actual cooling subsystem does. As soon as all the subsystems have been verified, the subsystem simulation will be added together to form the simulation model of the mine's entire cooling system. Figure 35 is a visual representation of mine A's pre-cooling towers' simulation in PTB.

[3] Deon Arndt Partner of Enoveer Engineering Innovation

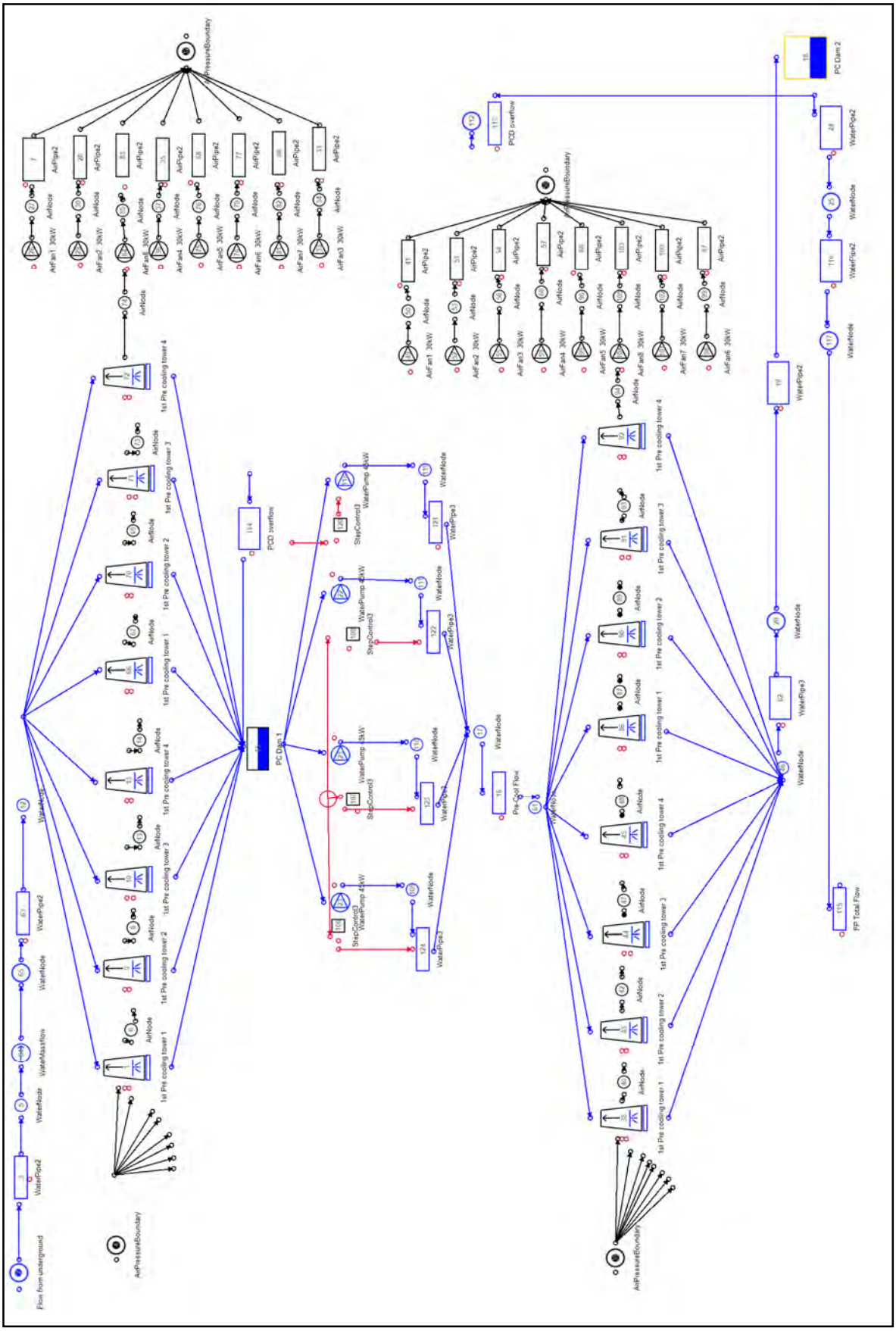

Figure 35: PTB simulation of mine A's pre-cooling towers

The two stage pre-cooling towers include 16 pre-cooling towers, 16 pre-cooling tower fans, 4 transfer pumps and 2 pre-cooling dams. The information required to accurately simulate the pre-cooling of mine A's cooling system is stipulated in Table 4.

Table 4: Pre-cooling tower information required for PTB simulation

Pre-Cooling Towers			
Requirement	**Unit**	**Value**	
		First Stage	**Second Stage**
16 Water-Air Cooling Towers			
Barometric Pressure	kPa	87.23	87.23
Water inlet Temp	˚C	25.1	18.5
Water Outlet Temp	˚C	18.5	17.07
Water Flow	ℓ/s	50	50
Air Inlet Temp	˚C	21	21
Air Inlet Relative Humidity	%	42.24	42.24
Air Flow	kg/s	50	50
16 Air Fans			
Fan Motor Power	kW	30	30
Fan Flow	kg/s	50	50
Fan Motor Efficiency	%	90	90
Fan Efficiency	%	90	90
Fan inlet Pressure	kPa	87.23	87.23
Fan Inlet Temp	˚C	21	21
2Water Dams			
Inlet Temp (Pre-Cooling)	˚C	18.5	17.07
Inlet Temp (BAC)	˚C	-	11.36
Inlet Temp (Recycle)	˚C	-	5.6
Outlet Temp	˚C	18.5	13.58
Flow (Pre-Cooling)	ℓ/s	400	400
Flow (BAC)	ℓ/s	-	399
Flow (Recycle)	ℓ/s	-	201
Ambient Temp	˚C	21	21
Heat Transfer Coefficient	$kW/m^2/˚C$	0	0
Volume	m^3	5000	5000
4 Pre-Cool Transfer Pumps			
Pump Motor Power	kW	45	
Pump Flow	ℓ/s	200	
Pump Motor Efficiency	%	95	
Pump Efficiency	%	95	
Pumping Elevation	M	0	

The outlet water temperature of the second pre-cooling dam is less than the water out of the second stage pre-cooling towers. This is due to a water air pre-cooling tower cannot reduce the water temperature lower than 2ºC below ambient WB temperature[4]. This temperature is however above the FPs designed inlet water temperature. Therefor the BAC return water and the recycled chilled water is dumped into the second stage pre-cooling dam. This lowers the second stage pre-cooling dam temperature which ensures that the FPs are supplied with their design inlet water temperature.

The BAC return water is 11.36ºC and enters the second stage pre-cooling dam 5.71ºC below the outlet water temperature of the second stage pre-cooling towers. The water flow from the BACs are 399 ℓ/s. Cooling will be wasted if the BAC return water is dumped with the warm water from underground since the water can only be cooled up to 2ºC below the ambient WB temperature.

Mine A's pre-cooling towers and the BAC return water is inadequate to lower the water temperature down to the FPs design inlet water temperature. This causes the FPs to be unable to lower the water temperature down to the required FPs outlet water temperature. The mine then recycles some of the cooled FP outlet water with the water in the pre-cool dam two. The recycled chilled water enters the second stage pre-cool dam at 5.6ºC, 11.47ºC below the outlet water temperature of the second stage pre-cooling towers. 210ℓ/s of chilled water is being recycled.

The simulation of the pre-cooling towers will be iterated until the simulation outputs correlate with the actual values. As soon as the simulation proves to be within an acceptable range of the actual values, the next subsystem is added to the simulation. Mine A's FPs, condenser and evaporator cycle will be added next. Figure 36 represents the PTB simulation of the FPs, evaporator pumps, condenser pumps and chill dam.

[4] Deon Arndt Partner of Enoveer Engineering Innovation

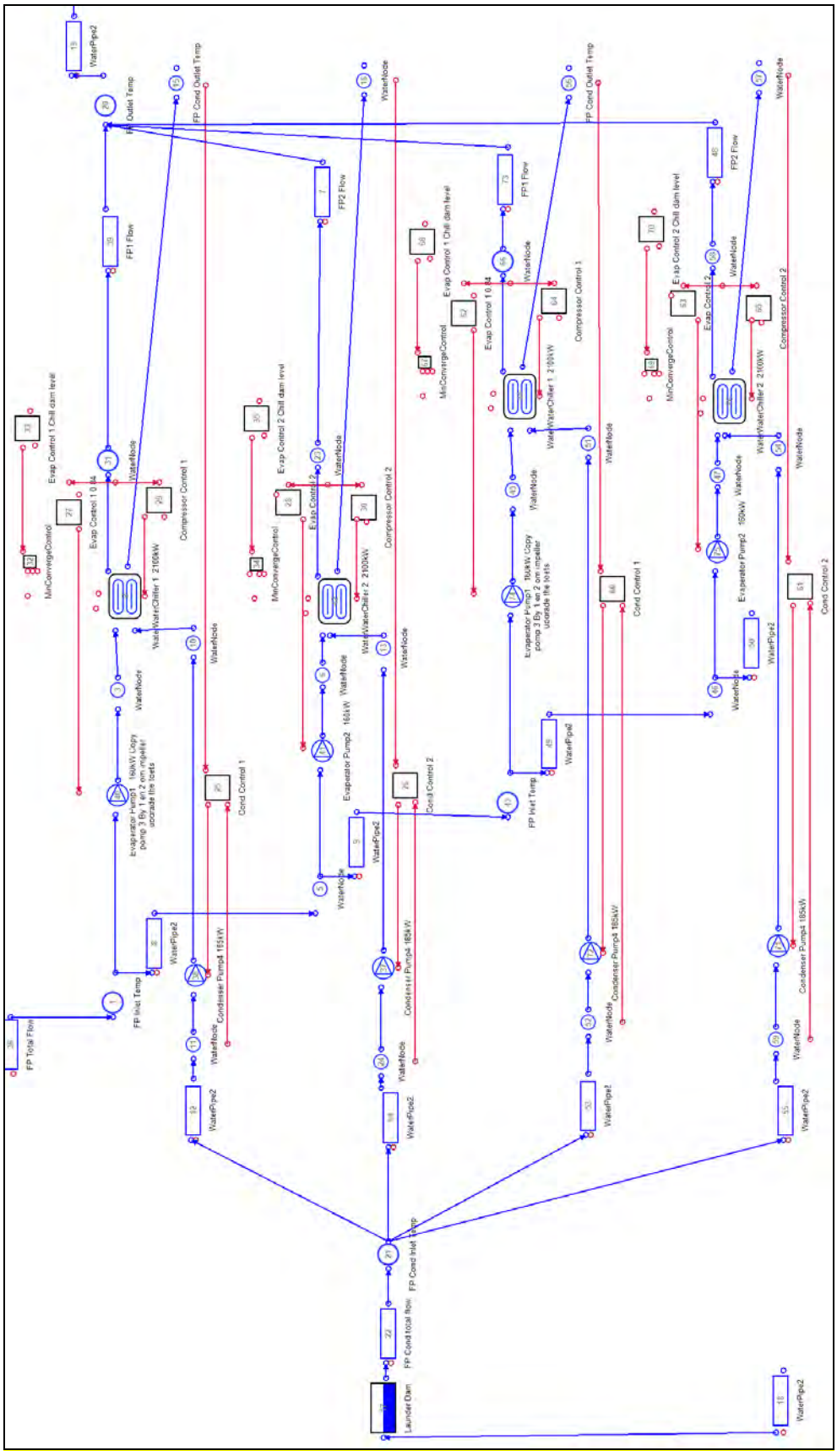

Figure 36: PTB simulation of mine A's FPs

Mine A's cooling system consists of four FPs in parallel. Each of these FPs has their own condenser and evaporator pump in series with the FPs. The evaporator water enters the FPs from the second stage pre-cooling dam. The FPs cool the water and store the chilled water in the chill dam before it is distributed to the various chilled water consumers. The PTB simulation was developed accordingly.

The FPs cannot be simulated without the condenser cycle. The condenser cycle will be discussed next. Table 5 represents all the information required to accurately develop a PTB simulation of mine A's FPs and the evaporator cycle.

Table 5: FPs information required for PTB simulation

Fridge Plants		
Requirement	**Unit**	**Value**
4 Fridge Plants		
Evaporator Outlet Temp	˚C	5.5
Evaporator Inlet Temp	˚C	15.32
Evaporator Flow	ℓ/s	250
Condenser Outlet Temp	˚C	31
Condenser Inlet Temp	˚C	26
Compressor Motor Power	kW	2100
Condenser Flow	ℓ/s	540
4 Evaporator Pumps		
Pump Motor Power	kW	160
Pump Flow	ℓ/s	250
Pump Motor Efficiency	%	95
Pump Efficiency	%	70
Pumping Elevation	m	0
Fan Inlet Temp	˚C	21
1 Chill Dam		
Inlet Temp	˚C	5.5
Outlet Temp	˚C	5.6
Flow (Underground)	ℓ/s	400
Flow (BAC)	ℓ/s	399
Flow (Recycle)	ℓ/s	201
Ambient Temp	˚C	21
Heat Transfer Coefficient	kW/ m^2/˚C	0
Volume	m^3	2000

The PTB simulation cannot solve the FPs' simulation without a condenser cycle. Figure 37 is a visual representation of mine A's condenser cooling towers developed in the PTB simulation software.

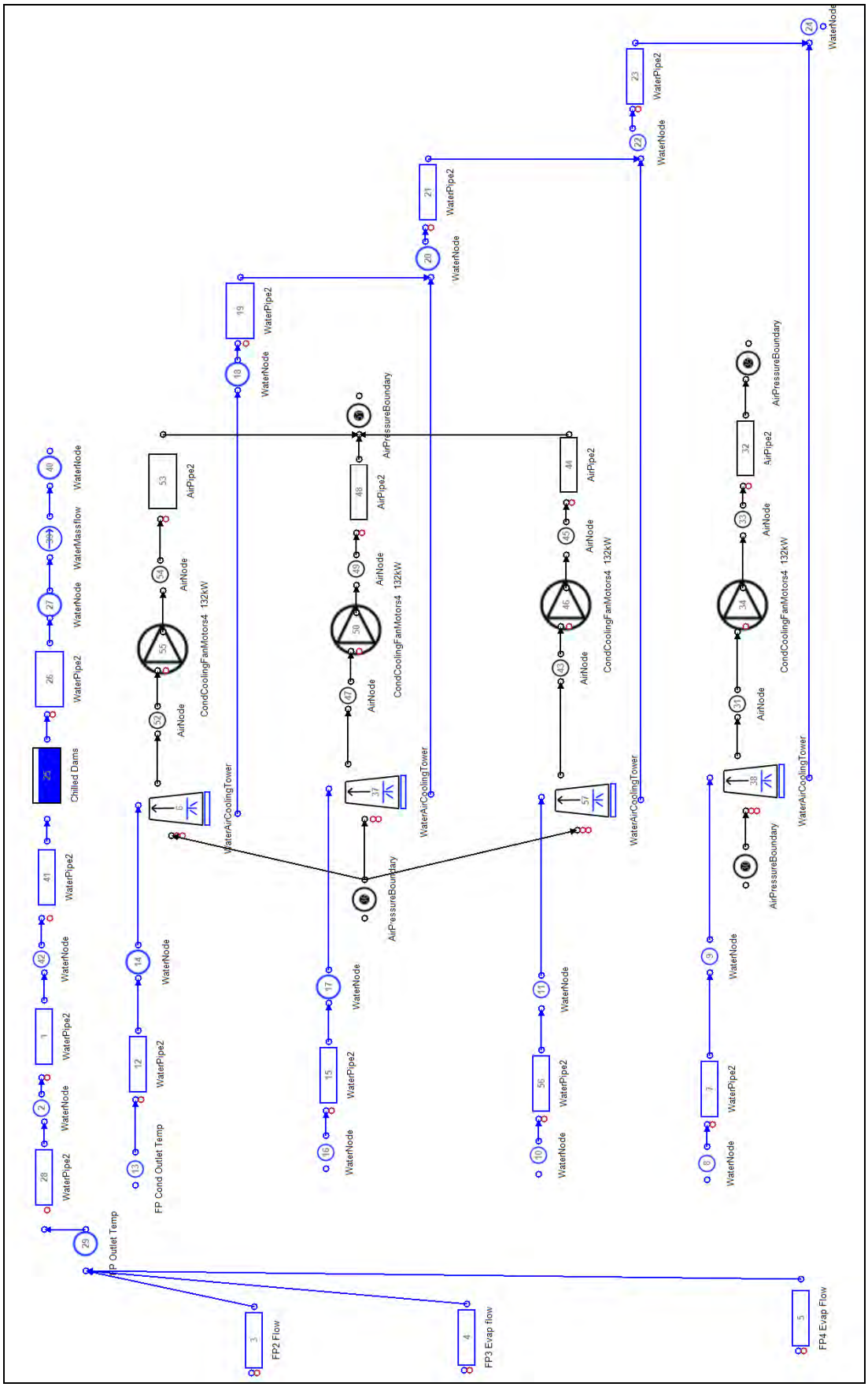

Figure 37: PTB simulation of mine A's condenser cycle

Mine A's four condenser pumps pump the water through the FPs' condenser vessels and the condenser cooling towers. Each condenser pump pumps the condenser water through its own condenser cooling tower. The cooled condenser water is gathered in a launder dam to ensure the correct condenser inlet water temperature is maintained. Table 6 represents the information required to accurately develop the PTB simulation of mine A's condenser cooling towers.

Table 6: Condenser cycle information required for PTB simulation

Condenser Cycle		
Requirement	**Unit**	**Value**
4 Condenser Pumps		
Pump Motor Power	kW	185
Pump Flow	ℓ/s	420
Pump Motor Efficiency	%	95
Pump Efficiency	%	75
Pumping Elevation	m	0
4 Condenser Cooling Towers		
Barometric Pressure	kPa	87.23
Water Inlet Temp	˚C	31
Water Outlet Temp	˚C	26
Water Flow	ℓ/s	420
Air Inlet Temp	˚C	21
Air Inlet Relative Humidity	%	42.24
Air Flow	kg/s	252
4 Air Fans		
Fan Motor Power	kW	132
Fan Flow	kg/s	252
Fan Motor Efficiency	%	90
Fan Efficiency	%	75
Fan inlet Pressure	kPa	87.23
Fan Inlet Temp	˚C	21
1 Launder Dam		
Inlet Temp	˚C	26
Outlet Temp	˚C	26
Flow	ℓ/s	1680
Ambient Temp	˚C	21
Heat Transfer Coefficient	$kW/m^2/˚C$	0
Volume	m^3	5000

The pre-cooling towers, FPs with the condenser and evaporator cycles will be developed with the PTB simulation software. The FPs, condenser and evaporator cycles will be iterated

until their information correlates with the actual data. The BAC is the final subsystem that will be added to the simulation model in order to accurately simulate mine A's cooling system. Figure 38 represents the PTB simulation of mine A's BACs.

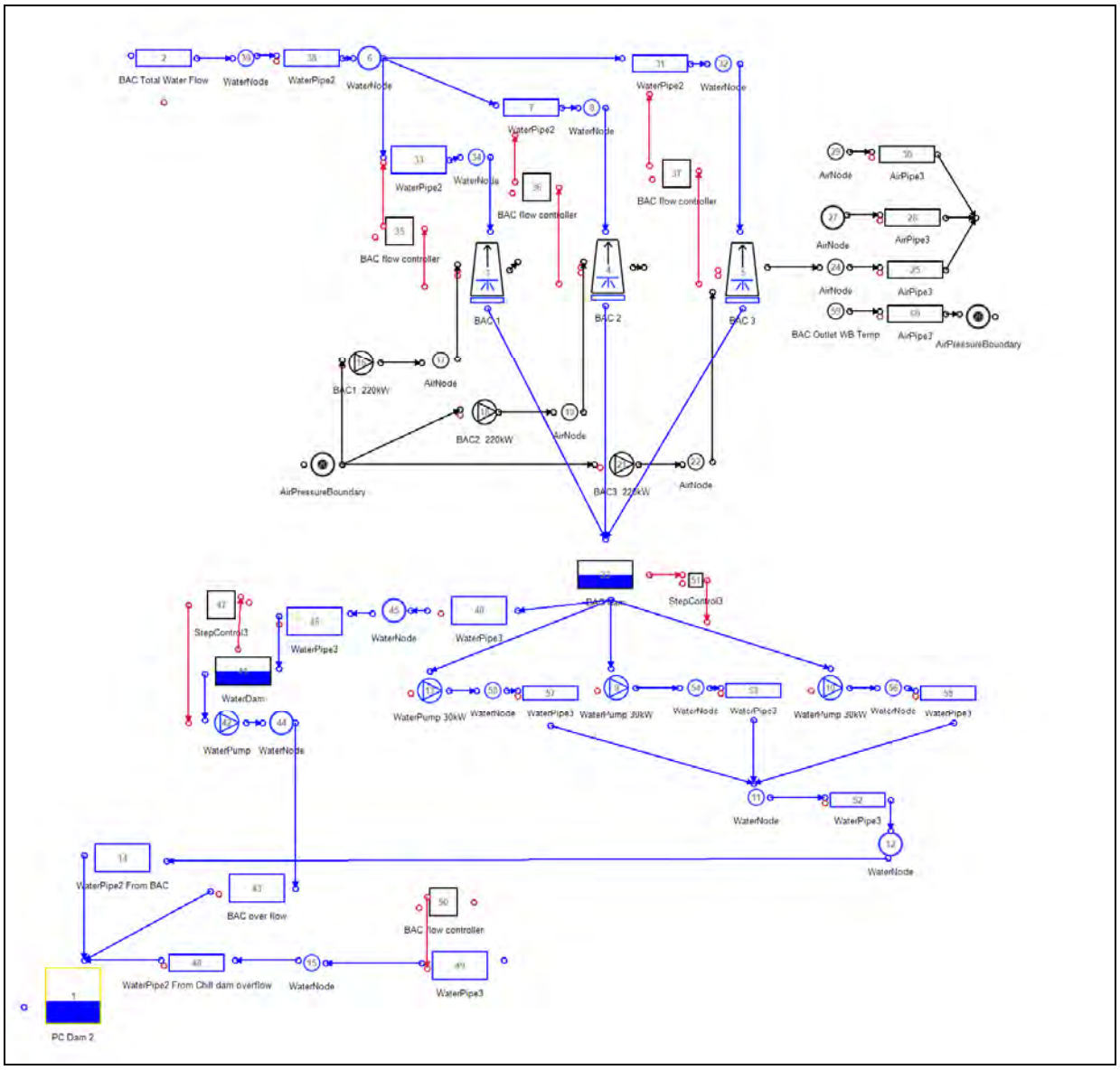

Figure 38: PTB simulation of mine A's BACs

Mine A's BACs consist of a three chamber BAC with three fans. The BAC has one sump dam. Three valves at the BAC inlet maintain a constant inlet chill water flow of 133 ℓ/s into each of the BAC chambers. Three BAC pumps are responsible for returning the BAC outlet water to the second stage pre-cooling dam. The BAC sump dam has an overflow dam with a small pump to allow the BAC sump dam to overflow, should one of the sump pumps experience a breakdown. The BAC return water is cooled by the FPs before it re-enters the BACs. Table 7 stipulates all the information required to accurately simulate mine A's BACs.

Table 7: BAC information required for PTB simulation

Bulk Air Cooler (BAC)		
Requirement	**Unit**	**Value**
3 BACs		
Barometric Pressure	kPa	87.23
Water Inlet Temp	˚C	5.6
Water Outlet Temp	˚C	11.36
Water Flow	ℓ/s	133
Air Inlet Temp	˚C	21
Air Inlet Relative Humidity	%	42.24
Air Flow	kg/s	133
3 Air Fans		
Fan Motor Power	kW	220
Fan Flow	kg/s	133
Fan Motor Efficiency	%	95
Fan Efficiency	%	95
Fan inlet Pressure	kPa	87.23
Fan Inlet Temp	˚C	21
3 BAC Sump Pumps		
Pump Motor Power	kW	30
Pump Flow	ℓ/s	133
Pump Motor Efficiency	%	95
Pump Efficiency	%	95
Pumping Elevation	m	0
1 BAC Sump Dam		
Inlet Temp	˚C	11.36
Outlet Temp	˚C	11.36
Flow	ℓ/s	399
Ambient Temp	˚C	21
Heat Transfer Coefficient	$kW/m^2/˚C$	0
Volume	m^3	1000
1 BAC Over Flow Pump		
Pump Motor Power	kW	25
Pump Flow	ℓ/s	40
Pump Motor Efficiency	%	90
Pump Efficiency	%	90
Pumping Elevation	m	0

With this information mine A's cooling system can be iterated until an accurate simulation model has been developed. The PTB simulation will provide results of all the components. The different component results will be discussed in the following section. As soon as the simulation outputs correlate with the default values of mine A's cooling system, the simulation model can be considered as verified and the validation process may commence.

Simulation results

All the components' results can be evaluated after the simulation has been solved. The results will be given in a 24-hour profile. The results can then be evaluated for each hour individually. The simulation is capable of instantly drafting a graph with the selected results to analyse the data. Alternatively, the data can be copied to a spread sheet to compare the data with actual data. Table 8 represents the results and units that can be expected from all of the components in the PTB simulation.

Table 8: PTB simulation components' results

PTB Simulation Component Outputs			
Outputs	**Unit**	**Outputs**	**Unit**
Water Node		***Air Node***	
Barometric Pressure	kPa	Pressure	kPa
Water Inlet Temp	˚C	Temperature	°C
Water Outlet Temp	˚C	Enthalpy	kJ/kg
Pipe		Humidity	kg/kg
Flow	ℓ/s	Temperature Wet Bulb	°C
Cooling Tower		Density	kg/m^3
Water Flow	ℓ/s	***Water Pump***	
Air Flow	kg/s	Water Pressure	kPa
Cooling Duty	kW	Water Flow	ℓ/s
Fridge Plants		Pump Efficiency	%
Evaporator Water Flow	ℓ/s	Fan Speed	-
Condenser Water Flow	ℓ/s	Fan Power	kW
Cooling Duty	kW	Fan Power Cost	R
Compressor Power	kW	***Air Fan***	
Load Fraction	-	Air Pressure	kPa
COP	-	Air Flow	kg/s
Chiller Power Cost	R	Fan Efficiency	%
Dams		Fan Speed	-
Level	%	Fan Power	kW
Temperature	°C	Fan Power Cost	R
Enthalpy	kJ/kg		

3.4. MINE A'S SIMULATION VERIFICATION

The simulation was developed from the available data. Unfortunately mine A did not have the required data in 24-hour profiles for the different variables to compare the data on a daily basis. Therefore, the verification process will be done by comparing the simulated and actual average outputs against each other. If data were available in 24-hour profiles the simulated and actual profiles could have been compared. The new installation of mine A included instrumentation to enable mine A to log the required variables of the cooling system. This will ensure the simulation can be properly validated.

The newly developed simulation model from the available summer data will be considered as the baseline simulation. The simulation model was compared to the available power and temperature data to verify the simulation model. The average input values of a summer period are represented in Table 9.

Table 9: Simulation average input values

Simulation Inputs	Unit	Values
Water from Underground Temperature	°C	25.98
Ambient Temperature	°C	27.81
Humidity	%	29.07
Pressure	kPa	86.78
Evaporator Compressor Setpoint	°C	5.00
Evaporator Pump Setpoint	°C	5.00

The same inputs as displayed in Table 9 were utilised to develop the simulation model for the simulation validation. The evaporator output setpoint was set at 5℃, the same setpoint as the mine A's setpoint before any installations occurred. All of the cooling equipment of mine A was added to the simulation model. The simulation model control was developed according to the mine's different equipment's control philosophies at that stage. Figure 39 represents the comparison of the actual and simulated 24 hour power profile for the average summer period input data.

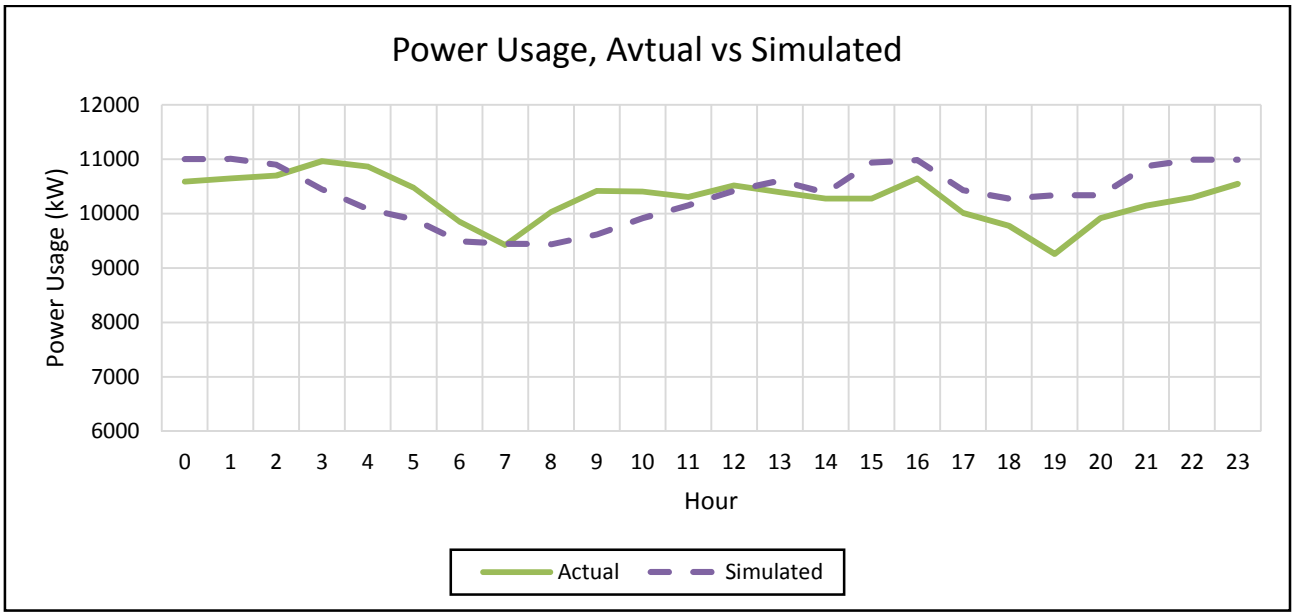

Figure 39: Power profile (actual vs. simulated)

From Figure 39 it is evident that the two profiles follow the same trend. However, there is a slight deviation in the two profiles, which is due to data shortage. The mine could not provide pump and fan status data for this period; therefore, the profiles do not correlate 100%. The actual power data is less at some time periods due to components tripping or due to load shifts. The actual power data can be higher than the simulated value as plant operators could have started equipment at a certain time and not according to a dam level of output temperatures.

The most important outputs from the simulation will be compared against the actual data to validate the simulation model's performance and accuracy. Table 10 compares the daily average values of the simulation and the actual average values with each other. The table also depicts the percentage deviation between the two values. It is evident that the simulation is an accurate representation of mine A's cooling system as the largest deviation is 5.09 %. Therefore, the simulation can be considered as accurate and the identified reconfigurations can be implemented. As soon as the reconfigurations have been implemented on mine A's cooling system, the simulation will be validated with actual data.

Table 10: Verification of mine A's simulation average output values

Outputs	Unit	Average Actual	Average Simulate	Percentage (%) Deviation
Power Usage	kW	10279.03	10373.65	0.91
FP Total Evaporator Water Flow	ℓ/s	1050.00	1023.00	2.57
FP Evaporator Inlet Temperature	°C	13.66	14.07	2.98
FP Evaporator Outlet Temperature	°C	5.2	5.05	2.88
FP Total Condenser Total Flow	ℓ/s	2058.32	2163.00	4.84
Condenser Inlet Temperature	°C	26.12	25.73	1.49
Condenser Outlet Temperature	°C	30.49	30.84	1.13
BAC Total Water Flow	ℓ/s	390.00	381.00	2.31
Ambient DB Temperature	°C	24.89	24.89	0.00
Chill Dam Temperature	°C	5.95	5.65	5.04
BAC Outlet Air Temperature WB	°C	11.63	11.42	1.81
BAC Outlet Water Temperature	°C	11.85	11.32	4.47
Water from Underground Temperature	°C	24.33	24.38	0.21
Pre-cooling Dam 1 Water Temperature	°C	19.39	19.70	1.59
Pre-cool Dam 2 Water Temperature	°C	12.61	12.92	2.38

Mine A's simulation model of the cooling system proved to be within range of the actual values. Therefore, the simulation model can be considered as verified. The simulation model can be validated as soon as all the new instrumentation has been installed to measure the required variables.

3.5. MINE A'S SIMULATION VALIDATION

The validation of mine A's cooling system simulation included the installation of VSDs. This is due to the fact that the project included VSD installation and instrumentation installations. A detailed explanation VSD installation can be found in section 4.2.

The simulation was validated by simulating the model with the same ambient conditions as on a specific day. The water flow in and out of the simulation was kept constant at 370 ℓ/s. The important variables are water temperature from underground, ambient humidity, atmospheric pressure, ambient temperature and FP setpoints. Figure 40 depicts the 24 hour profiles of the different variables that were used as inputs for the validation of the simulation.

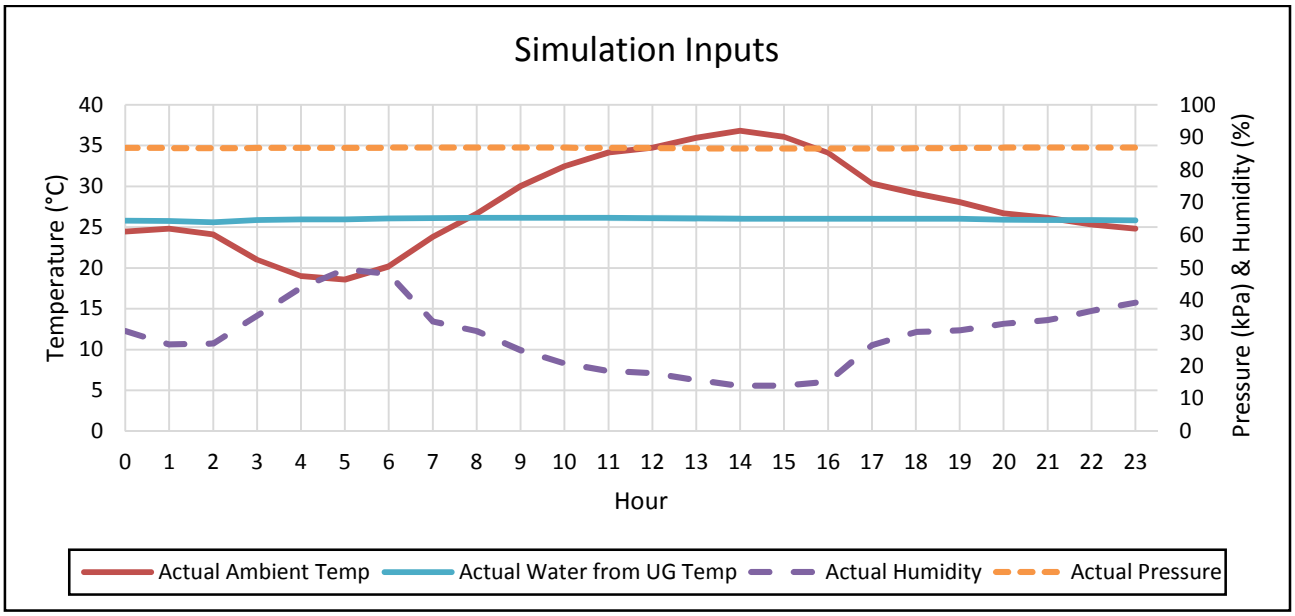

Figure 40: Cooling systems' simulation inputs

The simulation components' statuses were updated with the components running statuses of the specific day. Figure 41 represents the FPs' statuses of the actual day, while the simulation FPs' schedules were updated accordingly.

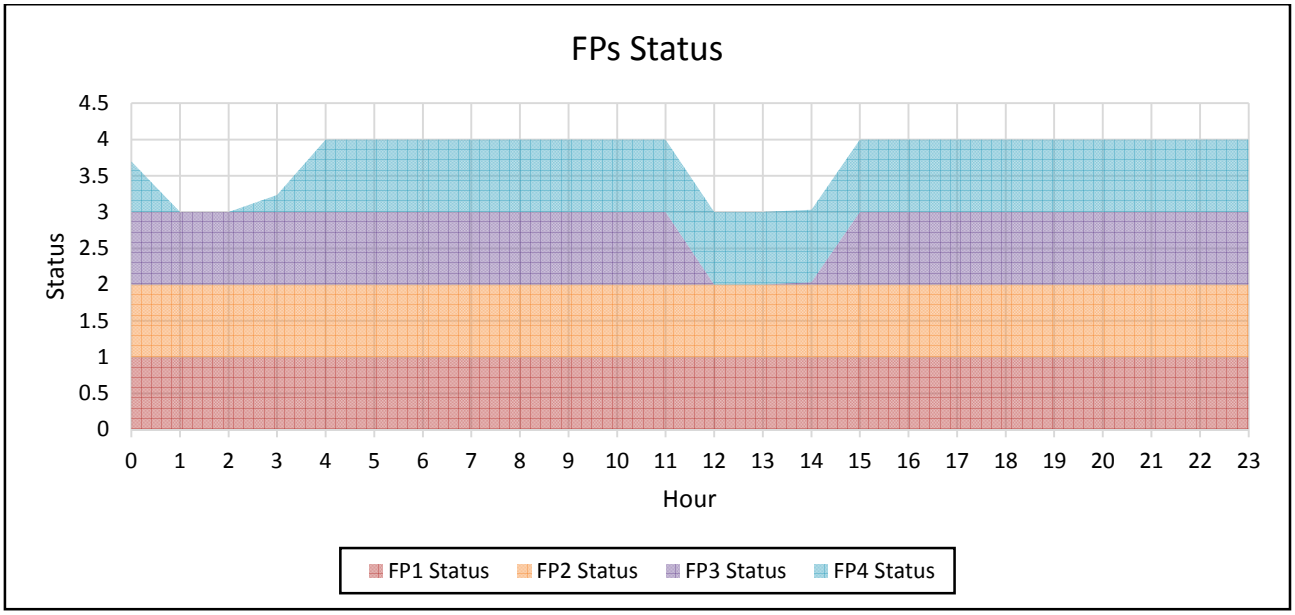

Figure 41: FPs status summary of actual day

From Figure 41 it is evident FP 4 tripped between 01:00 03:00 in the morning. During this period the evaporator and condenser pumps were kept on. FP 3 tripped between 12:00 and 14:00 in the afternoon. During this period the corresponding condenser and evaporator

pumps were switched off. As soon as an evaporator pump is switched off the amount of chilled water that is produced is reduced, which resulted in a BAC being starved during this period. Mining personnel could not say why the FPs tripped.

The FPs setpoints and control philosophies were kept the same as far as possible. For the validation the evaporator and FP compressor setpoint was set to 4℃ which is the same as the actual FP setpoint for the specific day.

There are multiple outputs from the simulation comparable to the actual data to validate the simulation accuracy. The following section will compare the total power usage, crucial water flow and temperature outputs of FPs, BACs and Pre-cooling towers. Table 11 is a summary of the crucial simulation output variables for simulation validation.

Table 11: Validation of mine A's simulation average output values summary

Outputs	Unit	Average Actual	Average Simulate	Percentage (%) Deviation
FP Total Evaporator Water Flow	ℓ/s	866.19	912.69	5.09
FP Evaporator Inlet Temperature	°C	13.66	13.16	3.62
FP Evaporator Outlet Temperature	°C	4.53	4.39	3.12
FP Total Condenser Water Flow	ℓ/s	2058.33	2030.20	1.37
FP Condenser Inlet Temperature	°C	26.12	25.59	2.04
FP Condenser Outlet Temperature	°C	30.49	30.29	0.65
BAC Total Water Flow	ℓ/s	382.14	382.32	0.05
Ambient WB Temperature	°C	15.96	15.14	5.15
Chill Dam Temperature	°C	5.31	5.08	4.29
BAC Outlet Air Temperature WB	°C	11.63	11.29	2.91
BAC Outlet Water Temperature	°C	11.40	10.93	4.11
Water from Underground Temperature	°C	25.98	25.98	0.01
Pre-cooling Dam 1 Water Temperature	°C	19.39	19.28	0.55
Pre-cool Dam 2 Water Temperature	°C	12.61	12.61	0.06

Table 11 depicts that on average the simulation has a good correlation with the actual data. The largest deviation the simulation has with the actual data is 5.15%. Therefore, the simulation can be deemed as validated with a 94% accuracy.

Power:

Figure 42 compares the actual and simulated hourly average total power usage of all the cooling equipment.

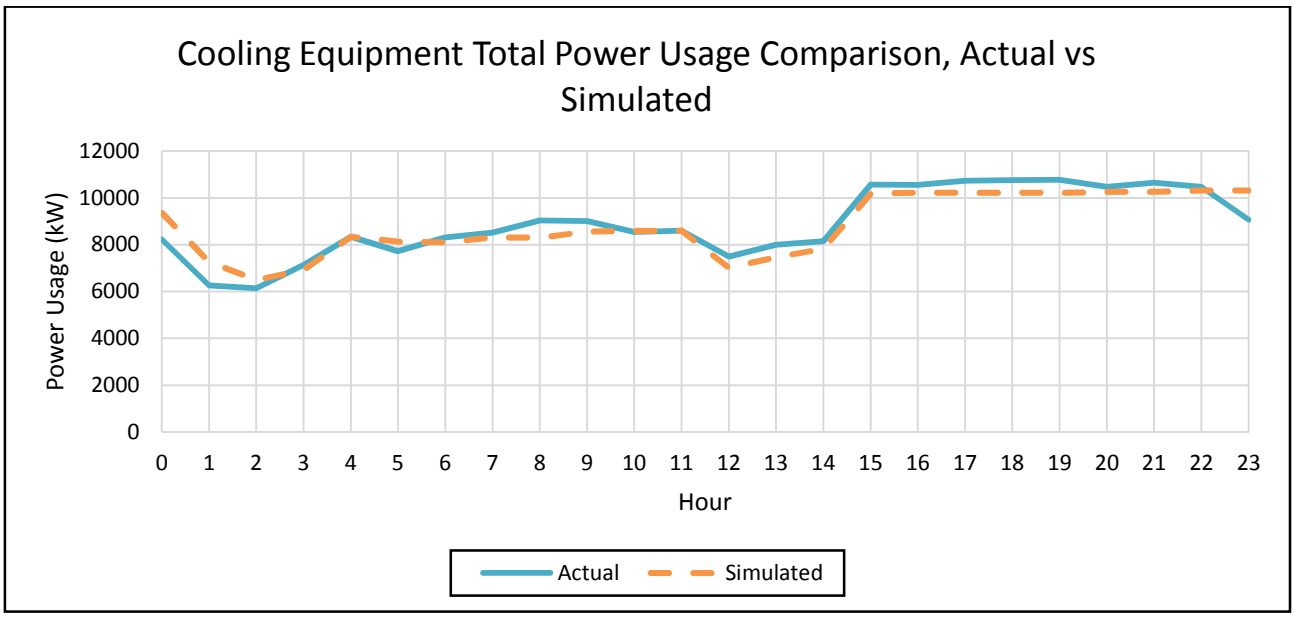

Figure 42: Cooling equipment total power usage comparison, actual vs. simulated

The power drop between 01:00-02:00 and 12:00-14:00 represented by Figure 42 is due to an FP tripping between these periods. On average the actual and simulated power data deviates from each other with 0.93% and a coefficient of determination of 85.94%. Therefore, the simulation predicts the same power profile for the same input values as the actual power consumption.

Evaporator cycle:

Figure 43 compares the actual and simulated hourly average total water flow through all four FPs' evaporator circuit.

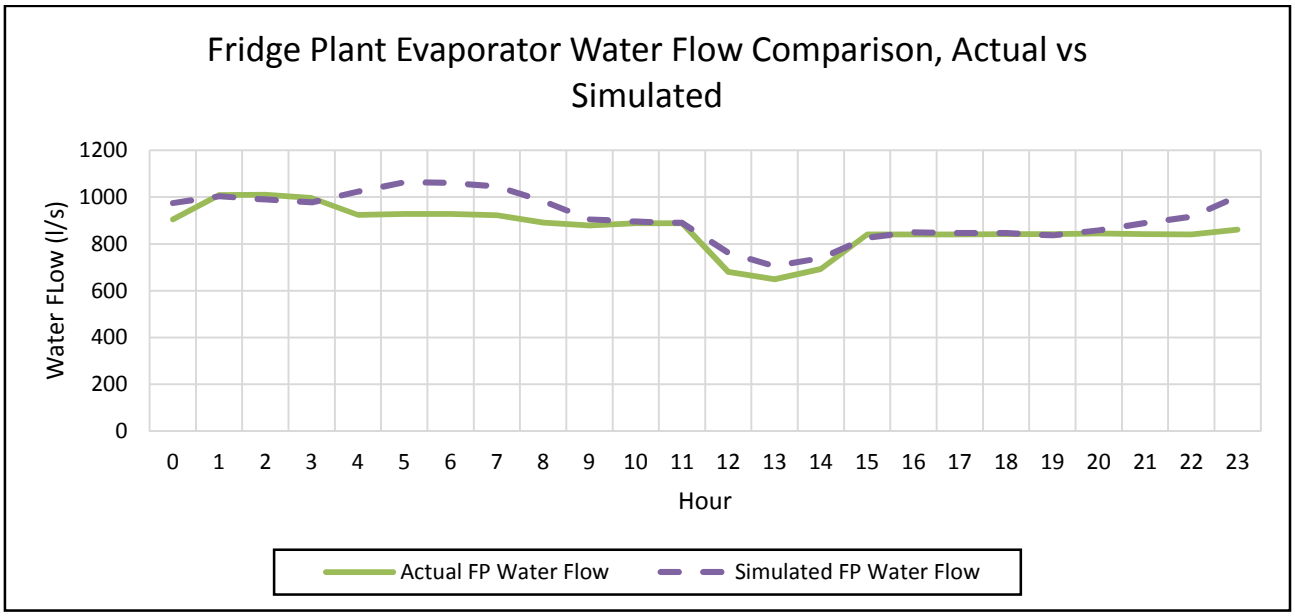

Figure 43: FP evaporator water flow comparison, actual vs. simulated

Figure 43 shows the simulated water flow through the FPs' evaporator circuit is higher than the actual flow during certain periods of the day. This issue will be addressed in section 4.3. In principle the actual and simulated control philosophies are identical. As Table 11 depicts, the simulated and actual daily average water flow through the FPs' evaporator side deviate with 5.09%. Figure 44 compares the actual and simulated hourly average inlet and outlet water temperatures through the FPs' evaporator side.

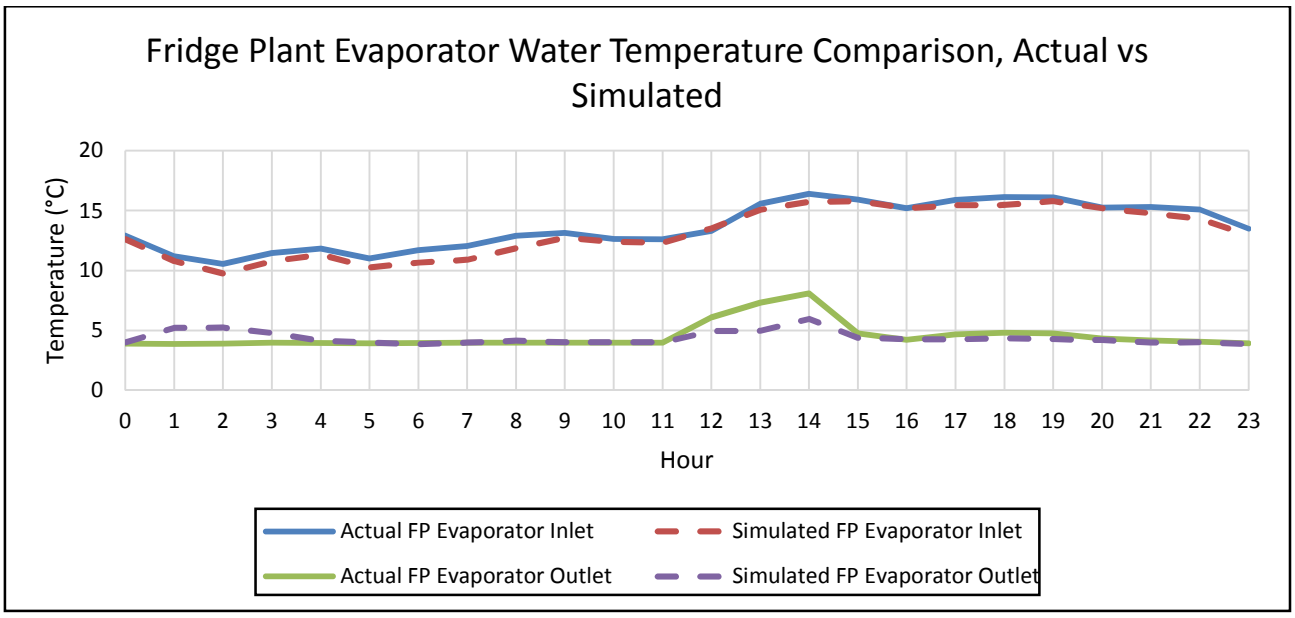

Figure 44: FP evaporator water temperature comparison, actual vs. simulated

From Figure 44 it is evident the simulated inlet and outlet water temperatures through the FPs' evaporator circuit correlate and follow the same trend as the actual FP inlet and outlet evaporator water temperatures. Table 11 depicts the simulated and actual daily average inlet and outlet water temperatures through the FPs, which deviate with 3.62% and 3.12% respectively.

Both the actual and simulated evaporator outlet water temperatures show a temperature increase in evaporator outlet temperature between 11:00-15:00. This period is the period during and after an FP and pump trip, as depicted by Figure 41. During the morning period one of the FPs tripped but the corresponding evaporator and condenser pumps were kept on. This, however, did not affect the actual output temperature as the inlet water temperature was relatively cold during this period, and the flow stayed constant. In the simulation this effect was immediately detected and counteracted by the control philosophy, which lead to an output temperature increase.

Condenser cycle:

Figure 45 compares the actual and simulated hourly average total water flow through the FPs' condenser circuit.

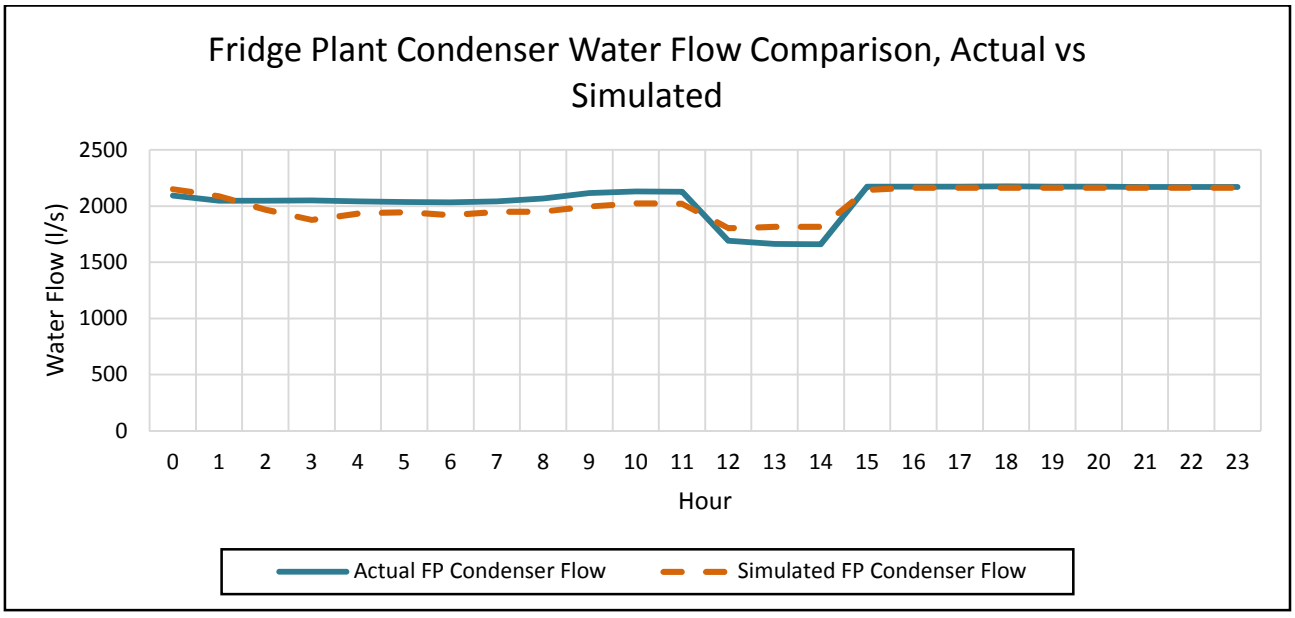

Figure 45: FP condenser total water flow comparison, actual vs. simulated

From Figure 45 it is evident that the simulated and actual total water flow through the FPs' condenser sides closely correlate. The condenser flow control could be simulated more

accurately as the correct condenser pump characteristics' data was available from project inception. The condenser pump control philosophy parameters do not change as much as the evaporator control parameters, as a result the simulation is more accurate. Table 11 depicts that the simulated and actual daily average water flow through the FP's condenser circuit deviates with 1.37%. Figure 46 compares the actual and simulated hourly average inlet and outlet water temperatures through the FPs' condenser circuit.

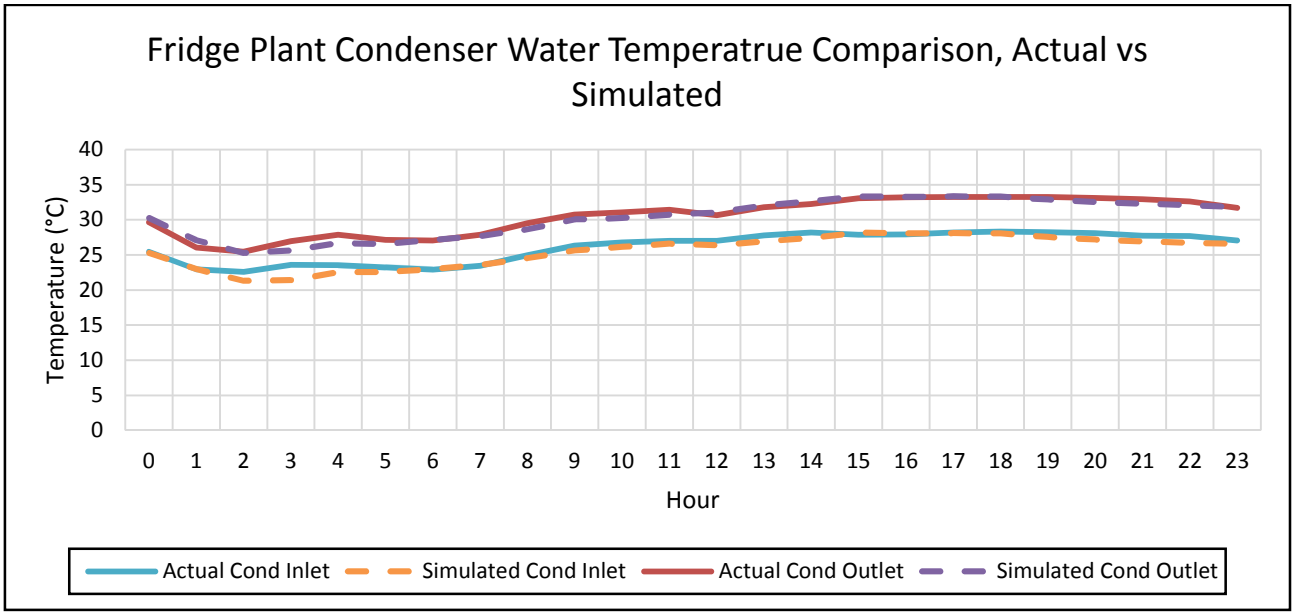

Figure 46: FP condenser water temperature comparison, actual vs. simulated

From Figure 46 it is evident that the simulated inlet and outlet water temperatures through the FPs' condenser circuit correlate and follow the same trend as the actual FP inlet and outlet condenser water temperatures. Table 11 indicates that the simulated and actual daily average inlet and outlet water temperatures through the FPs' condenser circuit deviates with 2.04% and 0.65% respectively.

Bulk air cooler:

Figure 47 compares the actual and simulated hourly average total water flow through the BACs.

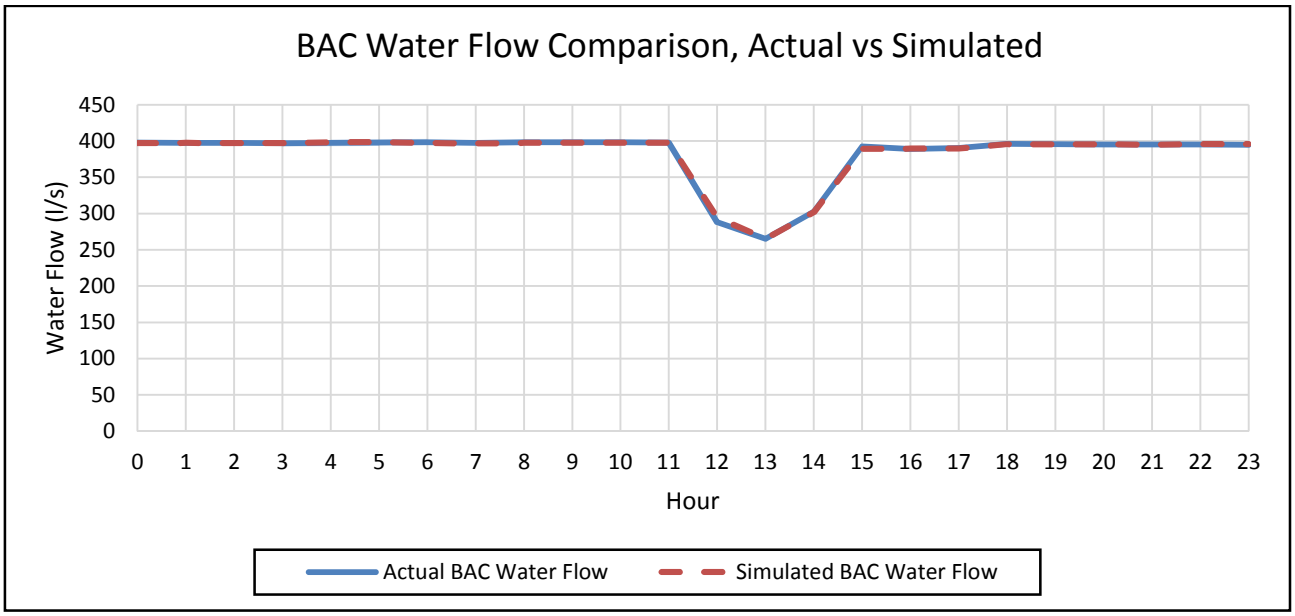

Figure 47: BAC total water flow comparison, actual vs. simulated

From Figure 47 it is evident that the simulated and actual total water flow through the BACs are the same. The reduction in water flow between 11:00 and 15:00 is due to one of the four FPs tripping during the day. This caused a reduction in chilled water flow to the BACs. The BAC sump dam level was lower during this period, reducing the amount of pumping that is required. Table 11 indicates that the simulated and actual daily average total water flow through the BACs deviates with 0.05%. Figure 48 compares the actual and simulated hourly average outlet WB air temperatures through the BACs. It also depicts the ambient WB air temperature input of the simulation.

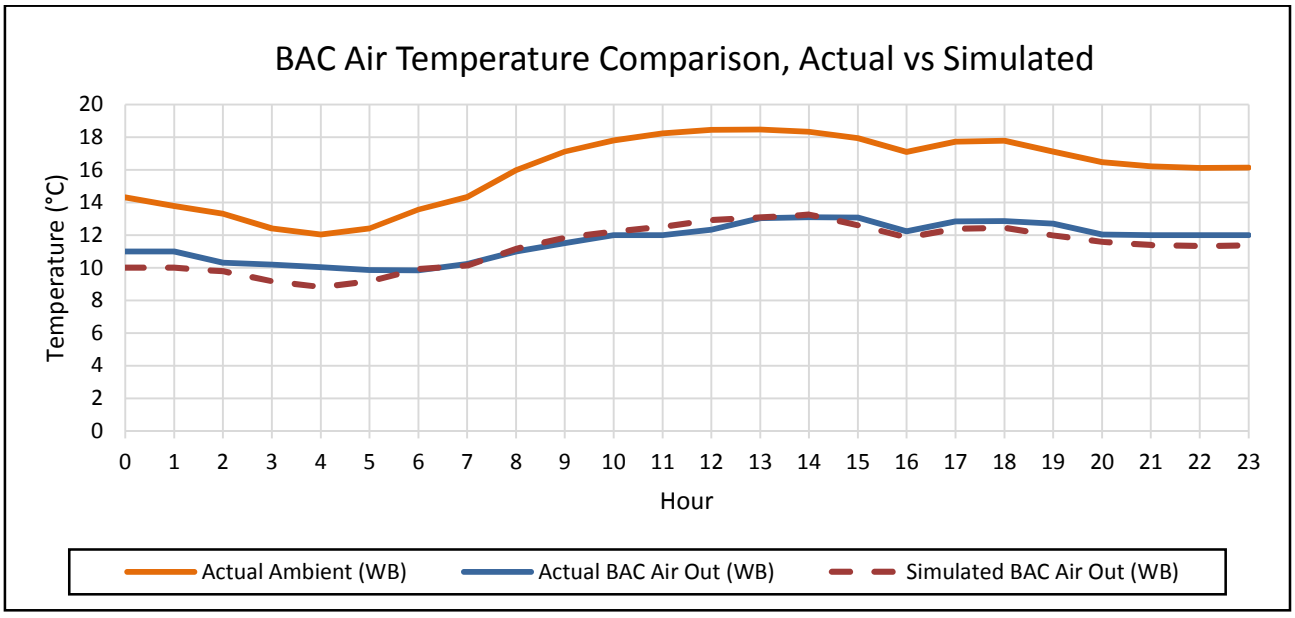

Figure 48: BAC air temperature comparison, actual vs. simulated

From Figure 48 it is evident the simulated BACs' outlet WB air temperatures correlate with the actual data. Table 11 shows that the simulated and actual daily average BACs' outlet WB air temperatures deviate with 2.91%. Figure 49 compares the actual and simulated hourly average inlet and outlet water temperatures through the BACs.

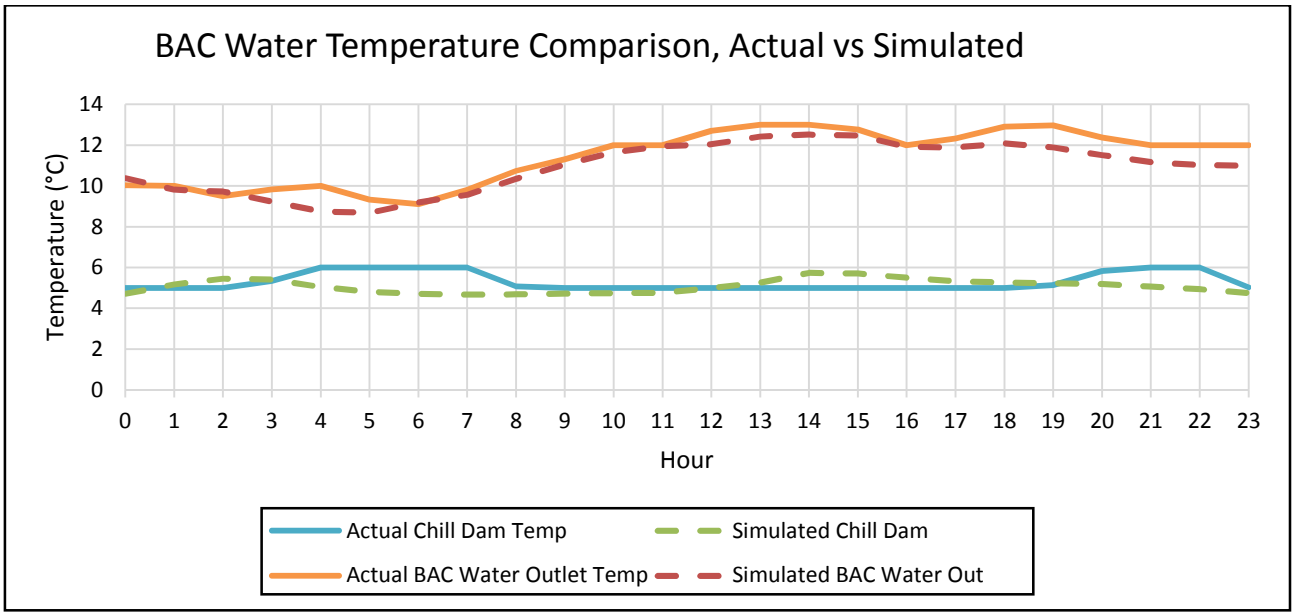

Figure 49: BAC water temperature comparison, actual vs. simulated

From Figure 49 it is evident the simulated inlet and outlet water temperatures through the BACs correlate with one another and follow the same trend. Table 11 depicts the simulated and actual daily average inlet and outlet water temperatures through the BACs, which deviate with 4.29% and 4.11% respectively.

Pre-cooling towers:

Figure 50 compares the actual and simulated hourly average inlet and outlet water temperatures from underground, pre-cool stage 1 and finally pre-cool stage 2.

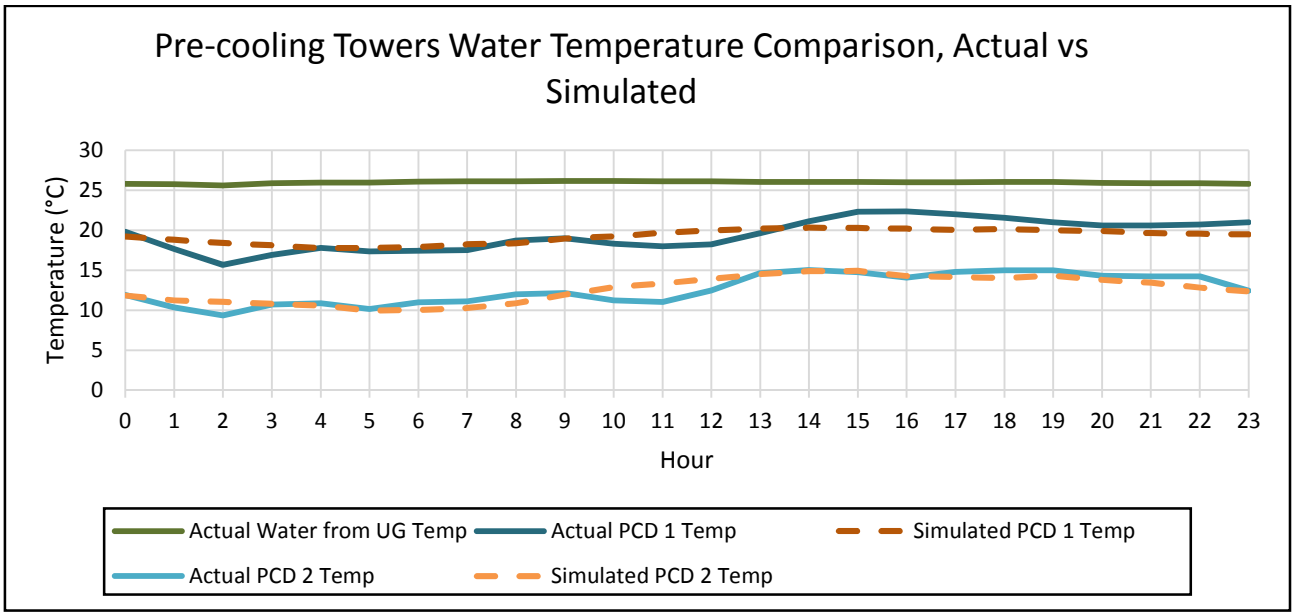

Figure 50: Pre-cooling water temperature comparison, actual vs. simulated

From Figure 50 it is evident the simulated inlet and outlet water temperatures through the two stage pre-cooling towers correlate with one another and follow the same trend. Table 11 depicts the simulated and actual daily average water from underground, pre-cool stage 1 and pre-cool stage 2 temperatures, which deviate with 0.01%, 0.55% and 0.06% respectively.

When comparing the crucial simulation and actual values, it is evident that the simulation responds almost identically to the input values as the actual cooling system would under the same circumstances.

3.6. CONCLUSION

This chapter formulated a strategy to reconfigure mine cooling auxiliaries for optimal operations. The procedure to identify the inefficient components was discussed. The method to physically reconfigure the cooling subsystems and to determine the ideal control philosophy was identified. Finally the simulation verification and validation processes were discussed and a simulation model was developed, verified and validated.

The strategy will be applied to four case studies of mine A's cooling subsystems in the following chapter. The case studies will be used to validate the strategy and determine the practical impact they have on a mine's cooling system.

Chapter 4. CASE STUDY- IMPLEMENTATION OF PROPOSED SOLUTIONS ON MINE A'S COOLING SYSTEM

KJ Oberholzer

"Don't watch the clock; do what it does. Keep going." - Sam Levenson

4.1. INTRODUCTION

Background

Utilising the information available from the literature review in chapter 2, a universal reconfiguration methodology is developed in chapter 3. The optimisation methodology will be tested on different components within a mine's cooling system. Mine A's cooling system was identified to be inefficient and required reconfiguration for optimal operation.

According to the mine A's personnel and the name plates of the FPs, three of the four FPs and their cooling auxiliaries were installed during 1992. The fourth FP was added in 2013, to increase the recycled chilled water from the chill dam to the second stage pre-cooling dam [5]. The recycled water will decrease the FP inlet water temperature and in return will lower the FP outlet water temperature. Table 12 indicates mine A's cooling systems' current design and expected outputs.

Table 12: Summary of cooling system's outputs

Summary of Average Cooling System's Outputs.				
Variable	**Unit**	**Current**	**Design**	**Mine Expectation**
Water Flow per BAC	ℓ/s	133	133	133
Total Water Flow to BAC's	ℓ/s	399	450	399
Water Flow to Underground	ℓ/s	400	400	400
Evaporator Water Flow per FP	ℓ/s	250	309	230
Total Evaporator Water Flow	ℓ/s	1000	1236	920
Recycled Water	ℓ/s	201	437	121
Condenser Water Flow per FP	ℓ/s	540	570	540
Total Condenser water Flow	ℓ/s	2160	2280	2160
Condenser Inlet Water Temperature	°C	25	26	26
BAC Outlet WB Air Temperature	°C	12.5	9	11 -12
FP Outlet Water Temperature	°C	5.1	3	4

During the initial project investigation in 2013 mine personnel were satisfied with a 5℃ evaporator outlet water temperature and a 12.5℃ BAC outlet air WB temperature. During project implementation mine personnel changed the expected output temperatures to 4℃ evaporator outlet water and 11-12℃ BAC outlet air WB temperature. Therefore reconfiguration of the cooling auxiliaries will aim to provide an operation as close to the equipment's design specifications, realising in maximum power savings.

[5] Tony Kleinschmidt Senior Instrumentation Technician

From Table 12 it is evident that the mine A's evaporator outlet water temperature and BAC outlet WB air Temperature are above the system's OEM design specifications. This is due do certain components being inefficient. Identifying these inefficient components and reconfiguring them for optimal operation will be beneficial for the mine. An optimal operating system can lead to increased cost savings under the same service delivery or increased service delivery with a decrease in power savings. Figure 51 identifies mine A's components which can possibly be considered for reconfiguration.

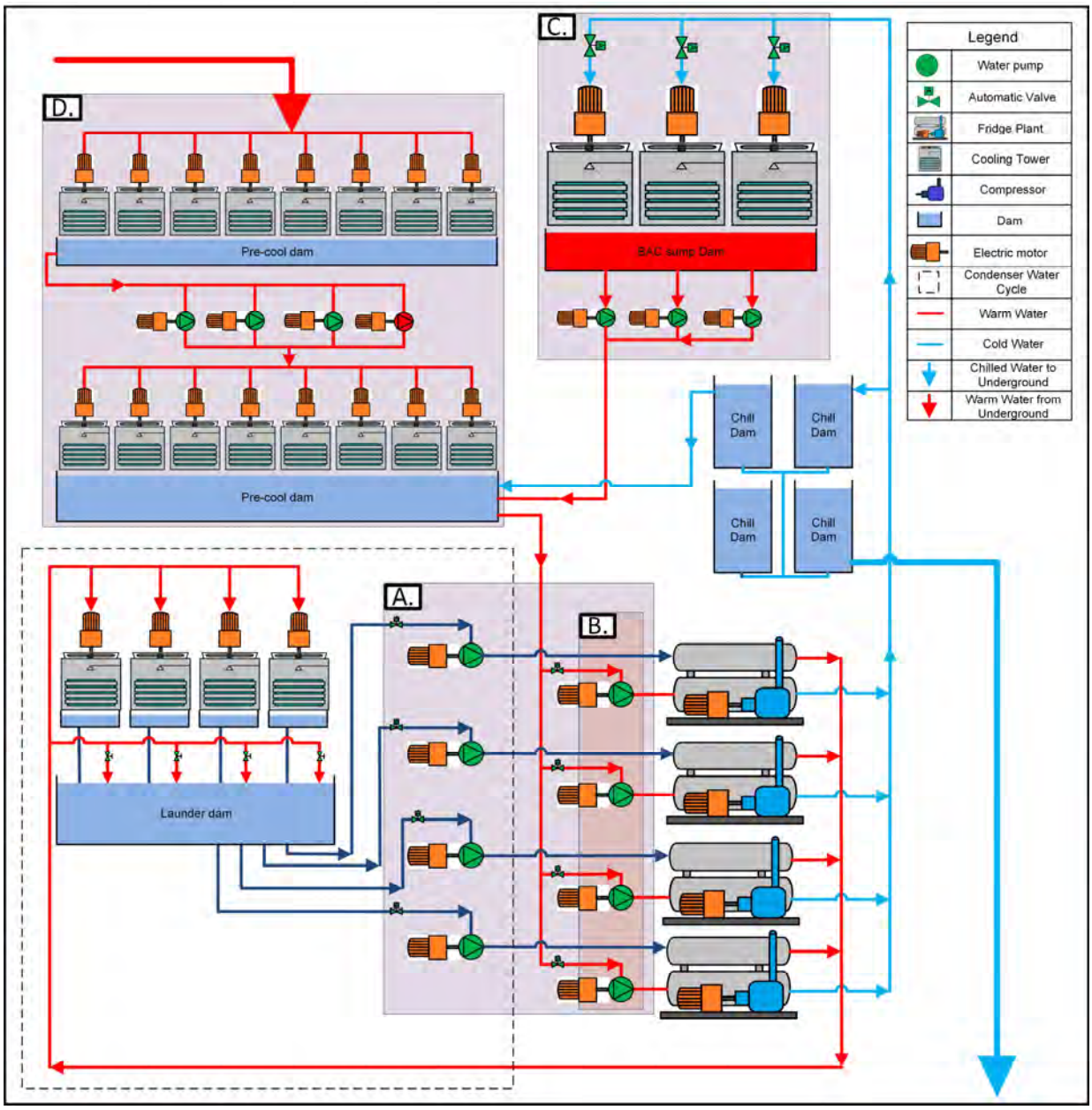

Figure 51: Identification of inefficient operation for reconfiguring

Figure 51 identifies inefficient components A to D. All of these components operate in alliance with one another to meet the mine's cooling demand. A brief description of the components follows:

A. Reconfiguration of FP pumps' flow control

Installing VSDs on the FP condenser and evaporator pumps to regulate the water flow through the FPs will ensure that the correct condenser inlet temperature is maintained. The evaporator VSD will allow maximum heat transfer between the evaporator water and the refrigerant gas. This could lead to improve the FPs' COP which in return will result in power savings or improved service delivery.

B. Reconfiguration of evaporator pump impellers

After implementing the FP pump flow control, the FPs' COP was not improved as expected. This was due to the alterations to the pump characteristics. The mine reduced the evaporator pump impellers size to reduce the water flow through the FPs. According to mine personnel, this was common practice before VSDs were available or affordable [6&7].

Reconfiguring the pump impellers to full size impellers will increase the range at which the VSD can control the evaporator water flow. It will also enable the mine to increase the water flow to the design specification when needed. Increased water flow could realize cost savings during the winter months when the lower ambient conditions allow colder evaporator inlet temperatures. Evaporator pumps are started to meet the water demand with the FPs switched off, as the evaporator inlet water is cold enough. Therefore, if all pumps are installed with full size pump impellers, fewer pumps will be needed to meet the water demand during the winter months.

C. Reconfiguration of bulk air coolers

From Table 12 it is evident that the BAC outlet WB temperature and water flow do not meet the OEM design specification. This is due to restricted sump dam capacity, leading to under-cooling during the day. Over-cooling can also occur when the ambient air temperature drops and the BAC cannot utilise all of the provided cooling. Reconfiguring the pipe configuration at the BAC sump dam will allow the mine to provide the BAC with its required water flow for

[6] Johan Barnard — Mechanical Foreman
[7] Tony Kleinschmidt — Senior Instrumentation Technician

maximum service delivery. This will also enable the mine to adjust the BAC inlet water flow control philosophy to maintain a constant BACs output air WB temperature. This will ensure no cooling is wasted as the BACs will be supplied with the correct amount of chilled water.

D. Reconfiguration of pre-cooling towers

The cooling realised from the pre-cooling towers can be considered as free cooling when considering the temperature difference it produces at a relatively low power consumption [8]. Therefore, replacing the pre-cooling tower with cooling towers with improved efficiencies will increase the temperature difference achievable by the pre-cooling towers. The new design of the pre-cooling towers will also allow hassle free maintenance and reduced downtime during a breakdown. An improved temperature difference will ensure colder FP inlet water temperature which could lead to power savings.

4.2. RECONFIGURATION OF FP PUMP FLOW CONTROL

Introduction

Mine A's cooling system consists of four FPs in parallel. Each FPs has its own condenser and evaporator pumps. These pumps are in series with the each of the FPs' condenser and evaporator circuits. Figure 52 is a visual representation of mine A's FPs and pump configuration. Before reconfiguration of the mine's flow control, the mine used to operate all eight pumps at full load. The excess chilled water was recycled to the second stage pre-cooling dam to lower the evaporator inlet water temperature to reduce the evaporator outlet water temperature. The FPs compressor's guide vanes cut back when the outlet water temperature is close to the desired setpoint temperature.

[8] Deon Arndt Partner of Enoveer Engineering Innovation

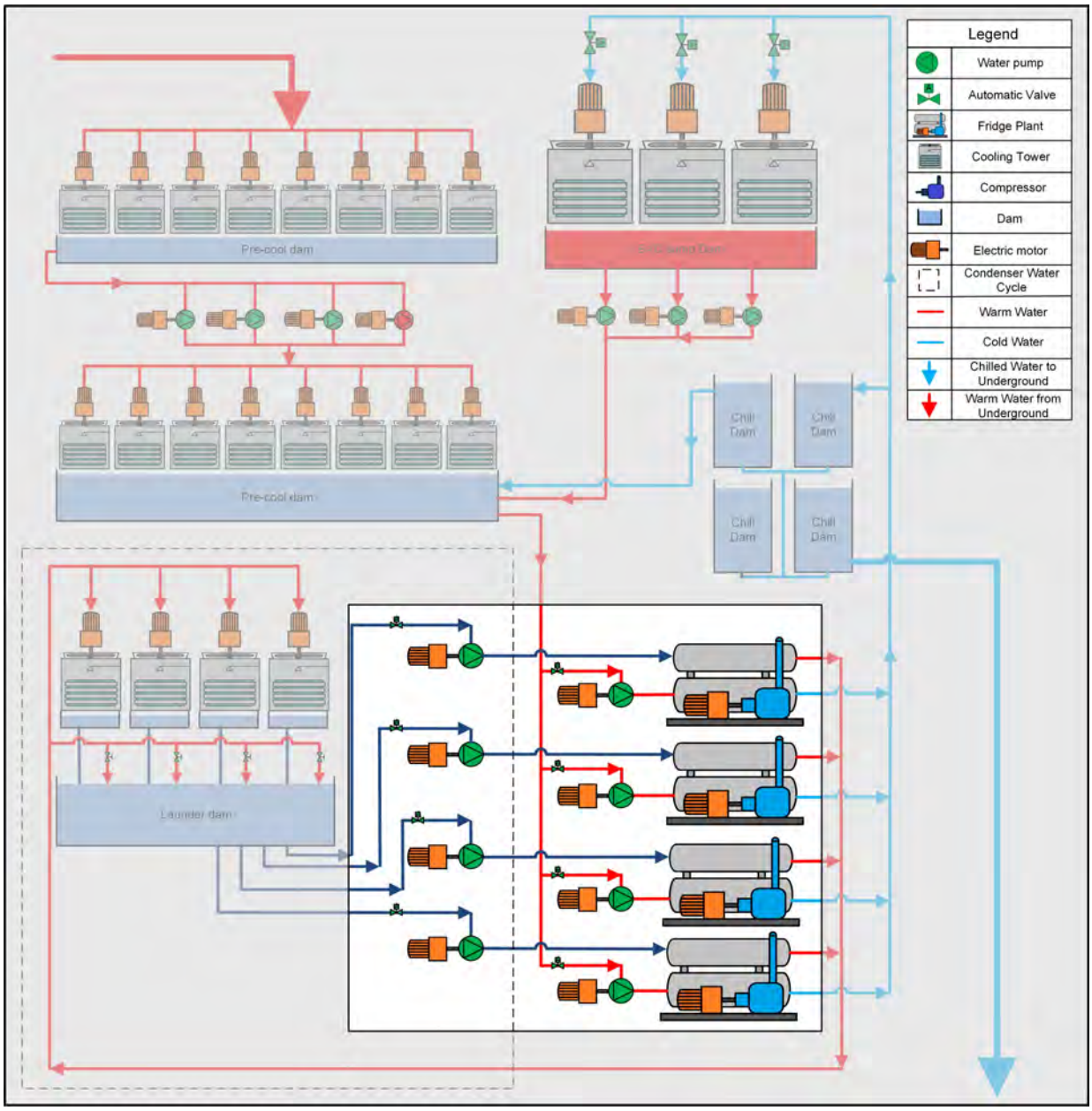

Figure 52: Mine A's FPs, pump configuration

Figure 52 depicts the condenser pumps, which are in a closed loop on surface whilst the evaporator pumps are in a semi-closed loop, providing chilled water to underground and the BACs. Table 12 specifies the FP current water flow and temperature's properties. It also indicates the design and expected properties. The evaporator water flow is higher than the chilled water demand, causing chilled water to be recycled. Although recycled chilled water lowers the evaporator inlet temperature, it also increases the power consumption unnecessary as chilled water has to be re-cooled and extra pumping is required.

Identifying the inefficient operation for reconfiguring:

The evaporator pumps provide constant maximum water flow through the FPs' evaporator circuits. Figure 53 represents the evaporator setpoint and actual outlet water temperature.

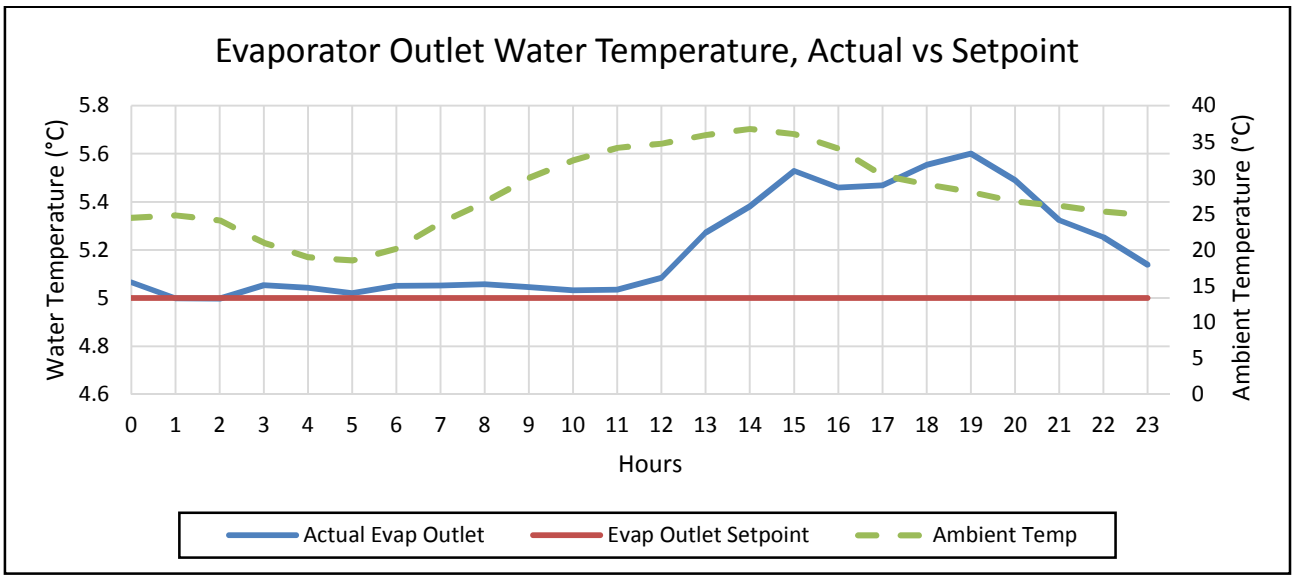

Figure 53: Evaporator outlet water temperature

Figure 53 indicates that the FPs cannot maintain the evaporator outlet water temperature close to the desired setpoint temperature when the ambient temperature increases. The water flow through the evaporator pressure vessel is too high to allow sufficient heat transfer. Reducing the water flow rate through the evaporator cycle will allow sufficient heat to be transferred from the water to the refrigerant gas and reduce the amount of chilled water being recycled. Figure 54 represents the daily average chilled water being recycled before VSDs were installed on the pumps.

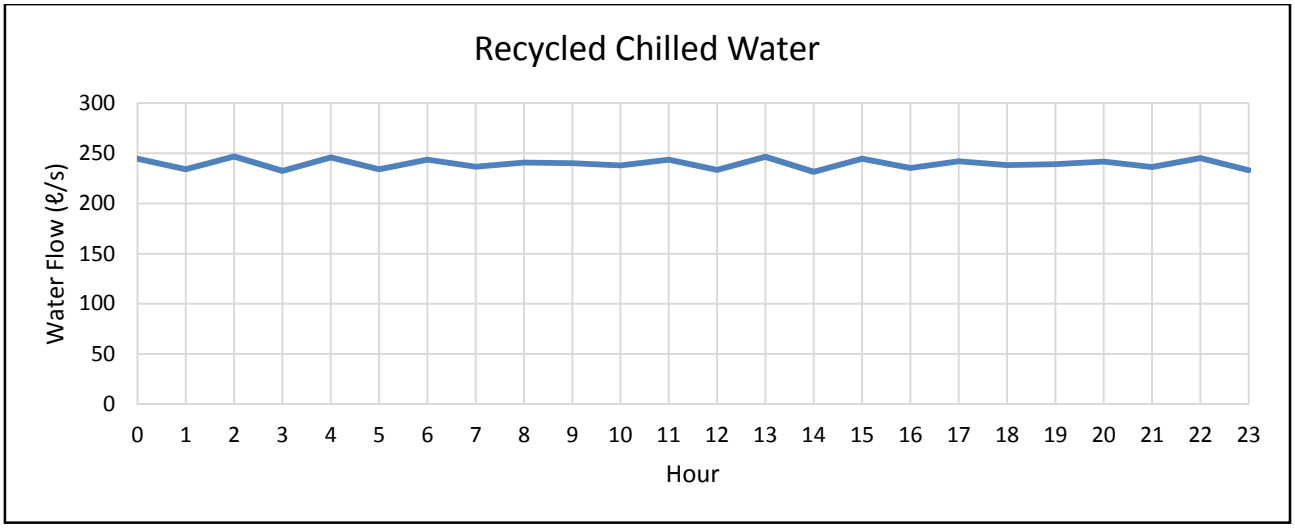

Figure 54: Recycled chilled water

From Figure 54 it is evident that chilled water is almost constantly being recycled throughout the day. Reducing the amount of chilled water being recycled by lowering the evaporator water flow will decrease the amount of cooling that is being wasted. This allows the required outlet temperature to be achieved in one pass. Figure 55 represents the daily average condenser water temperatures.

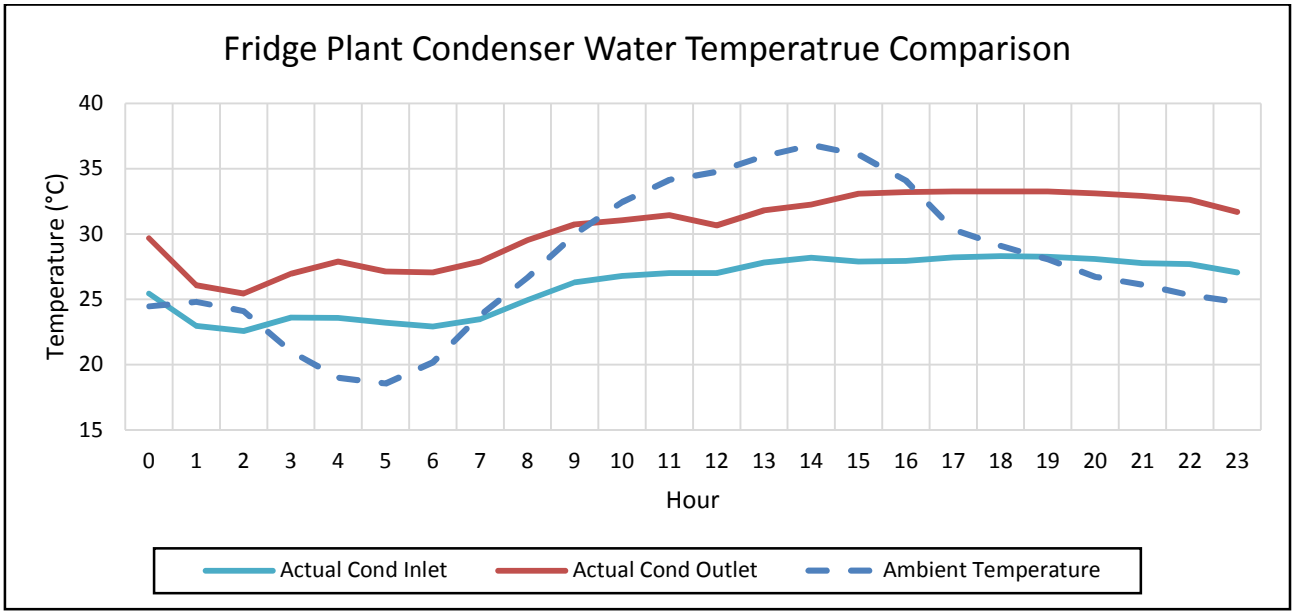

Figure 55: Condenser water temperatures

The condenser cycle design inlet water temperature specification is 26℃. From Figure 55 it is evident that the condenser inlet water temperature is above the designed 26℃ inlet temperature during the warmer periods of the day. Adding control to the condenser pump flow will enable the mine to maintain a condenser inlet water temperature of 26℃ throughout the day. Figure 56 is a schematic representation of the VSD installation at mine A.

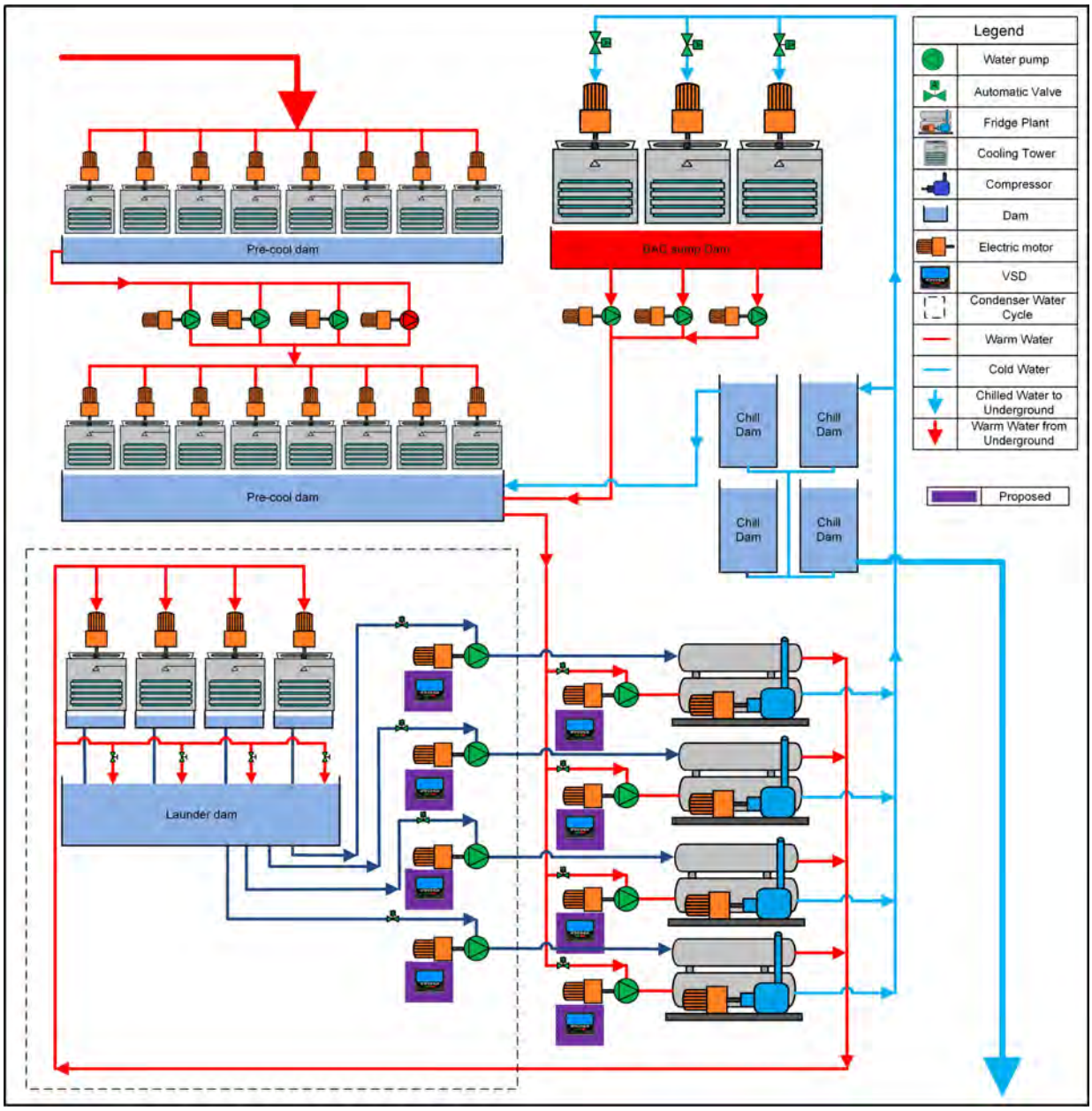

Figure 56: Schematic Representation of the VSD installations at mine A

The following improvements can realise from installing VSDs on FP condenser and evaporator pumps with standard pump characteristics [21]:

- control the FP's evaporator output temperature more accurately;
- maintain a condenser inlet water temperature below 26℃;
- improve the FP's COP;
- reduce the amount of recycled chilled water;
- meet the chilled water demand more accurately, and depending on the setpoint;
- realise a cost savings.

Control philosophy reconfiguration

The new equipment required a control philosophy update as the VSDs will control the evaporator pump flows to achieve a specific FP's output water temperature. The VSDs also control the condenser pump flows to maintain the FPs' correct condenser inlet water temperature. The newly developed control philosophy should not increase or decrease the water flow through the FPs beyond the OEM design specifications. Table 13 represents the FPs OEM design, minimum and maximum flow rate through the evaporator and condenser vessels respectively.

Table 13: Summary of FPs' OEM design specifications

Summary of FPs OEM design specifications				
Variable	**Unit**	**Minimum**	**Design**	**Maximum**
Evaporator Water Flow	ℓ/s	210	309	350
Condenser Water Flow	ℓ/s	500	570	640

Evaporator control strategy:

All four FP's on: -The VSDs control the evaporator pump water flow to achieve an output setpoint temperature of 4℃.
-The FP compressors setpoint will be set to 4℃.

One or more FPs off: -The VSDs control the evaporator pump water flow to meet the chilled water demand.
- The FP compressor's setpoint will be set to 4℃.

If the output water temperature is above the setpoint temperature, the VSDs will cut back to the specified minimum flow rate to increase the heat transfer from the water to the refrigerant gas. At this stage the FP's compressor GV will be 100% open. As the output temperature approaches the output temperature setpoint, the VSDs will increase the flow through the FPs. The compressor's GV will start to cut back as soon as the output temperature reaches the setpoint temperature. With this control philosophy recycling of chilled water will be kept to a minimum and will only occur when all four FPs are on.

Condenser control strategy:

- The temperature drop over the FP's condenser cycle will be set to 3.5℃ when the condenser inlet temperature is greater than 26℃. The VSD will increase the condenser pump flow to maximum flow to obtain a temperature difference of 3.5℃ over the FP's condenser cycle.

- The temperature over the FP's condenser cycle will be set to 5℃ when the condenser inlet temperature is equal or less than 26℃. The VSD will decrease the condenser pump flow to maintain a temperature difference of 5℃ over the FP's condenser cycle when the inlet water temperature is less than 26℃.

Changing the water flow through the FPs' condenser side will ensure the condenser cooling towers can maintain a condenser inlet water temperature of 26℃. This will ensure the condenser cycle is as optimal as possible and prevent the FPs from tripping unnecessarily.

Simulation validation process

Mine A's simulation could only be validated after the installation of the VSDs since the installation included instrumentation to log all the required variables. All the different subsystems of mine A's cooling systems were validated in section 3.5.

Results

The results were obtained from the simulation as the simulation was validated in the preceding chapter. The results will be discussed in three sections. The first results will be aimed at maximum power savings under the mine's old evaporator water temperature output setpoints. The second results will determine the power savings that could be realised under the mines current required outputs. The third set of results will determine the maximum service delivery that could be realised by the initiative.

The actual temperature outputs and control philosophies were used as inputs for the baseline simulation. For the baseline none of the pump flow control measure was implemented. The FP compressor setpoints were set to 5℃ to determine the equipment's cooling capabilities before project implementation. For the implemented simulation the Evaporator and FP compressor hourly setpoints were updated with the hourly average temperature output from the baseline simulation. This will ensure the cooling is kept constant to determine the maximum power savings that could be realised. Figure 57 represents the power usage of the cooling equipment for the baseline and simulated savings.

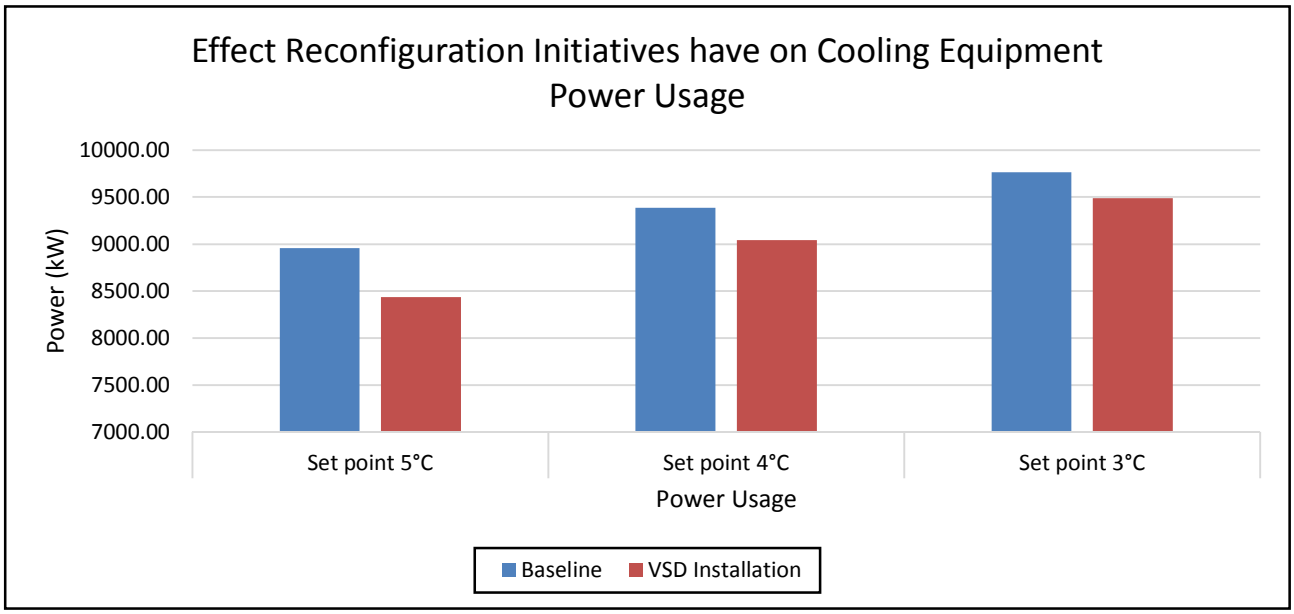

Figure 57: Cooling equipment total power usage comparison

From the baseline simulations it is evident that the power usage increases on average 400 kW for every 1℃ drop in desired evaporator outlet water temperature. The power savings also decrease as the desired evaporator outlet water temperature decreases. It is important to note that the power savings are calculated from different baselines as the desired temperature setpoints are changed. Figure 58 represents the power savings realised from installing VSDs on the FPs evaporator and condenser pumps.

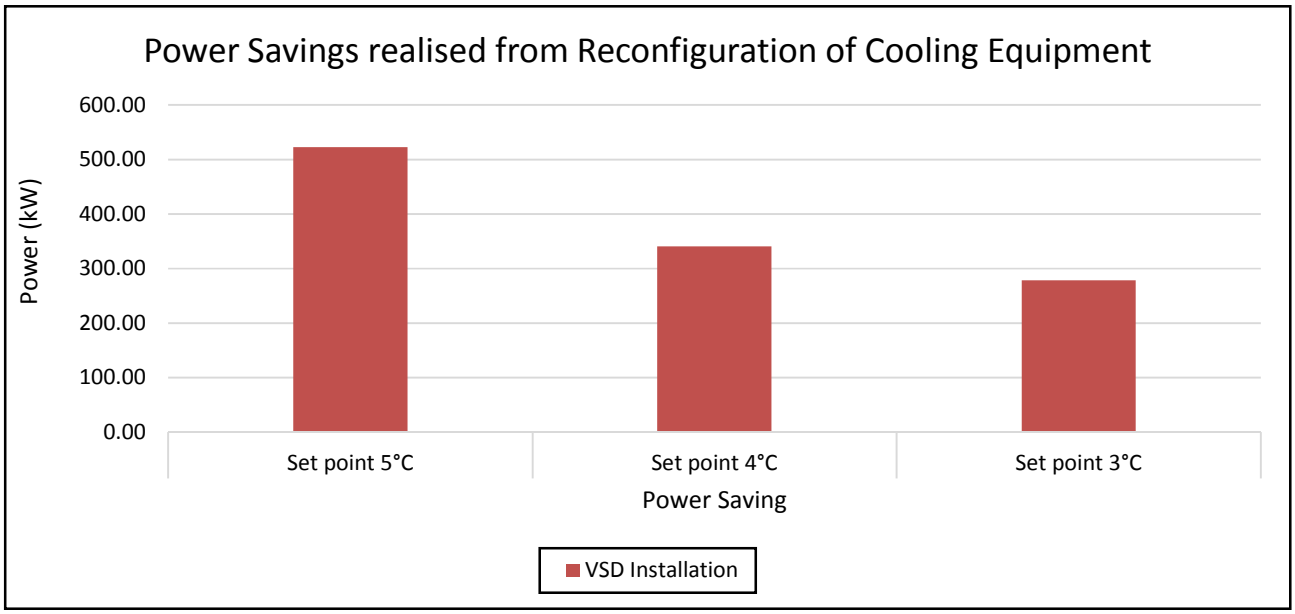

Figure 58: Power savings realised from reconfiguration of a mine's cooling equipment

Figure 58 shows the saving achieved by installing VSDs on mine A's FP pumps. To maintain an evaporator output temperature of 5℃, 4℃ and 3℃ a power saving of 522.41 kW, 340,69 kW and 278.06 kW will be realised respectively. Figure 59 shows the effect installing VSDs on FPs pumps, to control the water flow, has on the FPs' water and BAC WB air temperatures.

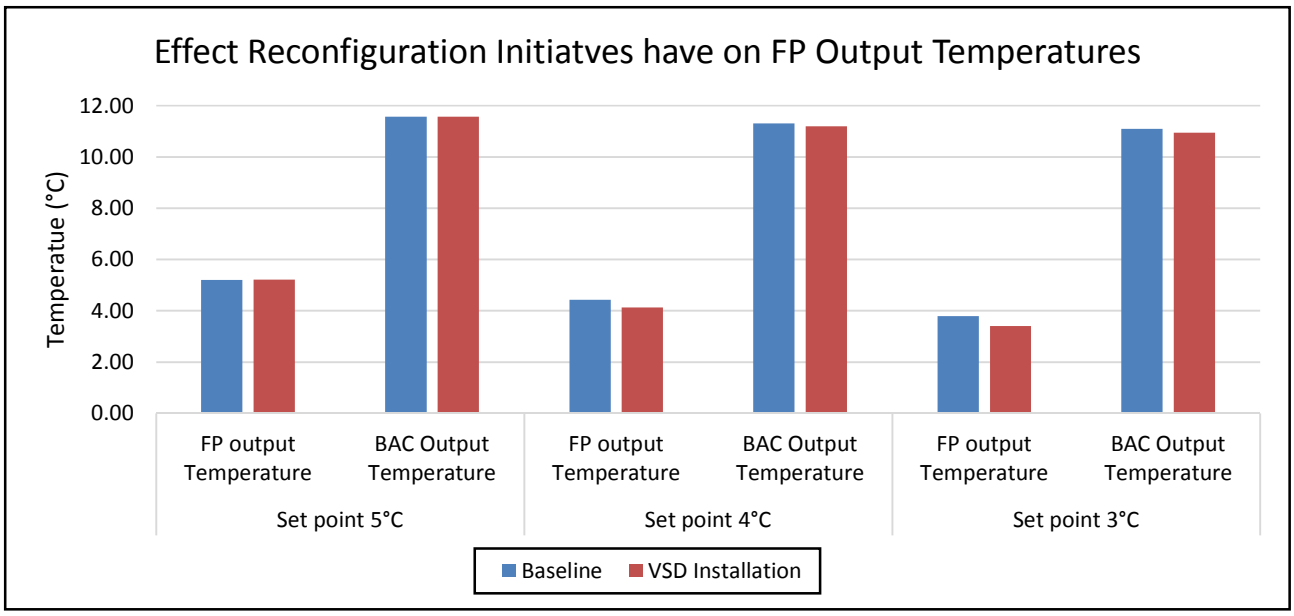

Figure 59: Effect reconfiguration initiatives have on FP outlet temperatures

Figure 59 indicates that, for the first set of simulations with the setpoint of 5℃, the average FP evaporator outlet temperature increased with 0.01℃. This is due to the reduced water flow through the FP's evaporator resulting in less water to be recycled. This caused the evaporator inlet water temperature to increase. The BAC outlet WB air temperature remained unchanged. Therefore, the evaporator setpoint at 5℃ for energy savings will result in an energy saving of 522.41 kW without affecting the system's service delivery.

For the second set of simulations, with the setpoint set to 4℃, the average FP evaporator outlet temperature decreased from 4.43℃ (baseline simulation) to 4.13℃. The BAC outlet WB air temperature decreased from 11.30℃ to 11.19℃ due to the decreased evaporator output temperatures. Therefore, the evaporator setpoint at 4℃ for improved service delivery will result in an average evaporator water and BAC WB air temperature improvement of 6.79% and 0.98% respectively and a power saving of 340.69 kW.

For the third set of simulations the evaporator outlet water temperature setpoint was set to 3℃ where the outlet temperature decreased from 3.79℃ (baseline simulation) to 3.40℃.

The reduced evaporator outlet water temperature caused the BAC outlet WB air temperature to decrease with 0.14℃. The improved service delivery lead to a power saving of 278.86 kW.

A detailed analyses of the effect the new pump flow control had on the cooling system can be found in Appendix C.

Conclusion - Reconfiguration of FP pump flow control

The need for an FP water flow control was identified. Two sets of simulations, baseline and implemented, were simulated for each scenario, to determine the effect the reconfiguration has on the system whilst keeping the ambient psychrometric conditions 100.00% identical. Each scenario consisted of a baseline and post implementation simulation. The first set of simulations was focused on energy savings with the same chilled water setpoint of 5℃. The second set of simulation was focused on improved service delivery and possible cost savings with a chilled water setpoint of 4℃. The third set focused on producing the maximum service delivery from the cooling system with an evaporator outlet water temperature setpoint of 3℃.

It will be in the best interest for the mine to maintain an evaporator output temperature of 5℃ with the VSD initiative. It will realise in the most power savings for the mine whilst maintaining the same underground working conditions.

4.3. RECONFIGURATION OF EVAPORATOR PUMP IMPELLERS

Introduction

Figure 60 is a visual representation of mine A's cooling equipment. The evaporator pumps are located between the pre-cooling towers and the FPs. The evaporator pumps transport warm water from the second stage pre-cooling dam through the FPs to the BACs and chill dams. The FPs refrigerant gas extracts the heat from the warm water to produce chilled water. The longer the warm water is in the evaporator vessel the more heat can be transferred. Therefore, if the compressor guide vanes are already 100% open and the setpoint temperature is not achieved, the water flow rate can be reduced to lower the output evaporator water temperature.

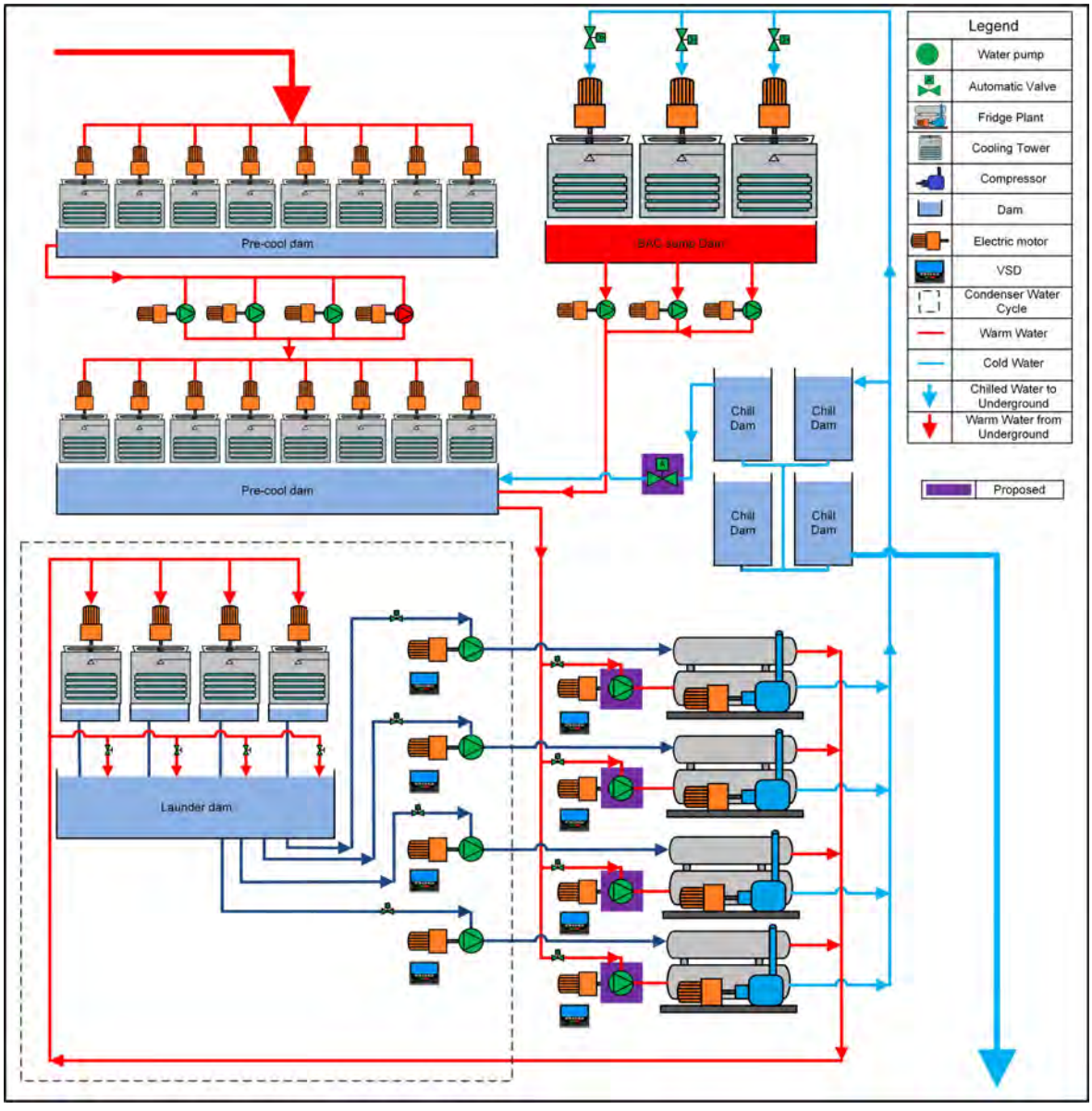

Figure 60: Mines A's cooling equipment layout

If funds are available, VSDs are installed on the evaporator pumps to regulate the water flow through the FPs. The VSDs reduce the water flow to ensure the output temperature is maintained. The water flow is increased when the water demand increases. According to mine employees, before VSD technology was available and affordable, it would be common practice to reduce the pump impeller size to reduce the water flow through the FPs[9&10]. The impeller size is reduced for a reduced water flow to increase the heat transfer, whilst at the same time meeting the water demand. An impeller with a reduced size for less flow has to be replaced with a full size impeller to restore the initial flow rate.

These changes are not always properly logged. It is of outmost importance for mine personnel to inform external investigating companies of these changes during project investigation. These changes were not noticed during the investigation stage of the project as the flow data for individual pumps was not available. The issue arose when analysing the improvements of the FPs COP after installing VSDs on the FP pumps for flow control because the plant COP did not improve as was expected.

Identifying inefficient operations

The OEM design specification of the FPs' evaporator water flow is 309 ℓ/s as Table 13 depicts. The evaporator water flow can be reduced to a minimum of 210 ℓ/s with the help of a VSD to decrease the evaporator output temperature. The evaporator water flow can be increased to a maximum of 350 ℓ/s if required to meet the mine's water demand during emergencies. From Equation 1 and Equation 5 it is evident that that when the water flow is reduced and the evaporator outlet water temperature decreases, the FPs' COP will increase. Figure 61 represent the FPs' average COP improvement after installation of the VSD initiative with and evaporator setpoint temperature of 5℃.

[9] Johan Barnard Mechanical Foreman
[10] Tony Kleinschmidt Senior Instrumentation Technician

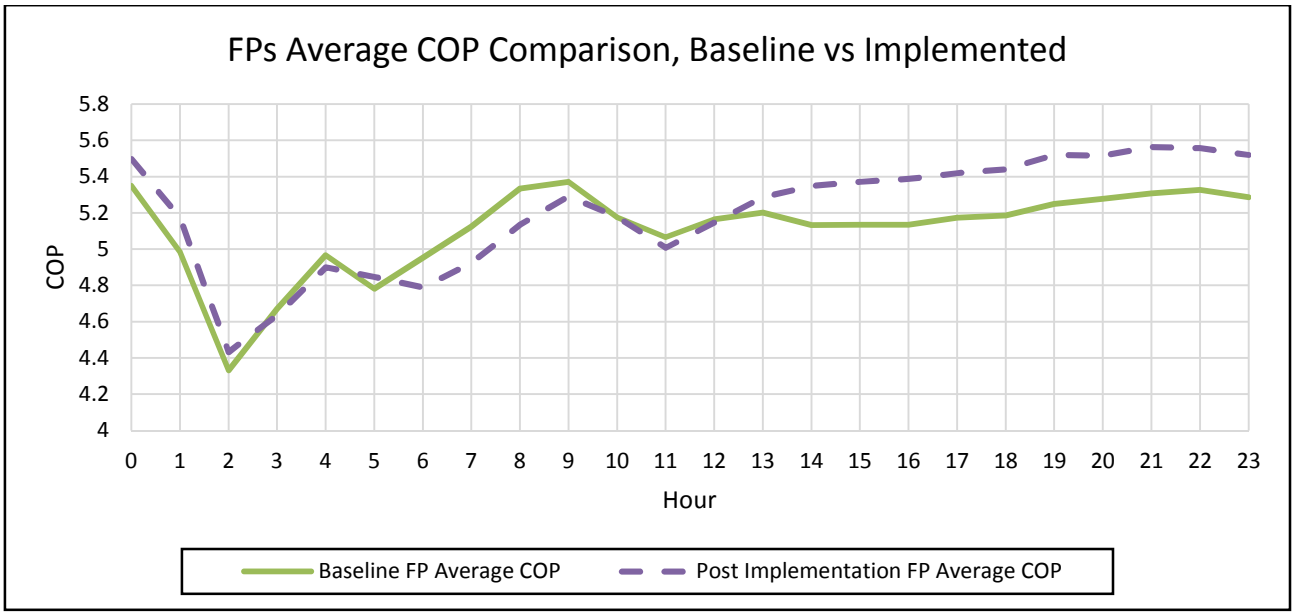

Figure 61: FPs average COP comparison, baseline vs. implemented for a 5℃ setpoint

Figure 61 indicates that, from implementing the VSD initiative, an average COP improvement of 1.78% was experienced with an evaporator outlet temperature setpoint of 5℃. Other researchers on VSD have proved implementation of VSD on FP evaporator circuits can result in a COP increase of up to 36% [15], [16], [21], [23], [28]. An improved COP relies on reduced flow and improved output temperature at reduced power consumption.

Three of Mine A's evaporator pump flows were already close to their minimum OEM water flow design specification; therefore there was little scope for a vast improved COP. Upon investigation mine personnel did not acknowledge that the pump impellers' sizes were reduced and that they delivered water flow below the FPs' design specification. If the evaporator water flow rate was at the normal design specification, the COP could have easily shown a vast improvement by installing VSDs to control the water flow, as explained in section 2.2.

A VSD controls the water flow by controlling the power supply's frequency. At 50 Hz the pump will deliver its maximum flow rate. Figure 62 represents the four FP's evaporator pump water flow plotted against different frequencies.

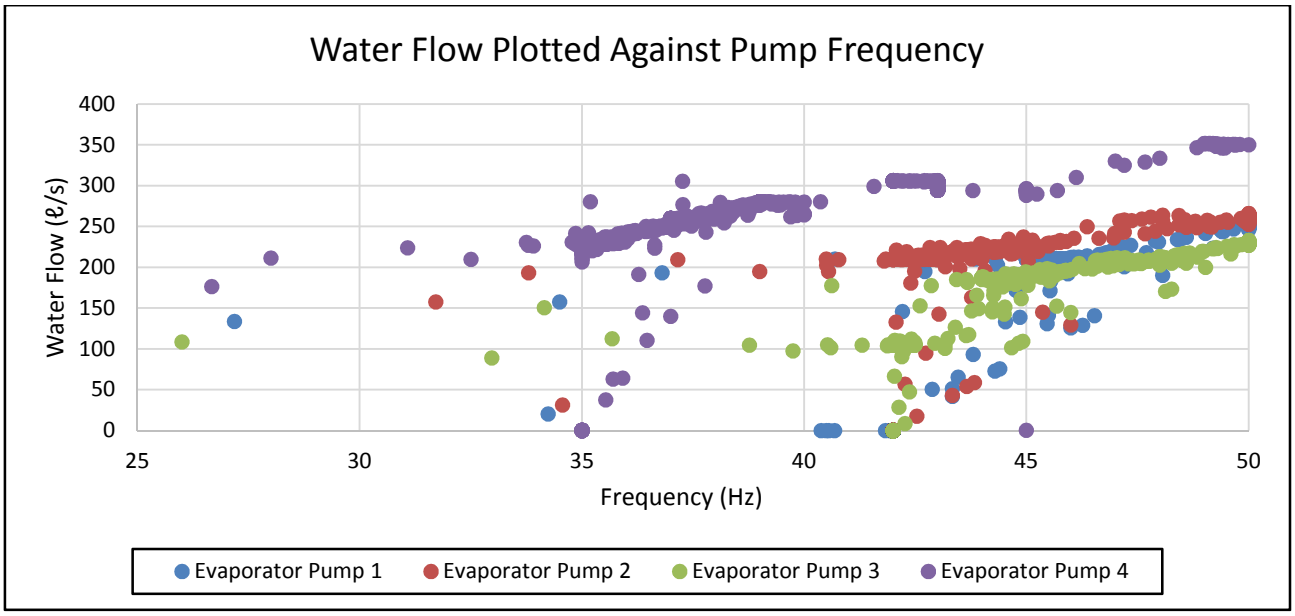

Figure 62: Evaporator pumps' water flows at different frequencies

Figure 62 indicates evaporator pump four is the only pump delivering the designed water flow rate. The evaporator pumps one to three do not deliver a water flow rate close to their design specification. At maximum frequency (50 Hz) these three pumps deliver a flow of between 230 and 250 ℓ/s, 22% below the FPs' OEM design water flow rate. It is evident from the cluster of plots that the VSD's control philosophy usually controls pumps one to three between 42 and 50 Hz, whilst pump four is usually controlled between 35 Hz and 40 Hz.

Mine personnel confirmed pump one to three's impellers were reduced to maintain a reduced flow rate[11&12]. FP four is a newly installed FP with correct specified condenser and evaporator pumps. Therefore, evaporator pump four delivers the correct water flow rate at maximum frequency. Figure 63 represents three FPs' evaporator pump power plotted against different frequencies.

[11] Johan Barnard — Mechanical Foreman
[12] Tony Kleinschmidt — Senior Instrumentation Technician

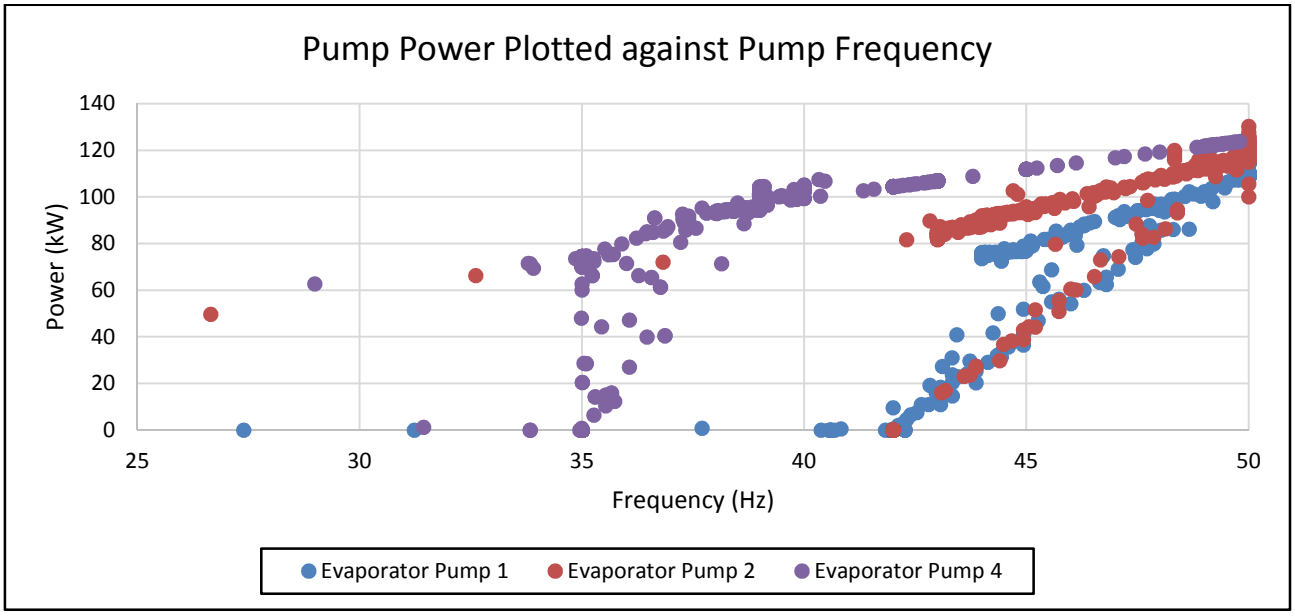

Figure 63: Evaporator pumps' power consumptions at different frequencies

From Figure 63 it can be seen that pump four's power utilisation is in the same vicinity as pumps one and two. However, between 35 and 40 Hz pump four utilises an average power of 78.5 kW to deliver an average water flow of 235.73 ℓ/s; conversely, between 40 Hz and 50 Hz pump one and two utilise an average power of 93.92 kW and 97.33 kW to deliver an average water flow of 210.05 ℓ/s and 198.71 ℓ/s respectively. Pump one and two are less efficient as they utilise more power than pump four to transport less water. Power data for pump three was not available during this period.

Replacing the pumps, or replacing only impellers of pumps one to three with a full size impeller to deliver the same water flow and efficiency as pump four, will be beneficial for the mine. During the summer months the pumps will consume less power to provide the same amount of water flow. The new pump impellers will enable the mine to increase the evaporator water flow rate to meet the mine's water demand in case of an emergency. During the winter months the mine will be able to run fewer evaporator pumps and still meet the underground water demand, since the BACs require less water. This will reduce the amount of chilled water being recycled during the winter months. Figure 64 represents the effect the reduction of evaporator water flow to ensure a lower evaporator outlet when the ambient temperature increase has on the amount of chilled water being recycled.

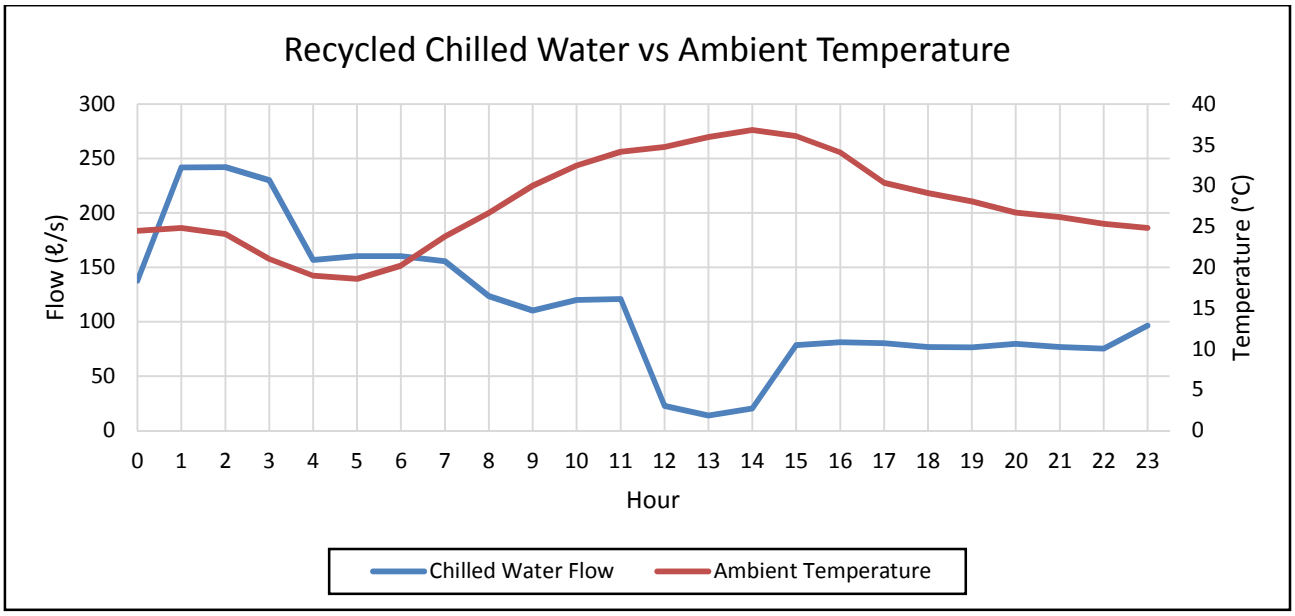

Figure 64: Recycled chilled water compared against ambient temperature

Figure 64 shows that when the ambient temperature is higher, the amount of chilled water being recycled is less than when compared to the amount of chilled water being recycled when the ambient temperature is lower. This is due to the VSDs reducing the water flow during the warmer parts of the day to maintain a constant evaporator outlet water temperature. This results in a decrease in recycled chilled water. Adding a control valve to the recycled chilled water will ensure the water is only recycled when it will be beneficial to the FPs' performance. This will reduce the amount of chilled water that is being recycled when the evaporator inlet water temperature is below a certain setpoint, and in return will reduce the amount of cooling that is being wasted.

Control philosophy reconfiguration

The impeller reconfiguration requires an adjustment to the current evaporator flow control philosophy. All the other control philosophies remain the same as in the preceding section. Two control strategies, one for summer and one for winter, will be developed for optimal operation. The summer control strategy will ensure the water demand and required output temperatures are met whilst utilising less power. The winter control strategy will focus on meeting the underground water demand whilst utilising the least number of pumps and still providing the lowest required water temperature.

Evaporator control strategy:

The following adjustments to the evaporator control strategy are applicable to both summer and winter control strategies:

- Replace the impellers of pump one to three with full size impellers to deliver the same water flow and efficiency as pump four.
- Change the evaporator pump's outlet temperature setpoint to 0.5℃ below the FP's compressor's guide vane evaporator outlet water temperature setpoint.
- Install an electronic valve with PI control on the recycled chilled water pipe line. The valve should control the recycled water flow to maintain a second stage pre-cool dam temperature below 14℃. This will ensure no cooling is lost due to chilled water being recycled when the evaporator inlet water temperature is below the required inlet temperature.

Evaporator summer control strategy:

All four FP's on: -The control philosophy will control the evaporator pump water flow to achieve an output setpoint temperature of 3.5℃ and maintain the chill dam level at 60%. The VSDs will be controlled according to the value returning the smallest from these two control philosophy.
-The FP compressors setpoint will be set to 4℃.

This will reduce the amount of chilled water being recycled whilst maintaining the optimal output chilled water temperature.

One or more FPs off: -The VSDs control the evaporator pump water flow to meet the chilled water demand.
- The FP compressor's setpoint will be set too 4℃.

During the winter months the ambient temperature drops drastically, causing the ambient psychrometric conditions to change. These changes increase the BACs and pre-cooling towers' service delivery, compared to the summer months. Improved BACs service deliveries allow the mine to isolate the BACs' chilled water flow and switch off some of the BACs until all three the BAC are switched off. The negative pressure from the extraction fans causes cool ambient air to be drawn underground to cool the underground environment during the winter months.

Isolated BACs resulted in a 399 ℓ/s chilled water demand decrease. In return almost two FPs can be isolated for maintenance if the correct control philosophy is implemented on the

other two FPs and evaporator pumps. The improved service delivery of the pre-cooling towers causes the evaporator inlet temperature to decrease below the minimum evaporator inlet temperatures. The FPs' tubes can freeze if the evaporator cools the water below 0℃, resulting in burst tubes. Therefore, all four FPs are switched off if the inlet temperature decreases below 10℃. As the water temperature increases, more FPs are switched on; up to a maximum of three FPs during the winter.

Sometimes three evaporator pumps are running with only one FP being on to meet the underground water demand. These three evaporator pumps deliver more water flow than the underground water demand, resulting in an increased recycled chill water. Running only two evaporator pumps will not meet the chill water demand. If an additional pump is started it will cause the pump to cycle in order to maintain the chill dam at 60%. Pump cycle can cause mechanical failure of the pump.

The maximum amount of FPs will be switched on depending on the ambient psychrometric conditions. This will ensure the optimal chilled water temperature is maintained.

Evaporator winter control strategy:

Two or more FPs switched on: -The VSD controls the evaporator pump water flow to achieve an output setpoint temperature of 5℃.
-The FP compressors setpoint will be set too 5℃.

Less than two FPs available : -The VSD controls the evaporator pump water flow to meet the underground water demand utilising Equation 24.

$$\dot{m}_{EvapVSDWater\ FP\ Off} = \dot{m}_{WaterDemand} - \dot{m}_{EvapVSDWater\ FP\ On} \quad (24)$$

$\dot{m}_{WaterDemand}$ = Underground Water Demand (kg/s)
$\dot{m}_{EvapVSDWater\ FP\ Off}$ = VSD Evaporator Water Flow FPs Off(kg/s)
$\dot{m}_{EvapVSDWater\ FP\ On}$ = VSD Evaporator Water Flow FPs On(kg/s)

The control philosophy will ensure the water demand is always met whilst obtaining the maximum service delivery from the FPs that are on. The evaporator pumps from the FPs that are off will allow the minimum water flow to maintain a constant chill dam level and

prevent the chill dam temperature from increasing too drastically. As soon as the ambient psychrometric conditions allow an additional FPs to be switched on, the evaporator pumps will be controlled to maintain the evaporator outlet temperature setpoint. If the chill dam level is within its control range the VSD's minimum frequencies will be determined by Equation 24.

Should the chill dam level be below its allowable ranges, the minimum water flow will be determined with Equation 25. The evaporator water flow will be increased by 10% until the chill dam level is within its allowable ranges. Then the evaporator water flow will be set to meet the chill water demand. This will ensure the chill dam level increases without increasing the chill dam water temperature with water that was not cooled.

$$\dot{m}_{EvapMinWater} = \frac{(\dot{m}_{WaterDemand}) * 110\%}{N_{Available\ FPs}} \quad (25)$$

$\dot{m}_{WaterDemand}$ = Underground Water Demand (kg/s)

$\dot{m}_{EvapVSDMinWater}$ = VSD Minimum Evaporator Water Flow(kg/s)

$N_{Available\ FPs}$ = Number of Available FPs (-)

Simulation validation process

Complications between the contractor and mine A resulted in only the evaporator pump three impeller being replaced. The simulation will be validated with the actual data from the pump with the replaced impeller. The inefficient pumps within the simulation will be updated with the same data as the validated pump. This will ensure that accurate prediction can be made from the simulation outputs. The pump with the replaced impeller ensures an overall water flow improvement at a lower frequency as seen from Figure 65.

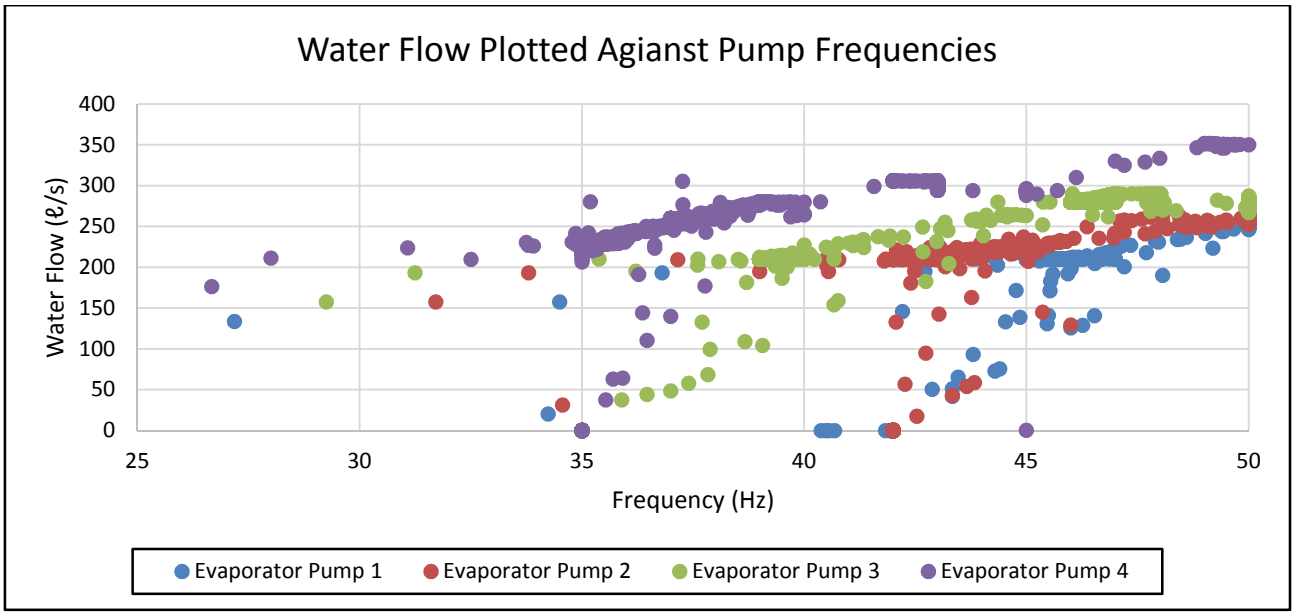

Figure 65: New evaporator impeller improved water flow plotted against different frequencies

Figure 65 depicts the new impeller of pump three, which delivers an improved water flow rate, better than the old impellers but not as good as the evaporator pump four. The maximum water flow that pump three can deliver is 290 ℓ/s, 19 ℓ/s below the design flow rate. This is due to inefficiencies in the pump housing and electric motor. Figure 66 depicts the new pump impellers power consumption plotted against different frequencies.

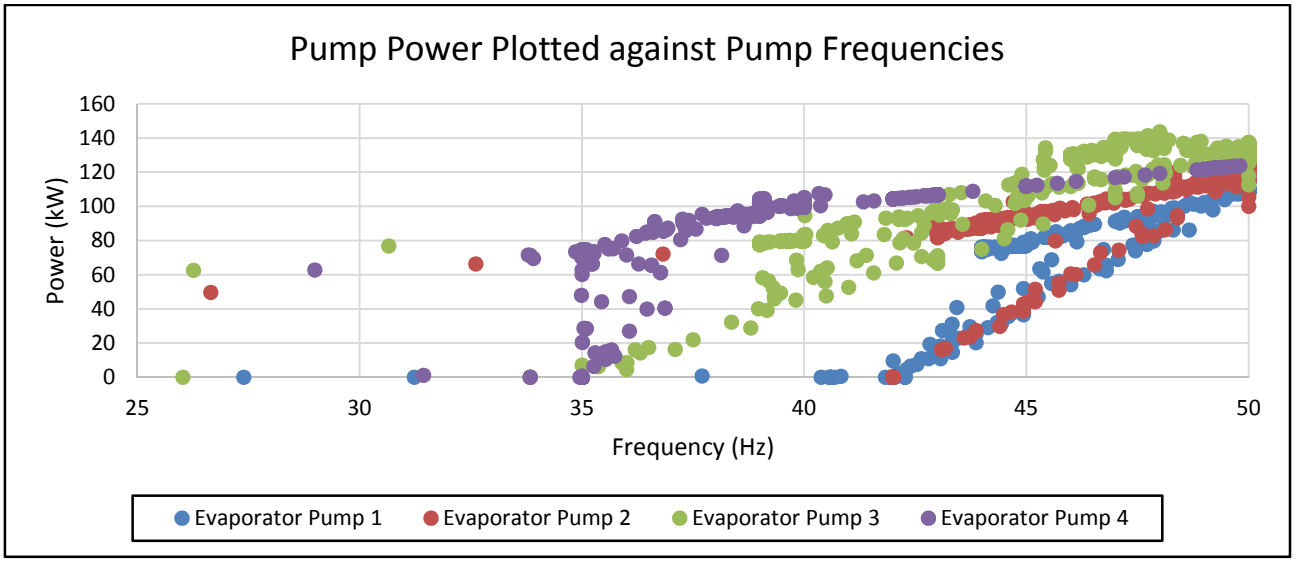

Figure 66: New evaporator impeller power plotted against different frequencies

Figure 66 indicates that pump three's power is between 45 and 50 Hz more than the other pumps. This is due to the pump housing and motor being inefficient. Fortunately the pump will be controlled between 37 and 42 Hz to provide an average flow of 210 ℓ/s. At this flow

rate the pump will utilise 80 kW power. If evaporator pumps one and two were to be replaced with a similar impeller delivering the same amount of water flow as pump two power savings can be realised. Figure 67 and Figure 68 represent a comparison between, actual water flow of a specific day with the VSD controlling the evaporator pumps, the simulated water flow with the same control philosophy and the maximum simulated water flow of evaporator pump three and four respectively.

The simulation evaporator pumps were set to maximum flow rate for a day to determine the simulated maximum water flow. This can also be seen in Figure 67.

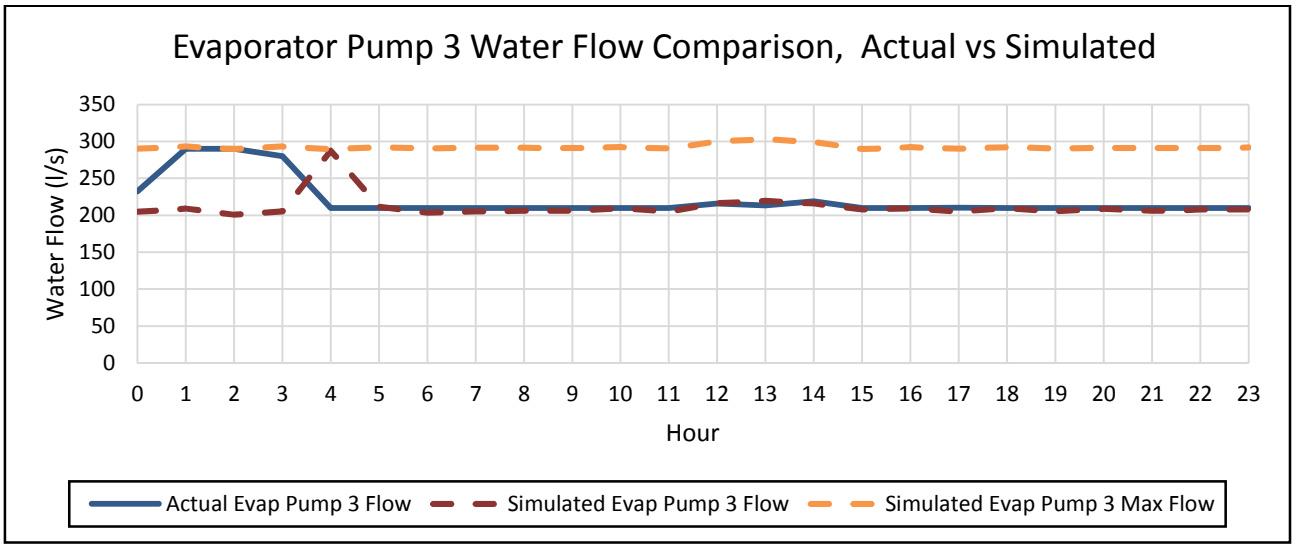

Figure 67: Evaporator pump 3 water flow comparison, baseline vs. implemented

Figure 67 depicts the minimum water flow of the simulation and the actual data, which correlate with one another. The simulation does not reduce the water flow more than the VSD reduces the actual water flow. The simulated evaporator pump three maximum water flow is in the vicinity of 290 ℓ/s; when compared to Figure 65 one can see the simulation allows the same maximum water flow as the actual pump at its full capacity (50Hz). Figure 68 represents the actual and simulated water flow properties of evaporator pump four.

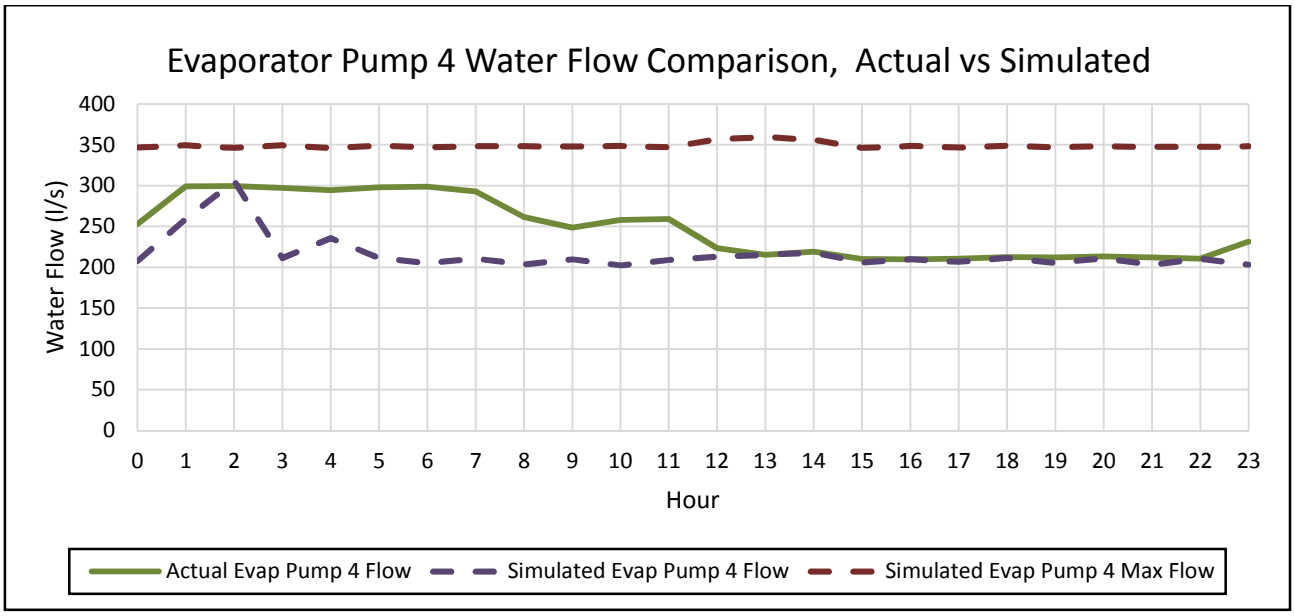

Figure 68: Evaporator pump 4 water flow comparison, baseline vs. implemented

Figure 68 shows that the minimum water flow of the simulation and the actual data correlate with one another. The simulation does not reduce the water flow more than the VSDs reduce the actual water flow. The simulated evaporator pump four's maximum water flow is in the vicinity of 350 ℓ/s; comparing this to Figure 65 one can see the simulation allows the same maximum water flow as the actual pump at its full capacity (50Hz).

The assumption can be made that, if pump one and two are replaced with a pump with the same properties as pump three, the maximum water flow would be achieved with all three the pumps. The simulation was adapted accordingly.

Results

The simulation of the pump flow control will be considered as the baseline simulation, as mine A already made the reconfiguration and any additional reconfiguration would include the pump flow control upgrade. A winter baseline was developed with the average winter ambient psychrometric conditions. The new control philosophies were simulated for the summer and winter conditions. Table 14 represents the daily average ambient psychrometric conditions for the summer and winter conditions.

Table 14: Winter and summer daily average ambient psychrometric conditions

Outputs	Unit	Summer		Winter	
		Average Baseline	Average Implemented	Average Baseline	Average Implemented
Water from Underground Temperature	°C	25.98	25.98	25.98	25.98
Ambient Temperature	°C	22.07	22.07	10.25	10.25
Humidity	%	67.67	67.67	52.44	52.44
Pressure	kPa	80.00	80.00	80.00	80.00

From Table 14 it is evident that the same ambient psychrometric conditions were used when determining the power savings or improved service delivery. Figure 69 is a representation of the daily average winter and summer ambient psychrometric conditions.

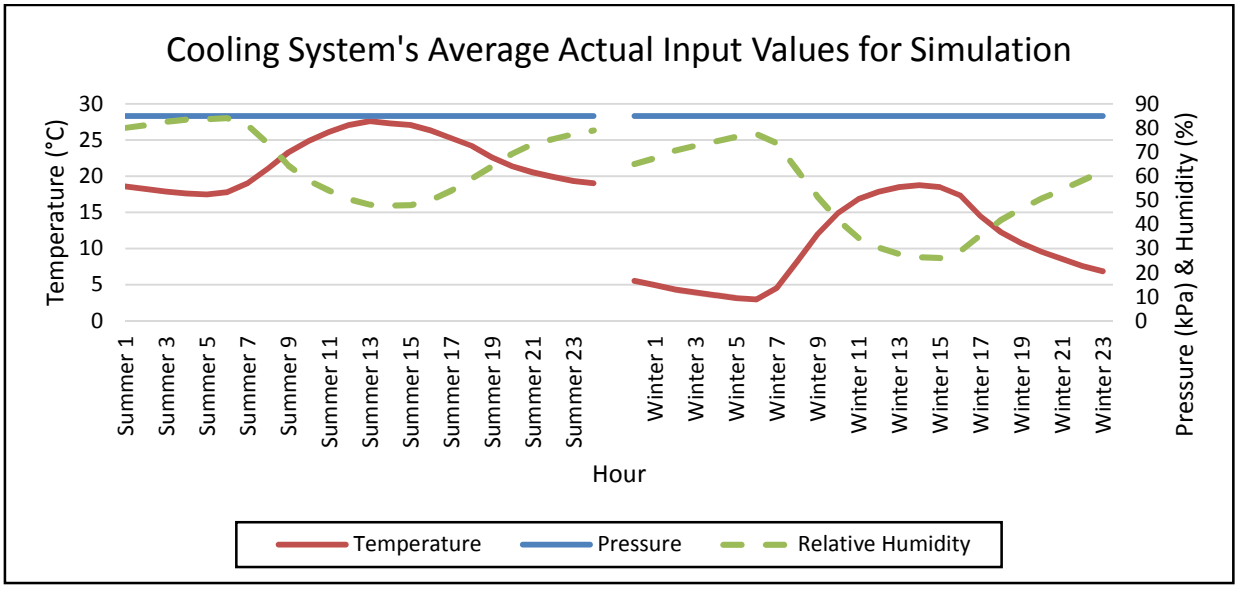

Figure 69: Winter and summer daily average ambient psychrometric conditions

It is evident from Figure 69 that the average ambient temperature is much lower during the winter season than in the summer season. The average atmospheric pressure stays constant at 85 kPa. The humidity is lower during the winter months. During the summer and winter season the humidity decreases as the temperature increases and vice versa.

The simulated results will be divided into a summer and winter section, whereby the summer results consist of three simulations; one for maximum energy savings with an evaporator setpoint of 5℃ , one for the mine's preferred setpoint of 4℃ and one for maximum service delivery with a setpoint of 3℃. The winter simulations will only focus on energy savings with a setpoint of 5℃. The increased setpoint will enable the mine to start the FPs sooner as

the colder ambient conditions cause the FPs to trip on low evaporator inlet water temperature.

Summer

The replacement of the evaporator pump impellers will not have a vast impact on the summer month's power savings or service delivery as the VSDs will reduce the flow to the same minimum flow for maximum heat transfer. However, the control philosophy adjustment and the installation of a control valve on the recycle chilled water valve will increase the power savings as wastage of cooling will be kept to a minimum. Figure 70 depicts the power usage of the cooling equipment.

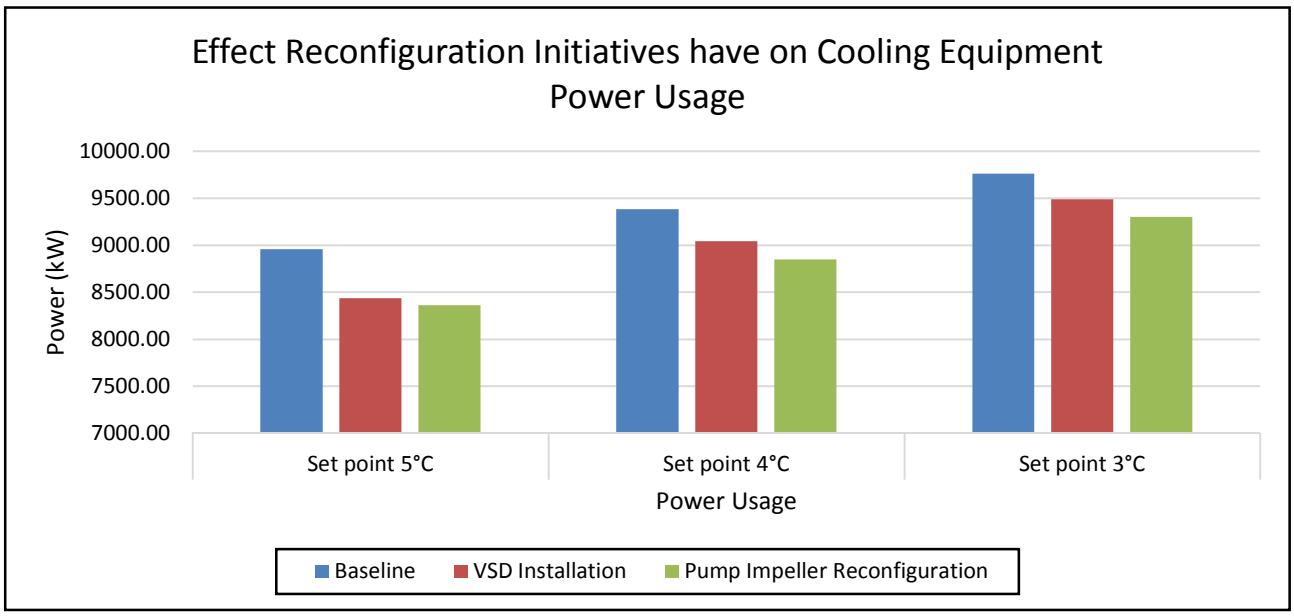

Figure 70: Cooling equipment total power usage comparison

From Figure 70 it is evident that the new control philosophy resulted in a reduced power consumption for all three of the different evaporator output water temperature setpoints. Figure 71 represents the accumulative power savings realised by adding the FPs' pump control, replacement of the pump impellers and the new control philosophy.

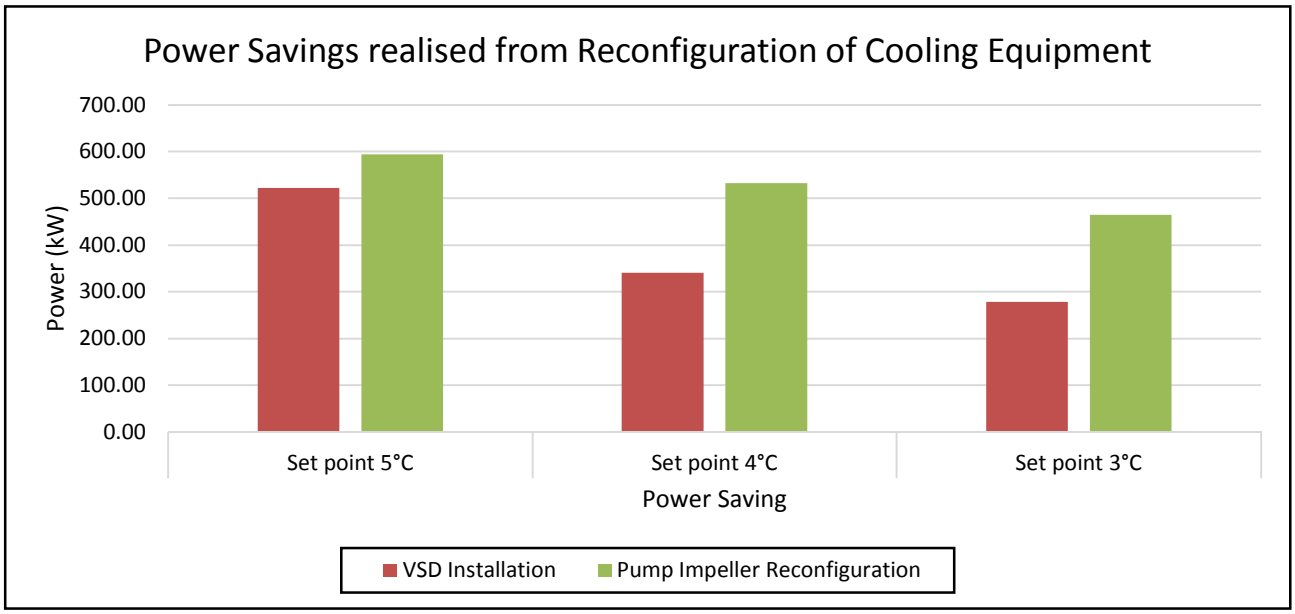

Figure 71: Power savings realised from reconfiguration of a mine's cooling equipment

Figure 71 shows that a greater power saving will realise when the evaporator outlet water temperature setpoint is 4℃ and 3℃, compared to a setpoint of 5℃. This is due to the fact that less chilled water has to be recycled, if the chilled water temperature of the recycled water is lower. This allowed the evaporator pumps to reduce the flow through the FPs and maintain the required chill dam level. Figure 72 compares the effect that all the reconfigurations have on the cooling system's output temperatures if the setpoint is 5℃.

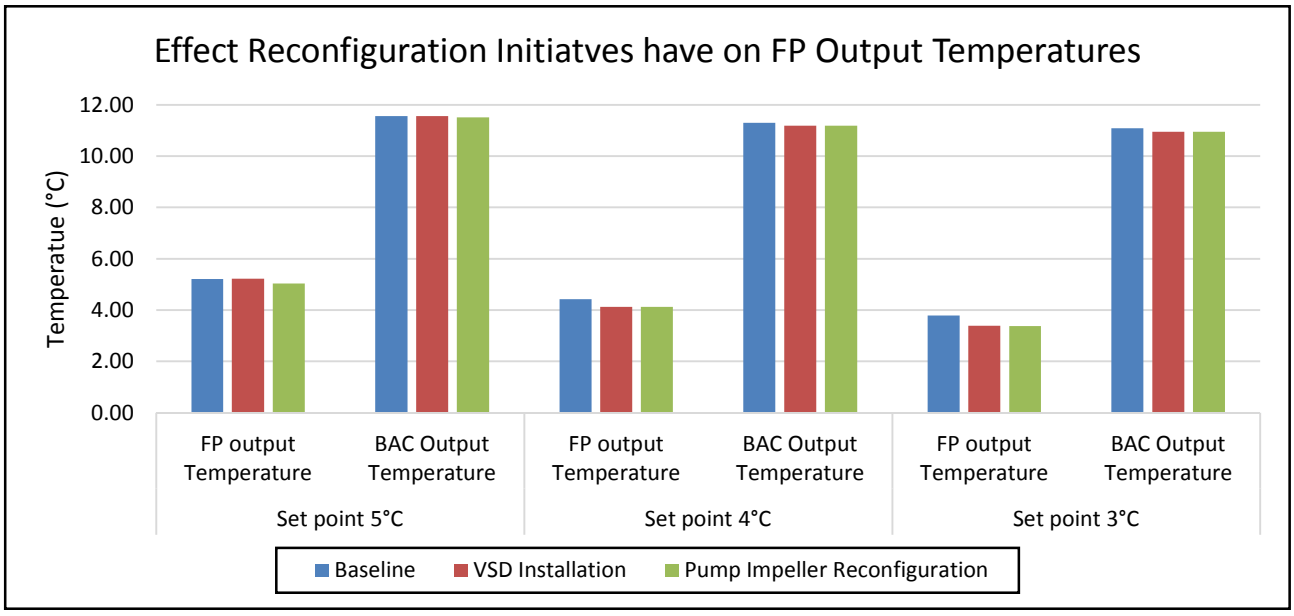

Figure 72: Effect reconfiguring initiatives have on cooling system outlet temperatures

Figure 72 depicts the 5℃ simulation service delivery increased by 3.44% and 0.46% for the FPs outlet water and BAC outlet WB air temperatures, respectively. The service deliveries for the evaporator outlet water temperature setpoint set to 4℃ and 3℃ were not affected by the replaced impellers. The majority of the power savings for the reconfiguration of the pump impellers will realise during the winter months. The winter power savings will have a vast impact on the mine's electricity cost as the electricity tariffs are more than double the summer price during the Eskom winter peak periods [102].

Winter

A new winter baseline simulation was developed with three months average winter ambient psychrometric conditions. The prescribed winter control philosophy was simulated with the replaced pump impellers and compared against the winter baseline simulation with the old impellers and control philosophy. Figure 73 depicts a summary of the winter simulation's power and evaporator output water temperatures. The results do not compare the BACs' outputs conditions as the BACs are switched off during the winter months.

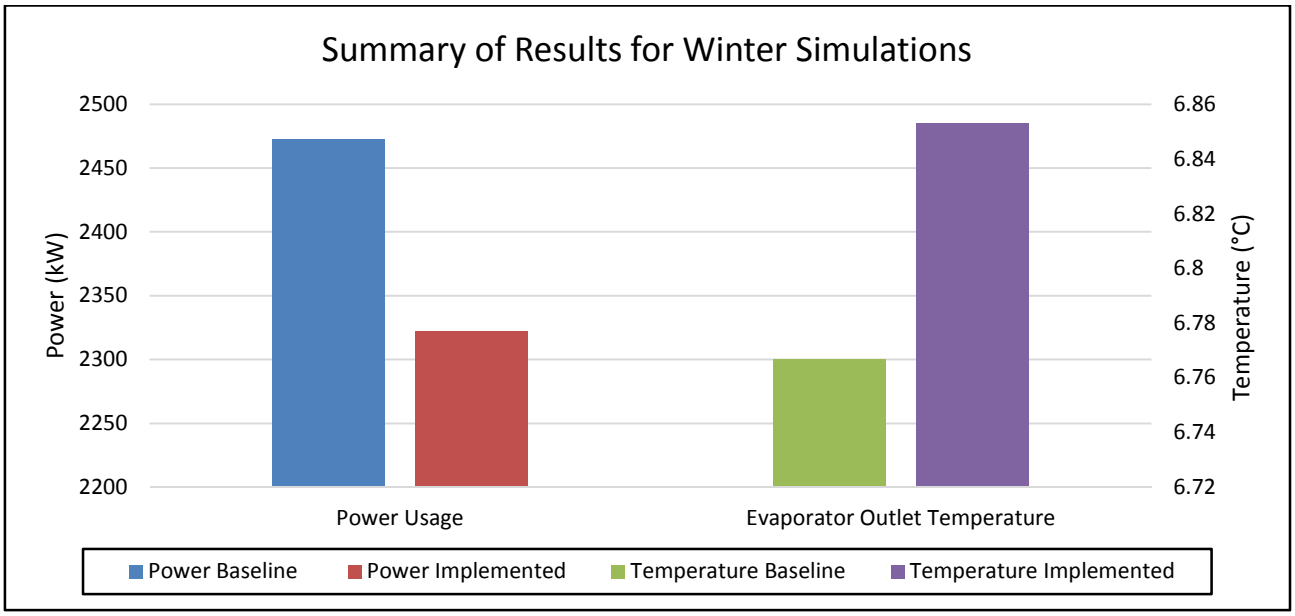

Figure 73: Effect that reconfiguring of evaporator pump impellers has on the FPs outputs during the winter months

Figure 73 depicts that a power saving of 150.62 kW will be realised during the winter months by switching of an additional pump. A power saving of 6.09% on a 2 321.83 kW power usage is a significant power saving. During the summer months a saving of 0.85% can be realised on a power usage of 8 363.48 kW. An evaporator outlet water temperature increase of 0.81℃ will not affect the underground working conditions significantly.

The increase in evaporator outlet water temperature is due to the evaporator flow being decreased. This causes less chilled water to be recycled, increasing the evaporator inlet water temperature. A detailed analysis of the effect replacing the evaporator pump impellers has on the cooling system can be found in Appendix D.

Conclusion - Reconfiguration of evaporator pump impellers

The need for replacing the evaporator pump impellers was identified. The effect that the reconfiguration has on the cooling system was simulated as the mine has not completed the installation of the new evaporator pump impellers. The installation of the control valve on the recycled chilled water and the updated control philosophy will ensure cost savings during the summer months without affecting the system's service delivery. However, the evaporator pump impeller reconfiguration will result in significant power saving during the winter months.

4.4. RECONFIGURATION OF BULK AIR COOLERS

Introduction

At mine A, three BACs are utilised to cool the ambient air before it is sent underground. The BACs utilise chilled water from the FPs to cool the underground environment. The warmer BACs' return water is pumped to the second stage pre-cooling dam before it is cooled by the FPs. The cooled air reduces the air temperature and dehumidifies the underground working conditions. Table 15 summarises the BACs' current operations, OEM design and mine's expected operating conditions.

Table 15: BACs' specifications

Summary of Average Cooling System's Outputs.				
Variable	**Unit**	**Current**	**Design**	**Mine Expectation**
Water Flow to a BAC	ℓ/s	133	150	133
BAC Outlet WB Air Temperature	°C	12.5	9	11 - 12

From Table 15 it is clear that the BACs are operating below the design specifications. Upon investigation the BACs were identified as inefficient. The first initiative will ensure no cooling is wasted to increase the power savings and the second initiative will help improve the service delivery of the BAC. Figure 74 shows the location of the BAC at mine A and identifies the components requiring reconfiguration.

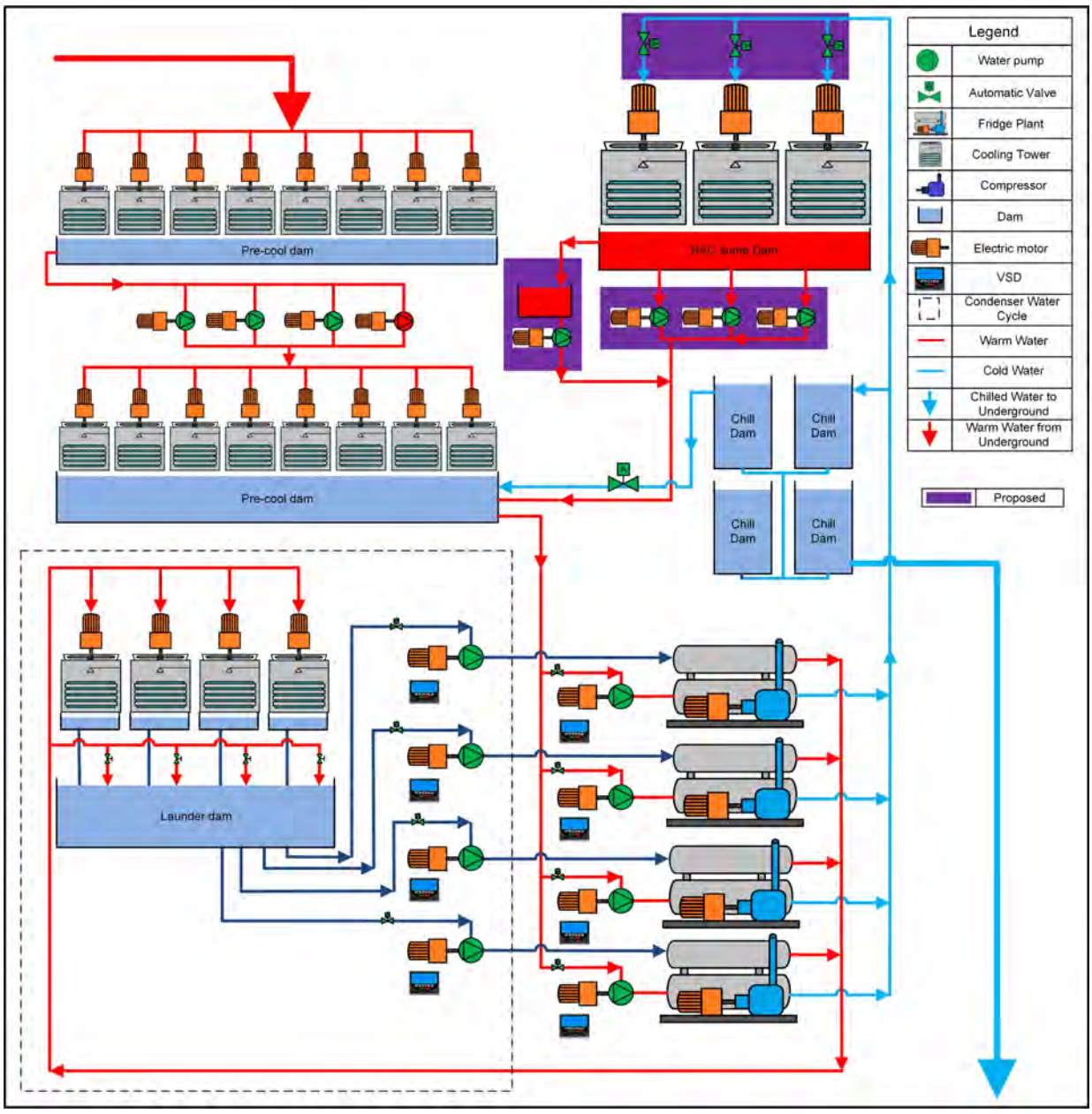

Figure 74: Mine A's BAC reconfiguration

Figure 74 indicates that the BACs' chilled water is provided by the FPs' evaporator cycle. The BACs are geologically lower than the FPs, allowing the chilled water to be gravity fed to the BACs. Currently, valves are throttled to maintain a constant chilled water flow through the BACs. BAC sump pumps maintain the BAC sump dam level between the allowable limits. The BAC overflow dam allows the BAC water to overflow. The BAC overflow dam is emptied with a small 8 kW pump.

Identifying inefficient operations

The valves are throttled to provide each BAC with a constant water flow of 133 ℓ/s. However, if the ambient temperature decreases, chilled water is being wasted. The BACs are provided with too much chilled water, this is evident from the reduction in BAC outlet water temperature when the ambient temperature decreases. Figure 75 represents the BAC's actual inlet water -, ambient DB - and outlet water temperatures with a constant chilled water flow of 399 ℓ/s through the BACs.

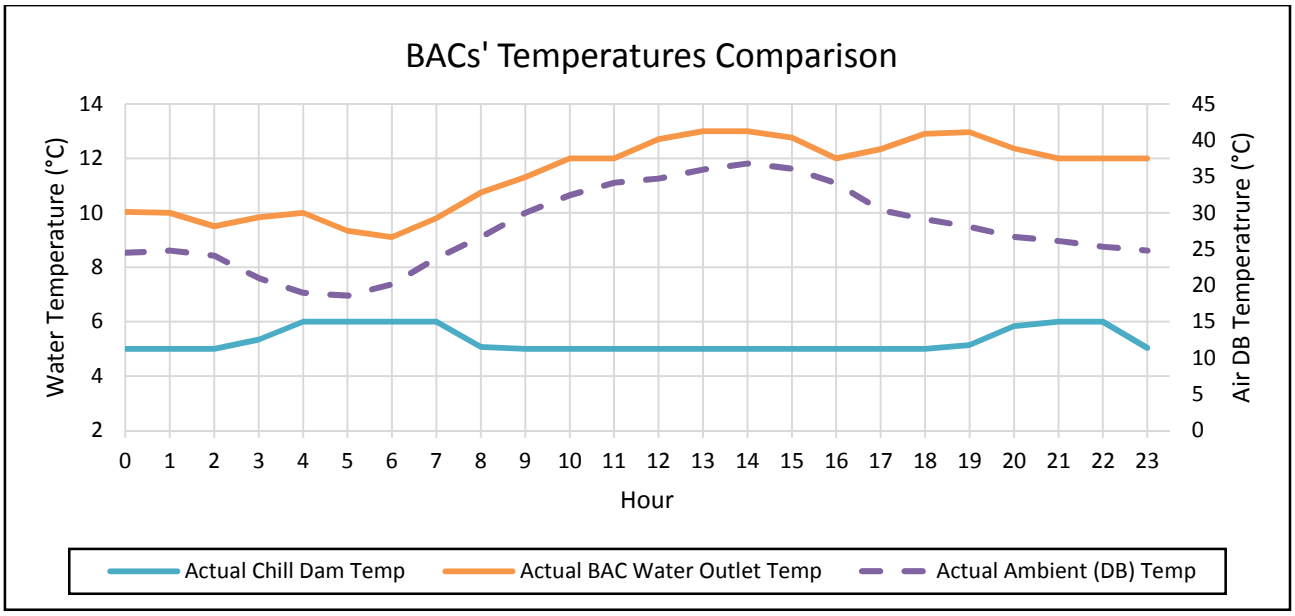

Figure 75: BACs actual temperature comparisons

From Figure 75 it is evident that, when the ambient temperature decreases, the BAC outlet water temperature decreases due the BAC not utilising all of the cooling provided by the chilled water. During this period the chilled water flow through the BACs can be reduced to ensure the BAC utilises all the provided cooling. Automating valves will enable the mine to provide the BACs with the correct amount of chilled water flow to maintain a constant BAC outlet WB air temperature. Figure 76 represents the BACs' daily average water flow and pump statuses.

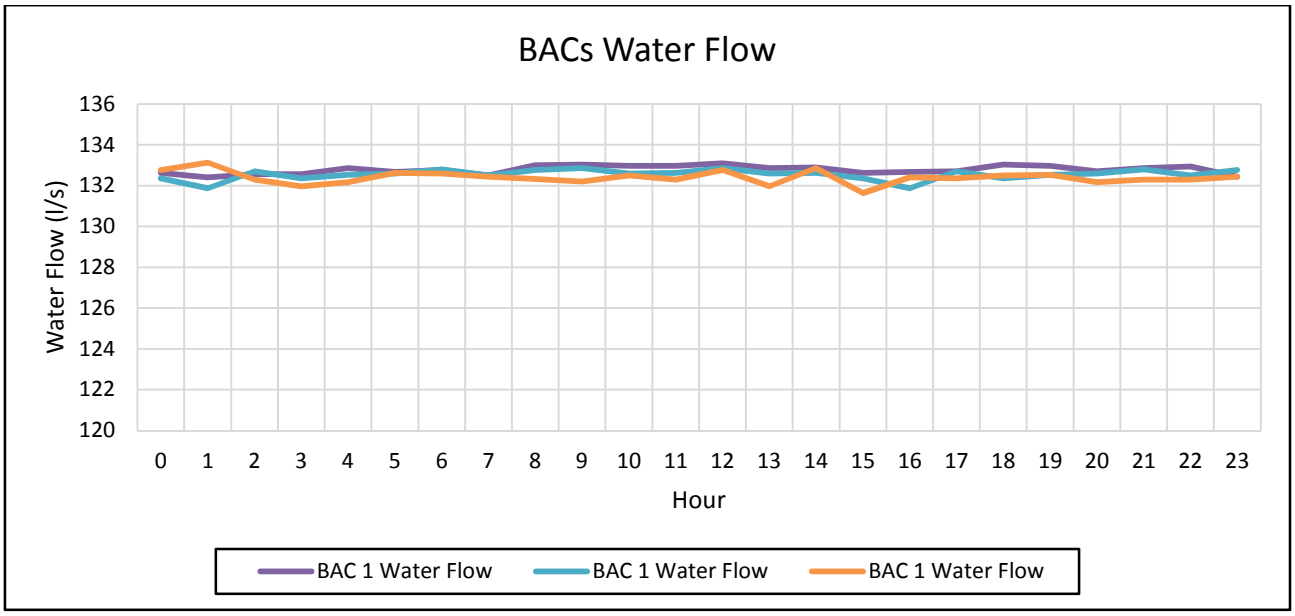

Figure 76: BAC pumps water flow

Figure 76 depicts that the average chilled water flow into a BAC is 133 ℓ/s. Currently, mine A throttles manual valves to maintain a constant chilled water flow into the BACs. Figure 77 represents statuses of the BAC sump dam pumps.

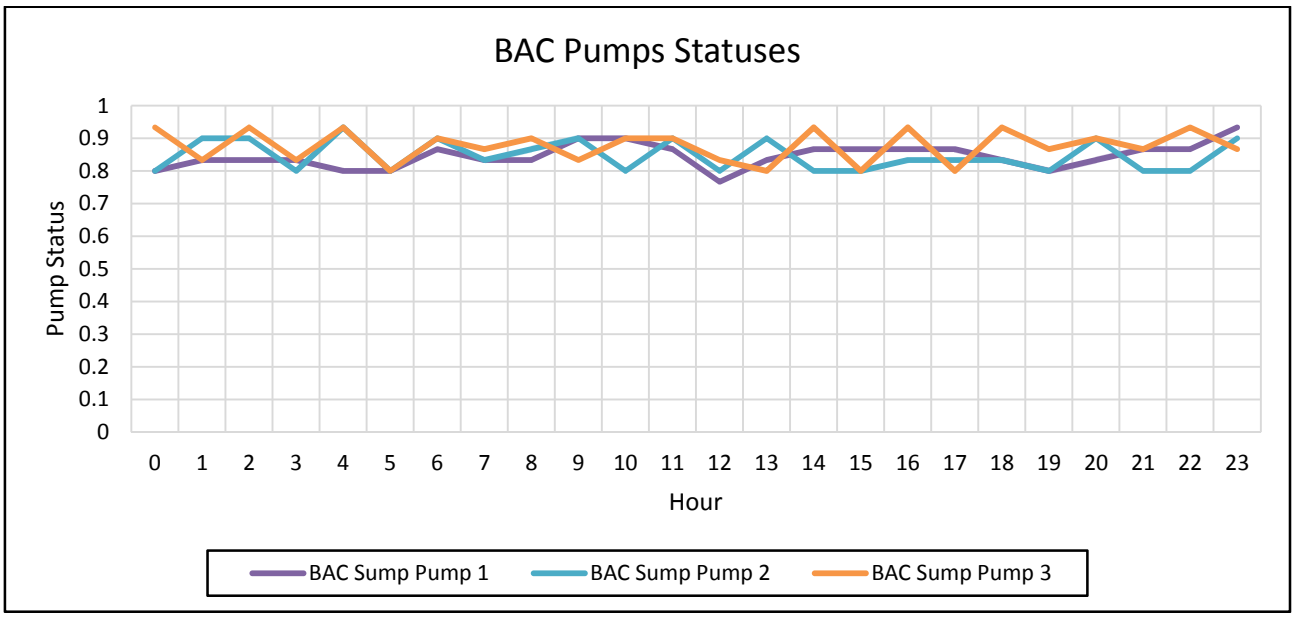

Figure 77: BAC pump statuses

Figure 77 depicts the BAC sump dam pump's pumping status to maintain an acceptable BAC sump dam level. The BAC sump pumps are controlled to maintain BAC sump dam levels between 40% and 75%. Each BAC pump can deliver more than 133 ℓ/s as the pumps

are utilised 85% of the day. Unfortunately there is no water flow meter installed to measure the BAC pump's flow rate. Figure 78 represents the average BAC water flow plotted against the average BAC pump status to theoretically calculate the maximum BAC sump pump water flow.

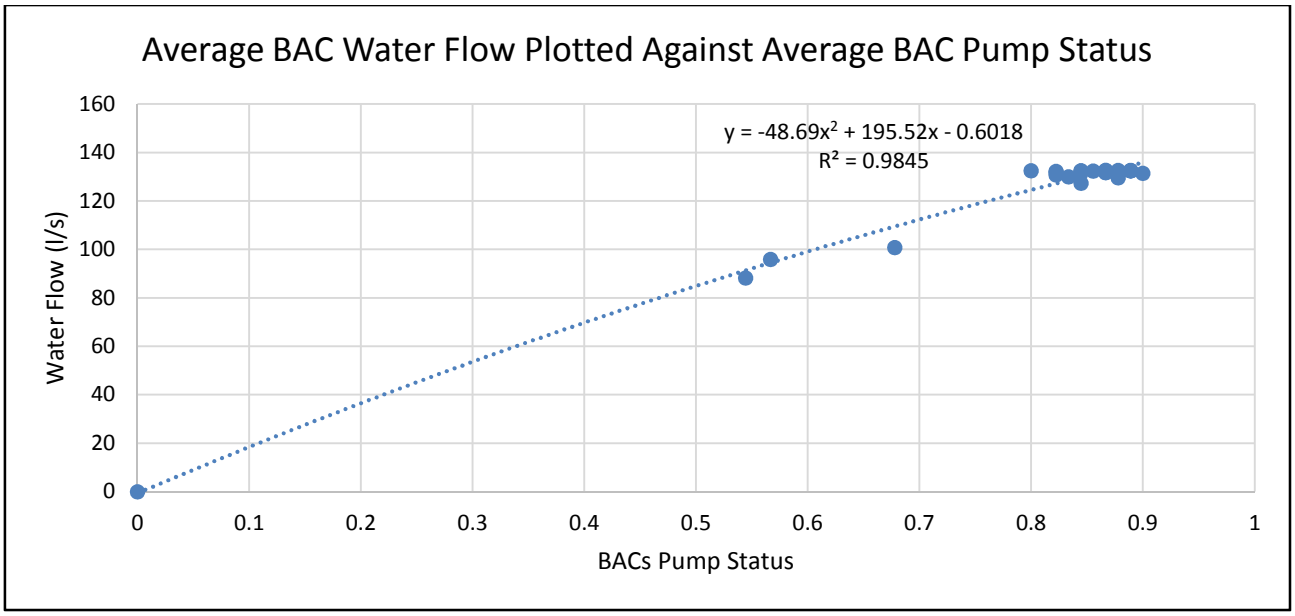

Figure 78: Average BAC water flow plotted against average BAC pump status

From Figure 78 it is evident the data has a 97.70% coefficient of correlation. The regression line formula is also represented on the graph. Submitting a running status of one in the formula will determine that the maximum water flow that a BAC sump dam pump can deliver, is 146.23 ℓ/s. Therefore, the maximum chilled water through the BACs can be set to the design specification of 150 ℓ/s. The additional 3.77 ℓ/s will overflow into the BAC overflow dam and be returned to the second stage pre-cooling dam via the overflow pump. This will not only improve the service delivery of the BAC, but will also increase the power consumption of the FPs as more chilled water is needed.

If the BAC sump pumps are not able to handle the increased water flow, the sump dam will overflow into the BAC overflow dam. Currently the dam is very small with an 8 kW pump. It will be more cost effective for the mine to increase the overflow dam capacity and the pump than to replace all three the BAC sump dam pumps. The overflow pump should have the same specifications as the BAC sump dam pumps to provide a water flow of 150 ℓ/s. This will help the mine with the maintenance of the pumps as they could be swapped around if one of the pumps should fail.

The prescribed control philosophy will also allow the mine to lower the BAC sump dam level when the chilled water flow into the BACs are reduced due to lower ambient temperatures.

Control philosophy reconfiguration

The control philosophy will be divided into two sections. The first section will aim to increase the power savings whilst maintaining the same service delivery. Section two will focus on improving the BACs' service delivery. The chilled water flow will be increased to the BACs' OEM design specification water flow of 150 ℓ/s, whilst utilising the same control philosophy to reduce the chilled water flow when the ambient temperature decreases.

BACs' control strategy for energy savings:
Automate the BACs inlet chilled water valves. Control the BAC inlet valves to maintain a BACs outlet WB air temperature according a setpoint. The valves should not allow more than the maximum water flow of 133l /s through the BAC. The BAC outlet WB air temperature setpoint should be set to the average achievable WB temperature without the valve flow control. This will ensure that the same average BAC outlet WB air temperature is maintained.

BACs control strategy for maximum service delivery:
The BAC water flow control valves are controlled to the same prescribed control philosophy. The maximum water flow is set to 150 ℓ/s. For a safety precaution, the BAC overflow dam capacity is increased and upgraded with a larger pump. The overflow pump should have the same specifications as the BACs' sump dam pumps delivering the same amount of water flow. This will ensure pump versatility during an unforeseen pump breakdown.

The valve control philosophy will prevent the BAC sump dam from continuously overflowing. This will only occur during the warmer periods of the day when maximum cooling is required from the BACs and the pumps cannot empty the dams in time. When the ambient conditions are more favourable, the BACs' inlet valves will reduce the chilled water flow to the BACs. During these periods the BAC pumps will be able to lower the BAC dam level in order to prepare for the increased water flow during the warmer periods of the day.

Simulation validation process

The currently installed BAC simulation was validated in section 3.5. The reconfiguration was simulated to obtain the results. Unfortunately mine A did not have funds available to do the PLC development for the valve control or the reconfiguring of their BAC overflow dam and pumps.

In the simulation the BAC sump dam pumps are specified to deliver a maximum water flow rate of 150 ℓ/s. The pumps are then controlled by a step controller to maintain a BAC sump dam level between 40% and 75%. Currently the BAC inlet chilled water flow is set at a constant flow of 133 ℓ/s.

Results

The preceding simulation with the reconfigured pump impellers will be considered as the baseline as mine A already commenced with replacing of the pump impellers. The results will be divided into two section. The first section will include the automation of the BAC chilled water valves for energy savings with a maximum chilled water flow of 133 ℓ/s. The second section will include the updated chilled water valve control philosophies, however the maximum chilled water flow rate will be increased to 150 ℓ/s for optimal operation. Figure 79 represents the BACs' outlet air WB temperature for the baseline simulation and the setpoints for the implemented simulations.

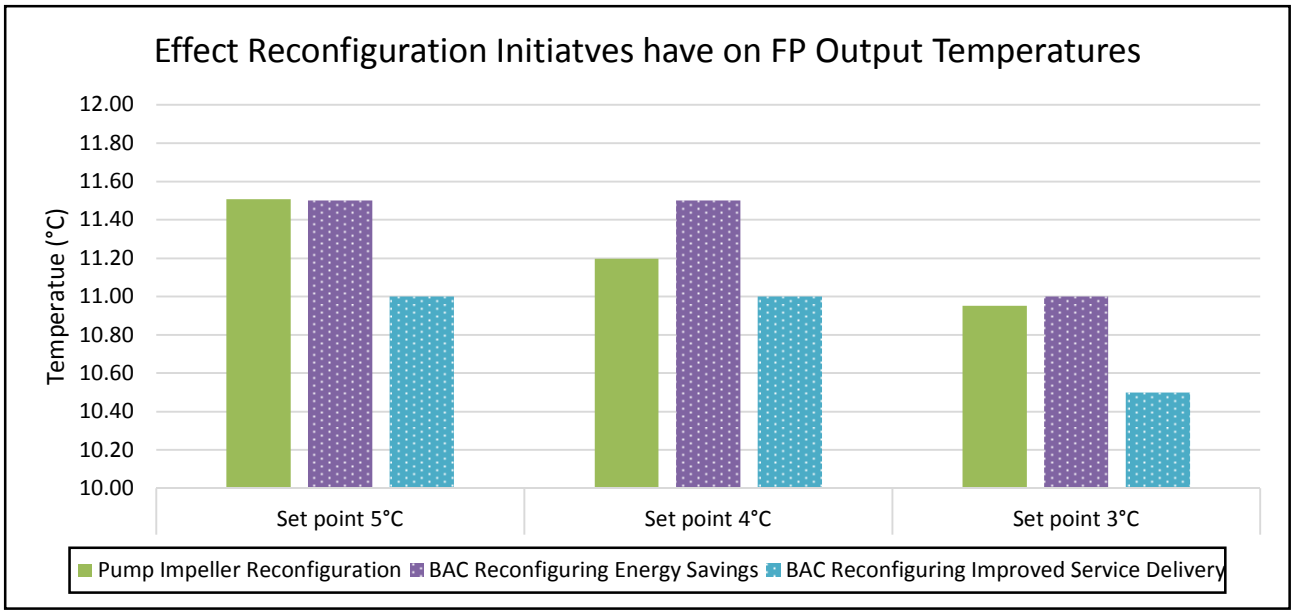

Figure 79: BACs' outlet air WB temperature setpoint for different simulations

Figure 79 depicts the outlet air WB temperature maintained during the baseline simulations with the evaporator outlet temperature set to 5℃, 4℃ and 3℃ respectively. The BAC outlet air WB temperature was set to 11.5℃ to maintain an acceptable underground working environment and increase the power savings.

The BAC outlet air WB temperature setpoint for improved service delivery was determined by updating the simulation with a BAC setpoint of 9℃ to determine minimum achievable output temperature by the BACs. The BACs' valve control was updated to control the chilled water flow to maintain the specific outlet air WB temperature. This will ensure the chilled water demand is decreased when the ambient temperature decreases and will prevent wastage of cooling. Figure 80 represents the effect the different reconfiguration initiatives have on the cooling systems' power usage.

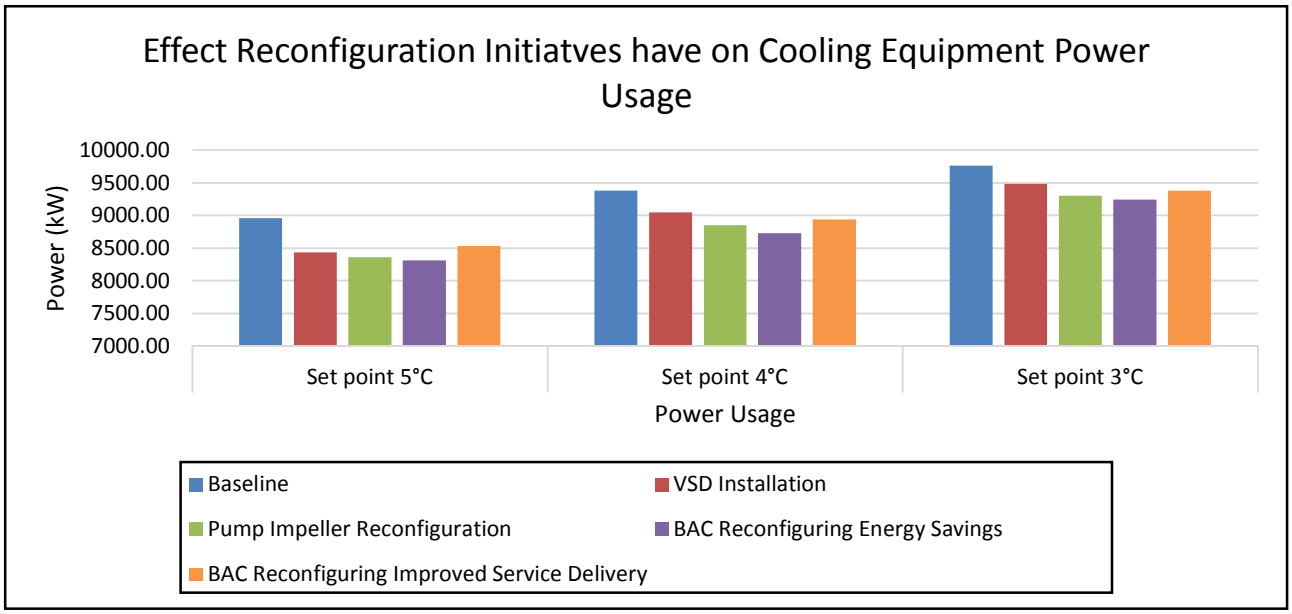

Figure 80: Cooling equipment total power usage comparison

Figure 80 depicts that the power usage increased as the evaporator output setpoint decreases. The power usage increases as the BACs service delivery increases due to an increased chilled water demand, resulting in an increased power usage by the FPs and the BAC return pumps. Figure 81 represents the accumulative power savings realised from the addition of the FPs pump control, replacement of the evaporator pump impellers and the BAC reconfiguration.

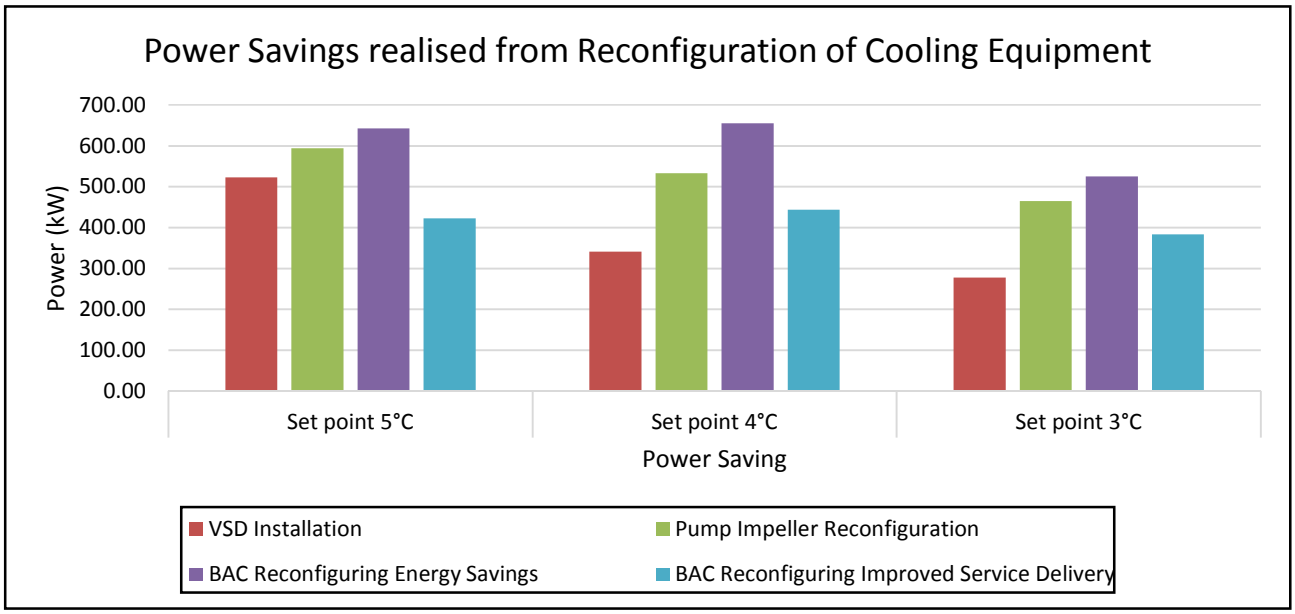

Figure 81: Power savings realised from reconfiguration of a mine's cooling equipment

Figure 81 depicts an increase in power saving for the BAC valve control. The power saving realised as the chilled water demand decreases during certain periods of the day. This enables the VSDs to reduce the water flow through the FPs, resulting in an increased power saving. The simulation with increased service delivery reduced the power savings by 21%, utilising the power savings realised from the other reconfiguration initiatives for a slightly improved BAC service delivery. Figure 82 represents the effect the reconfiguration had on the cooling systems output values.

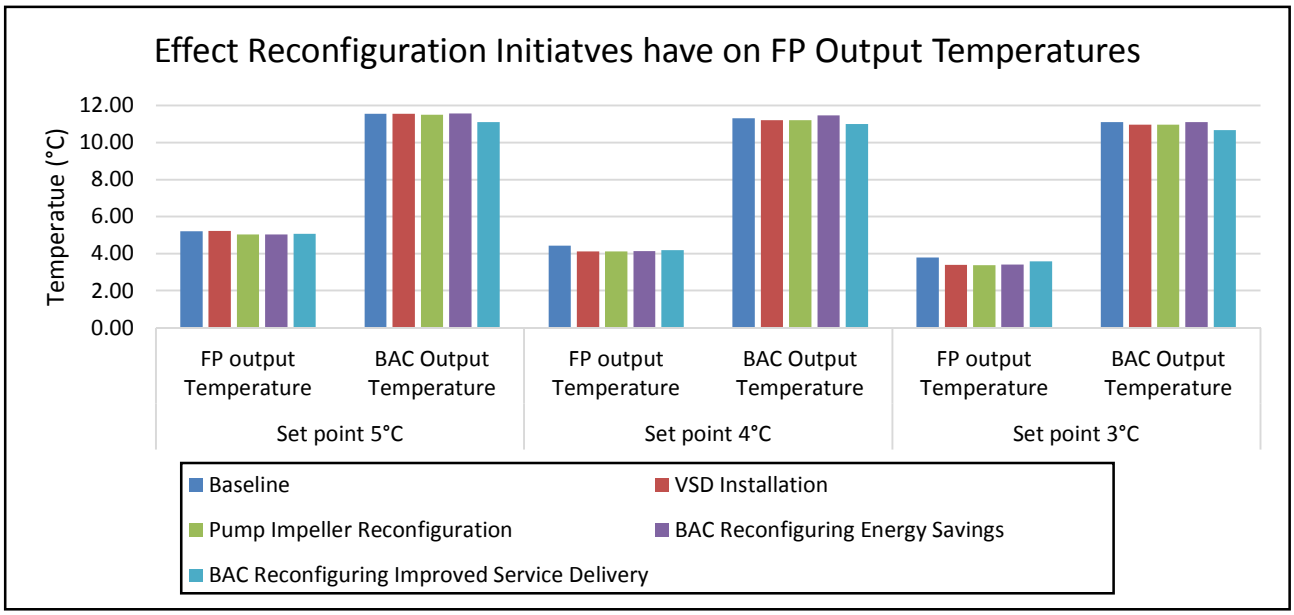

Figure 82: Effect reconfiguration initiatives have on cooling system outlet temperatures

Figure 82 indicates that the evaporator outlet water temperature was not affected by the BAC reconfiguration for power savings. The BAC outlet air WB temperature increased with 0.60%, 2.42% and 1.37% with an evaporator setpoint of 5℃, 4℃ and 3℃ respectively. The larger temperature increase for the simulation with an evaporator outlet water temperature setpoint of 4℃ is due to a 0.3℃ higher BAC outlet setpoint temperature. However, the increase is small and will have minimal effect on the underground working environment.

The evaporator outlet water temperature was not affected by the BAC reconfiguration for the simulations with a 5℃ and 4℃ evaporator outlet water temperature setpoint. With the evaporator outlet water temperature set to 3℃ and the BACs' chilled water flow demand increase, caused less water to be recycled. In return it caused the evaporator inlet water temperature to increase with 2.11% resulting in a 0.11℃ evaporator outlet water temperature increase.

The BAC's service delivery for the evaporator outlet water temperature setpoint of 5℃, 4℃ and 3℃ improved with 3.63%, 1.79% and 2.63% respectively. The service delivery is much lower than anticipated. A detailed analysis of the effect that reconfiguring the BACs has on the cooling system can be found in Appendix E.

Conclusion - Reconfiguration of bulk air coolers

The need for reconfiguration of the BACs was identified. The simulation proved it is worthwhile to update the chilled water flow control through the BACs for power savings. The service delivery will not be affected by the updated control and power savings will be realised. The simulations indicated that it will not be worthwhile to reconfigure the BAC sump pumps. It will increase the cooling system's operating costs without sufficiently improving the system's service delivery. The mine should consider replacing the BAC fill to improve the BAC's heat transfer to obtain the BAC's design outlet specification.

4.5. RECONFIGURATION OF PRE-COOLING TOWERS

Introduction

Mine A's pre-cooling towers consist of two stages, each stage having eight towers with 30 kW installed fan motors. The pre-cooling towers are utilised to pre-cool the warm water from underground before the FPs' evaporator cycle further cools the water. The water is transported from the pre-cool dam one through the second stage pre-cooling towers via four 45 kW pumps. An efficient pre-cooling tower can cool the water from underground to 2℃ above the ambient WB temperature [13]. Figure 83 represents the location and layout of mine A's current pre-cooling installation.

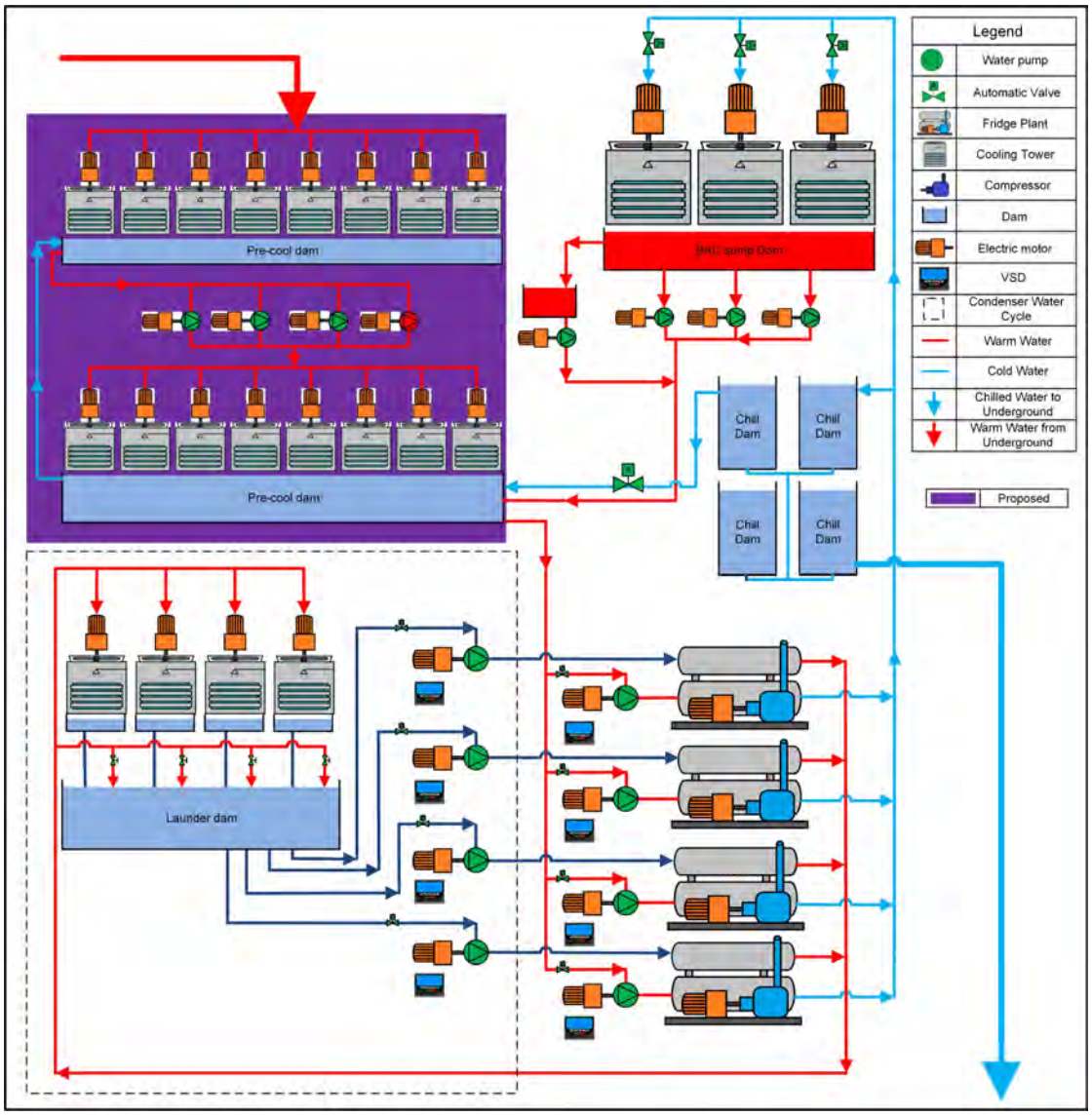

Figure 83: Location of Mine A's pre-cooling towers

[13] Deon Arndt Partner of Enoveer Engineering Innovation

Figure 83 depicts that the BAC return and recycled chilled water is dumped in the second stage pre-cool dam. The BACs' return water is dumped in the dam as the return water is colder than the ambient WB air temperature. Cooling will be wasted if the BAC return water is sent through the pre-cooling towers. Chilled water is recycled to lower the FP's inlet temperature as the pre-cooling towers cannot cool the water from underground sufficiently.

The pre-cooling towers' outlet water is directly dumped into the pre-cooling dams. Therefore, only the performance of the pre-cooling stage one can accurately be determined, as the second stage pre-cooling dam water is mixed with cold water from the BAC and recycled chilled water. If the water flowing into pre-cool dam two is more than the evaporator inlet water flow, the water from pre-cool dam two will overflow to pre-cool dam one.

Identifying inefficient operations

Mine A's pre-cooling towers were installed simultaneously and their maintenance plans were identical; therefore, their service delivery will be the same. Currently maintaining these machines proved to be troublesome as the fans are big and cannot be replaced by mine personnel. If a pre-cooling tower has a breakdown, mine A will delay the repair until two or more cooling tower fans have failed to ensure the callout is worthwhile. This reduces the pre-cooling tower service delivery unnecessarily. Mine A's current pre-cool water temperatures are summarised in Table 16.

Table 16: Pre-cooling average water temperature evaluation

Description	Temperature (°C)
Water from UG	25.98
Pre-cool Dam1 Water	19.39
Pre-cool Dam2 Water	12.61
Ambient (WB)	15.96
BAC Return Water	11.40
Recycled Chilled water	5.31

From Table 16 it is evident that the pre-cooling towers' stage 1 is able to lower the water from underground to 3.43℃ above the ambient WB temperature. The pre-cool dam two's water temperature is 3.35℃ below the ambient WB temperature. These low temperatures are achieved by dumping a large volume of the BAC return water and chilled water with an average temperature of 11.40℃ and 5.31℃ respectively into the second stage pre-cool dam. Figure 84 is a visual representation of the pre-cooling towers' daily water temperatures.

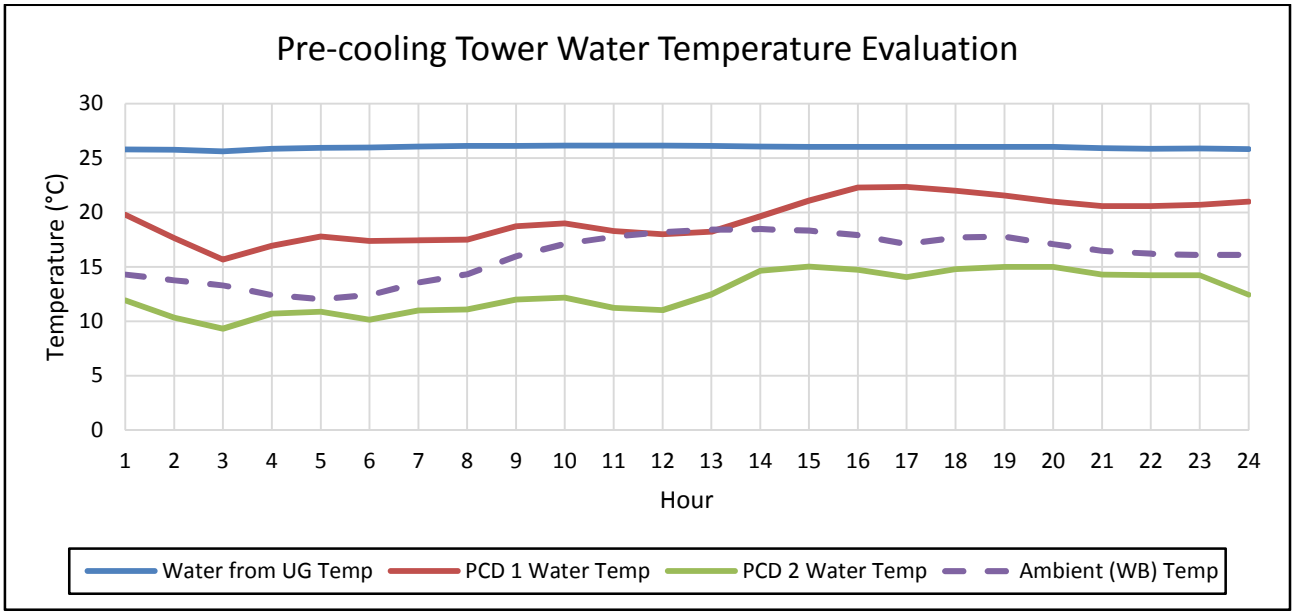

Figure 84: Pre-cooling water temperature evaluation

Figure 84 depicts that the warm water from underground remains constant at 25.98℃. The first stage pre-cooling water outlet temperature is on average 3℃ above the ambient WB air temperature. Between 11:00 and 13:00 the first stage pre-cooling water temperature is reduced to the ambient WB temperature. This is due to the second stage pre-cooling dam overflowing into the first stage pre-cool dam.

The simulation software can provide a simulated value of the output water temperature from the second pre-cooling towers before the water is mixed with the BAC return water and recycled chilled water. Figure 85 represents the simulated water temperatures of the pre-cooling towers compared against the ambient WB air temperatures.

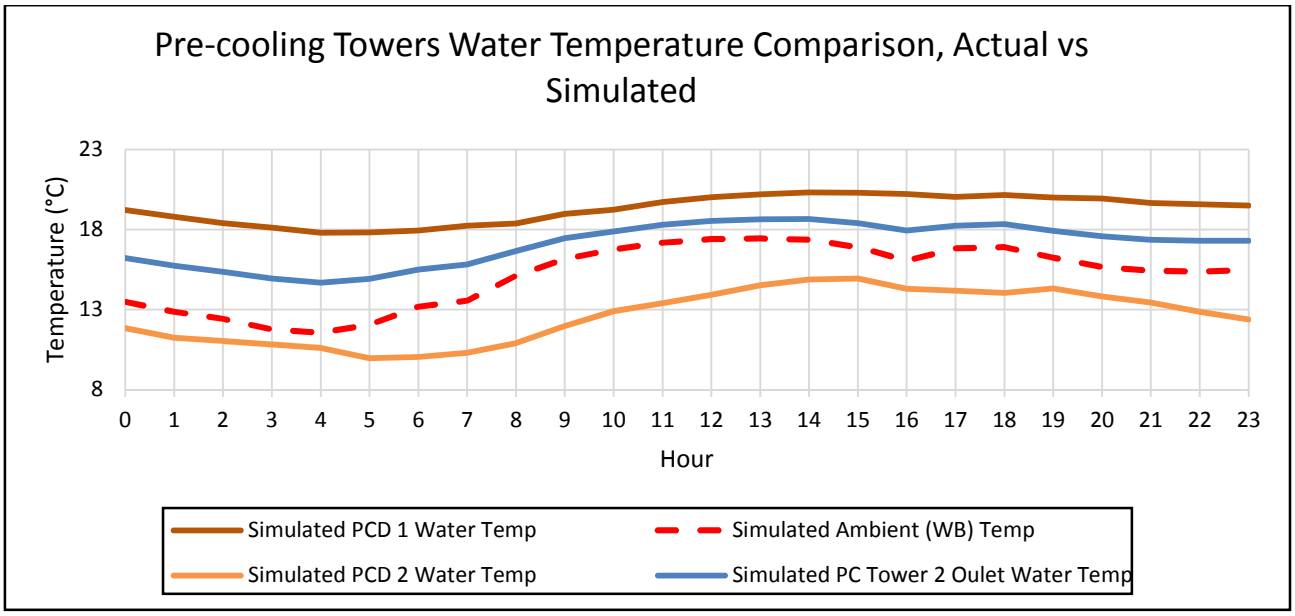

Figure 85: Simulated pre-cooling outlet water temperatures

Figure 85 represents the second stage pre-cooling towers, where the water temperature is lowered by 2.31℃ whilst the first stage pre-cooling towers reduced the water temperature from underground by 6.6℃ on average. Both these subsystems utilise the same amount of power. The COP of the two machines can be compared against each other as the data was simulated under the same ambient conditions. Utilising Equation 6 and Equation 7 the COP of the cooling towers was calculated and summarised in Figure 86.

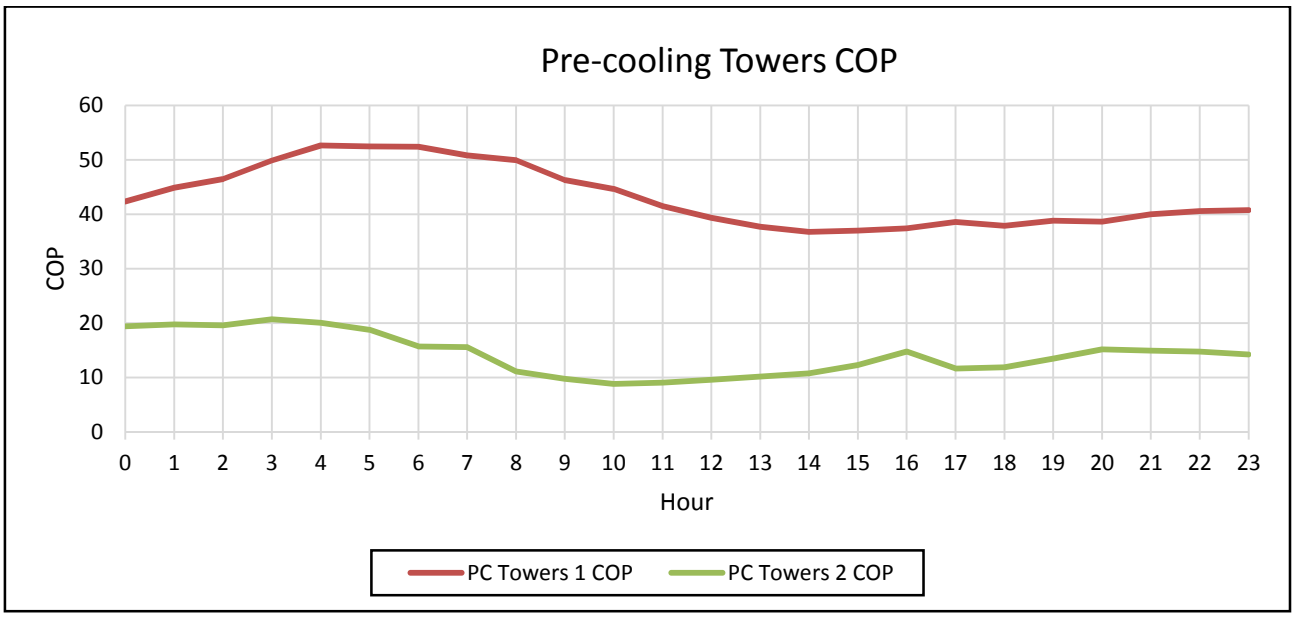

Figure 86: Pre-cooling towers' simulated COP

Figure 86 depicts that the COP of the first stage pre-cooling towers is three times better than the COP of the second stage pre-cooling towers. This is due to pre-cooling stage one temperature reduction being three times better than the second stage. Mine A's pre-cooling towers' water side efficiency is good due to its relatively low water flow from underground. The mine is wasting power by running both stages pre-cooling towers.

Control philosophy reconfiguration

Replacing the second stage pre-cooling towers with state-of-the-art pre-cooling towers with improved service delivery will allow the mine to only run one stage of the cooling towers whilst maintaining an outlet water temperature of 2℃ above the ambient WB air temperature. The first stage pre-cooling towers can be switched off to reduce the power consumption.

Warm water from underground will be pumped through the first stage pre-cooling towers with the fans switched off. This will allow some form of heat transfer without consuming additional power. The first stage pre-cool dam will act as a hot water storage dam before the water is pumped through the upgraded second stage pre-cooling towers.

All eight of the currently installed second stage pre-cooling towers will be replaced with new cooling towers. Each of the new cooling towers will have four 5.5 kW fan motors. The new cooling towers will simplify the maintenance of the pre-cooling towers as the motors are lighter and can be replaced by mine employees. Fans can be switched off individually if the outlet water temperature stabilises 2℃ above the ambient WB air temperature.

Simulation validation process

The simulation was validated in section 3.5, where the pre-cooling outputs of the first and second stage deviated with 0.55% and 0.06 % respectively from the actual cooling towers' performance. Mine A did not have funds available to upgrade the pre-cooling towers. However, Mine F upgraded their outdated pre-cooling towers, which allowed the savings to be verified on mine F.

Mine F's pre-cooling towers consisted of one stage pre-cooling towers. Mine F also had 30 kW fan motors installed on all eight of their pre-cooling towers. Each cooling tower was replaced with a cooling tower consisting of four 5.5 kW installed fans. Mine F's pre-cooling towers' water efficiency improved from 50% to 78% without BAC return or recycled chilled

water [21]. A maximum pre-cooling water side efficiency of 78% can be expected from reconfiguration of the mine's pre-cooling towers.

Results

The effect of the reconfiguration of the pre-cooling towers will be compared against the output simulation values of the pump impeller reconfiguration. The simulation will not include the reconfiguring of the BACs as the BACs' reconfiguration had not been implemented at mine A. The simulation model was updated to include the pre-described reconfiguration of the pre-cooling towers. The pre-cooling towers are an independent subsystem from the entire cooling system. Changes to the evaporator setpoint will not greatly affect the pre-cooling tower's operation. Therefore the pre-cooling tower's performance will remain the same for the different evaporator output temperatures.

The performance of the pre-cooling towers will, however, affect the performance of the rest of the cooling equipment. Therefore, the power saving realised will be calculated for three scenarios with an evaporator setpoint of 5℃, 4℃ and 3℃. Figure 87 represents the evaporator water temperatures of the baseline and implemented simulations.

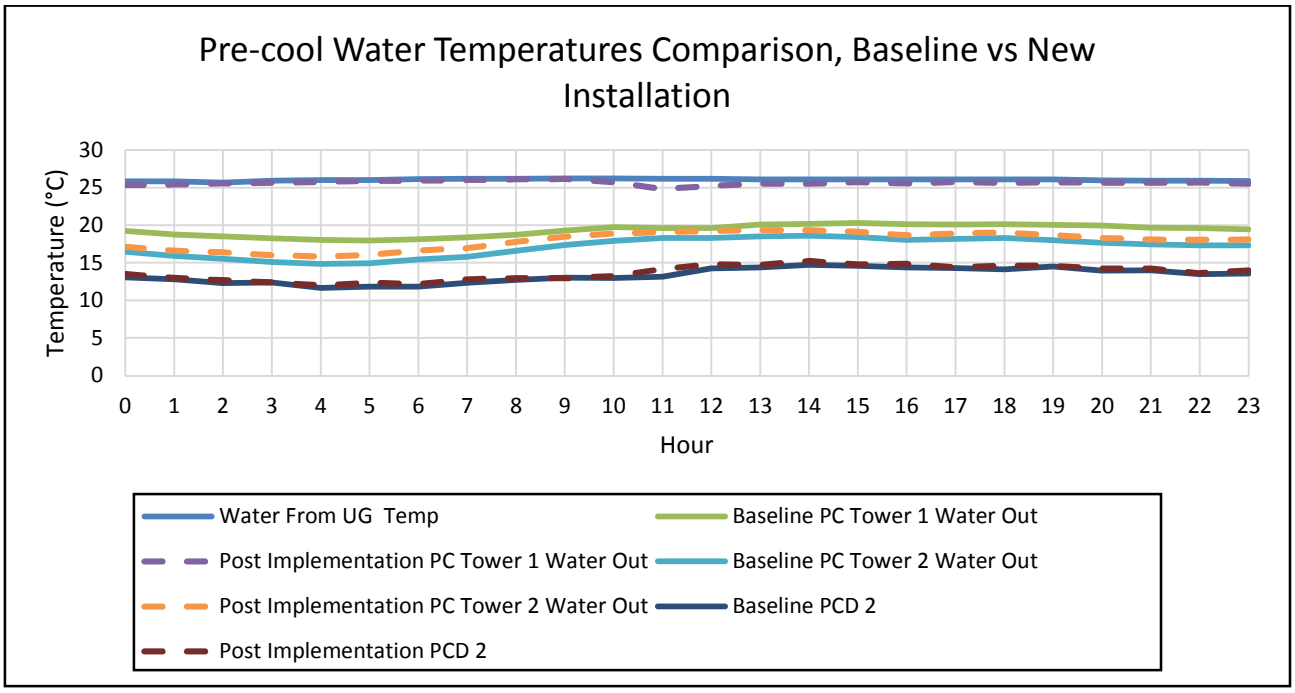

Figure 87: Pre-cool towers' water temperatures with a 4℃ evaporator setpoint temperature

Figure 87 depicts that the water temperature from underground remained the same for both simulations. The first stage pre-cooling towers reduced the water temperature on average with 0.38℃. The second stage with the replaced pre-cooling towers managed to reduce the

water temperature to 17.96℃, 0.87℃ warmer than the second stage pre-cooling tower outlet temperature of the baseline simulation. The recycled chilled water was increased to 7.24% to maintain an evaporator inlet water temperature of 14.29℃, 2.14% above the baseline inlet temperature. Figure 88 summarises the pre-cooling towers' water efficiencies of the baseline and implemented simulations.

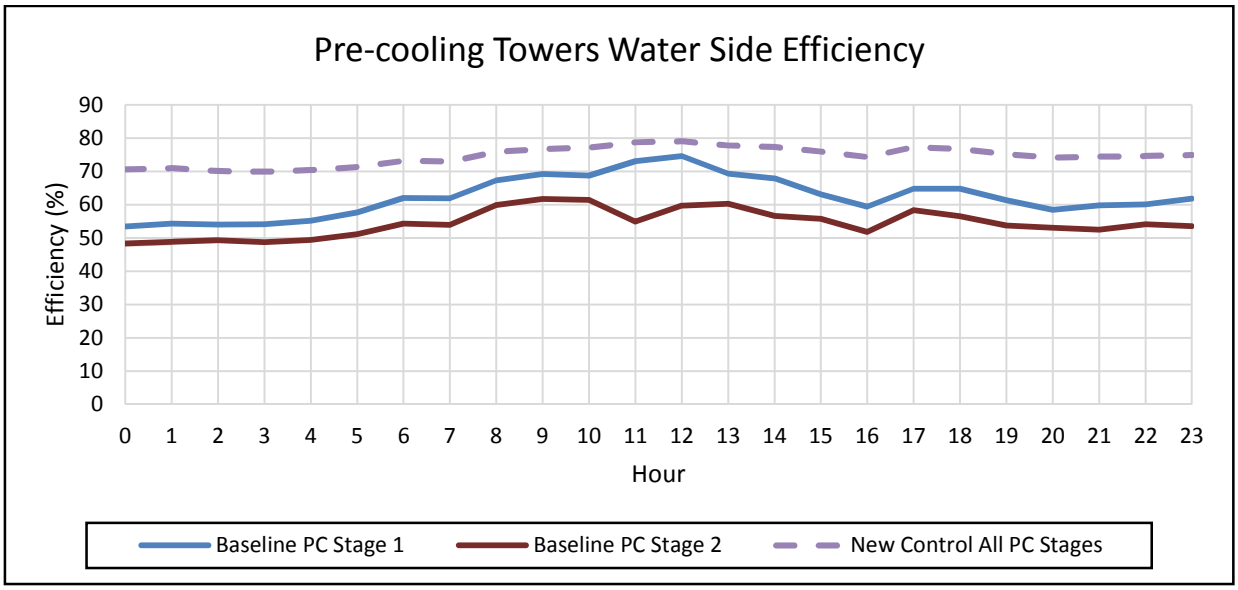

Figure 88: Pre-cool towers' water side efficiency with a 3℃ evaporator setpoint temperature

Figure 88 depicts that the baseline water side efficiency for both pre-cooling stages are less than the implemented water side efficiency. The baseline simulation depicts an average water side efficiency of 62.34% and 54.49% of the first and second stage pre-cooling towers respectively. The implemented simulation realised a water side efficiency of 74.59%.

The efficiency is calculated from the water from underground temperature to the second stage pre-cooling tower outlet water temperature as the first stage pre-cooling tower's fans were switched off. This is a realistic service delivery and efficiency from the simulation of the pre-cooling towers of mine A, as a water side efficiency of 78% has been recorded for the same amount of pre-cooling towers at mine F [21]. Figure 89 represents the effect that different reconfiguration initiatives have on the power usage of mine A's cooling systems.

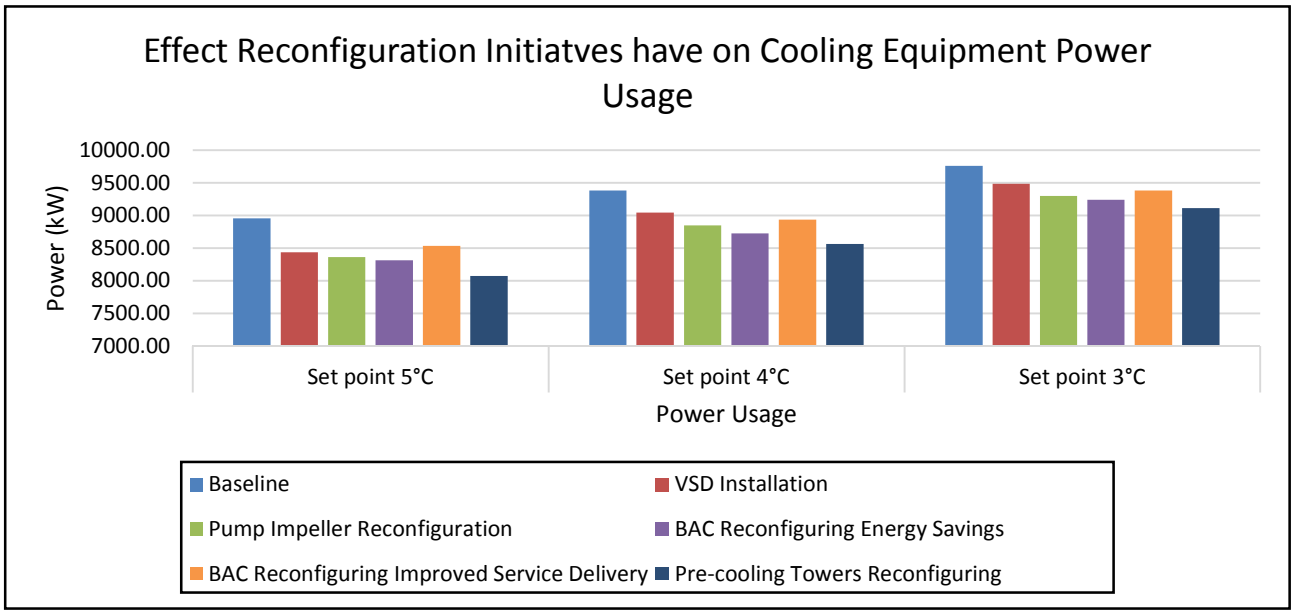

Figure 89: Cooling equipment total power usage comparison

From Figure 89 it is evident that the reconfiguration of the pre-cooling towers resulted in a reduced power consumption. The pre-cooling reconfiguration did not include the BACs reconfiguration, as mine A had not commenced with the implementation of the BACs reconfiguration. Figure 90 represents the accumulative power savings of the VSDs' installation, evaporator pump impeller replacement and the pre-cooling tower reconfiguration.

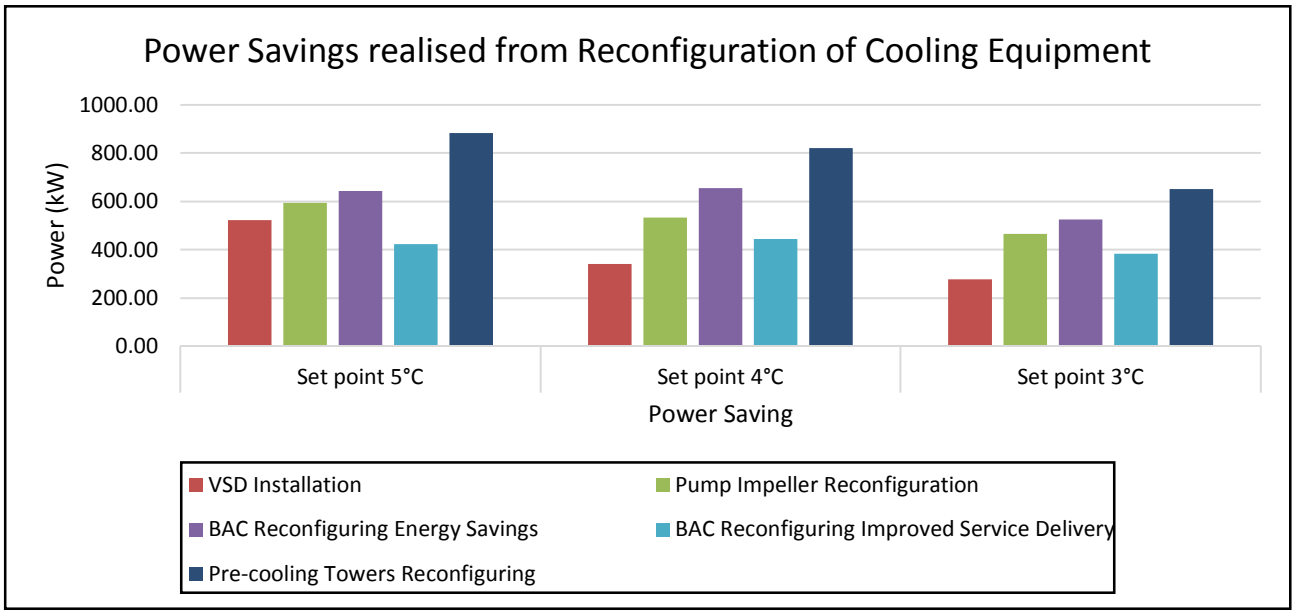

Figure 90: Power savings realised from reconfiguration of a mine's cooling equipment

Figure 90 depicts that the savings realised from the reconfiguration of the pre-cooling towers remained at 287 kW for an evaporator outlet water temperature setpoint of 5℃ and 4℃. However, the savings deteriorated to 185.82 kW with an evaporator outlet water temperature of 3℃ as the FPs had to work harder to maintain a lower evaporator outlet water temperature. Figure 91 represents the effect that the reconfiguration of the pre-cooling tower had on the cooling systems' output values.

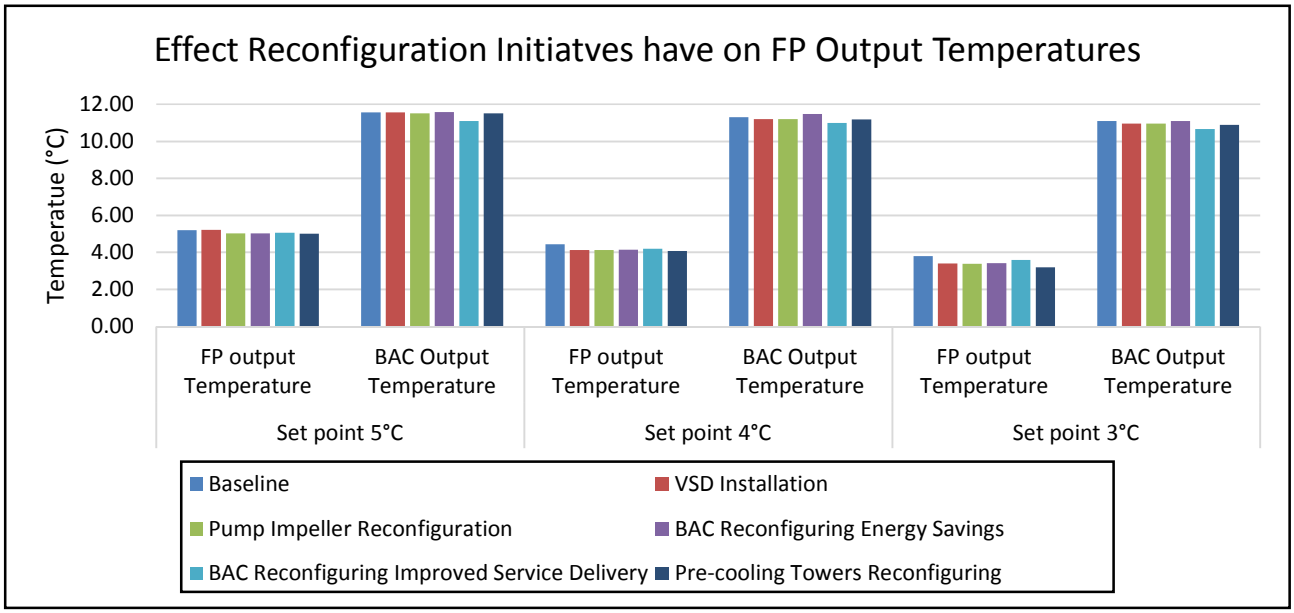

Figure 91: Effect reconfiguration initiatives have on cooling system outlet temperatures

Figure 91 depicts that the replacement of the pre-cooling towers was beneficial for the cooling system's service delivery. A 0.40%, 1.40% and 5.33% improvement in evaporator outlet water temperature was experienced for an evaporator output temperature setpoint of 5℃, 4℃ and 3℃ respectively. The slightly higher evaporator inlet water temperature allowed for the FP's compressor to increase the temperature drop. This, however, did not drastically improve the plant COP as the power consumed by the FPs compressors increased as well.

The improved evaporator outlet water temperature resulted in an improved service delivery to the BACs. The BAC outlet air temperature was improved with 0.06%, 0.18% and 0.54% with an evaporator outlet temperature setpoint of 5℃, 4℃ and 3℃ respectively. A detailed analysis of the effect replacing the second stage pre-cooling towers has on the cooling system can be found in Appendix F.

Conclusion - Reconfiguration of pre-cooling towers

The need for reconfiguring of mine A's pre-cooling towers was identified. Replacing the mine's second stage pre-cooling towers will ensure an improved water side efficiency of 74.59%. The improved efficiency will allow the mine to switch off the first stage pre-cooling towers for increased power savings. The improved second stage pre-cooling towers managed to deliver the maximum service delivery and lowering the water temperature to 2℃ above the ambient WB air temperature. The recycled chilled water and BAC return water reduced the pre-cool dam two's temperature to ensure the optimal evaporator inlet water temperature is maintained for maximum service delivery.

4.6. CONCLUSION

Mine A will definitely benefit from reconfiguring their cooling system. Setting their evaporator setpoint will influence their power savings drastically. With an evaporator output temperature of 5℃, the maximum power savings will be realised by sacrificing the service delivery of the cooling system. Changing the evaporator output water temperature to 3℃ will improve the service delivery of the FPs' evaporator output water temperature drastically whilst sacrificing the power savings. The 3℃ evaporator outlet water temperature did not improve the BACs' outlet air WB temperature as expected.

With an evaporator outlet water temperature setpoint of 4℃, mine A will benefit from improved service delivery and power savings. Figure 92 represents the accumulated power savings realised for the different reconfigurations with an evaporator outlet water temperature of 4℃.

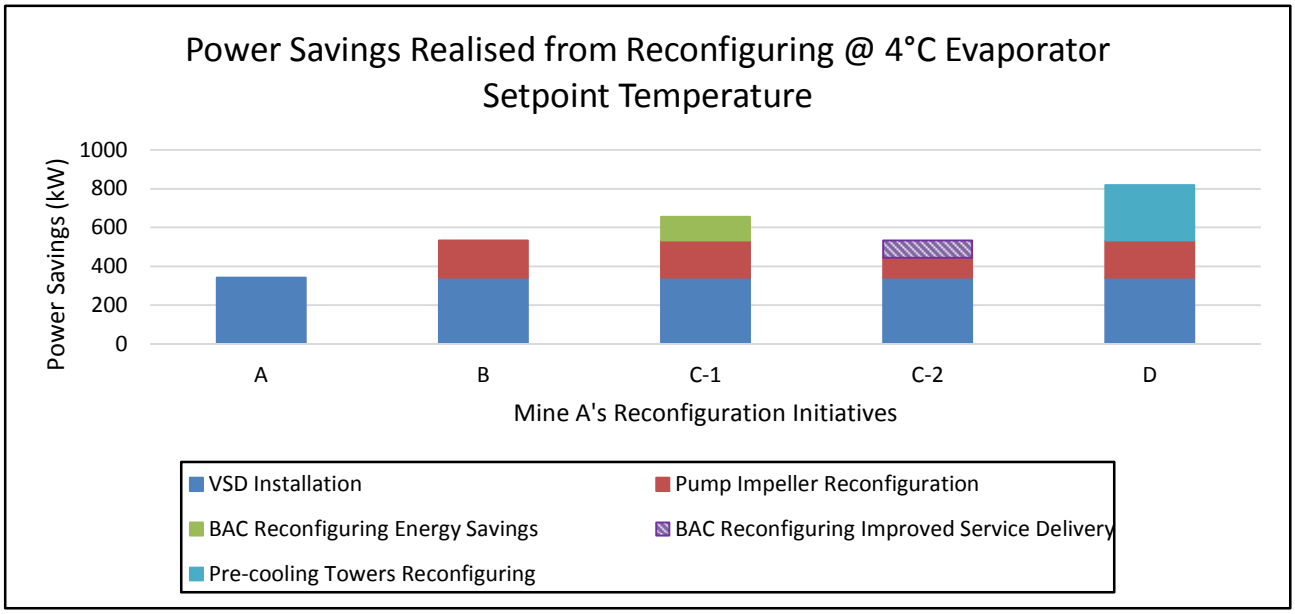

Figure 92: Power savings realised from different reconfigurations of cooling equipment at mine A

Figure 92 depicts that, with an evaporator outlet water temperature setpoint of 4℃, the largest energy savings of 340.69 kW will be realised from the implementing of the flow control on the FP pumps. The replacement of the pump impellers including the upgrading of the recycled chilled water valve will realise a saving of 191.90 kW, 2.17% of the total power consumption, during the summer months. This is a significant power saving; however, the upgrade will benefit the mine more during the winter months. The Eskom electricity tariff is almost double during the winter peak periods; therefore, any amount of power saving realised during the winter months will be beneficial for the mine. A power

saving of 150.62 kW, 6.09% of the total power consumption, will be realised during the winter months.

Improving of the BACs' inlet water valves' control philosophy to maintain a constant BAC outlet WB air temperature will realise a power saving of 122.32 kW. This is a relatively small cost saving and a slight sacrifice of the system's service delivery. However the installation will have a fairly low installation cost. Reconfiguration of the BACs' pump configuration for improved service delivery will increase the cooling system power consumption with 88.89 kW. This will result in a decreased evaporator outlet water service delivery and insignificant increase in the BACs' service delivery. Consequently, it would be advisable to only install the BACs control valves and neglect the reconfiguration of the BACs sump dam overflow dam and pump.

Reconfiguration of the pre-cooling towers will achieve the second most power saving of all the reconfiguration initiatives. A power saving of 287.08 kW will be realised and an insignificant improvement of the cooling system service delivery. Figure 93 depicts the cooling system's service delivery improvement with an evaporator outlet water temperatures set to 4℃.

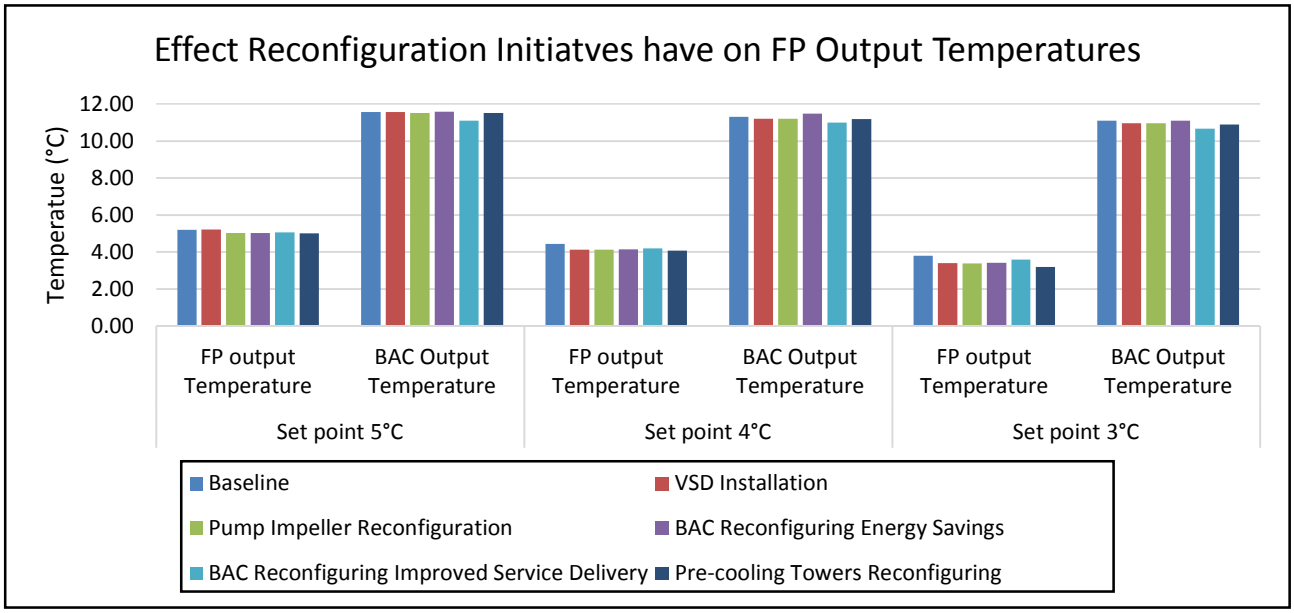

Figure 93: Improved service delivery of mine A's cooling systems from different reconfiguration initiatives

Figure 93 depicts all of the energy initiatives contributed to improved service delivery of both the evaporator outlet water and BACs outlet WB air temperature. The evaporator outlet water temperature service delivery improved until the setpoint temperature was obtained. The FPs then managed to maintain the evaporator outlet water temperature at the setpoint

temperature. The reconfiguration of the BACs sump dam pumps realised in an insignificant improvement of the BACs outlet air WB temperature and a decreased service delivery of the evaporator outlet temperature. The decrease in evaporator outlet water temperature is due to an increased chilled water demand.

Chapter 5. CONCLUSION AND RECOMMENDATIONS

"Failure will never overtake me if my determination to succeed is strong enough." -Og Mandino

5.1. OUTCOME OF DISSERTATION

Potential of reconfiguring mining cooling auxiliaries for optimal operations

Research proved that mine cooling systems are one of the most essential systems found on deep level gold mines. Cooling systems are responsible for maintaining acceptable underground working conditions. The majority of these cooling systems found on mines are outdated as they were installed a few years after mine inception. Inadequate and incorrect maintenance of the cooling systems causes the cooling system to be inefficient.

These inefficient subsystems have been identified by ESCos and DSM projects have been implemented on an ad hoc basis on mine cooling systems. The ESCos do not consider a total reconfiguration of mine cooling systems since the ESCos are not rewarded by Eskom for over- performance. This scenario creates an opportunity for reconfiguration of the mine's cooling auxiliaries for optimal operation. Therefore, a universal reconfiguration strategy was developed to identify and improve a mine's inefficient cooling subsystems and to ensure the reconfigured subsystems are synchronised with the older components.

Investigation and strategy development

Mine A's cooling system was identified as outdated and inefficient due to the fact that its cooling system was not able to maintain the evaporator outlet water temperature at a setpoint of 5℃. However, the cooling system's OEM design specification is to deliver an evaporator outlet water temperature of 3℃. Mine A's personnel will, however, be satisfied with an evaporator outlet water temperature of 4℃, even though the cooling provided with an evaporator outlet water temperature of 5℃ are sufficient.

A universal methodology was developed to reconfigure mine A's cooling subsystems for optimal operation. The reconfigurations were theoretically simulated through an iterative process to obtain the optimal operation of mine A's cooling system. Four of mine A's cooling subsystems were identified as inefficient and required reconfiguring.

VSDs were added to the FPs' evaporator and condenser pumps to control the water flow through the FPs. The VSDs control the water flow to increase the heat transfer between the water and the refrigerant gas for optimal operation. This allowed the FPs' compressors to

cut back on their guide vanes as the setpoint temperature will be maintained throughout the majority of the day.

Mine A's installed evaporator pump impeller sizes were reduced to reduce the flow through the FPs. Previously this used to be common practice before VSD technologies were available and affordable. Replacing the pump impellers with correctly sized impellers will allow the mine to utilise the VSDs to their full potential and enable the mine to increase the water flow to the FP's design specification. The new impellers will not have a significant effect on the cooling system during the summer months as the VSDs will reduce the water flow. However, power savings will be realised during the winter months when the ambient psychrometric conditions are more favourable and fewer pumps are required to meet the underground water demand.

Mine A's BAC service delivery was below the OEM design specification. The BACs did not utilise all the cooling that was provided by the chilled water, therefore the BACs could be reconfigured for increased power savings or improved service delivery. The BACs cannot utilise all the cooling provided when the ambient psychrometric conditions are lowered; therefore, during this period the chilled water flow through the BACs can be reduced to maintain a constant BAC outlet WB air temperature. This caused a reduction in the chilled water demand, which in return realised in increased cost savings.

The chilled water flowing through the BACs is below the BACs' OEM design specification due to the BACs' sump damp pumps restricting the maximum chilled water flow rate. Reconfiguring the pump's control philosophy and increasing the BAC overflow dam and pump capacities, will enable the mine to increase the chilled water flow to the design specification for maximum service delivery from the BACs.

Analysing mine A's pre-cooling towers' water side efficiencies provided proof that the pre-cooling towers are inefficient. Replacing the second stage pre-cooling towers with modern and more efficient pre-cooling towers will enable the mine to switch off their first stage pre-cooling towers. The replaced second stage pre-cooling towers will produce sufficient cooling. The recycled chilled and BAC return water will lower the FPs' evaporator inlet water temperature to the design inlet water temperature. Table 17 summarises the effect that different evaporator outlet water temperature will have on mine A's cooling system's service delivery and power savings if all the reconfigurations are implemented. This was determined through PTB simulation software. The simulation model was developed with the system's

actual data and validated using the cooling present operation data. The simulation model was found to have an accuracy of 94%.

Table 17: Effect reconfiguration has on mine A's cooling system with an evaporator setpoint of 5, 4 and 3℃

Effect Total Reconfiguration has on Mine A's Cooling System with an Evaporator Setpoint of 5, 4 and 3°C					
Simulation	**Power Usage (kW)**	**Power Savings (kW)**	**Power Savings (%)**	**Evaporator Outlet Water Temp (°C)**	**BAC Outlet WB Air Temp (°C)**
Desired Evaporator Outlet Water Temperature of 5°C					
Baseline	8957.69	928.12	10.36	5.21	11.57
Implemented	8029.57			5.02	11.57
Desired Evaporator Outlet Water Temperature of 4°C					
Baseline	9384.71	1093.63	11.65	4.43	11.30
Implemented	8291.07			4.08	11.46
Desired Evaporator Outlet Water Temperature of 3°C					
Baseline	9765.25	762.72	7.81	3.79	11.09
Implemented	9002.53			3.22	11.04

From Table 17 it is evident that the power usage increased as the evaporator outlet water temperature decreased. This is due to an increased heat load from the increased chilled water temperature demand. With an evaporator outlet water temperature of 5℃, maximum service delivery will realise while maintaining an acceptable underground working environment. Changing the evaporator outlet water temperature setpoint to 3℃ will realise maximum service delivery from the cooling system at a cost of increased electricity consumption of 1.08% from the original baseline.

Setting the evaporator outlet water temperature to 4℃ will allow the mine to benefit from an increased service delivery and power savings. A power saving of 10.04% will realise when comparing it against the baseline with an evaporator setpoint of 4℃. A power reduction of 666.63 kW power saving and a service delivery improvement of 21.88% will realise from the chilled water when compared against the original baseline with an evaporator outlet water temperature setpoint of 5℃. Therefore, the optimal operation for mine A’s cooling systems will be at an evaporator outlet water temperature setpoint of 4℃.

Implementation and results

Due to financial constraints not all of the reconfigurations have been implemented at mine A. The reconfiguration of mine A’s FPs’ pump control has been successfully implemented.

For this reconfiguration the simulation model was validated with the actual implemented data. The reconfiguration realised a 0.30℃ and 0.11℃ improvement on the chilled water and BAC outlet WB air temperature respectively. The reconfiguration of the FP pump flow control realised in a power saving of 3.36%. The effect different reconfigurations have on mine A's cooling system with an evaporator output setpoint of 4℃ is summarised in Table 18.

Table 18: Effect different reconfigurations have on Mine A's cooling system with an evaporator setpoint of 4℃

Effect Different Reconfigurations have on Mine A's Cooling System with an Evaporator Setpoint of 4°C					
Simulation	**Power Usage (kW)**	**Power Savings (kW)**	**Power Savings (%)**	**Evaporator Outlet Water Temp (°C)**	**BAC Outlet WB Air Temp (°C)**
A. Reconfiguration of FP Pumps Flow Control					
Baseline	9384.71	340.69	3.63	4.43	11.30
Implemented	9044.02			4.13	11.19
B. Reconfiguring of Evaporator Pump Impellers					
Baseline	9044.02	191.90	2.12	4.13	11.19
Implemented	8852.12			4.13	11.20
C. Reconfiguring of Bulk Air Coolers for Cost Savings					
Baseline	8852.12	122.32	1.38	4.13	11.20
Implemented	8729.80			4.14	11.48
D. Reconfiguring of pre-cooling towers					
Baseline	8852.12	438.73	4.96	4.14	11.48
Implemented	8413.39			4.08	11.46
Total Reconfiguration for Optimal Operation					
Baseline	9384.71	1093.63	11.65	4.43	11.30
Implemented	8291.07			4.08	11.46

Table 18 depicts the reconfiguration of the evaporator pump impellers and a control philosophy adjustment, which will realise in additional power saving of 2.12%, whilst maintaining a constant evaporator outlet water temperature of 4.13℃ and BAC outlet air WB temperature of 11.19℃ during the summer months. The implemented VSD simulation was considered as the baseline simulation, as the VSDs' installation had been completed at mine A. The Baseline simulation was utilised to determine the effect that the other reconfigurations have on the cooling system's performance.

Up to date only one of mine A's evaporator pump impellers has been replaced. The evaporator pump flow simulation was validated with the actual water flow data from the one reconfigured pump. The simulation was updated and utilised to predict the results from the validated simulation. The validated simulation proved that during the winter months a power

saving of 6.09% realised on a power usage of 2 321.83 kW. This is an improvement for mine A's electricity bill as Eskom electricity tariffs are significantly higher during the winter months.

The validated simulation provided proof that the reconfiguration of the BACs for power savings will realise in a 1.38% power saving. The cooling system's service delivery was, however, negatively affected. The evaporator outlet water and BACs outlet air WB temperatures increased with 0.01℃ and 0.28℃ respectively. The increase in evaporator outlet water temperature is due to the BAC return water being warmer, resulting in a higher evaporator inlet temperature. The BAC outlet air WB temperature was set to 11.5℃ to maintain an acceptable underground working environment and increase the power savings. The average BAC outlet air WB temperature was 0.02℃ below the setpoint. The reconfiguration of the BACs for improved service delivery is not represented in Table 18, since the BACs' service delivery did not improve as expected.

The reconfiguration of mine A's secondary pre-cooling towers was simulated as there was not enough funds available to reconfigure the pre-cooling towers. The validated simulation proved that, with the first stage pre-cooling towers switched off and the new second pre-cooling towers, an improved water side efficiency of 74.59% will realise. This is a realistic improvement of the water side efficiency as a water side efficiency of 78% has been reported at mine F with the same amount of newly replaced pre-cooling towers [21]. The reconfiguration realised in a power reduction of 3.24% whilst improving the service delivery of the cooling system.

It will in the best interest of mine A to implement all the reconfiguration on the mine's cooling system. The reconfiguration will ensure optimal operation of the cooling system. The optimal operation will not only be focused on improved service delivery, but will include power savings whilst maintaining acceptable underground working conditions. It is evident that the reconfigurations that were implemented on mine A's cooling system improved the service delivery while reducing the power consumption.

5.2. RECOMMENDATIONS

The study focused on reconfiguring a South African mine's surface cooling auxiliaries' subsystems for optimal operation, particularly on reconfiguration a mine's different cooling subsystems on surface. The study proved that mine cooling equipment is inefficient and

that various DSMs have been implemented on ad hoc bases on mines' cooling subsystems. These DSM initiatives do not always consider synchronisation of old and new equipment for optimal operation. Therefore, a universal reconfiguration strategy was developed and tested on Mine A's cooling subsystems to ensure the cooling system operates at its optimum.

The author is of the opinion that if the ESCos were to be rewarded by Eskom or the mine for over-performance on the DSM initiatives, the ESCo will ensure the old and new equipment is synchronised with one another. The ESCos should also inform the mine of possible future upgrades to their cooling system that will improve the performance of the mine's cooling system.

The universal reconfiguration strategy should be tested on other mines and industries to optimise their outdated and inefficient cooling systems. The strategy can be applied to surface and underground cooling systems. The strategy is also applicable to other cooling subsystems where efficiencies are bound to decrease over time.

Furthermore, it is advised to improve mine A's BACs' service delivery to ensure the BACs are capable of performing as closely to its OEM design specification as possible. It is important for mine personnel to record all the maintenance procedures and decisions as the recordings will help with future improvements and maintenance decisions.

Finally, it is recommended to investigate the installation of VSDs on the BAC fans and FP's compressors. This will improve the cooling system's operation and contribute to this field of study. Additionally, the effect that repairing the underground chilled water leaks will have on the cooling systems performance, should be investigated.

The proposed investigations will ensure a valuable contribution to this field of study. This will not only benefit the academic field but also contribute to the mines' financial standings. In the end the mine's main goal is to produce gold safely at the lowest running cost to ensure maximum profitability.

REFERENCES:

[1] "South African History Online -Local Goverment," *Colonial History and Development of Johannesburg - Discovery of the Gold in 1884*. [Online]. Available: http://www.sahistory.org.za/discovery-gold-1884. [Accessed: 02-Feb-2015].

[2] C. W. de Kiewiet, *A History of South Africa*. Oxford, 1941.

[3] L. Mackay, S. Bluhm, and J. van Rensburg, "Refrigeration and cooling concepts for ultra-deep platinum mining," in *The 4th Platinum in Transition*, 2010, pp. 285–292.

[4] M. J. McPherson, *Subsurface ventilation and environmental engineering*. London: Chapman and Hall., 1993.

[5] C. A. Nixon, A. D. S. Gillies, and M. J. Howes, "Analysis of heat sources in a large mechanized development end at Mount Isa Mine," in *Proceedings Fifth International Mine Ventilation Congress*, 1992, pp. 109–117.

[6] L. F. van der Zee and D. R. Pelzer, "Modelling of electricity cost risks and opportunities in the gold mining industry," North-West University, 2014.

[7] M. Kosaka, M. Yamane, R. Ogai, T. Kato, N. Ohnishi, and E. Simon, "Human body temperature regulation in extremely stressful environment: Epidemiology and pathophysiology of heat stroke," *Journal of Thermal Biology*, vol. 29, pp. 495–501, 2004.

[8] K. Cloete, "Technology helps to keep mineworkers cool," *Mzambian Mining Magazine*, Jun-2014.

[9] RSA Government, "Mine Health and Safety Act 29 of 1996," no. 967, 2009.

[10] R. Pelzer, R. P. Richter, M. Kleingeld, and J. F. van Rensburg, "Performance comparison between manual and automated DSM pumping projects," *Industrial and Commercial Use of Energy*, 2009.

[11] A. M. Holman, "Benefits of improved performance monitoring of mine cooling systems," Masters Dissertation, NWU, Potchefstroom, South Africa, 2014.

[12] M. Kleingeld and J. H. Marais, "A high level strategy plan for reducing a mine group's dependence on compressed air," *Proc. Industrial and Commercial Use of Energy (ICUE), Cape Peninsula University of Technology*, 2010.

[13] D. J. Brake, "The application of refrigeration in mechanised mines," in *Proceedings of the Australasian Institute of Mining and Metallurgy*, 2001, vol. 306, pp. 1–10.

[14] I. Britt and P. L. J. Grobler, "Measurement and verification methodology of a fridge plant scheduling project in the mining industry," *Industrial and Commercial Use of Energy Conference (ICUE)*, pp. 1–4, 2006.

[15] A. J. Schutte, “An intergrated energy-efficiency strategy for deep-mine ventilation and refrigeration,” PhD Thesis, NWU, Potchefstroom, South Africa, 2013.

[16] D. C. Uys, “Converting an ice storage facility to a chilled water system for energy efficiency on a deep level gold mine,” Masters Dissertation, NWU, Potchefstroom, South Africa, 2014.

[17] J. Greyling, “Techno-economic application of modular air cooling units for deep level mining at Mponeng,” Masters Dissertation, NWU, Potchefstroom, South Africa, 2008.

[18] “The top ten deepest mines in the world.” [Online]. Available: www.mining-technology.com/features/feature-top-ten-deepest-mines-world-south-africa/. [Accessed: 15-Mar-2015].

[19] C. F. Scheepers, “Implementing energy efficiency measures on the compressed air network of old South African mines,” Masters Dissertation, NWU, Potchefstroom, South Africa, 2012.

[20] J. I. G. Bredenkamp, “Reconfiguring mining compressed air networks for cost savings,” Masters Dissertation, NWU, Potchefstroom, South Africa, 2014.

[21] G. E. Du Plessis, “A variable water flow strategy for energy savings in large cooling systems,” PhD Thesis, NWU, Potchefstroom, South Africa, 2013.

[22] M. Van Eldik, “An investigation into the DSM and energy efficiency potential of a modular underground air cooling unit applied in the South African mining industry,” Masters Dissertation, NWU, Potchefstroom, South Africa, 2006.

[23] P. Maré, “Improved implementation strategies to sustain energy saving measures on mine cooling systems,” Masters Dissertation, NWU, Potchefstroom, South Africa, 2014.

[24] C. Swart, “Optimising the operation of underground mine refrigeration plants and ventilation fans for minimum electricity cost,” PhD Thesis, NWU, Potchefstroom, South Africa, 2003.

[25] M. Li and Y. Liu, “Underground coal mine monitoring with wireless sensor networks,” *ACM Transactions on Sensor Networks (TOSN)*, vol. 5, no. 2, p. 10, 2009.

[26] T. Matlala, “Industrial demand side management in South Africa,” *Industrial and Commercial Use of Energy Conference (ICUE)*, 2004.

[27] F. H. Von Glehn and S. J. Bluhm, “Practical aspects of the ventilation of high-speed developing tunnels in hot working environments,” *Tunnelling and underground space technology*, vol. 15, no. 4, pp. 471–475, 2000.

[28] J. L. Buys, “Optimising the refrigeration and cooling system of a platinum mine,” Masters Dissertation, NWU, Potchefstroom, South Africa, 2014.

[29] M. P. J. Du Plessis, Mr D Hoffman, M. W. Marx, and M. R. van der Westhuizen, “Optimising ventilation and cooling systems for an operating mine,” *Aboriginal Multi-Media Society*, pp. 1–16, 2013.

[30] R. Els, “Potential for load shifting in ventilation and cooling systems,” Masters Dissertation, UP, Pretoria, Sou th Africa, 2000.

[31] E. H. Mathews, E. Van Heerden, and D. C. Arndt, “A tool for integrated HVAC, building, energy and control analysis Part 1: overview of QUICKcontrol,” *Building and Environment*, vol. 34, no. 4, pp. 429–449, 1999.

[32] W. C. Kukard, “Research on reducing costs of underground ventilation networks in South African mines,” Masters Dissertation, NWU, Potchefstroom, South Africa, 2007.

[33] J. de V Lambrechts, “The Estimation of Ventilation Air Temperatures in Deep Mines,” *Journal of the Chemical, Metallurgical and Mining Society of South Africa*, vol. 50, no. 8, pp. 184–198, 1950.

[34] D. Fusch, “Energy Efficiency: Partnering Successfully with an ESCO,” *Academic Impressions*.

[35] P. Mare, J. H. Marais, and C. J. R. Kriel, “Reducing energy consumption of mine cooling systems by controlling chilled water demand of mobile cooling units,” *Industrial and Commercial Use of Energy Conference (ICUE)*, pp. 1–6, 2014.

[36] C. Ma and X. Wu, “Study of cooling mode of heat mine based on the principle of CCHP,” *Procedia Engineering*, vol. 26, pp. 982–991, 2011.

[37] G. E. du Plessis, L. Liebenberg, and E. H. Mathews, “Case study: The effects of a variable flow energy saving strategy on a deep-mine cooling system,” *Applied Energy*, vol. 102, pp. 700–709, 2013.

[38] C. Borgnakke and R. E. Sonntag, *Fundamentals of Thermodynamics*, 7th ed. John Whiley & Sons, 2009.

[39] A. J. Schutte, “Demand-side energy management of a cascade mine surface refrigeration system,” Masters Dissertation, NWU, Potchefstroom, South Africa, 2007.

[40] Y. A. Cengel, *Heat and Mass Transfer: A Practical Approach*. New York, NY: McGraw-Hill, 2006.

[41] K. N. Widell and T. Eikevik, “Reducing power consumption in multi-compressor refrigeration systems,” *International Journal of Refrigeration*, vol. 33, no. 1, pp. 88–94, 2010.

[42] J. Van Der Bijl, “Sustainable DSM on deep mine refrigeration systems - A novel approach,” PhD Thesis, NWU, Potchefstroom, South Africa, 2008.

[43] H. L. Hartman, J. M. Mutmansky, R. V Ramani, and Y. J. Wang, *Mine Ventilation and Air Conditioning*. New York, NY: John Wiley & Sons, 2012.

[44] J. van der Walt and A. Whillier, “Considerations in the design of integrated systems for distributing refrigeration in deep mines,” *Journal of the South African Institute of Mining and Metallurgy*, pp. 109–124, 1978.

[45] A. J. Schutte, D. R. Pelzer, and P. E. H. Mathews, “Improving cooling system efficiency with pre-cooling,” *Industrial and Commercial Use of Energy Conference (ICUE)*, vol. 9, pp. 1–4, 2012.

[46] ASHRAE, *Handbook on equipment*. Atlanta: American Society of Heating, Refrigeration and Air conditioning Engineers, 1997.

[47] R. Hemp, W. Holding, and R. M. Stroh, *Environmental Engineering in South African Mines*. Cape Town, South Africa: Cape & Transvaal Printers, 1982.

[48] BPMA, “Variable speed driven pumps: Best practise guide,” British Pump Manufactures’ Association, Birmingham, 2004.

[49] F. M. White, *Fluid Mechanics*. Boston: McGraw-Hill, 2008.

[50] E. Ozdemir, “Energy conservation opportunities with a variable speed controller in a boiler house,” *Applied Thermal Engineering*, vol. 24, no. 7, pp. 981–993, 2004.

[51] E. da Costa Bortoni, “Are my motors oversized?,” *Energy Conversion and Management*, vol. 50, no. 9, pp. 2282–2287, 2009.

[52] C. J. R. Kriel, H. P. R. Joubert, and J. H. Marais., “The influence of VSDs on electric motor operating temperatures,” *Vector*, pp. 34–38.

[53] B. K. Bose, “Energy, environment, and advances in power electronics,” in *Industrial Electronics, 2000. ISIE 2000. Proceedings of the 2000 IEEE International Symposium*, 2000, vol. 15(4), pp. 688 – 701.

[54] M. Teitel, A. Levi, Y. Zhao, M. Barak, E. Bar-lev, and D. Shmuel, “Energy saving in agricultural buildings through fan motor control by variable frequency drives,” *Energy and Buildings*, vol. 40, no. 6, pp. 953–960, 2008.

[55] A. T. De Almeida, S. Greenberg, and C. Blumstein, “Demand-side management opportunities through the use of energy-efficient motor systems,” *Power Systems, IEEE Transactions on*, vol. 5, no. 3, pp. 852–861, 1990.

[56] R. Saidur, “A review on electrical motors energy use and energy savings,” *Renewable and Sustainable Energy Reviews*, no. 14, pp. 877–898, 2010.

[57] Y. Yao, Z. Lian, Z. Hou, and X. Zhou, “Optimal operation of a large cooling system based on an empirical model,” *Applied Thermal Engineering*, vol. 24, no. 16, pp. 2303–2321, 2004.

[58] R. Saidur, T. M. I. Mahlia, and M. Hasanuzzaman, “Developing energy performance standard, label and test procedures and impacts analysis for commercial chillers,” *Energy Education Science and Technology Part A: Energy Science and Research*, vol. 27, no. 1, pp. 175–190, 2011.

[59] J. Tolvanen, “Saving energy with variable speed drives,” *World pumps*, vol. 2008, no. 501, pp. 32–33, 2008.

[60] R. Saidur, S. Mekhilef, A. Safari, and H. A. Mohammed, “Applications of variable speed drive (VSD) in electrical motors energy savings,” *Renewable and Sustainable Energy Reviews*, no. 16, pp. 543–550, 2012.

[61] M. H. Rashid, *Power electronics handbook: devices, circuits and applications*. Academic press, 2010.

[62] P. Pulkki, “Not just speed control [variable speed AC drives],” in *Cement Industry Technical Conference, 2004. IEEE-IAS/PCA*, 2004, pp. 169–183.

[63] K. H. Sueker, *Power electronics design: a practitioner’s guide*. Elsevier, 2005.

[64] P. C. Sen, *Principles of electric machines and power electronics*. John Wiley & Sons, 2007.

[65] L. I. Abbott, “Power quality and cost analysis of industrial electrical distribution systems with adjustable speed drives.” Masters Dissertation, California State University, California, USA, 2006.

[66] M. Thirugnanasambandam, M. Hasanuzzaman, R. Saidur, M. B. Ali, S. Rajakarunakaran, D. Devaraj, and N. A. Rahim, “Analysis of electrical motors load actors and energy savings in an Indian cement industry,” *Energy*, vol. 36, pp. 4307–4314, 2011.

[67] S. Zhang and X. Xia, “Modelling and energy efficiency optimization of belt conveyors,” *Applied Energy*, vol. 88, no. 9, pp. 3061–3071, Sep. 2011.

[68] G. Irvine and I. H. Gibson, “The use of variable frequency drives as a final control element in the petroleum industry,” in *Industry Applications Conference, 2000. Conference Record of the 2000 IEEE*, 2000, vol. 4, pp. 2749–2758.

[69] A. Marchi, A. R. Simpson, and N. Ertugrul, “Assessing variable speed pump efficiency in water distribution systems,” *Drinking Water Engineering and Science Discussions*, vol. 5, no. 1, pp. 47–65, 2012.

[70] J. M. Gordon, K. C. Ng, H. T. Chua, and C. K. Lim, “How varying condenser coolant flow rate affects chiller performance: thermodynamic modelling and experimental confirmation,” *Applied Thermal Engineering*, vol. 20, pp. 1149–1159, 2000.

[71] J. A. Romero, J. Navarro-Esbrí, and J. M. Belman-Flores, “A simplified black-box model oriented to chilled water temperature control in a variable speed vapour compression system,” *Applied Thermal Engineering*, vol. 31, no. 2, pp. 329–335, 2011.

[72] J. Vosloo, L. Liebenberg, and D. Velleman, “Case study: Energy savings for a deep-mine water reticulation system,” *Applied Energy*, vol. 88, no. 1, pp. 328–335, 2011.

[73] W. L. Le Roux, “Notes on mine ventilation control.,” in *Mine Ventilation Society of South Africa*, 4th, Ed. Johannesburg, 1990.

[74] J. Van der Walt and E. M. De Kock, “Developments in the engineering of refrigeration installations for cooling mines,” *International Journal of Refrigeration*, vol. 7, no. 1, pp. 27–40, 1984.

[75] H. W. Stanford III, *HVAC Water Chillers and Cooling Towers – Fundamentals, Application, and Operation*. Boca Raton, FL: CRC Press, 2011.

[76] M. D. Stanton, “Development and Testing of an Underground Remote Refrigeration Plant,” Masters Dissertation, NWU, Potchefstroom, South Africa, 2003.

[77] G. E. Du Plessis, L. Liebenberg, and E. H. Mathews, “The use of variable speed drives for cost-effective energy savings in South African mine cooling systems,” *Applied Energy*, vol. 111, pp. 16–27, 2013.

[78] W. F. Stoecker and J. W. Jones, *Refrigeration and air conditioning*, vol. 3. McGraw-Hill London, 1958.

[79] D. G. Kröger, *Air-cooled heat exchangers and cooling towers: Thermal-flow performance evaluation and design*. Faculty of Mechanical Engineering: University of Stellenbosch, 1998.

[80] W. L. Le Roux, *Mine ventilation notes for beginners*. Mine Ventilation Society of South Africa, 1979.

[81] J. Van Rensburg, A Botha, and G. Bolt, “Energy efficiency via optimisation of water reticulation in deep mines,” *2011 Proceedings of the 8th Conference on the Industrial and Commercial Use of Energy*, pp. 124–132, 2011.

[82] A. Botha, “Optimising the demand of a mine water reticulation system to reduce electricity consumption,” Masters Dissertation, NWU, Potchefstroom, South Africa, 2010.

[83] Department of Health and Human Services, “Coal Mine Dust Exposures and Associated Health Outcomes,” 2011.

[84] M. Biffi and D. J. Stanton, “Cooling power for a new age,” in *Third International Platinum Conference “Platinum in Transformation”. The Southern African Institute of Mining and Metallurgy*, 2008, pp. 239–247.

[85] D. Stephenson, “Distribution of water in deep gold mines in South Africa,” *International journal of mine water*, vol. 2, no. 2, pp. 21–30, 1983.

[86] D. A. J. Ross-Watt, “A discipline for the future,” *Journal of the South African Institute of Mining and Metallurgy*, vol. 95, no. 6, pp. 241–268, 1995.

[87] “In stope equipment,” *HPE Hydro Power Equipment*, 2010. [Online]. Available: www.hpesa.com/. [Accessed: 17-Mar-2015].

[88] M. Karsten and L. Mackay, “Underground environmental challenges in deep platinum mining and some suggested solutions,” *The Southern African Institute of Mining and Metallurgy*, pp. 177–192, 2012.

[89] A. Vladimirescu, K. Zhang, A. R. Newton, D. O. Pederson, and A. Sangiovanni-Vincentelli, *SPICE Version 2G Users Guide*. Department of Electrical Engineering and Computer Sciences, University of California, 1981.

[90] J. J. Hirsch, F. C. Winkelmann, W. F. Buhl, K. L. Ellington, J. McMenamin, I. Rohmund, S. Criswell, A. Bhimani, B. Spurlock, and D. Borstein, “POWERDOE, a windows-based visually oriented analysis tool,” in *Proceedings of the 1995 IBPSA Building Simulation Conference*, 1995, pp. 669–673.

[91] U. of W.--M. S. E. Laboratory and S. A. Klein, *TRNSYS, a transient system simulation program*. Solar Energy Laboratory, University of Wisconsin--Madison, 1979.

[92] E. H. Mathews and E. Van Heerden, “A tool for integrated HVAC, building, energy and control analysis Part 2: control simulations with QUICKcontrol,” *Building and environment*, vol. 34, no. 4, pp. 451–467, 1999.

[93] J. C. Vosloo, “A new minimum cost model for water reticulation systems on deep mines.” PhD Thesis, NWU, Potchefstroom, South Africa, 2008.

[94] S. J. Bluhm, F. H. Von Glehn, W. M. Marx, and M. Biffi, “VUMA mine ventilation software,” *Journal of the Mine Ventilation Society of South Africa*, vol. 54, pp. 65–72, 2001.

[95] M. A. Cascia, “Digital controller for a cooling and heating plant having near-optimal global set point control strategy,” United States Patent No. US5963458, 27-Jul-1997, Publication No. US5963458, 5-Oct-1999.

[96] J. A. Zaloom, “Optimizing operational efficiency and reducing costs of major energy system at large facilities,” United States Patents No. US6366889, 18-May-1999, Publication No. US6366889, 2-Aprl-2002.

[97] J. W. Rautenbach and M. Kleingeld, “Engineering a novel automated pump control system for the mining environment,” *Industrial and Commercial Use of Energy*, pp. 89–91, 2008.

[98] E. H. Mathews, “A remote energy management system for HVAC systems,” South African Paten No. SA2004/1172, 2004.

[99] Honeywell Inc, “RTP ControlTM.” NJ 07962, Tel: +97 3455 2000, Fax: 973 455-4807, 101 Columbia Road, Morristown.

[100] E. H. Mathews, “Process Toolbox (PTB),” Preliminary South African Patent No. 2014/08034, 2014.

[101] J. Calitz, “Research and implementation of a load reduction system for a mine refrigeration system,” Masters Dissertation, NWU, Potchefstroom, 2006.

[102] E. H. S. Limited, “Schedule of standard prices for Eskom tariffs 1 April 2015 to 31 March 2016 for non-local authority supplies, and 1 July 2015 to 30 June 2016 for local authority supplies, and 1 July 2015 to 30 June 2016 for local authority supplies,” vol. 0207, no. April 2015, pp. 1–43.

Appendix A – DATA SHEETS

Table 19: Pre-cooling fans' information for PTB simulation

		Pre-Cooling Tower 1 Fans								Pre-Cooling Tower 2 Fans							
Name	**Unit**		**2**	**3**	**4**	**5**	**6**	**7**	**8**	**1**	**2**	**3**	**4**	**5**	**6**	**7**	**8**
PTB number			**159**		**163**		**167**		**171**		**207**		**211**		**215**		**219**
Fan Motor Power	kW	30	30	30	30	30	30	30	30	30	30	30	30	30	30	30	30
Fan Flow	kg/s	50	50	50	50	50	50	50	50	50	50	50	50	50	50	50	50
Fan Motor Efficiency		0.95	0.95	0.95	0.95	0.95	0.95	0.95	0.95	0.95	0.95	0.95	0.95	0.95	0.95	0.95	0.95
Fan Efficiency		0.95	0.95	0.95	0.95	0.95	0.95	0.95	0.95	0.95	0.95	0.95	0.95	0.95	0.95	0.95	0.95
Fan Inlet Pressure	kPa	87.2	87.2	87.2	87.2	87.2	87.2	87.2	87.2	87.2	87.2	87.2	87.2	87.2	87.2	87.2	87.2
Fan inlet Temperature	˚C	21	21	21	21	21	21	21	21	21	21	21	21	21	21	21	21

Table 20: Condenser cooling and BAC fans' information for PTB simulation

		Condenser-Cooling Towers Fans				BAC Fans		
Name	**Unit**	**1**	**2**	**3**	**4**	**1**	**2**	**3**
PTB number		**131**	**139**	**144**	**149**	**174**	**177**	**180**
Fan Motor Power	kW	132	132	132	132	220	220	220
Fan Flow	kg/s	252	252	252	252	133	133	133
Fan Motor Efficiency		0.95	0.95	0.95	0.95	0.95	0.95	0.95
Fan Efficiency		0.95	0.95	0.95	0.95	0.95	0.95	0.95
Fan inlet Pressure	kPa	87.23	87.23	87.23	87.23	87.23	87.23	87.23
Fan inlet Temperature	˚C	21	21	21	21	21	21	21

Table 21: Pre-cooling towers' information for PTB simulation

		Pre-Cooling Towers 1				Pre-Cooling Towers 2			
Name	**Unit**	**1**	**2**	**3**	**4**	**1**	**2**	**3**	**4**
PTB number		**1**	**9**	**10**	**11**	**192**	**197**	**198**	**199**
Barometric Pressure	kPa	87.23	87.23	87.23	87.23	87.23	87.23	87.23	87.23
Water inlet Temperature	˚C	25.1	25.1	25.1	25.1	25.1	25.1	25.1	25.1
Water Outlet Temperature	˚C	18.5	18.5	18.5	18.5	18.5	18.5	18.5	18.5
Water Flow	ℓ/s	50	50	50	50	50	50	50	50
Air Inlet Temperature	˚C	21	21	21	21	21	21	21	21
Air Inlet Relative Humidity	%	42.24	42.24	42.24	42.24	42.24	42.24	42.24	42.24
Air Flow	kg/s	50	50	50	50	50	50	50	50

Table 22: Condenser cooling towers' and BACs' information for PTB simulation

		Condenser-Cooling Towers				BAC		
Name	**Unit**	**1**	**2**	**3**	**4**	**1**	**2**	**3**
PTB number		**63**	**152**	**153**	**154**	**95**	**97**	**98**
Barometric Pressure	kPa	87.23	87.23	87.23	87.23	87.23	87.23	87.23
Water Inlet Temperature	˚C	31	31	31	31	31	31	31
Water Outlet Temperature	˚C	26	26	26	26	26	26	26
Water Flow	ℓ/s	420	420	420	420	133	133	133
Air Inlet Temperature	˚C	21	21	21	21	21	21	21
Air Inlet Relative Humidity	%	42.24	42.24	42.24	42.24	42.24	42.24	42.24
Air Flow	kg/s	252	252	252	252	133	133	133

Table 23: FPs' information for PTB simulation

		Fridge Plants			
Name	**Unit**	**1**	**2**	**3**	**4**
PTB number		**24**	**30**	**35**	**41**
Evaporator Outlet Temperature	˚C	6	6	6	6
Evaporator Inlet Temperature	˚C	15.32	15.32	15.32	15.32
Evaporator Flow	ℓ/s	300	300	300	300
Condenser Outlet Temperature	˚C	31	31	31	31
Condenser Inlet Temperature	˚C	26	26	26	26
Compressor Motor Power	kW	2100	2100	2100	2100
Condenser Flow	ℓ/s	540	540	540	540
Cooling Duty Condenser	kW	11702.658	11702.658	11702.658	11702.658
Cooling Duty Evaporator	kW	-11300.85	-11300.85	-11300.85	-11300.85

Table 24: Pre-cool and BAC pumps' information for PTB simulation

		Pre-cooling pumps				BAC Outlet Pumps		
Name	**Unit**	**1**	**2**	**3**		**1**	**2**	**3**
PTB number		**117**	**109**	**110**		**113**	**102**	**103**
Pump Motor Power	kW	45	45	45	45	30	30	30
Pump Flow	ℓ/s	200	200	200	200	133	133	133
Pump Motor Efficiency		0.75	0.75	0.75	0.75	0.75	0.75	0.75
Pump Efficiency		0.95	0.95	0.95	0.95	0.95	0.95	0.95
Pumping Elevation	m	0	0	0	0	0	0	0

Table 25: Evaporator and Condenser pumps' information for PTB simulation

		Evaporator Pumps				Condenser Pumps			
Name	**Unit**	**1**	**2**	**3**	**4**	**1**	**2**	**3**	**4**
PTB number		**114**	**28**	**33**	**39**	**18**	**52**	**55**	**59**
Pump Motor Power	kW	160	160	160	160	185	185	200	185
Pump Flow	ℓ/s	309	309	309	309	540	540	540	540
Pump Motor Efficiency		0.75	0.75	0.75	0.75	0.75	0.75	0.75	0.75
Pump Efficiency		0.95	0.95	0.95	0.95	0.95	0.95	0.95	0.95
Pumping Elevation	m	0	0	0	0	0	0	0	0
Minimum Cut Back from Maximum Design Flow Rate	%	30	30	30	30	30	30	30	30

Table 26: Dams' information for PTB simulation

		Pre-cooling dams		Launder dam	BAC dam	Chill dam
Name	**Unit**	**1**	**2**	**1**	**4**	**1**
PTB number		**15**	**20**	**70**	**222**	**87**
Temperature	˚C	19.3	12.6	25.5	10.93	5
Flow	kg/s	370	370		399	401
Ambient Temperature	˚C	21	21	21	21	21
Heat transfer Coefficient	$kW/m^2/˚C$	0	0	0	0	0
REMS Volume	m^3	5000	5000	5000		2000

Appendix B – PTB SIMULATION

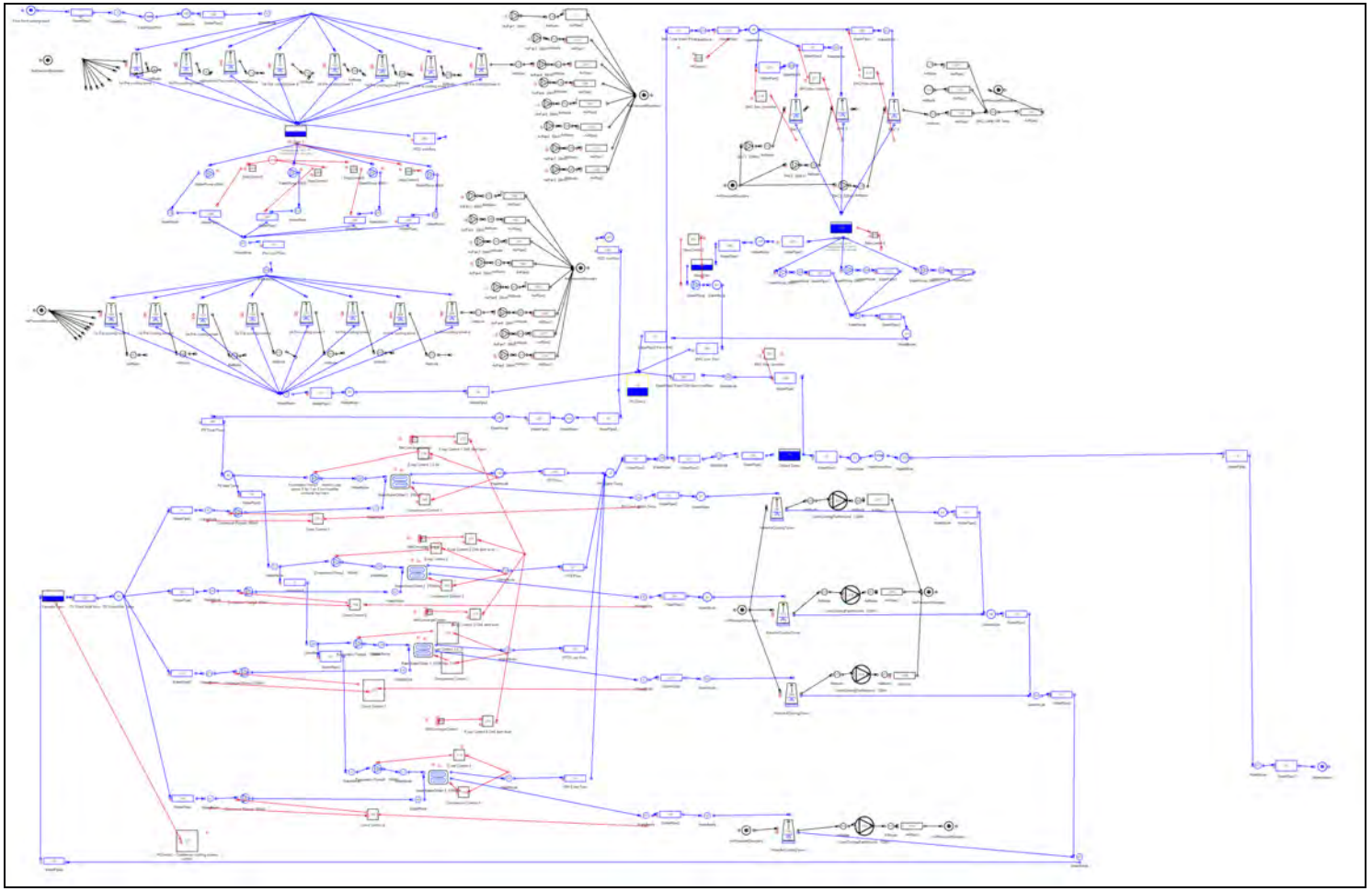

Figure 94: Screen shot of PTB simulation

Appendix C – RECONFIGURING OF MINE A'S PUMP FLOW CONTROL

5℃ Evaporator outlet water temperature setpoint:

Table 27 illustrates a comparison between the baseline and implemented input values for the simulation.

Table 27: Baseline and post implementation simulation input values for a VSD initiative with a 5℃ setpoint

Inputs	Unit	Average Baseline	Average Implemented	Percentage (%) Implemented
Water from Underground Temperature	°C	25.98	25.98	0.00
Ambient Temperature	°C	27.81	27.81	0.00
Humidity	%	29.07	29.07	0.00
Pressure	kPa	86.78	86.78	0.00
Evaporator Compressor Set point	°C	5.00	5.21	4.20
Evaporator Pump Set point	°C	-	5.21	-
Condenser Pump Delta Temp Set Point	°C	-	5.00	-

It is evident from Table 27 that all the inputs were kept the same during the baseline and implemented simulations. Only the FPs' compressor, evaporator and condenser pumps setpoints were updated. The evaporator compressor setpoint was increased with 4.20% as the installed cooling equipment was not capable of cooling the chilled water to the setpoint of 5℃.

The evaporator and condenser pump setpoint was added as the VSDs enabled the water flow to be controlled. Table 28 represents the baseline and after-implementation simulations' output values for the VSD initiative.

Table 28: Baseline and implemented simulation output values for VSD initiative with a 5℃ evaporator setpoint

Outputs	Unit	Average Baseline	Average Implemented	Percentage (%) Improvement
Power Usage	kW	8957.69	8435.28	5.83
FP Total Flow	ℓ/s	1108.44	918.41	17.14
FP Evaporator Inlet Temp	°C	12.07	13.59	-11.19
FP Evaporator Outlet Temp	°C	5.21	5.22	-0.19
Chill Dam Temp	°C	5.75	5.97	-3.60
FP Average COP	0	5.11	5.20	1.78
Condenser Flow	ℓ/s	2163.52	2033.00	6.03
Condenser Inlet	°C	25.12	25.23	0.46
Condenser Outlet	°C	29.01	29.43	1.43
BAC Total Water Flow	ℓ/s	399.00	399.00	0.00
BAC Outlet Air Temp WB	°C	11.57	11.57	0.00
BAC Outlet Water	°C	11.35	11.36	0.14
Recycled Chilled Water	ℓ/s	339.48	149.39	44.01

Table 28 depicts the important outputs and the outputs' percentage improvement. Figure 95 through to Figure 100 below are graphs representing the various outputs. The outputs will be evaluated after each graph. Figure 95 represents a comparison between the baseline and implemented simulation of the cooling equipment power usage.

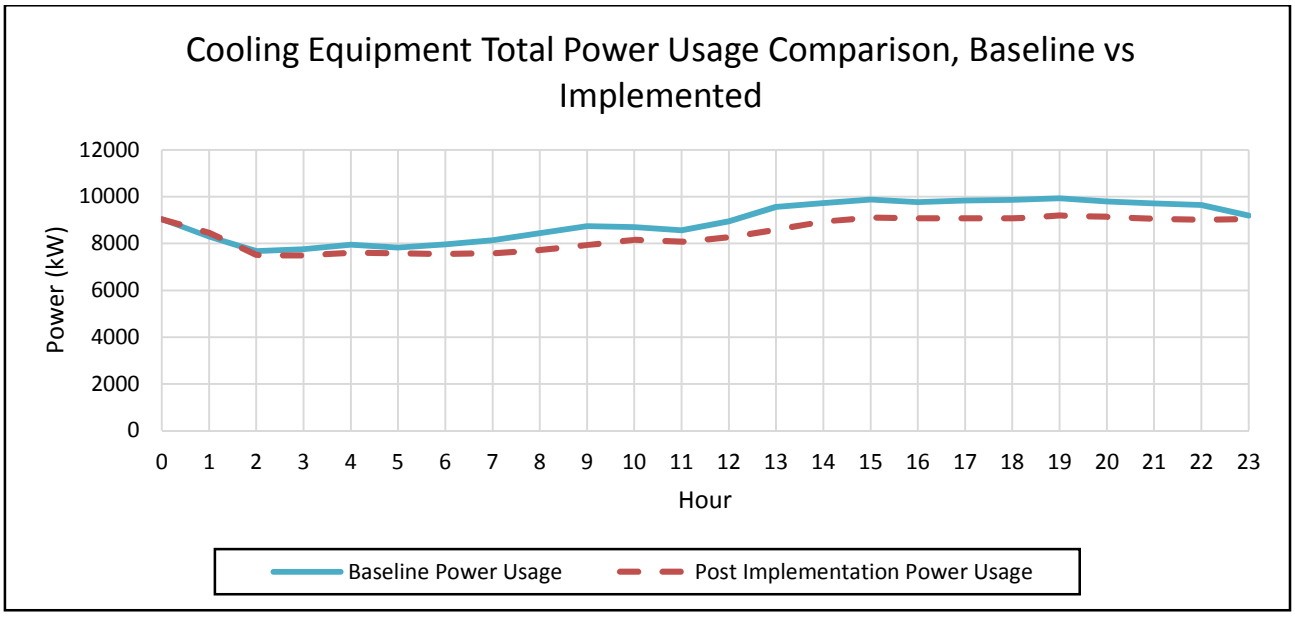

Figure 95: Cooling equipment total power usage comparison, baseline vs. implemented for a 5℃ setpoint

It is evident from Figure 95 that the power consumption was reduced after the implementation of the flow control initiative. The VSD initiative realised in an average power saving of 522.41 kW for the simulated day. Table 12 depicts a power reduction of 5.83%. The VSD initiative throttled the evaporator water flow rate to ensure maximum heat transfer is obtained. The realised power saving is a joint venture from the FPs' compressor guide vanes, evaporator and condenser. Figure 96 represents a comparison between the baseline and implemented simulation of the total water flow through the FPs.

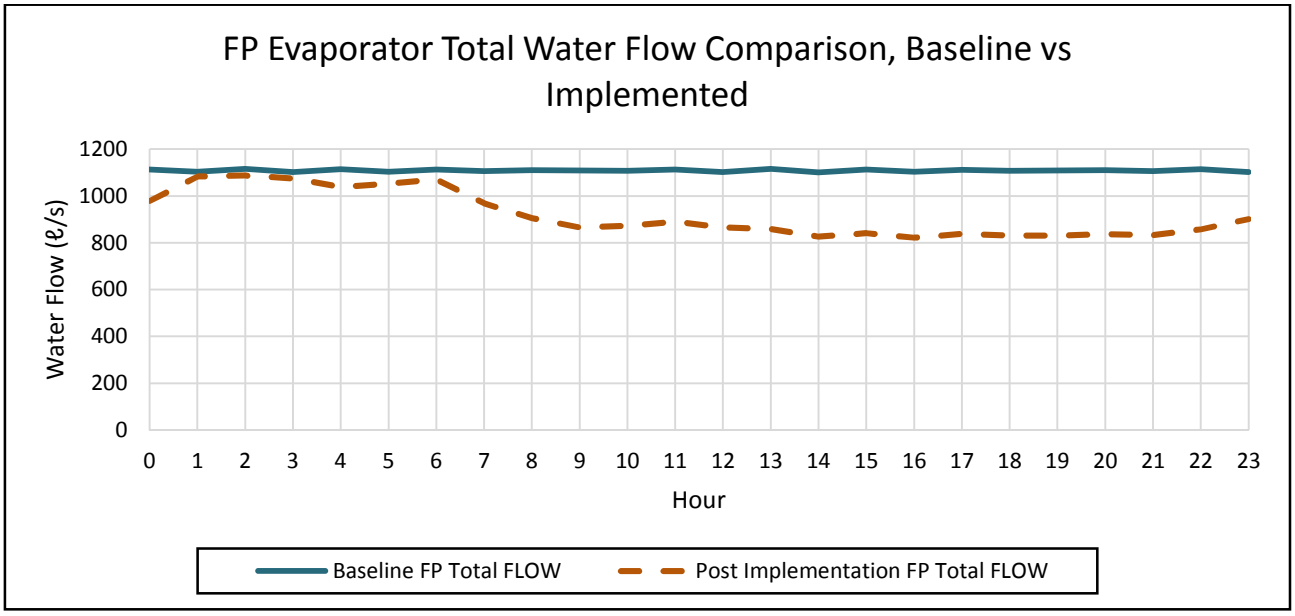

Figure 96: FP evaporator total water flow comparison, baseline vs. implemented for a 5℃ evaporator setpoint

From Figure 96 it is evident that the VSD reduced the water flow through the FPs. Table 12 depicts on average that the water flow was reduced with 17.14% or 190.03 ℓ/s. The reduced water flow allowed more heat to be transferred from the water to the refrigerant gas. This allowed the FP compressor to cut back and reduce the power consumption as the setpoint temperature could easier be established. Figure 97 represents a comparison between the baseline and implemented simulation of the evaporator water temperatures.

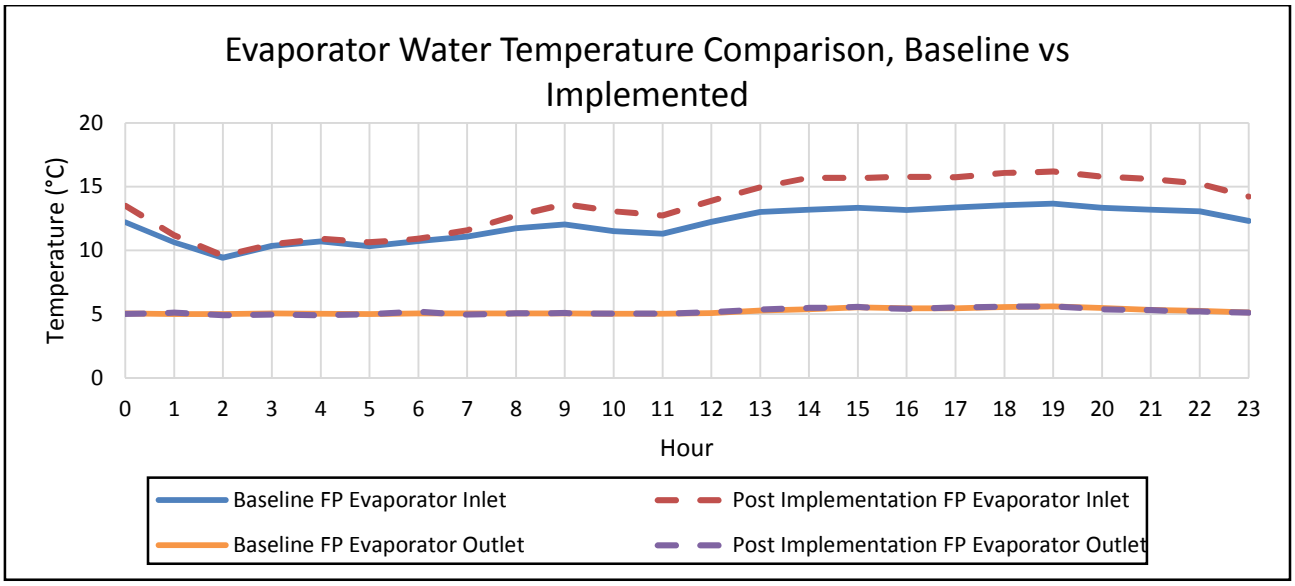

Figure 97: Evaporator water temperature comparison, baseline vs. implemented for a 5℃ evaporator setpoint

It is evident from Figure 97 that the inlet and outlet water temperatures are almost the same, with the implemented temperatures being slightly higher. Table 12 depicts that the post implementation inlet and outlet water temperature are on average 11.19% and 0.19% higher than the baseline simulation.

The increase in the inlet temperature is due to the reduced water flow through the FPs which caused less chilled water to be recycled. This caused the FPs' inlet water temperature to be higher. However, with an increased heat load, the FPs still manage to cool the water. Figure 98 represents a comparison between the baseline and implemented simulation of the FPs' average COP.

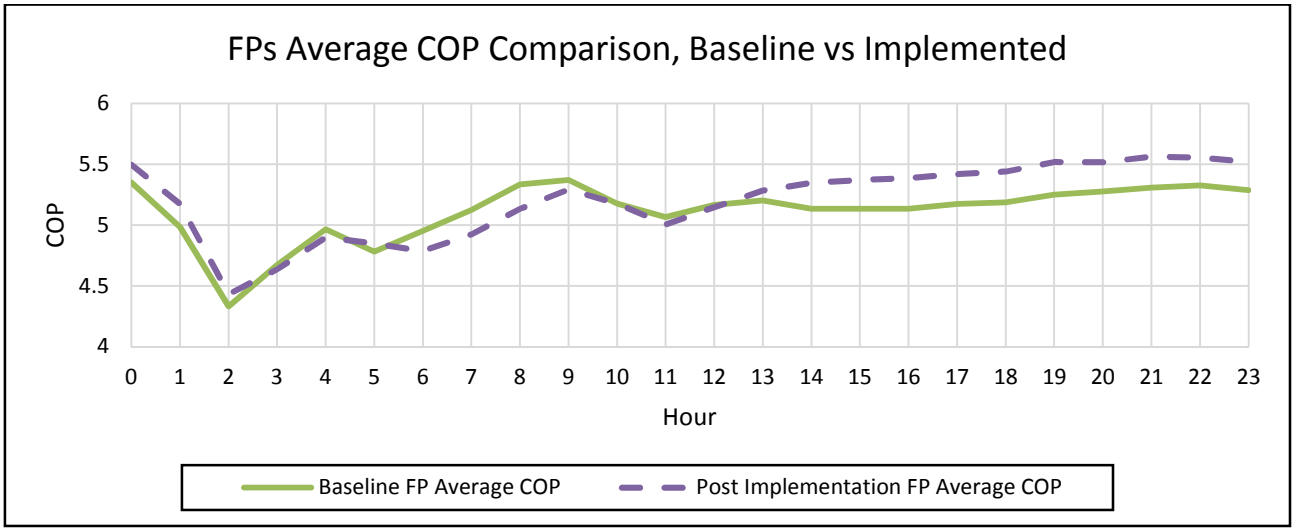

Figure 98: FPs average COP comparison, baseline vs. implemented for a 5℃ setpoint

Figure 98 shows that there is an increase in average COP of the plant throughout the majority of the day. This is due the increased heat load caused by an increase in FPs' inlet water temperature. Table 12 depicts an average COP improvement of 1.78%. Other researchers on VSD have proved implementation of VSD on FP evaporator circuits can result in a COP increase of up to 36% [28], [21], [23], [15], [16]. After further investigation it was discovered that the majority of the evaporator pumps' installed impellers were not full-size impellers. This was discussed in section 4.3. Figure 99 represents a comparison between the baseline and implemented simulation of the BAC air temperatures.

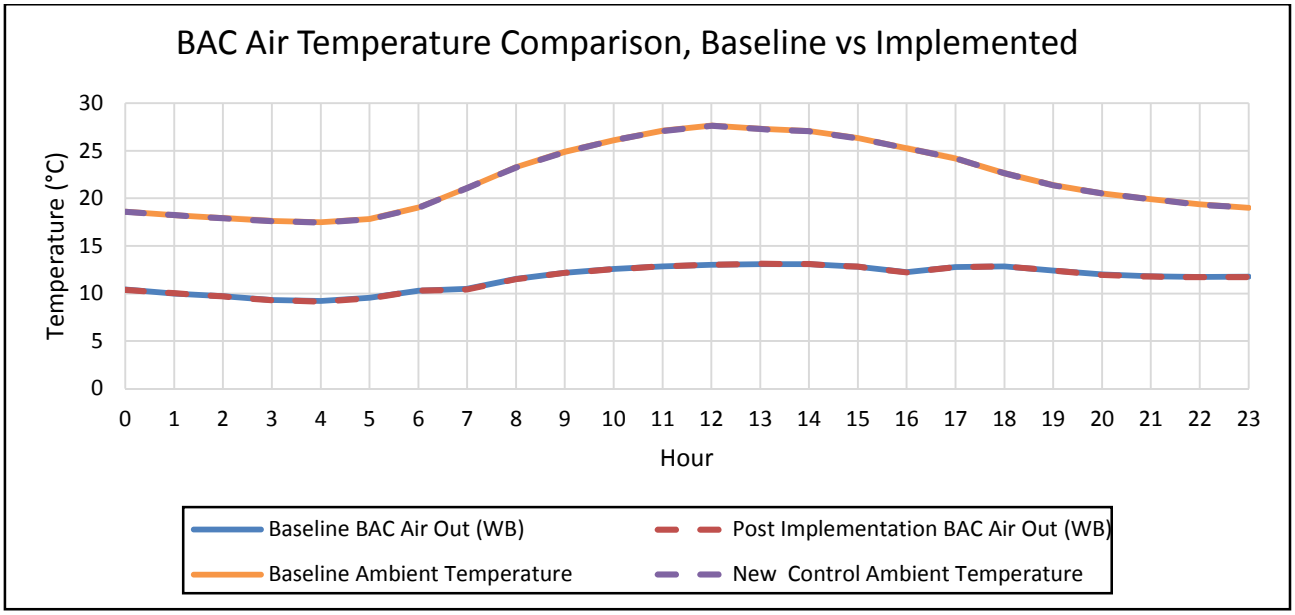

Figure 99: BAC air temperature comparison, baseline vs. implemented for a 5℃ setpoint

From Figure 99 it is evident that the ambient temperature stayed constant through both simulations. The BAC outlet WB air temperature remained unchanged. Figure 100 represents a comparison between the baseline and implemented simulation of the BAC water temperatures.

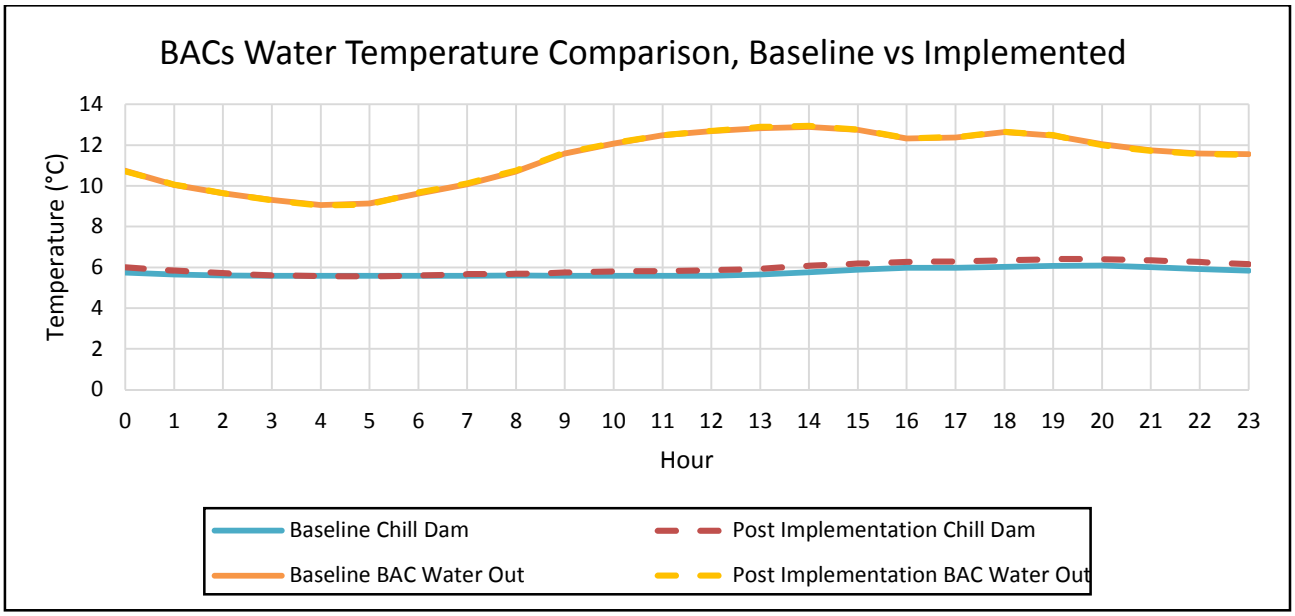

Figure 100: BACs water temperature comparison, baseline vs. implemented for a 5℃ evaporator setpoint

Figure 100 depicts the chill dam temperature or BAC inlet water temperature, which is on average 3.60% higher during day. The BAC outlet water temperature is on average 0.14% higher during the day as Table 12 depicts. This is due to the slight increase in evaporator outlet temperature. These increases in chill dam temperature did not affect the BAC output WB air temperature, as Figure 99 depicts.

4℃ Evaporator outlet water temperature setpoint:

The following set of results depicts the possible cooling mine A can achieve with a chilled water setpoint of 4℃. It also depicts the effect it has on the mine's power usage. A new baseline has to be developed as the evaporator output setpoint temperature was changed. If the same baseline was used, it would not be an accurate representation of the power saving that could be realised. Table 29 represents a comparison between the baseline and implemented input values for the simulations.

Table 29: Baseline and post implementation simulation input values for a VSD initiative with a 4℃ setpoint

Inputs	Unit	Average Baseline	Average Implemented	Percentage (%) Deviation
Water from Underground Temperature	°C	25.98	25.98	0.00
Ambient Temperature	°C	27.81	27.81	0.00
Humidity	%	29.07	29.07	0.00
Pressure	kPa	86.78	86.78	0.00
Evaporator Compressor Set point	°C	4.00	4.00	0.00
Evaporator Pump Set point	°C	-	4.00	-
Condenser Pump Delta Temp Set Point	°C	-	5.00	-

It is evident from Table 29 that all the input values were kept the same for both the baseline and implemented simulations. Table 30 represents a comparison between the baseline and implemented output values for the simulations.

Table 30: Baseline and implemented simulation output values for VSD initiative with a 4℃ evaporator setpoint

Outputs	Unit	Average Baseline	Average Implemented	Percentage (%) Deviation
Power Usage	kW	9384.71	9044.02	3.63
FP Total Flow	ℓ/s	1108.44	907.91	18.09
FP Evaporator Inlet Temp	°C	11.69	13.26	-11.81
FP Evaporator Outlet Temp	°C	4.43	4.13	6.79
Chill Dam Temp	°C	4.98	4.89	1.80
FP Average COP	0	5.09	5.13	0.70
Condenser Flow	ℓ/s	2163.52	2052.82	5.12
Condenser Inlet	°C	25.55	25.74	0.76
Condenser Outlet	°C	4.43	30.39	85.42
BAC Total Water Flow	ℓ/s	399.00	398.96	0.01
BAC Outlet Air Temp WB	°C	11.30	11.19	0.98
BAC Outlet Water	°C	10.97	10.83	1.24
Recycled Chilled Water	ℓ/s	339.45	138.94	40.93

From Table 30 it is evident that the changes to the chilled water setpoint had enormous effect on the output power and temperatures. The FPs' evaporator outlet temperature improved with 6.79% whilst realising in a 3.63% power saving. Figure 101 through to Figure 106 below are graphs representing the various outputs. The outputs will be evaluated after each graph. Figure 101 represents a comparison between the baseline and implemented simulation of the cooling systems' power usage

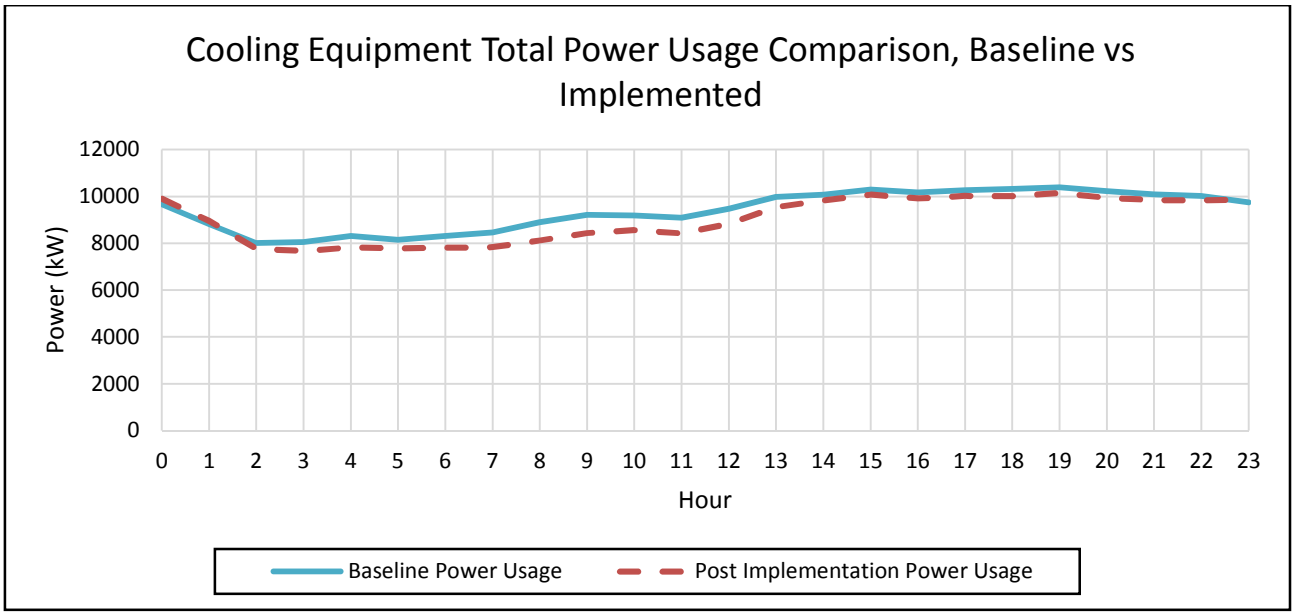

Figure 101: Cooling equipment total power usage comparison, baseline vs. implemented for a 4℃ setpoint

Figure 101 depicts that there is a slight power saving although the setpoint has been decreased to 4℃. The VSD initiative with the new setpoint of 4℃ realised in an average power saving of 340.69 kW for the simulated day. This is an average reduction of 3.63% on the baseline power consumption. The VSD initiative throttled the evaporator water flow rate for maximum heat transfer. The FPs' compressors had to open the guide vanes in order to further increase the cooling. Figure 102 represents a comparison between the baseline and implemented simulation of the total water flow through the FPs.

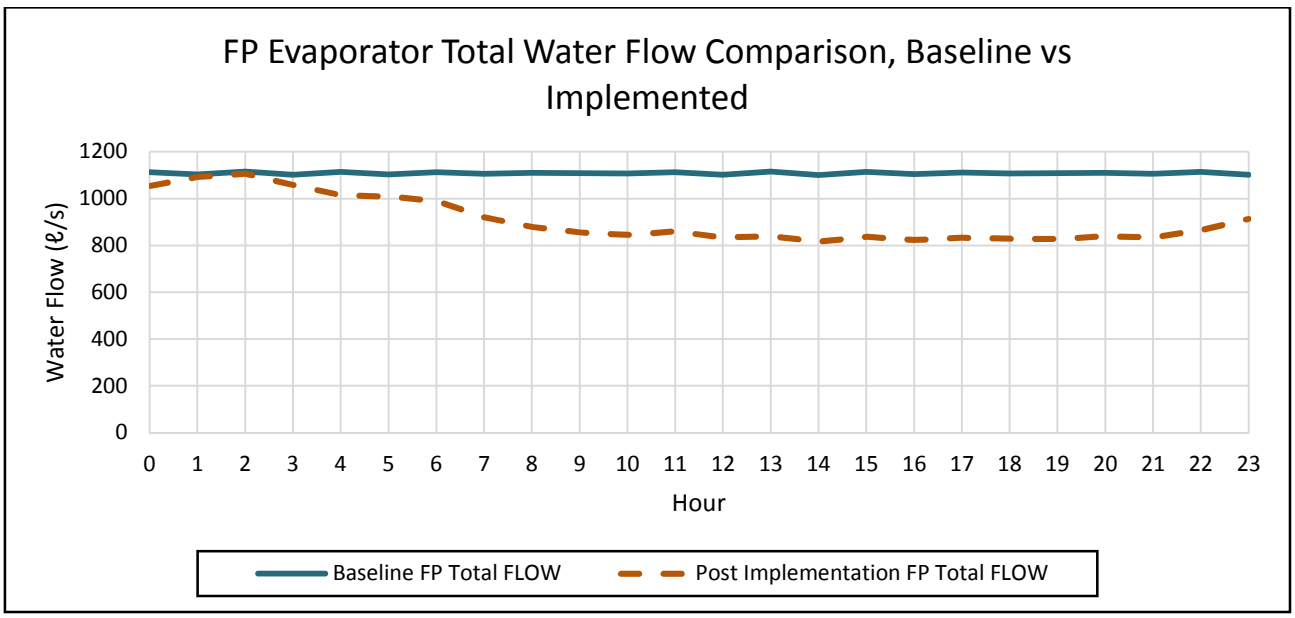

Figure 102: FP evaporator total water flow comparison, baseline vs. implemented for a 4℃ setpoint

Figure 102 depicts the evaporator flow, which was decreased throughout the day to increase the heat transfer between the evaporator water and the refrigerant gas. This allowed the water outlet temperature to be 6.79% lower than the baseline temperature, although the inlet water temperature was warmer. Figure 103 represents a comparison between the baseline and implemented simulation of the evaporator water temperatures.

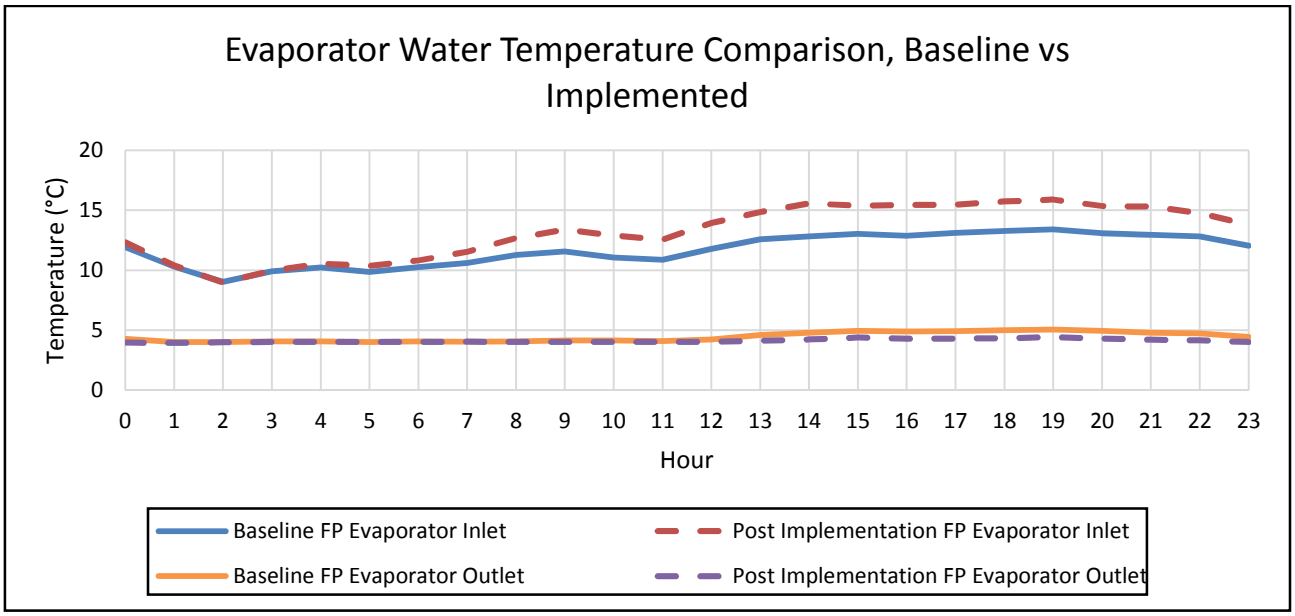

Figure 103: Evaporator water temperature comparison, baseline vs. implemented for a 4℃ setpoint

It is evident from Figure 103 that the inlet water temperature is higher than the baseline simulation due to a reduced recycled chilled water. However, the FPs still managed to maintain an evaporator outlet water temperature of 4.13℃. Table 30 shows that the inlet temperature is on average 11.81% higher and the outlet water temperature is on average 6.79% lower than the baseline simulation values. Figure 104 represents a comparison between the baseline and implemented FPs' average COP simulations.

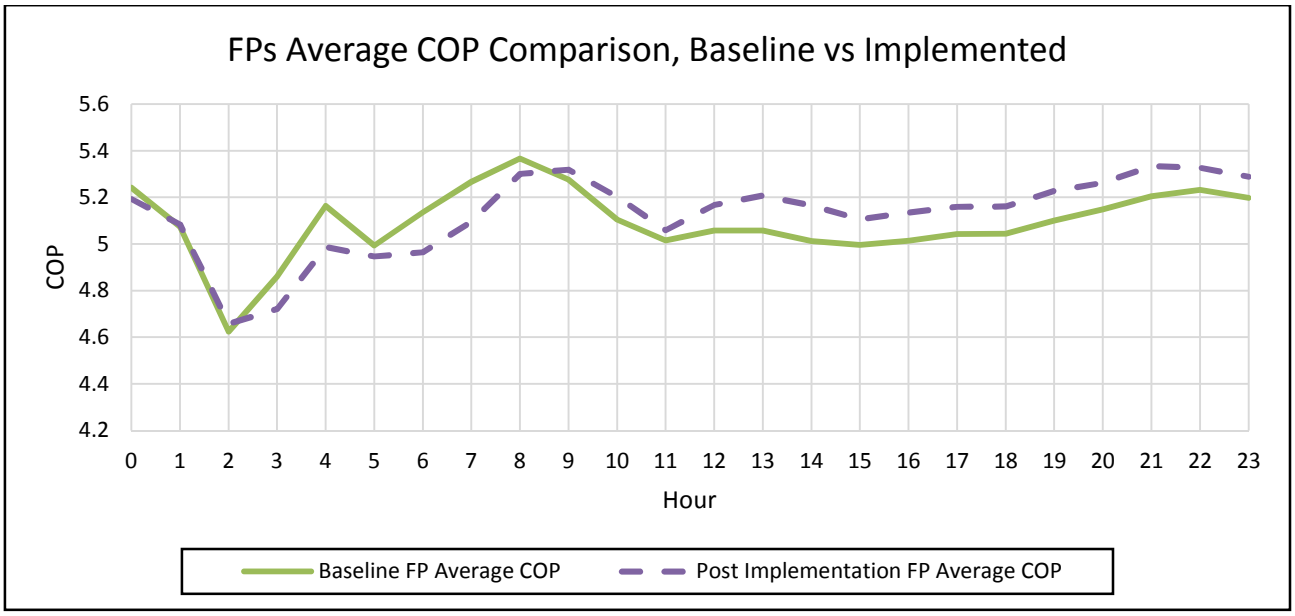

Figure 104: FPs average COP comparison, baseline vs. implemented for a 4℃ setpoint

Figure 104 shows that there is an overall increase in average COP of the FPs. This is due to the increased heat load caused by an increase FP inlet water temperature and a reduced compressor power. Table 30 depicts an average COP improvement of 0.70%. As mentioned in the preceding section, it was discovered that the majority of the evaporator pumps' installed impellers were not full-size impellers; this was discussed in section 4.3. Figure 105 represents a comparison between the baseline and implemented simulation of the BAC air temperatures.

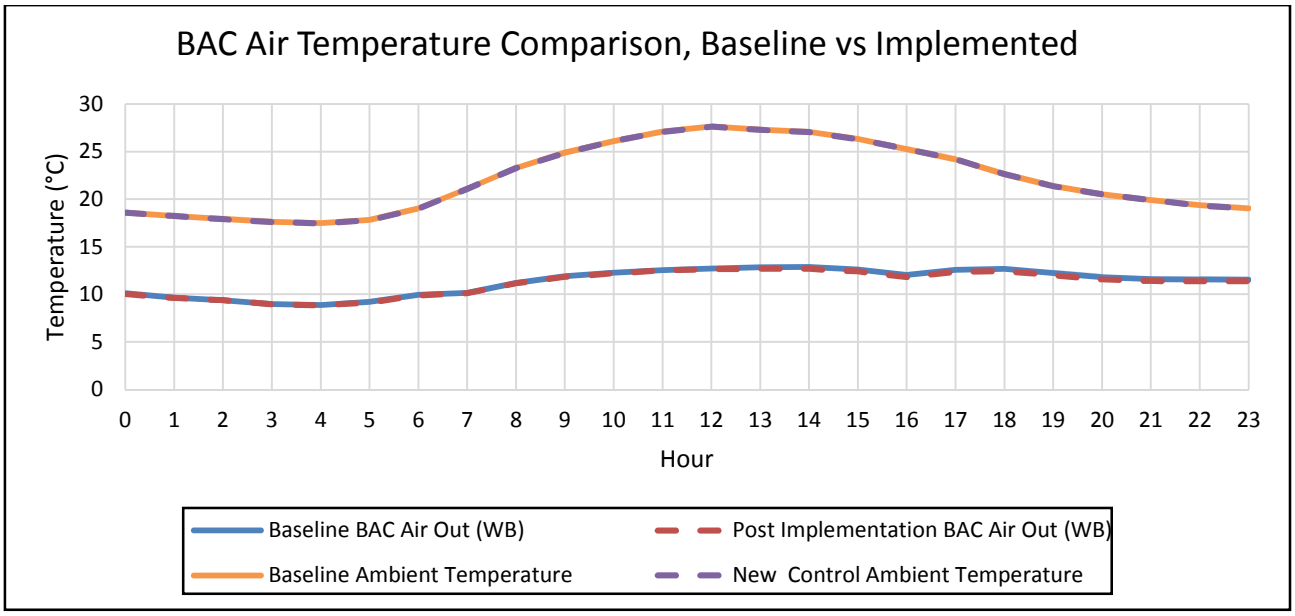

Figure 105: BAC air temperature comparison, baseline vs. implemented for a 4℃ setpoint

It is evident from Figure 105 that the inlet air conditions for both simulations are identical. However, the BAC outlet WB air temperature had a slight improvement. According to Table 30 the BAC outlet temperature improved with 0.98%. The improvement can be attributed to the lowered evaporator outlet water temperature. Figure 106 represents a comparison between the baseline and implemented simulation of the BAC water temperatures.

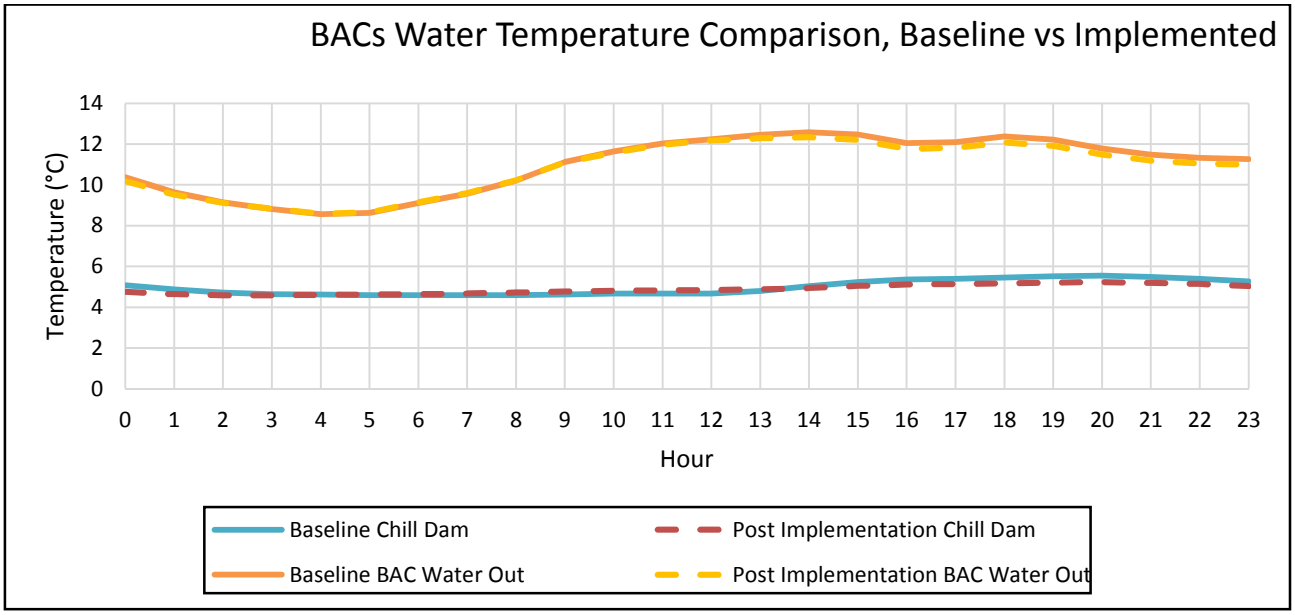

Figure 106: BACs water temperature comparison, baseline vs. implemented for a 4℃ evaporator setpoint

Figure 106 depicts the chill dam temperature, which are lower after implementation. This is due to lower evaporator outlet water temperatures. The BACs' outlet water temperature is also lower during certain periods during the day. The lowered outlet water temperature is due to the BAC not utilising all of the cooling that is provided and cooling is wasted during these periods. The BAC control can be optimised through control philosophy and possibly through physical reconfiguration. This was addressed in section 4.4.

3℃ Evaporator outlet water temperature setpoint:

A new baseline was developed with the ambient psychrometric conditions and input values provided in Table 31.

Table 31: Baseline and post implementation simulation input values for a VSD initiative with a 3℃ setpoint

Inputs	Unit	Average Baseline	Average Implemented	Percentage (%) Deviation
Water from Underground Temperature	°C	25.98	25.98	0.00
Ambient Temperature	°C	27.81	27.81	0.00
Humidity	%	29.07	29.07	0.00
Pressure	kPa	86.78	86.78	0.00
Evaporator Compressor Set point	°C	3.00	3.00	0.00
Evaporator Pump Set point	°C	-	3.00	-
Condenser Pump Delta Temp Set Point	°C	-	5.00	-

From Table 31 it is evident that the FPs' compressor setpoint for the baseline simulation was set at 3℃. The baseline simulation was developed to determine the pre-implementation maximum service delivery and the power consumed to deliver the specific service delivery. The implemented simulation was developed with the added VSD control on the evaporator and condenser pumps. The VSD and FP compressor setpoint was set to 3℃. Table 32 depicts the baseline and implemented simulation outputs.

Table 32: Baseline and implemented simulation output values for VSD initiative with a 3℃ evaporator setpoint

Outputs	Unit	Average Baseline	Average Implemented	Percentage (%) Deviation
Power Usage	kW	9765.25	9487.20	2.85
FP Total Flow	ℓ/s	1108.65	894.38	19.33
FP Evaporator Inlet Temp	°C	11.40	13.13	-13.16
FP Evaporator Outlet Temp	°C	3.79	3.40	10.37
Chill Dam Temp	°C	4.34	4.18	3.58
FP Average COP	0	5.03	5.10	1.44
Condenser Flow	ℓ/s	2107.41	2096.06	0.54
Condenser Inlet	°C	26.03	26.08	0.18
Condenser Outlet	°C	30.74	30.90	0.52
BAC Total Water Flow	ℓ/s	399.00	398.99	0.00
BAC Outlet Air Temp WB	°C	11.09	10.95	1.26
BAC Outlet Water	°C	10.65	10.46	1.76
Chilled Water Recycled	ℓ/s	339.67	125.41	36.92

Table 32 depicts the evaporator outlet water temperature setpoint of 3℃, which had an enormous effect on the power consumption and the output temperatures. The implementation of the VSDs on the FPs' pumps allowed the power consumption and the evaporator outlet temperatures to decrease with 2.85% and 10.37% respectively. Figure 107 up to Figure 112 are visual representations of the baseline and the implemented simulation outputs. Figure 107 presents the power consumption of both the baseline and implemented simulations.

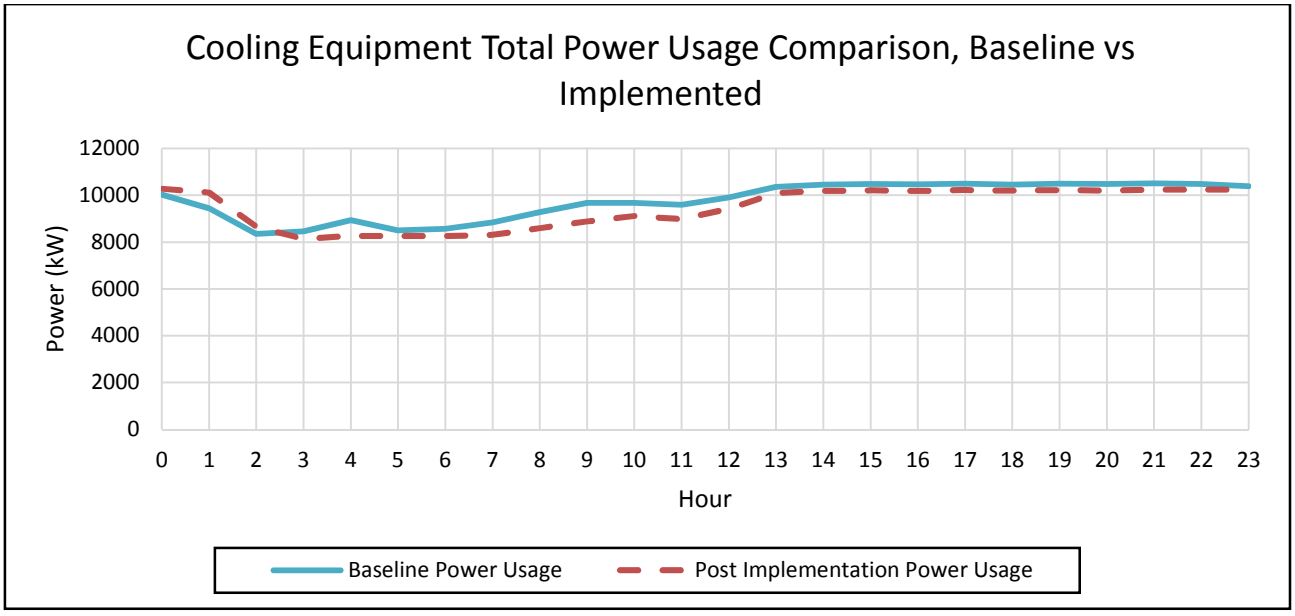

Figure 107: Cooling equipment total power usage comparison, baseline vs. implemented for a 3℃ setpoint

Figure 107 depicts the VSDs' implementation, which reduced the cooling equipment power usage with 278.05 kW. This is due to the VSDs increasing the contact time between the water and refrigerant gas for maximum heat transfer. This allowed the FPs' compressor guide vanes to cut back and increase the power savings. Figure 108 represents the total evaporator water flow through the FPs of the baseline and implemented simulations.

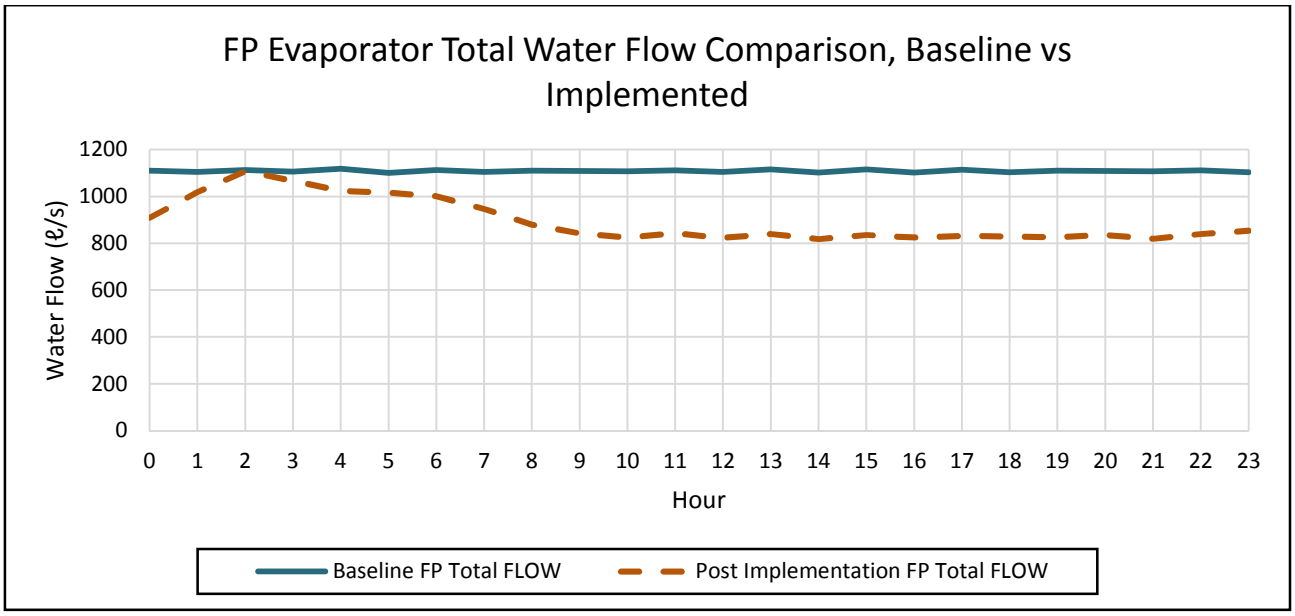

Figure 108: FP evaporator total water flow comparison, baseline vs. implemented for a 3℃ setpoint

From Figure 108 it is evident that the total evaporator water flow was reduced by 19.33%. The reduced flow rate resulted in a decrease in the recycled chilled water. The reduced flow rate allowed maximum heat transfer between the evaporator water and the refrigerant gas. Figure 109 represents the evaporator water temperatures for the baseline and implemented simulations.

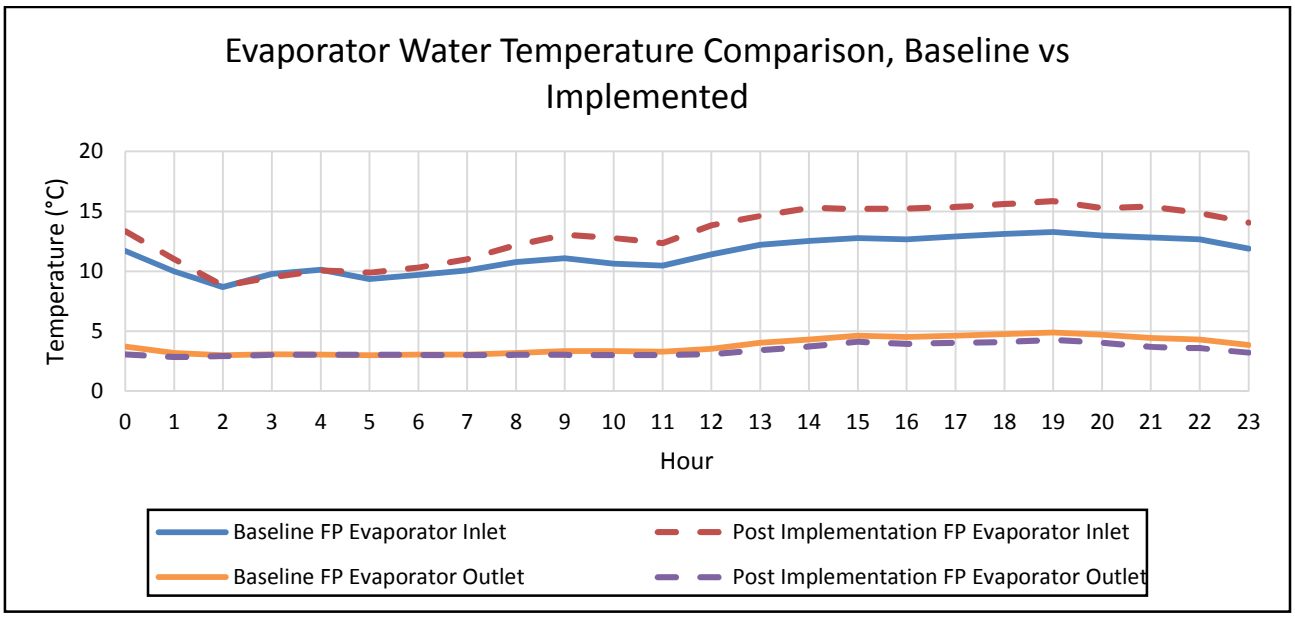

Figure 109: Evaporator water temperature comparison, baseline vs. implemented for a 3℃ setpoint

It is evident from Figure 109 that the inlet water temperature increased after the implementation of the VSDs. This is due to the reduced evaporator water flow rate allowing less chilled water to be recycled. However, the FPs still managed to maintain a 10.37% improved evaporator outlet water temperature of 3.40℃. An increased temperature drop over the evaporator water temperatures will ensure an overall COP increase. Figure 110 is a visual representation of the FPs' average COP's daily profile for both the baseline and implemented simulations.

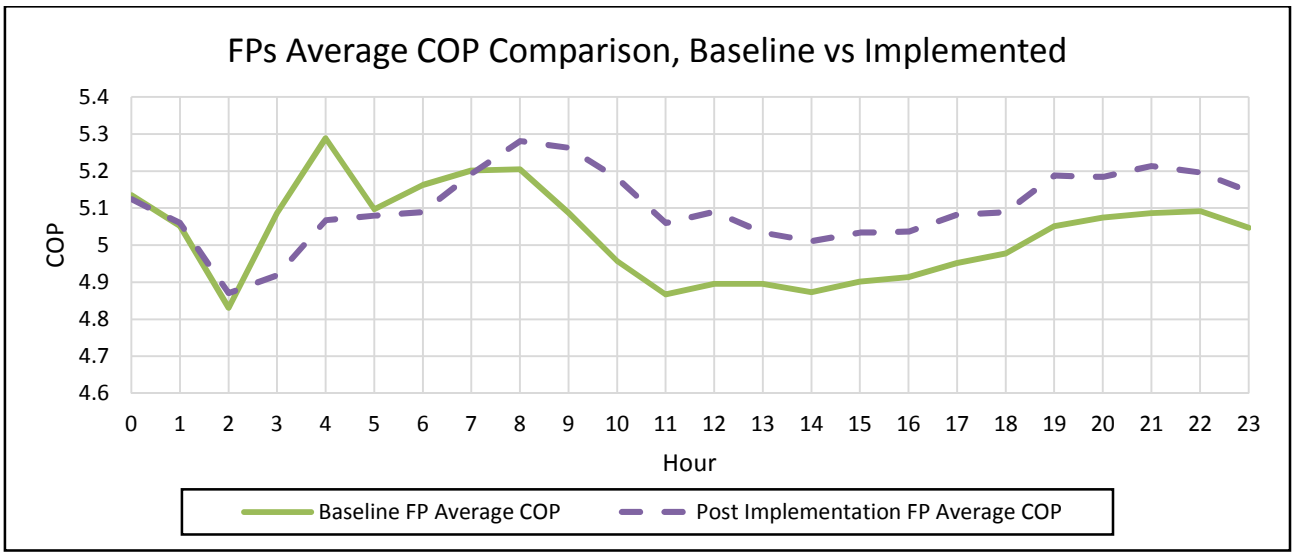

Figure 110: FPs average COP comparison, baseline vs. implemented for a 3℃ setpoint

Figure 110 depicts the FPs' average COP, which was improved throughout the majority of the day. According to Table 32 the daily average COP was increased with 1.44%. Figure 111 represents the BAC water temperature of the baseline and the implemented simulation.

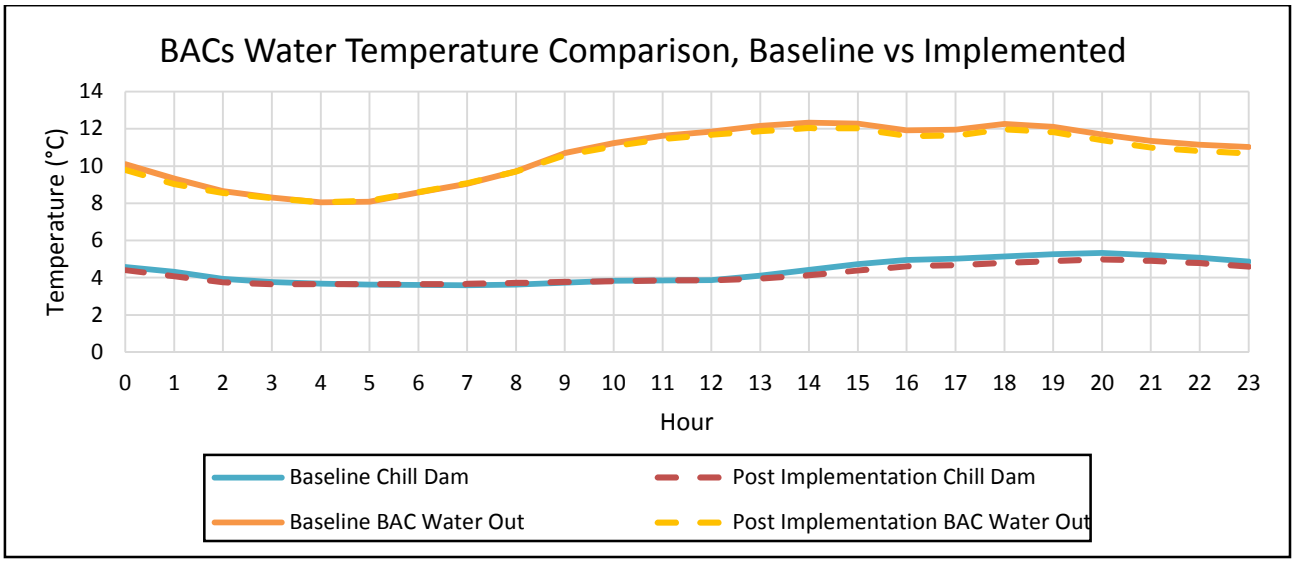

Figure 111: BACs water temperature comparison, baseline vs. implemented for a 3℃ evaporator setpoint

Figure 111 depicts the VSD reconfiguration, which did not affect the BACs' water temperatures. However, if the BACs are provided with colder chilled water, then the BACs should produce lower air temperatures. Figure 112 represents the BACs' air temperatures of both the baseline and implemented simulations.

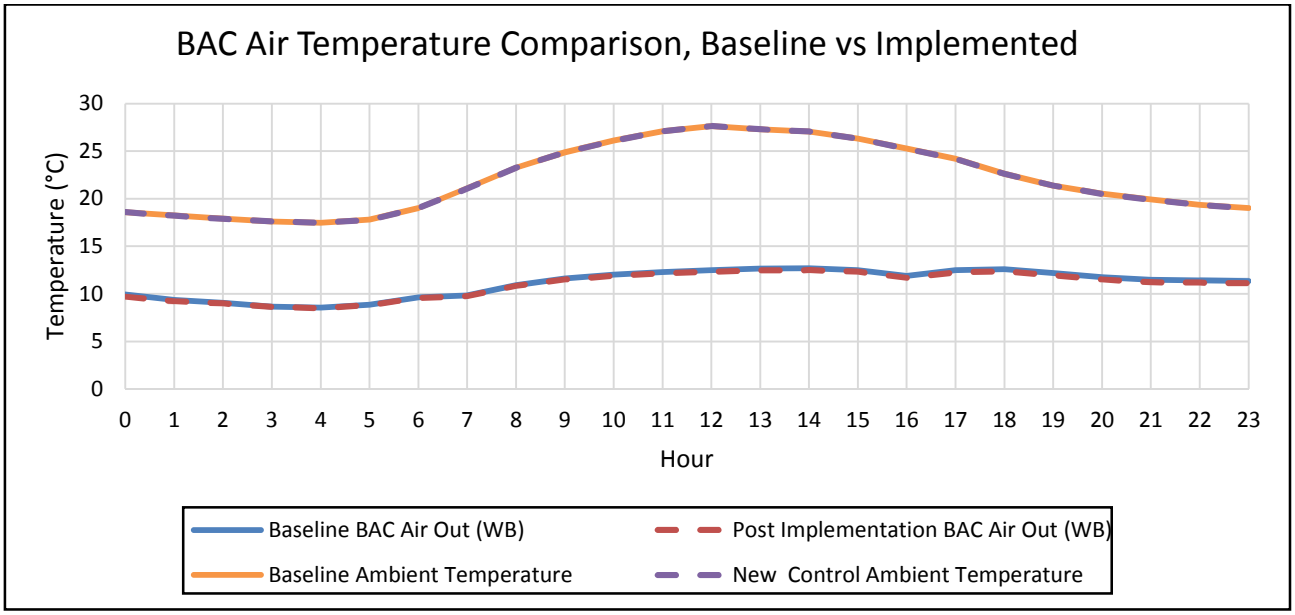

Figure 112: BACs air temperature comparison, baseline vs. implemented for a 3℃ setpoint

From Figure 112 it is evident that the BAC outlet air temperature was not affected by the VSD installation. However, the BACs' outlet WB air temperature did not decrease as expected when the chilled water temperature decreased. Cooling is wasted when too much

chilled water is sent to the BACs during the colder periods of the day. Improvement on the BACs' chilled water control valves can increase the power savings.

Appendix D – RECONFIGURING OF MINE A'S EVAPORATOR PUMP IMPELLERS

The simulation simulating the pump flow control will be considered as the baseline simulation, as mine A already made the reconfiguration and any additional reconfiguration will include the pump flow control upgrade. A winter baseline was developed with the winter ambient psychrometric conditions. The new control philosophies were simulated for the summer and winter condition respectively.

Summer:

5℃ Evaporator outlet water temperature setpoint:

The baseline simulation was simulated with the evaporator output water temperature set to 5℃. The implemented simulation was updated with the new impeller properties and new control philosophy and an evaporator outlet water temperature of 5℃. Table 33 compares the baseline and implemented simulation average outputs against each other.

Table 33: Baseline and implemented simulation output values pump impeller reconfiguring, 5℃ setpoint

Outputs	Unit	Average Baseline	Average Implemented	Percentage (%) Deviation
Power Usage	kW	8435.28	8363.48	0.85
FP Total Flow	ℓ/s	918.41	822.94	10.39
FP Evaporator Inlet Temp	°C	13.59	14.19	-4.25
FP Evaporator Outlet Temp	°C	5.22	5.04	3.44
Chill Dam Temp	°C	5.97	5.94	0.45
FP Average COP	0	5.20	5.18	-0.39
Condenser Flow	ℓ/s	2033.00	2019.32	0.67
Condenser Inlet	°C	25.23	25.24	0.04
Condenser Outlet	°C	29.43	29.62	0.65
BAC Total Water Flow	ℓ/s	399.00	398.99	0.00
BAC Outlet Air Temp WB	°C	11.56	11.51	0.46
BAC Outlet Water	°C	11.36	11.26	0.91
Chilled Water Recycled	ℓ/s	149.39	53.98	36.13

Table 33 depicts the impeller reconfiguring, which does not have a vast impact on the simulation outputs. The energy savings of 0.85% can be expected. Figure 113 is a visual comparison of the baseline and implemented simulation total power consumption.

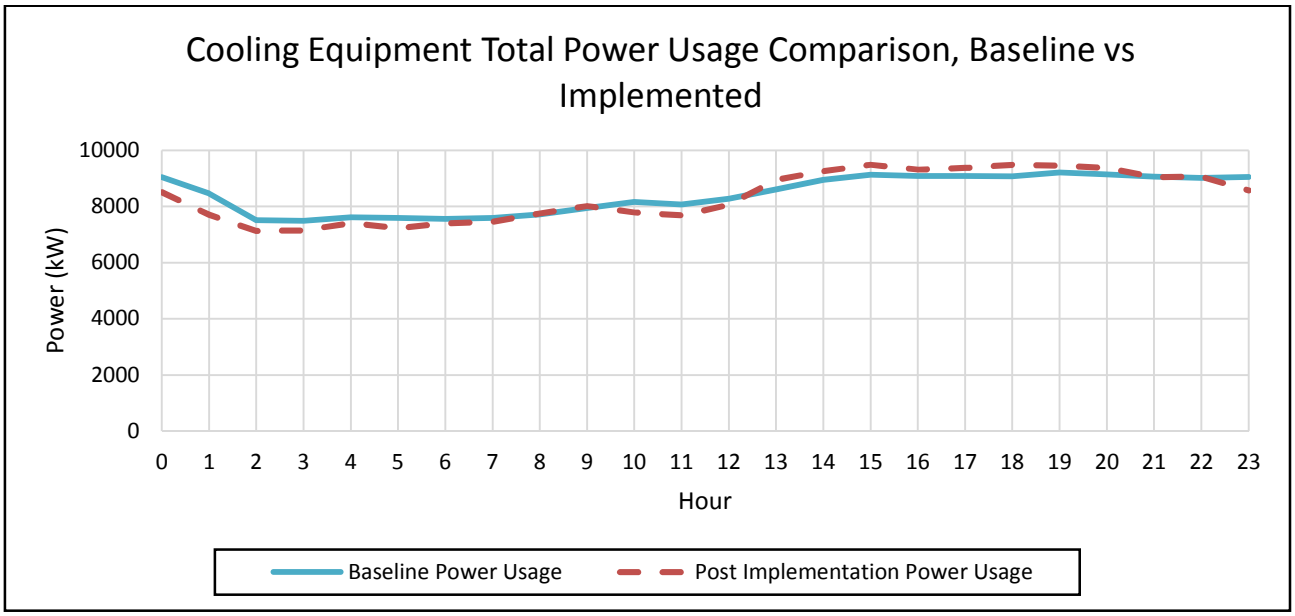

Figure 113: Cooling equipment total power usage comparison, baseline vs. implemented for a 5℃ setpoint

Figure 113 indicates that there is a slight power reduction of 71.80 kW due to the impeller reconfiguration and the control philosophy update. Figure 114 is a comparison of the baseline and implemented simulation water flow.

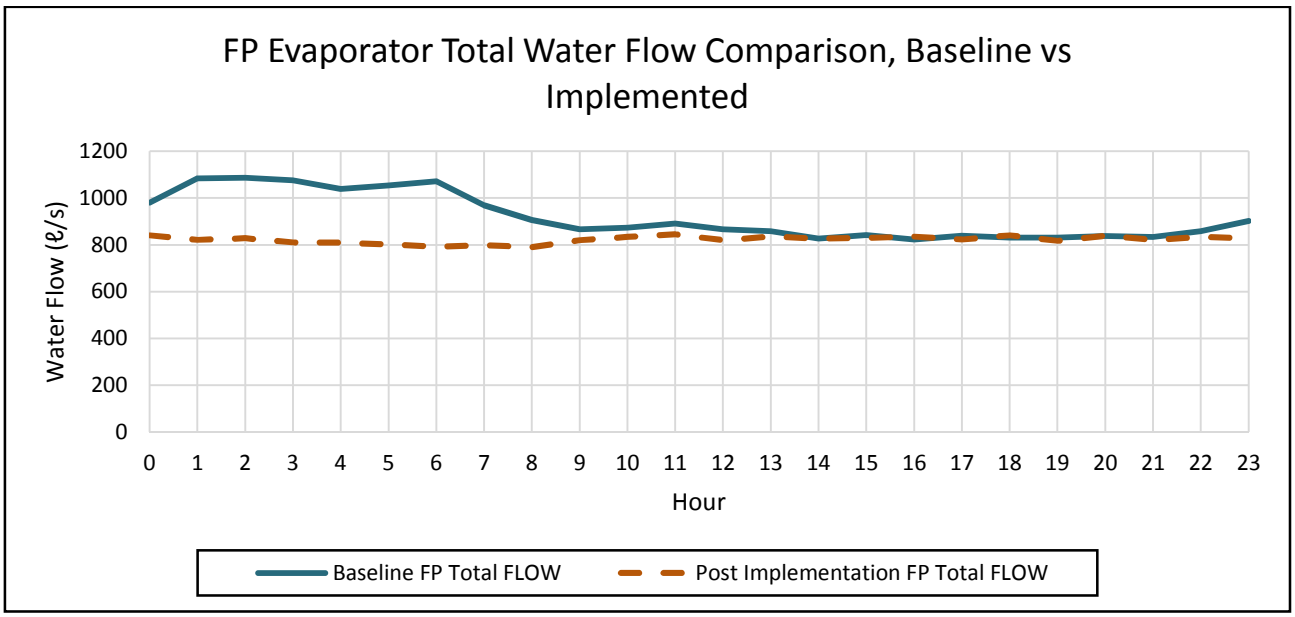

Figure 114: FP evaporator total water flow comparison, baseline vs. implemented for a 5℃ setpoint

From Figure 114 It is evident that the implemented evaporator water flow is less during certain periods of the day. This is due to the control philosophy update allowing the VSDs to cut back on the flow to maintain the correct chill dam level. This reduces the amount of chilled water being recycled. Figure 115 represents the evaporator water temperature for the baseline and implemented simulations.

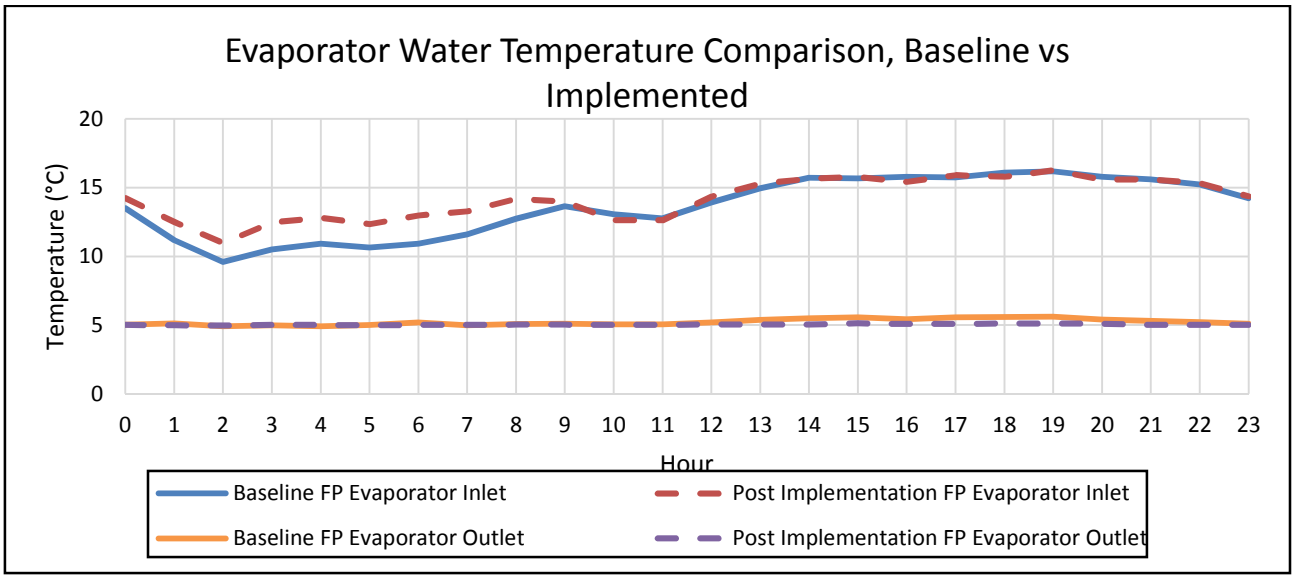

Figure 115: Evaporator water temperature comparison, baseline vs. implemented for a 5℃ setpoint

From Figure 115 it is evident that the evaporator inlet temperature increased during the morning period as the evaporator water reduced, causing the recycled chilled water to decrease. The FPs still managed to maintain an evaporator outlet water temperature of 5.04℃. Figure 116 represents the FPs' average COP of the baseline and the implemented simulations.

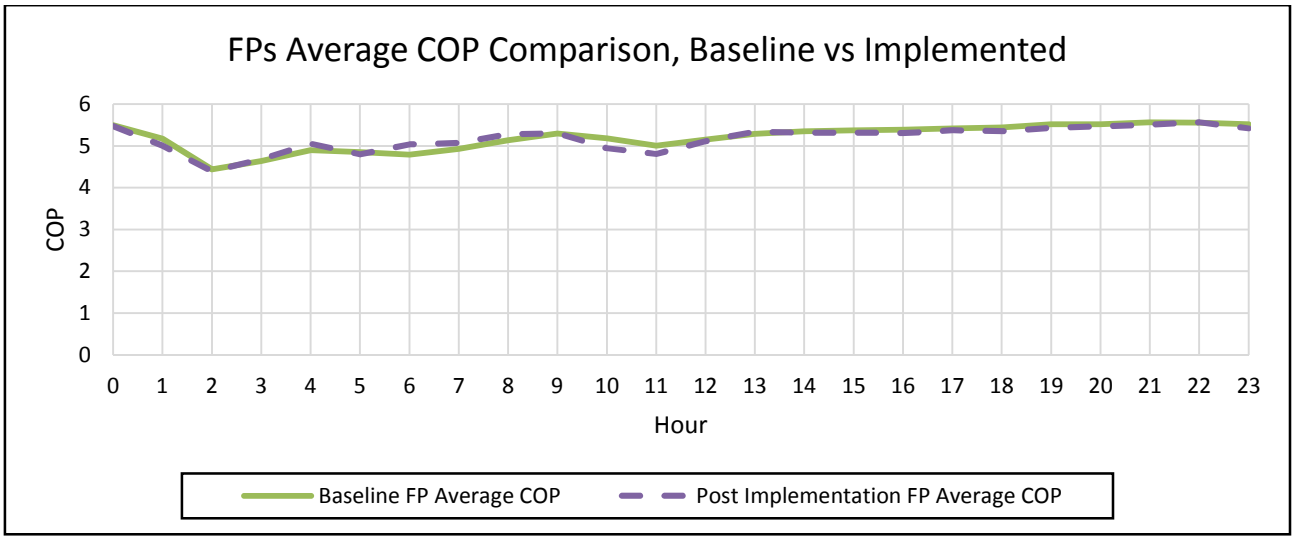

Figure 116: FPs average COP comparison, baseline vs. implemented for a 5℃ setpoint

Figure 116 depicts the FPs' COP, which was not affected by the evaporator pump impeller reconfiguration. Figure 117 represents the BACs' water temperature for the baseline and implemented simulations.

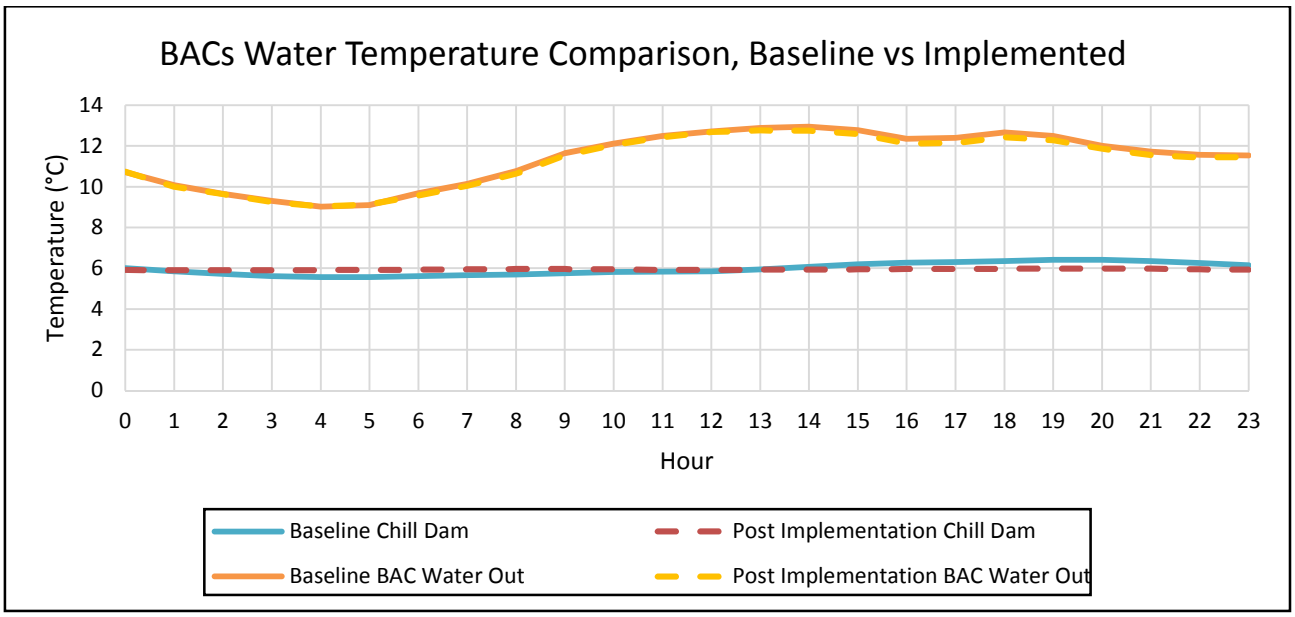

Figure 117: BACs water temperature comparison, baseline vs. implemented for a 5℃ evaporator setpoint

Figure 117 depicts the BAC outlet water temperature, which was not affected by the evaporator pump impeller reconfiguration. Figure 118 is a visual representation of the BACs' air temperatures for the baseline and implemented simulations.

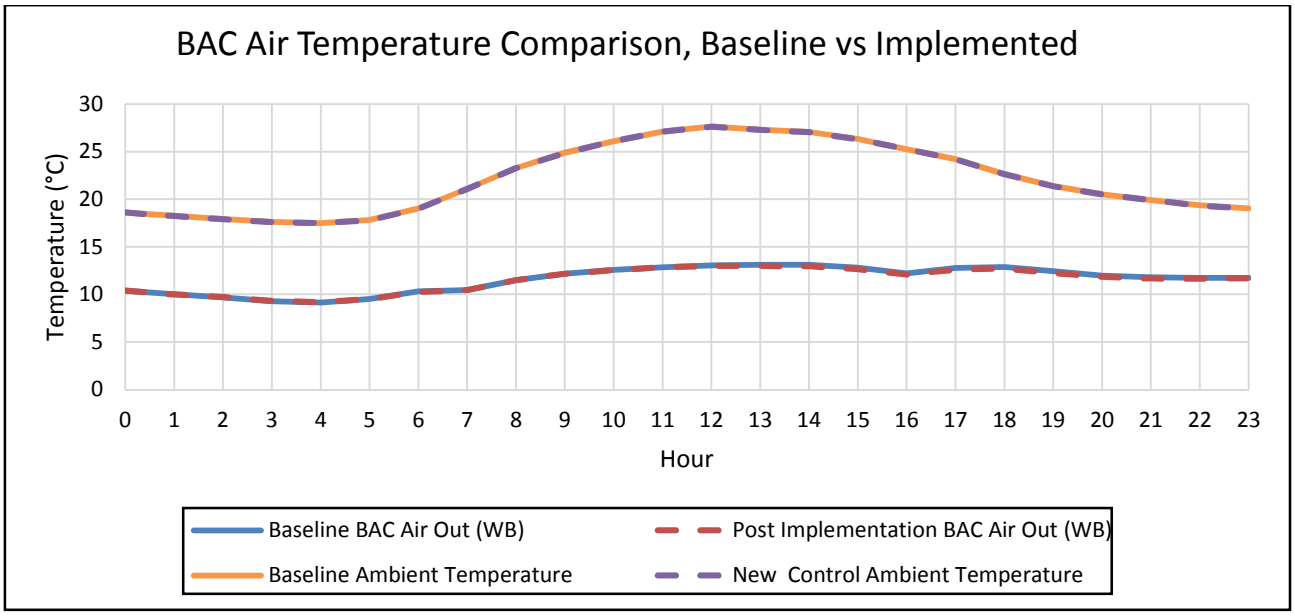

Figure 118: BACs air temperature comparison, baseline vs. implemented for a 5℃ setpoint

Figure 118 depicts the BAC's outlet WB air temperature, which was not affected by the evaporator pump impeller reconfiguration.

4℃ Evaporator outlet water temperature setpoint:

The evaporator output setpoint was changed to 4℃ and a new baseline was develop. The implemented simulation with the same setpoint was developed and compared against the baseline. Table 34 summarises of the baseline and the implemented daily average output values.

Table 34: Baseline and implemented simulation output values pump impeller reconfiguring, 4℃ setpoint

Outputs	Unit	Average Baseline	Average Implemented	Percentage (%) Deviation
Power Usage	kW	9044.02	8852.12	2.12
FP Total Flow	ℓ/s	907.91	821.19	9.55
FP Evaporator Inlet Temp	°C	13.26	13.94	-4.85
FP Evaporator Outlet Temp	°C	4.13	4.13	0.00
Chill Dam Temp	°C	4.89	4.89	0.00
FP Average COP	0	5.13	5.17	-0.87
Condenser Flow	ℓ/s	2052.82	2040.10	0.62
Condenser Inlet	°C	25.75	25.70	0.18
Condenser Outlet	°C	30.39	30.40	0.04
BAC Total Water Flow	ℓ/s	398.96	398.99	0.01
BAC Outlet Air Temp WB	°C	11.19	11.19	0.00
BAC Outlet Water	°C	10.83	10.81	0.16

Chilled Water Recycled	ℓ/s	139.32	52.22	37.48

From Table 34 it is evident that the pump reconfiguration did not affect the cooling system outputs at an evaporator output temperature of 4℃. Figure 119 represents the average total cooling equipment's power usage of the baseline and implemented simulations.

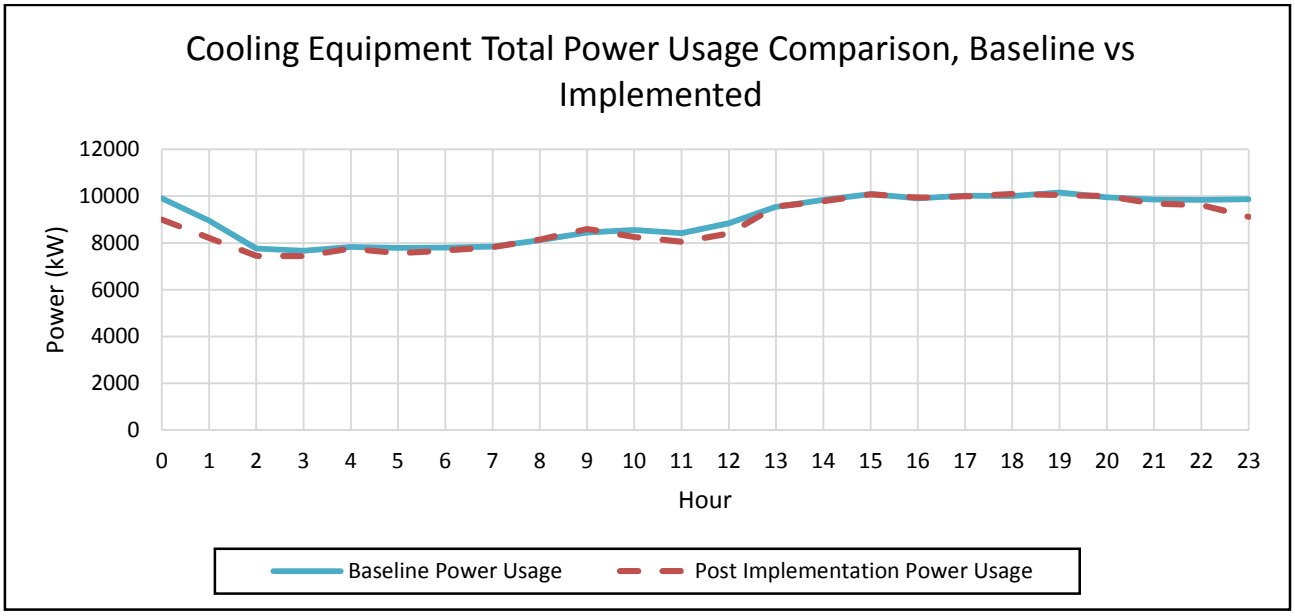

Figure 119: Cooling equipment total power usage comparison, baseline vs. implemented for a 4℃ setpoint

From Figure 119 it is evident that the evaporator pump reconfiguration did not affect cooling equipment power consumption. However, the power usage reduced on average with 191.90 kW due to the control philosophy reconfiguration. Figure 120 represents the total evaporator water flow through the FPs of the baseline and the implemented simulation.

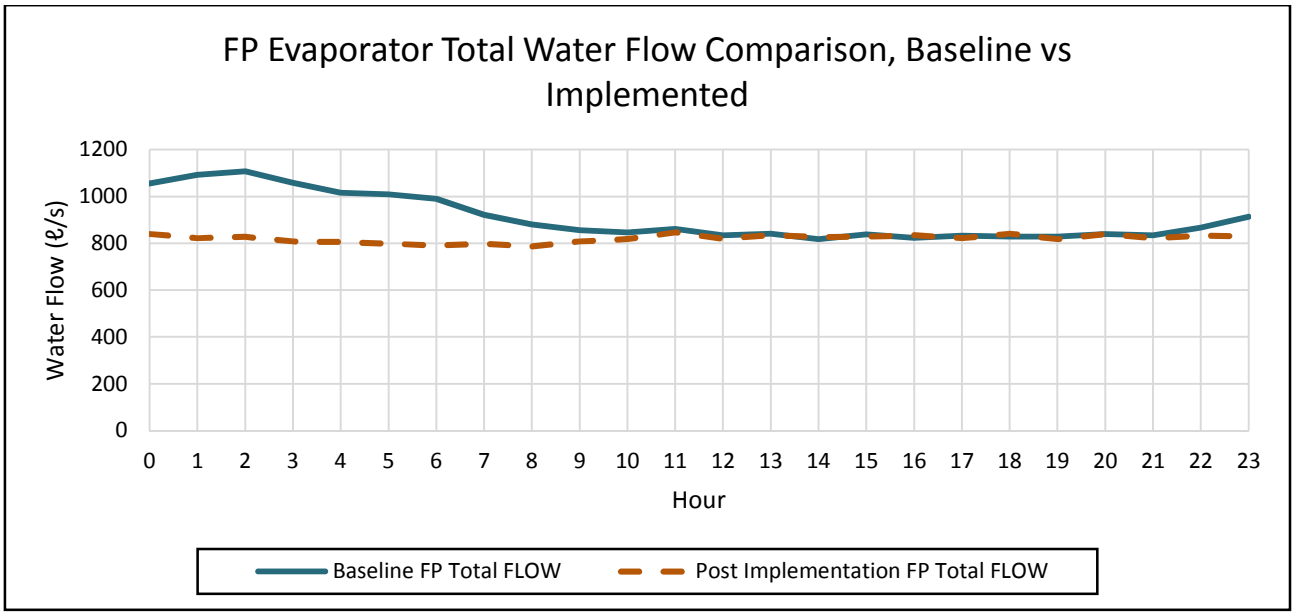

Figure 120: FP evaporator total water flow comparison, baseline vs. implemented for a 4℃ setpoint

From Figure 120 it is evident that the new control philosophy allows the VSDs to reduce the evaporator pump flow more during the day. The new control philosophy ensures the minimum chilled water to be recycled. Figure 121 represents the evaporator inlet and outlet water temperatures for both the baseline and implemented simulations.

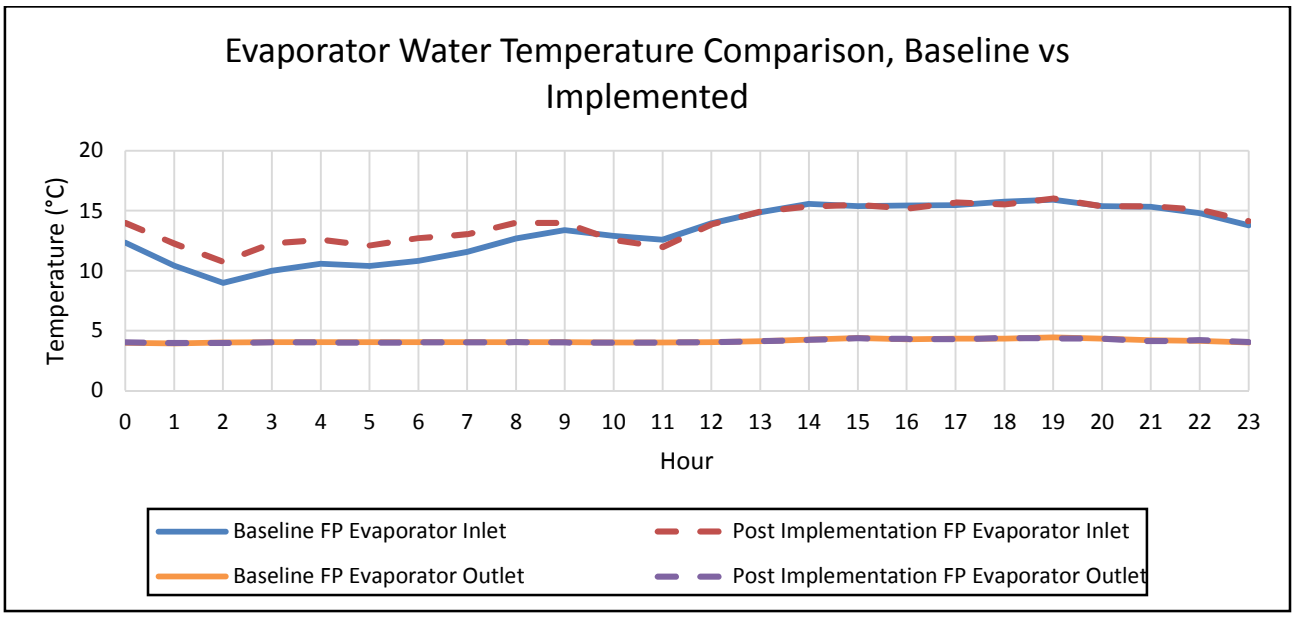

Figure 121: Evaporator water temperature comparison, baseline vs. implemented for a 4℃ setpoint

From Figure 121 it is evident that the evaporator outlet water temperatures were not affected by the pump impeller reconfiguration. The new control philosophy reduced the amount of chilled water being recycled and resulted in a slight increase evaporator inlet water temperature during certain periods of the day. The FPs, however, still managed to maintain an evaporator outlet water temperature of 4.13℃ during these periods. The will result in an improved FPs' COP as the water temperature drop has increased. Figure 122 is a visual representation of the average FPs' COP for both the baseline and implemented simulations.

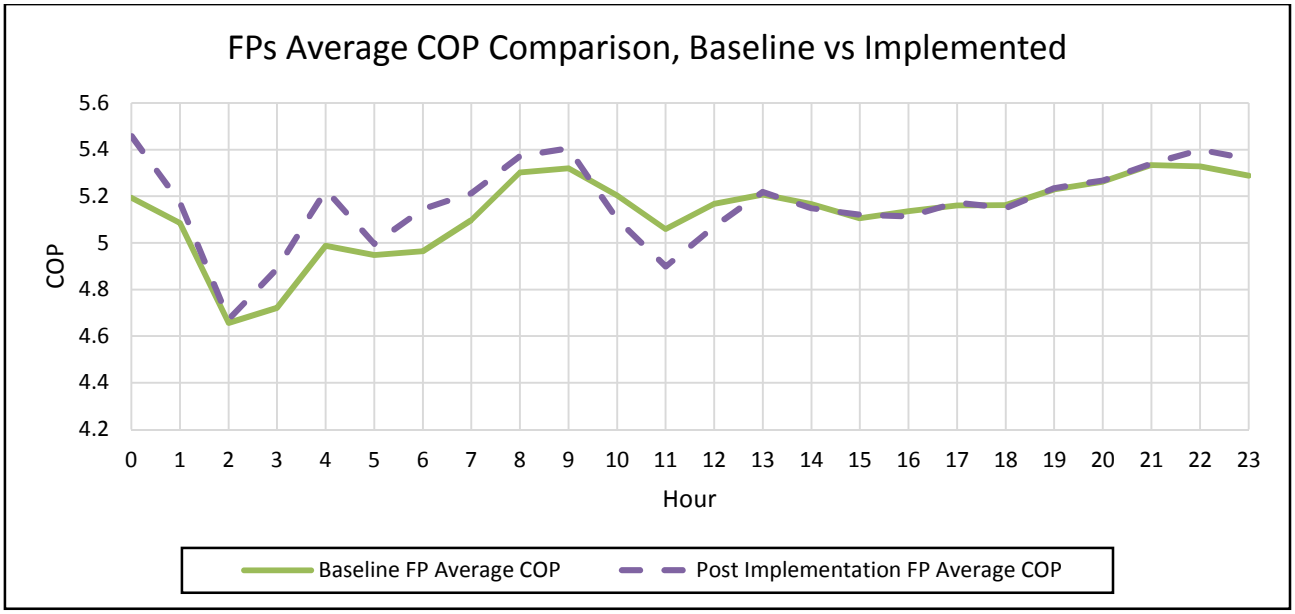

Figure 122: FPs average COP comparison, baseline vs. implemented for a 4℃ setpoint

Figure 122 indicates that the average FP's COP increased. According to Table 34 it increased with 0.87% on average. This is due to a reduced FP's water flow, whilst maintaining the same evaporator outlet water temperature and the FPs' compressors utilising the same or less amount of power. Figure 123 is a visual representation of the BACs' water temperatures' comparison between the baseline and implemented simulations.

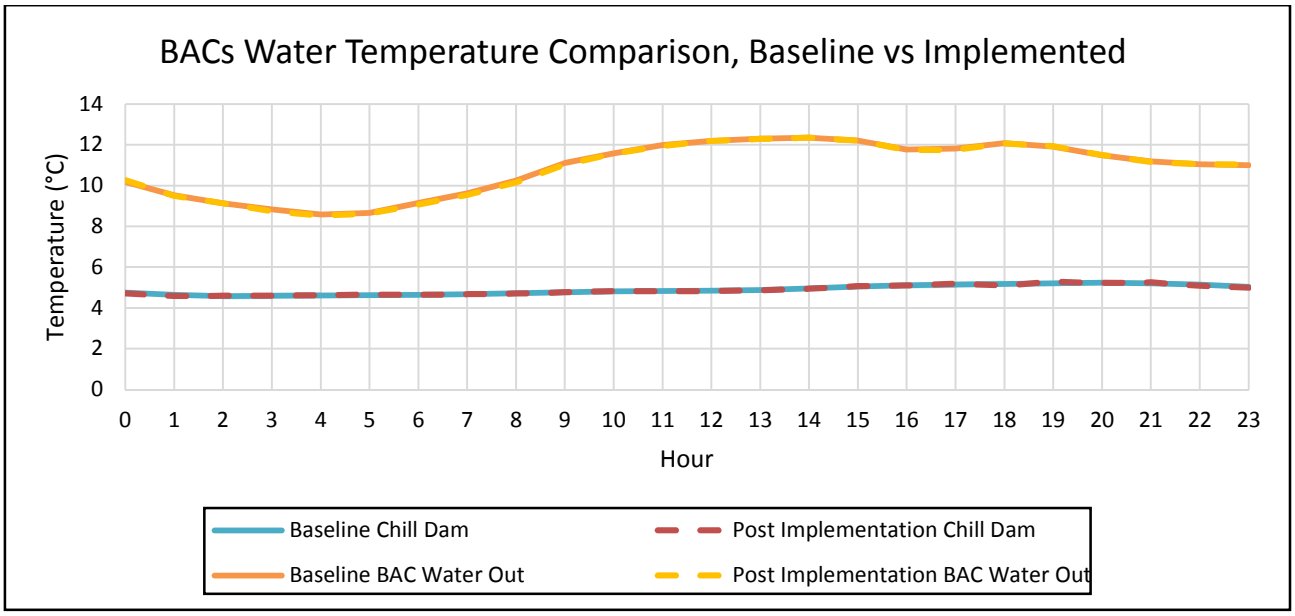

Figure 123: BACs water temperature comparison, baseline vs. implemented for a 4℃ evaporator setpoint

From Figure 123 it is evident that the BACs' outlet water temperature was not affected by the evaporator pump impeller change. Figure 124 represents the BACs' air temperatures of the baseline and implemented simulation.

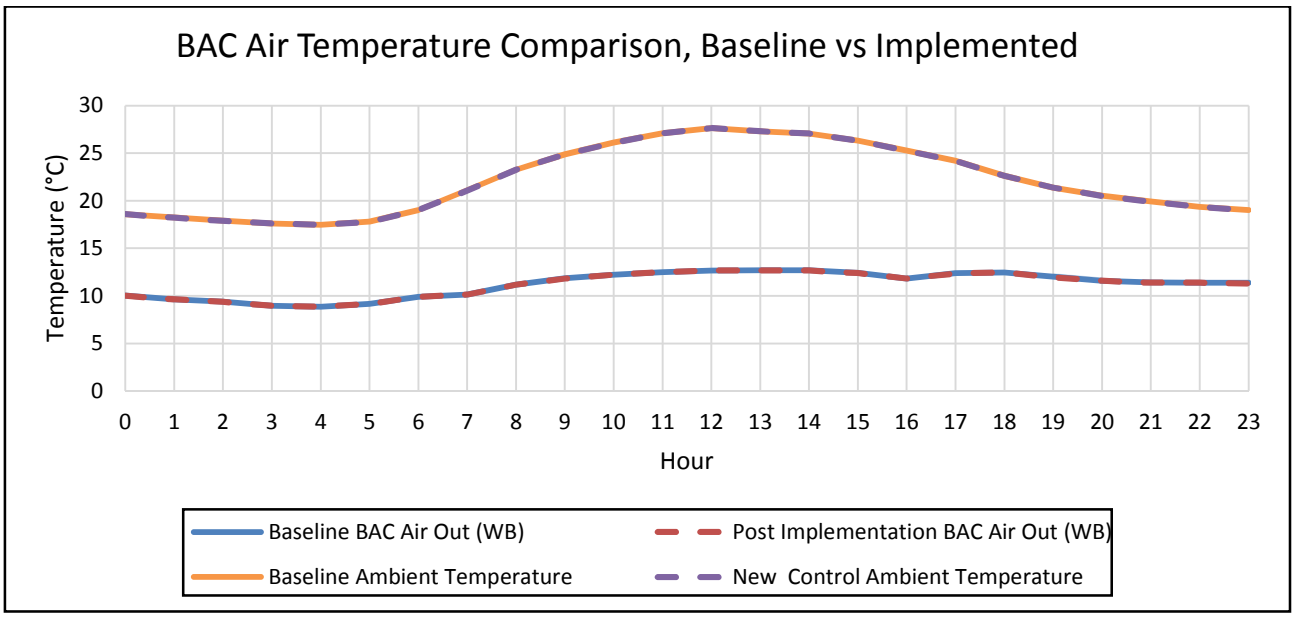

Figure 124: BACs air temperature comparison, baseline vs. implemented for a 4℃ setpoint

Figure 124 depicts the BAC outlet WB air temperature, which was not affected by the evaporator impeller reconfiguration.

3℃ Evaporator outlet water temperature setpoint:

The evaporator outlet water temperature setpoint was changed to 3℃. The implemented simulation was updated with the same setpoint and compared against the baseline simulation. Table 35 summarises the baseline and implemented simulation with an evaporator setpoint of 3℃.

Table 35: Baseline and implemented simulation output values pump impeller reconfiguring, 3℃ setpoint

Outputs	Unit	Average Baseline	Average Implemented	Percentage (%) Deviation
Power Usage	kW	9487.20	9300.38	1.97
FP Total Flow	ℓ/s	894.38	820.74	8.23
FP Evaporator Inlet Temp	°C	13.13	13.71	-4.22
FP Evaporator Outlet Temp	°C	3.40	3.38	0.58
Chill Dam Temp	°C	4.18	4.16	0.47
FP Average COP	0	5.10	5.15	0.93
Condenser Flow	ℓ/s	2096.06	2087.86	0.39
Condenser Inlet	°C	26.08	26.03	0.20
Condenser Outlet	°C	30.90	30.88	0.08
BAC Total Water Flow	ℓ/s	398.99	398.99	0.00
BAC Outlet Air Temp WB	°C	10.95	10.95	0.00
BAC Outlet Water	°C	10.46	10.44	0.19
Chilled Water Recycled	ℓ/s	125.41	51.76	41.28

From Table 35 it is evident that the implemented simulation output was not drastically affected by the evaporator pump impeller reconfiguration and the new control philosophy. Figure 125 represents the power consumed by the cooling equipment for both the baseline and implemented simulations.

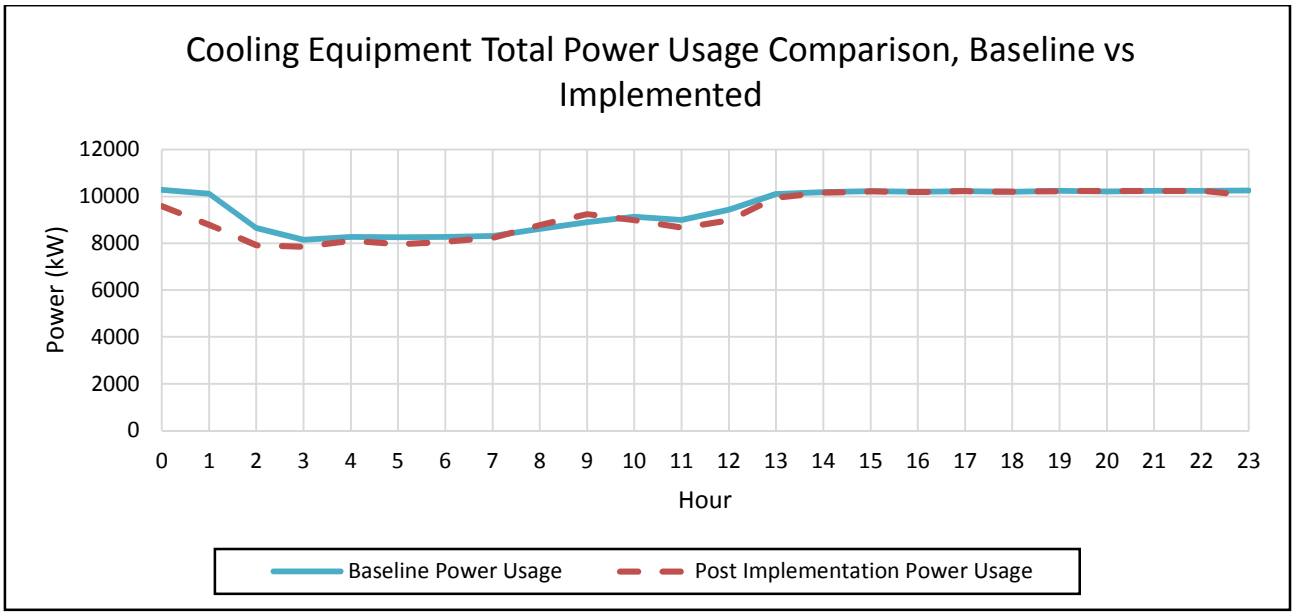

Figure 125: Cooling equipment total power usage comparison, baseline vs. implemented for a 3℃ setpoint

From Figure 125 it is evident that the cooling equipment's total power usage has been reduced during certain periods of the day due to the new control philosophy. On average the control philosophy upgrade can realise in a 186.82 kW power saving. Figure 126 represents the evaporator total water flow through the FPs for both the baseline and the implemented simulations.

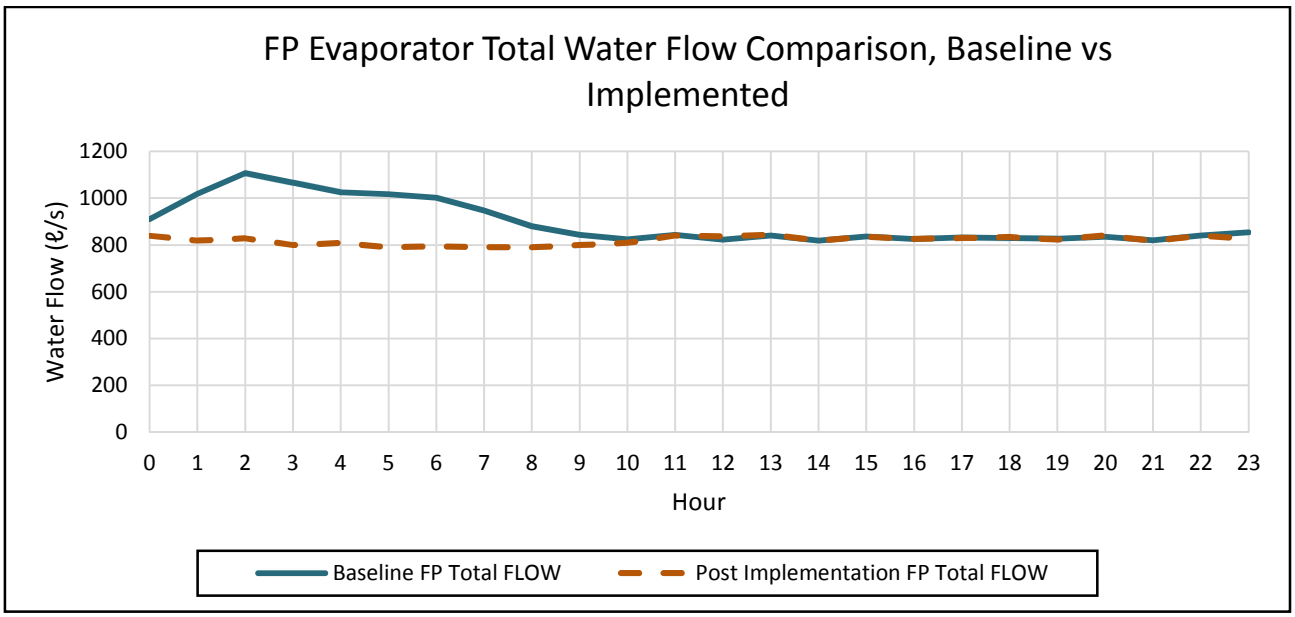

Figure 126: FP evaporator total water flow comparison, baseline vs. implemented for a 3℃ setpoint

Figure 126 depicts the evaporator flow, which was reduced during certain periods of the day with the new control philosophy. The evaporator reduced the water flow to maintain a certain chill dam level, while with the baseline simulation the water flow was increased as the inlet water temperature decreased. Figure 127 represents the evaporator water temperatures for both the baseline and implemented simulations.

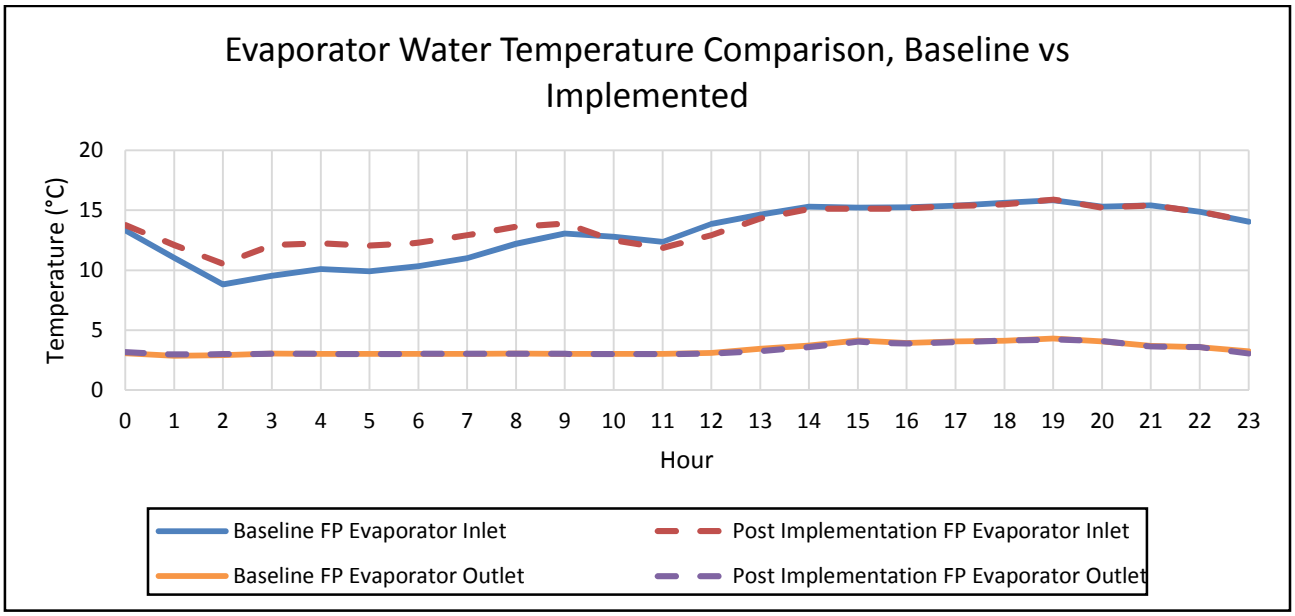

Figure 127: Evaporator water temperature comparison, baseline vs. implemented for a 3℃ setpoint

Figure 127 depicts the evaporator inlet water temperature, which slightly increased as the recycled water was reduced to maintain an evaporator inlet temperature of 14℃. However, the FPs still manage to maintain an evaporator outlet temperature of 3.38℃. This will result in an overall increase in the FPs' average COP. Figure 128 compares the FPs average COP of the baseline and implemented simulations.

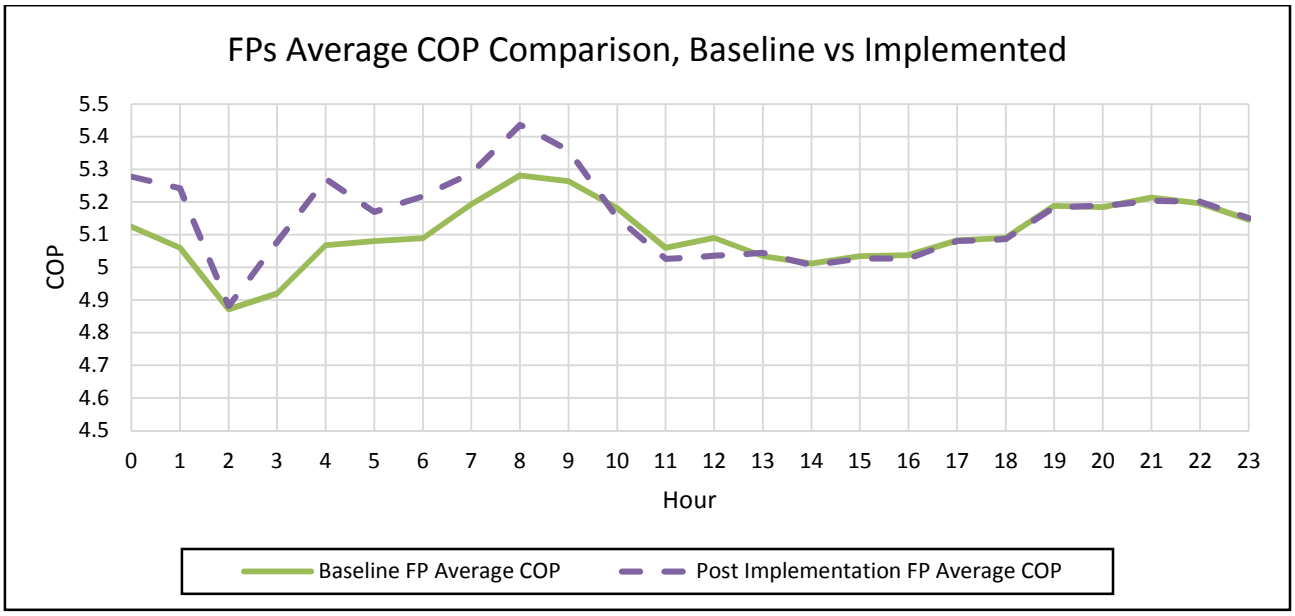

Figure 128: FPs average COP comparison, baseline vs. implemented for a 3℃ setpoint

From Figure 128 it is evident that the FPs' average COP has improved. According to Table 35 the daily average COP increased with 0.93%. This is due to the lowered evaporator water flow and allowing the FPs' compressor guide vanes to cut back and reduce the power consumed, whilst maintaining the same output water temperature. Figure 129 represents the BACs water temperatures of both the baseline and implemented simulation.

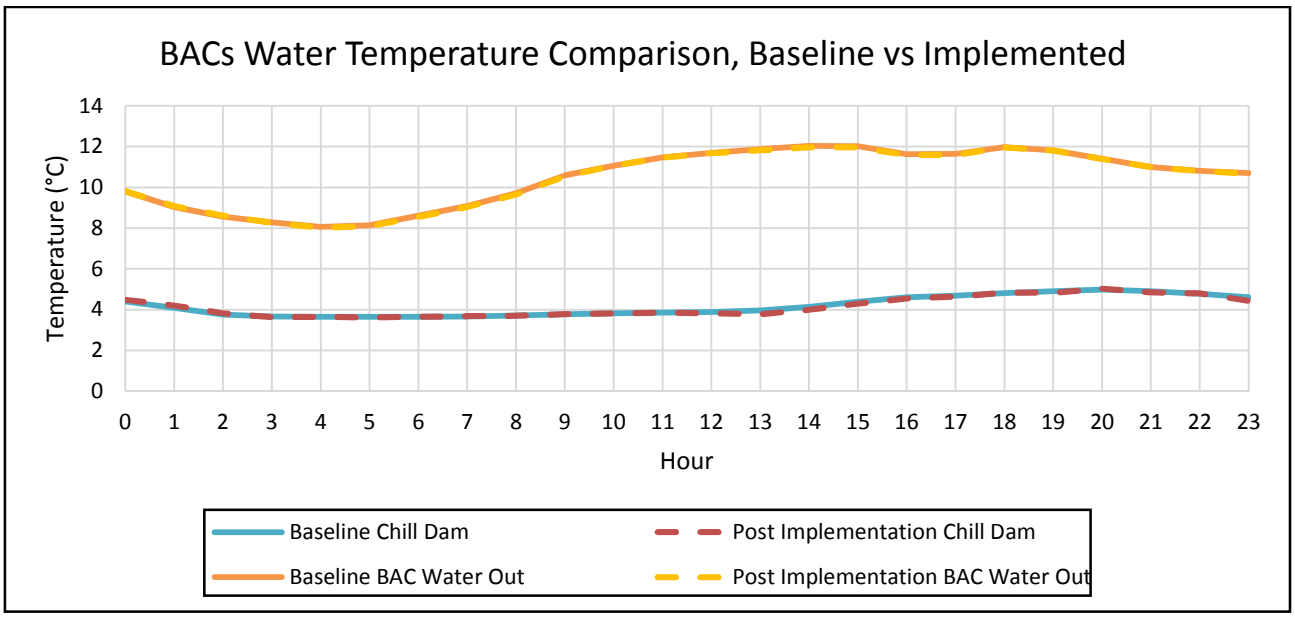

Figure 129: BACs water temperature comparison, baseline vs. implemented for a 3℃ evaporator setpoint

It is evident from Figure 129 that the BAC outlet temperature was not affected by the evaporator pump reconfiguration and the new control philosophy update. Figure 130 represents the BAC's air temperature of the baseline and the implemented simulation.

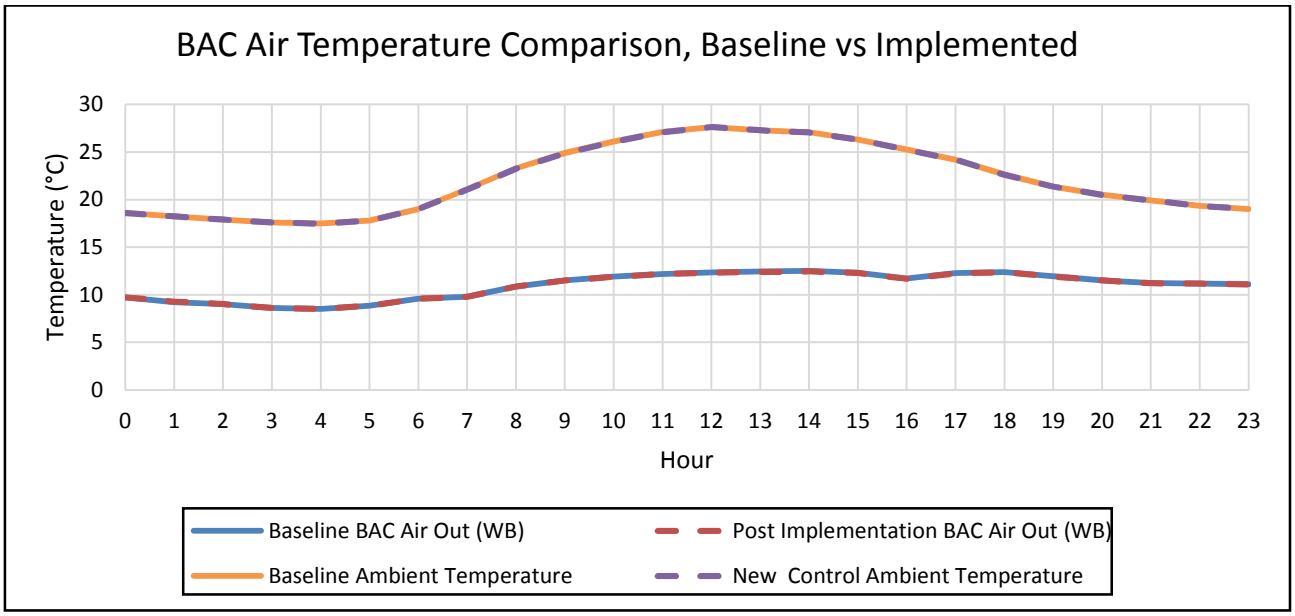

Figure 130: BACs air temperature comparison, baseline vs. implemented for a 3℃ setpoint

Figure 130 depicts the evaporator pump impeller reconfiguration, which did not affect the BAC outlet temperature.

Winter:

5℃ Evaporator outlet water temperature setpoint:

A new winter baseline simulation was developed from average winter ambient psychrometric conditions. The prescribed winter control philosophy was simulated with the replaced pump impellers and compared against the winter baseline simulation with the old impellers and control philosophy. Table 36 represents a comparison between the post implementation and baseline simulations with an output temperature setpoint of 5℃. The results do not include a comparison between the BACs' baseline and implemented simulation results as the BACs are switched off during the winter months.

Table 36: Baseline and implemented simulation output values for pump impeller reconfiguring with a 5℃ setpoint

Outputs	Unit	Average Baseline	Average Implemented	Percentage (%) Deviation
Power Usage	kW	2472.45	2321.83	6.09
FP Total Water Flow	ℓ/s	376.46	384.55	2.10
FP Evaporator Inlet Temp	°C	11.15	11.15	0.01
FP Evaporator Outlet Temp	°C	6.36	7.17	-11.34
Chill Dam Temp	°C	6.77	6.85	-1.26
Condenser Water Flow	ℓ/s	498.80	498.80	0.00
Condenser Inlet	°C	18.63	18.44	1.05
Condenser Outlet	°C	22.60	22.60	0.00

Table 36 depicts that a power saving of 150.82 kW will realise during the winter months, which equates to 6.09% on a 2 321.83 kW power consumption. This is a significant power saving as during the summer months a saving of 0.85% can be realised on an hourly average power usage of 8 363.48 kW. The total evaporator water flow increased with 2.10% and the evaporator outlet temperature increased with 11.34%. The condenser water flow and temperatures stayed unchanged. Figure 131 is a visual representation of the cooling equipment power usages for the baseline and post implementation simulations.

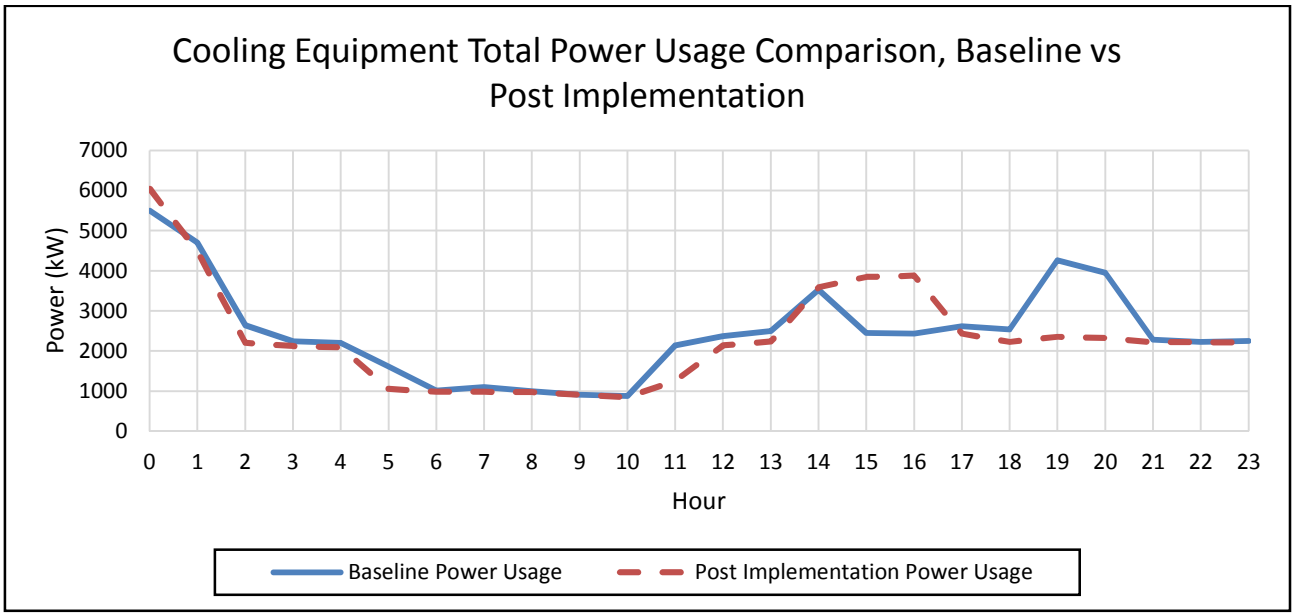

Figure 131: Cooling equipment total power usage comparison, baseline vs. implemented for the winter season

It is evident from Figure 131 that the components utilise less power throughout the day. It is only the control philosophy changes leading to power increases during different times of

the day. The average hourly power saving realised form the pump impeller reconfiguration during the winter months, is 150.62 kW. Even though this a relatively small power saving, it will have a vast impact on the electricity cost as the electricity tariffs are more than double the price during the Eskom winter peak periods [102]. Figure 132 is a visual representation of the FPs' total evaporator flow.

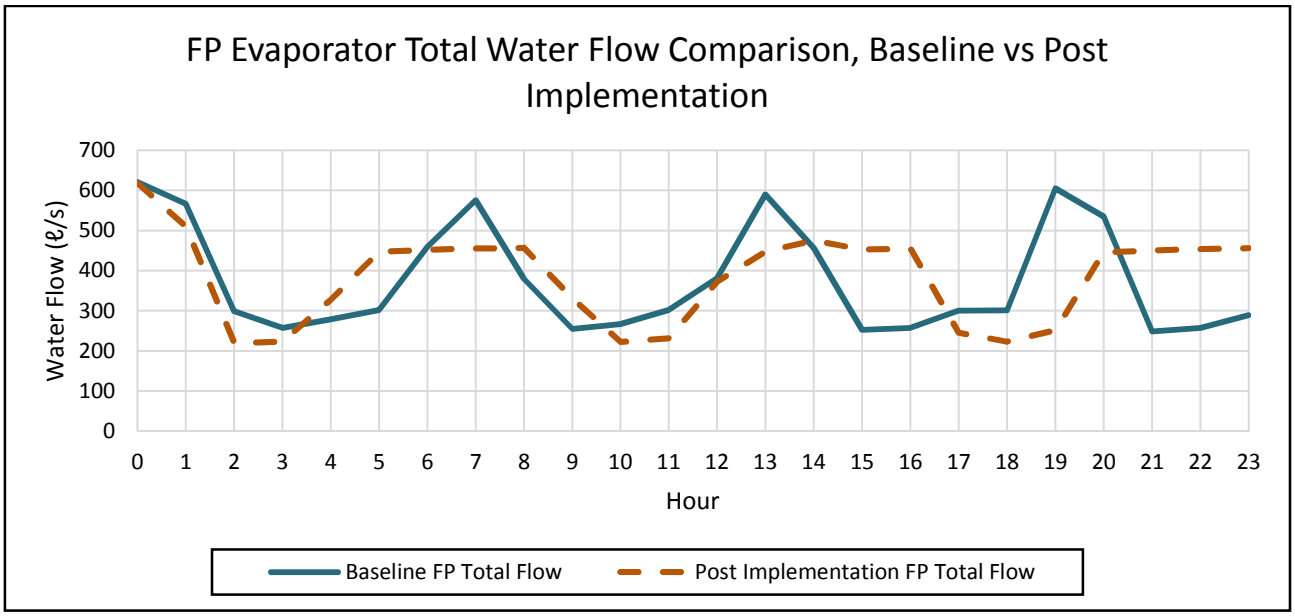

Figure 132: FP total evaporator water flow comparison, baseline vs. implemented for the winter season

From Figure 132 it is evident that the maximum water flow is less after replacement of the pump impellers. This is due to an increase volume flow rate per pump, enabling the mine to run two pumps to meet the water demand, instead of running three pumps to meet the water demand. This will allow mine personnel to do maintenance on two FPs and their cooling auxiliaries simultaneously. The higher volume flowrate causes the second pump to be running for longer periods to meet the demand. However, this does not affect the power savings and savings are still achieved. Figure 133 is a visual representation of the evaporator inlet and outlet water temperatures.

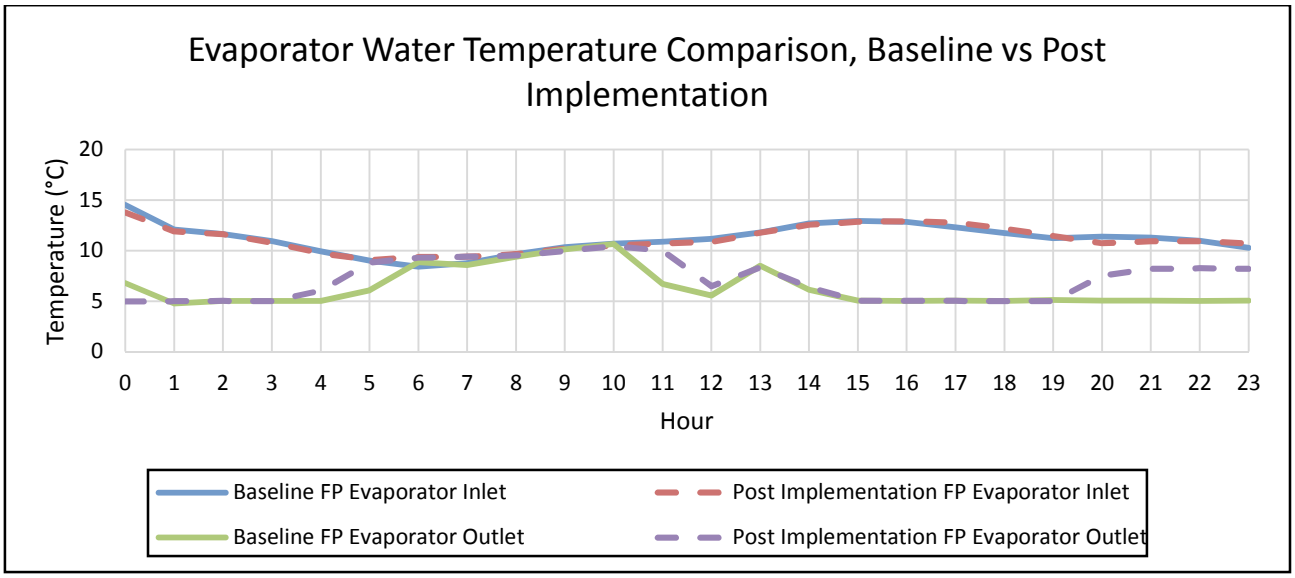

Figure 133: Evaporator water temperatures, baseline vs. implemented for the winter season

Figure 133 depicts the evaporator inlet temperatures, which are the same for the baseline and implementation simulations. However, the outlet water temperature is slightly higher during certain periods of the day due to the control philosophy update. The new control philosophy controls the chill dam level at a lower percentage reducing the running time of one FP. This causes the evaporator outlet temperature to be higher for longer periods. This, however, does not affect the chill dam temperature as seen in Figure 134.

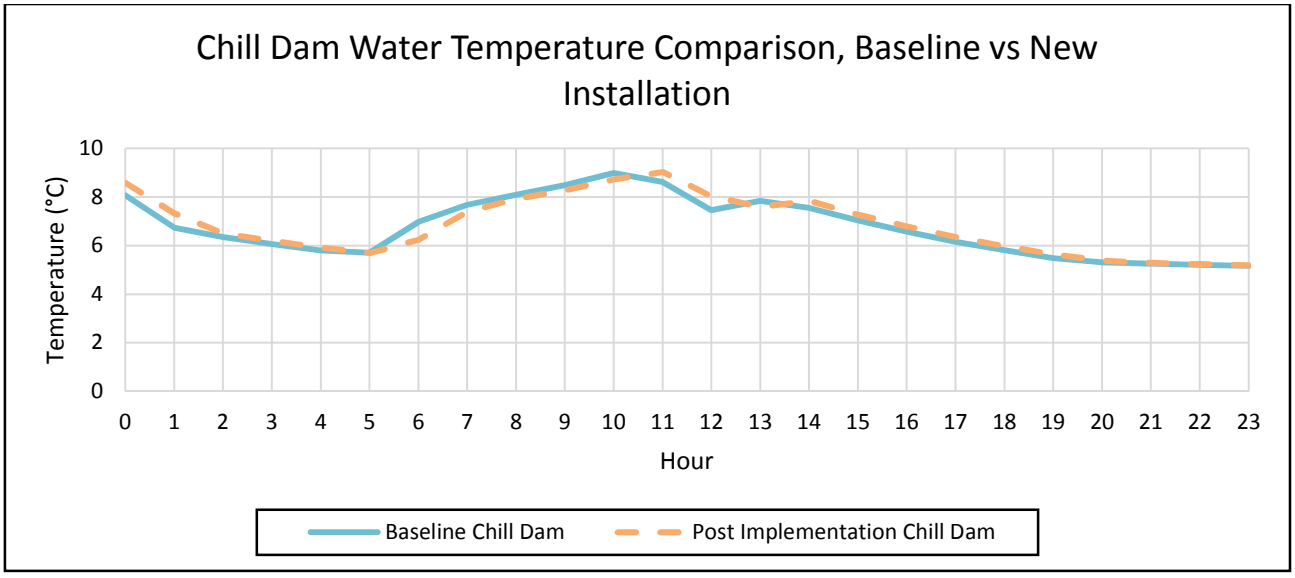

Figure 134: Chill dam water temperatures, baseline vs implemented for the winter season

Figure 134 depicts the hourly average chill dam temperature. It is evident that the chill dam temperature is not affected negatively by the new impeller installation.

Appendix E – RECONFIGURING OF MINE A'S BULK AIR COOLERS

Energy savings:

The energy efficient savings will be determined for an evaporator outlet water temperature of 5℃, 4℃ and 3℃. The BAC outlet WB air temperature setpoint will be set to the daily average output WB air temperature achieved with a constant chilled water flow of 133 ℓ/s through a BAC. This will ensure the underground environmental conditions are not affected by the BAC's reconfiguration.

5℃ Evaporator outlet water temperature setpoint:

The evaporator output water temperature setpoint was set to 5℃ to determine the effect the BAC valve control has on the power savings. Table 37 compares the baseline and implemented simulation's average output values and depicts the percentage deviation between the two.

Table 37: Baseline and implemented simulation output values BAC reconfiguration for energy saving, 5℃ setpoint

Outputs	Unit	Average Baseline	Average Implemented	Percentage (%) Deviation
Power Usage	kW	8363.48	8314.98	0.58
FP Total Flow	ℓ/s	822.94	811.14	1.43
FP Evaporator Inlet Temp	°C	14.19	14.31	-0.85
FP Evaporator Outlet Temp	°C	5.04	5.04	0.06
Chill Dam Temp	°C	5.94	5.96	-0.32
FP Average COP	0	5.18	5.14	-0.83
Condenser Flow	ℓ/s	2019.32	1990.92	1.41
Condenser Inlet	°C	25.25	25.33	0.33
Condenser Outlet	°C	29.62	29.78	0.55
BAC Total Water Flow	ℓ/s	398.99	386.73	3.07
BAC Outlet Air Temp WB	°C	11.51	11.58	-0.60
BAC Outlet Water	°C	11.26	11.26	0.04
Chilled Water Recycled	ℓ/s	53.98	48.47	89.80

Table 37 depicts the implemented simulation output values, which were not affected enormously. The baseline simulation shows that the average BAC outlet WB temperature

is 11.58℃. The BAC valve control was set to 11.51 C to prevent chilled water from being wasted unnecessarily. Figure 135 represents the power reduction realised from the BAC flow control improvement.

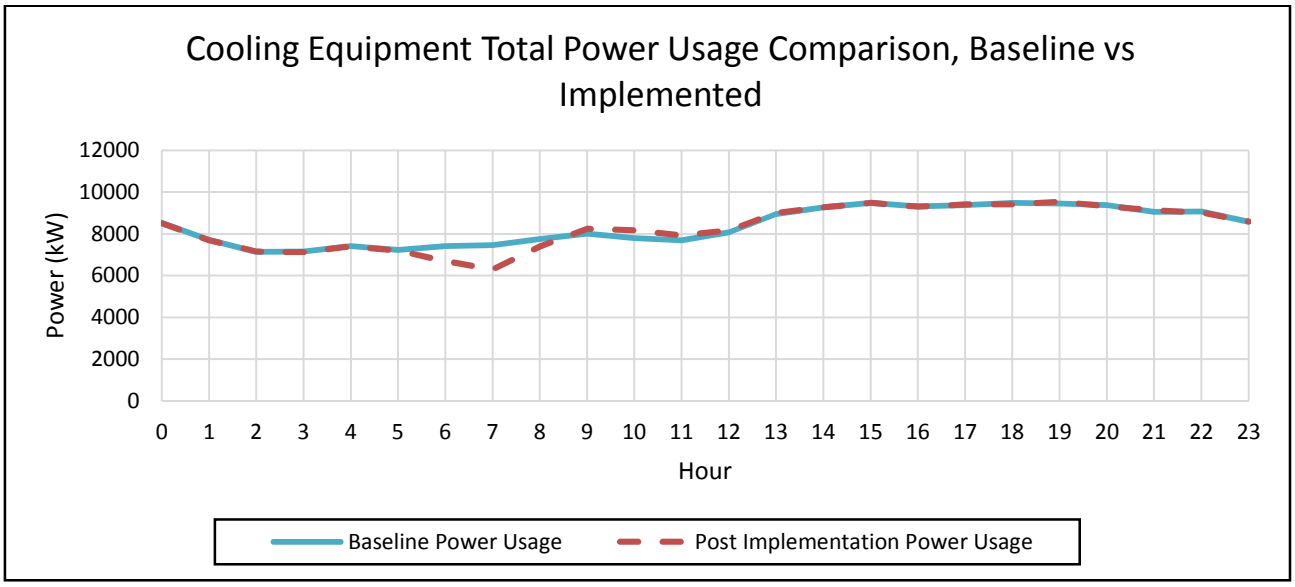

Figure 135: Cooling equipment total power usage comparison, baseline vs. implemented for a 5℃ setpoint

Figure 135 depicts the BAC valve control, which will reduce the cooling equipment between 05:00 and 08:00 when an FP is switch off due to a reduced chilled water demand during this period. The chilled water demand is reduced due to lower ambient temperatures during this period. The BAC improved control resulted in a daily average saving of 48.50 kW with the evaporator output water temperature set to 5℃. Figure 136 compares the total evaporator water flow through the FPs of both the baseline and implemented simulation.

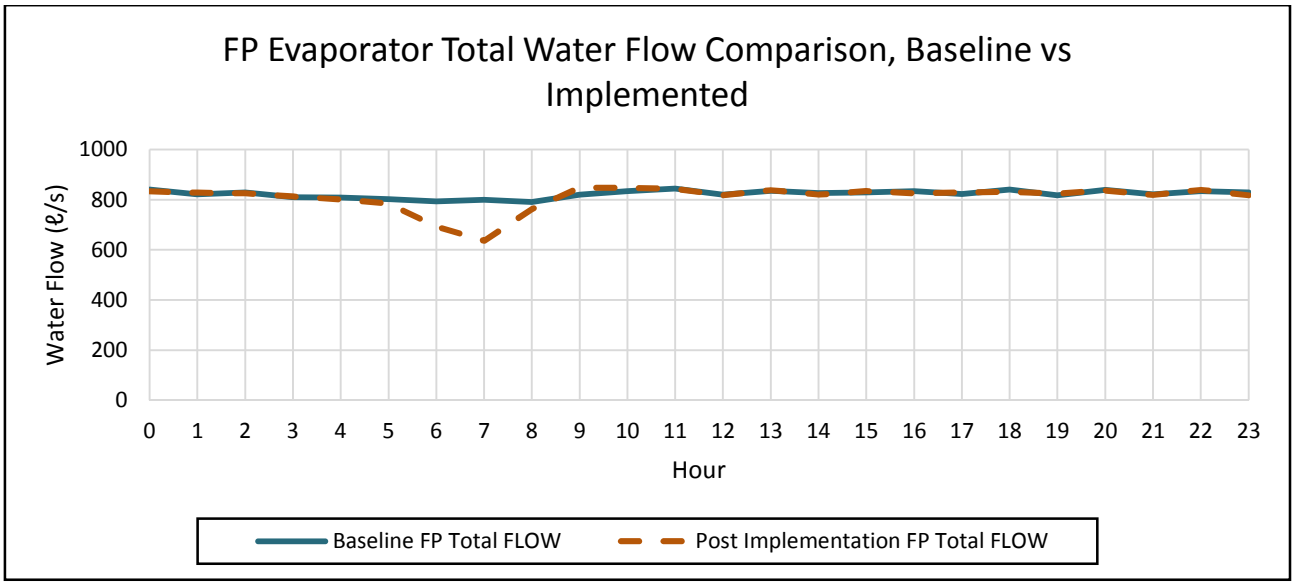

Figure 136: FP evaporator total water flow comparison, baseline vs. implemented for a 5℃ evaporator setpoint

Figure 136 depicts the evaporator, which decreased between 05:00 and 08:00 as the BAC chilled water demand decreased during this period. One FP and its pumps were switched off for this period reducing the amount of chilled water being recycled. Figure 137 compares the evaporator inlet and outlet water temperatures of the baseline simulation against the implemented simulation.

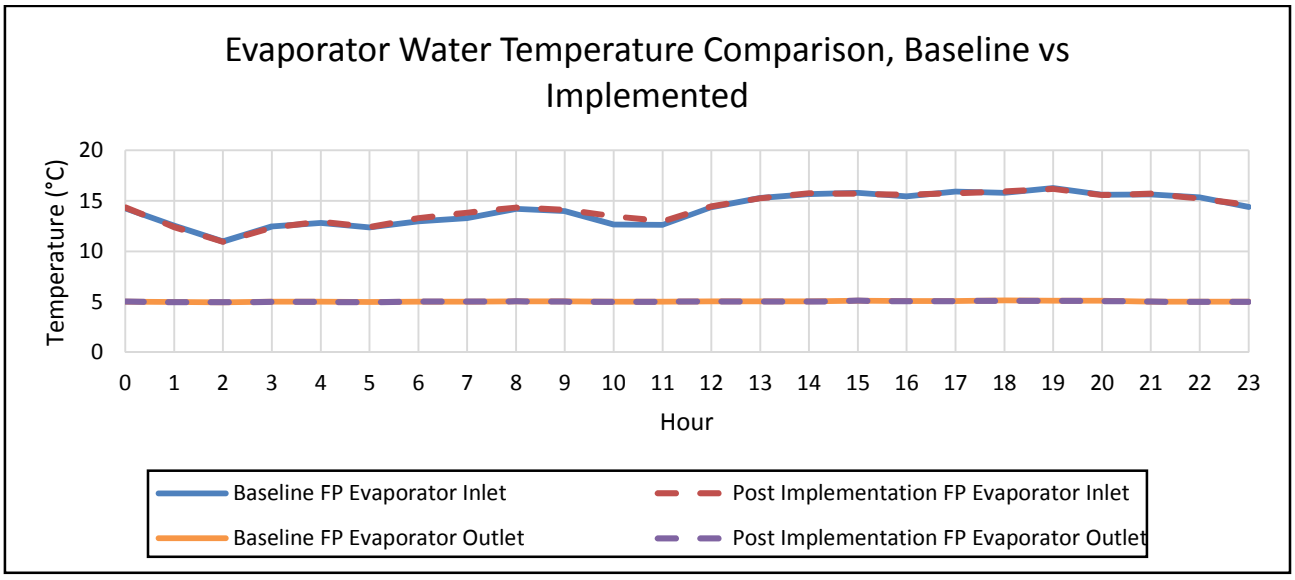

Figure 137: Evaporator water temperature comparison, baseline vs. implemented for a 5℃ evaporator setpoint

From Figure 137 it is evident that the evaporator inlet temperature increased during the period when one of the FPs was switched off. The switched off FP and pumps resulted in

less chilled water to be recycled. The FPs managed to maintain an evaporator outlet temperature of 5℃ with the increased inlet temperature. Figure 138 represents the BAC total chilled water flow for the baseline and implemented simulation.

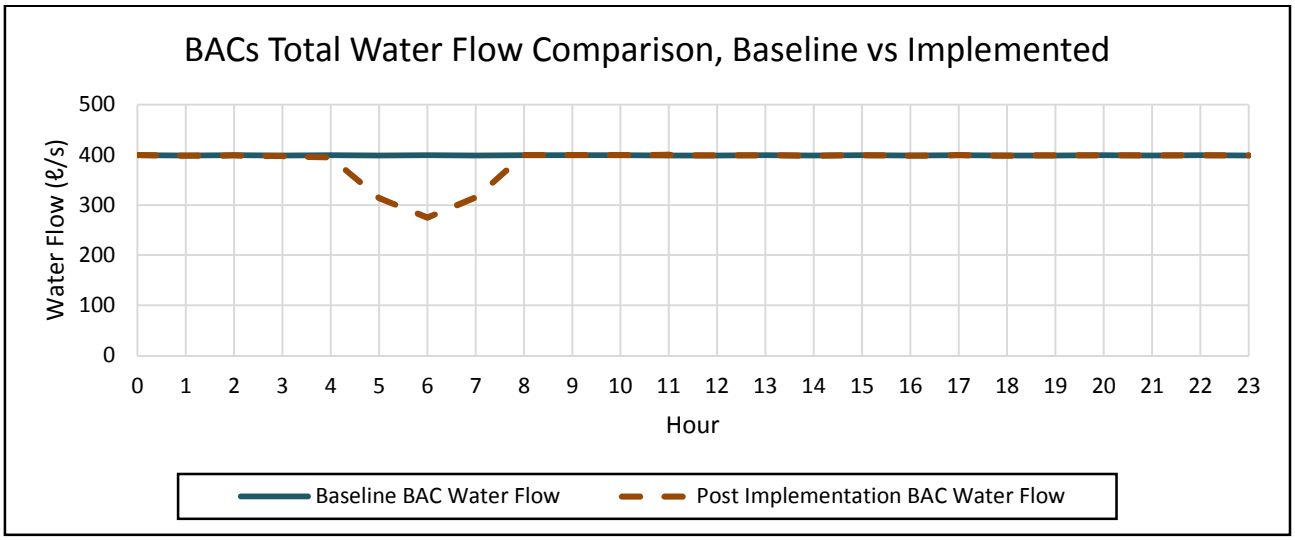

Figure 138: BAC water flow comparison, baseline vs. implemented for a 5℃ setpoint

Figure 138 depicts the BAC valves, which decreased the water flow up to a minimum of 275 ℓ/s between 04:00 and 08:00 as the ambient temperature decreased during this period. The BAC required less water through the BAC to maintain the output WB air temperature setpoint. Figure 139 compares the BAC water temperatures for the baseline and implemented simulations with each other.

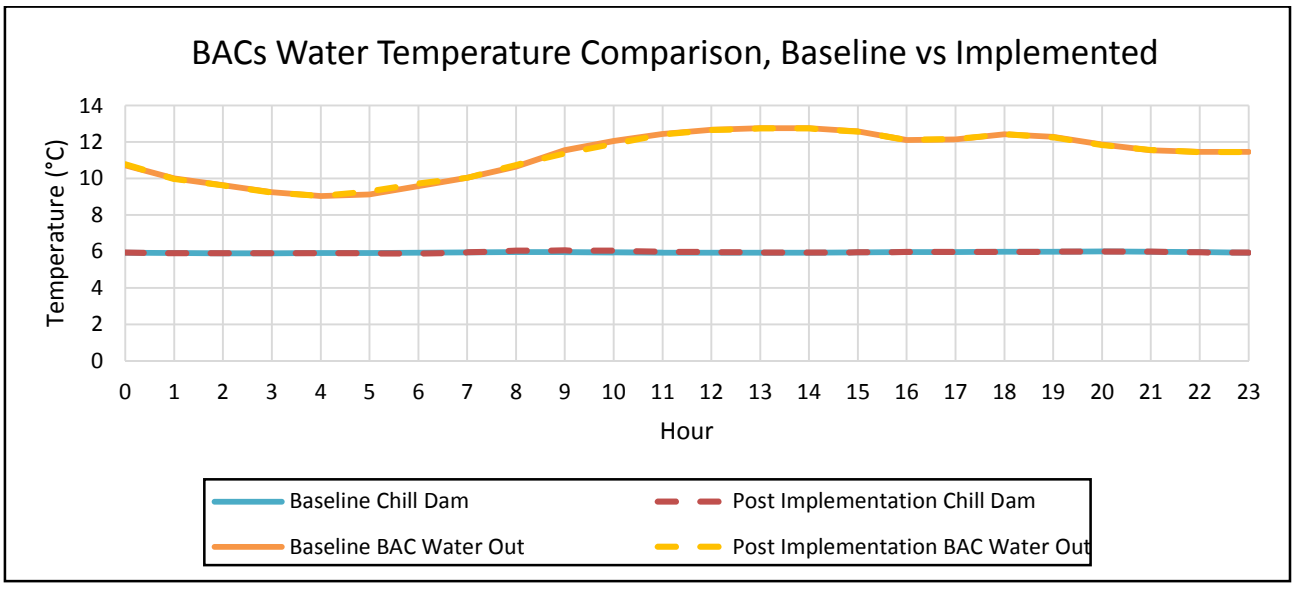

Figure 139: BACs water temperature comparison, baseline vs. implemented for a 5℃ evaporator setpoint

Figure 139 depicts the BAC inlet and outlet water temperatures, which were not affected by the BAC valve control update. Figure 140 represents the BAC air temperatures for the baseline and implemented simulations.

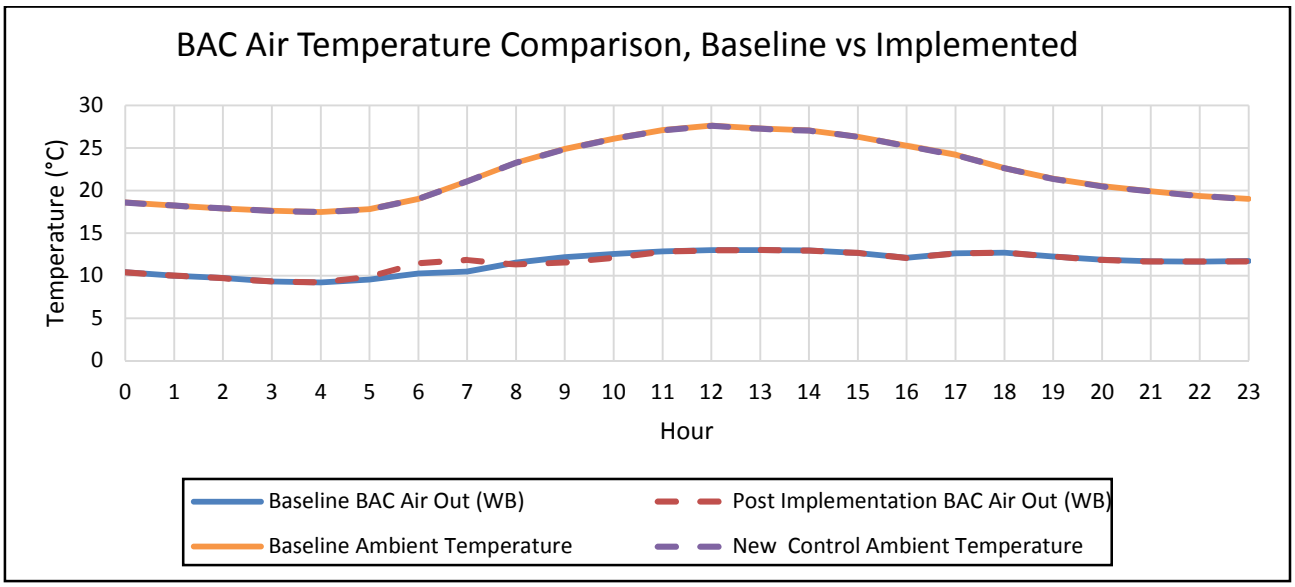

Figure 140: BACs air temperature comparison, baseline vs. implemented for a 5℃ setpoint

Figure 140 depicts the ambient temperature, which was not changed during the simulations. The BAC output WB air temperature slightly increased between 05:00 and 08:00 due to the reduced chilled water flow through the BACs. However, the BAC outlet water temperature did not increase above baseline simulation's maximum outlet temperature. On average the BAC outlet temperature increased with 0.07℃ throughout the day.

4℃ Evaporator outlet water temperature setpoint:

The evaporator output water temperature setpoint was set to 4℃ to determine the affect the BAC valve control will have on the power savings with the mine's preferred evaporator setpoint temperature. Table 38 summarises the baseline and implemented simulation output values.

Table 38: Baseline and implemented simulation output values BAC reconfiguration for energy saving, 4℃ setpoint

Outputs	Unit	Average Baseline	Average Implemented	Percentage (%) Deviation
Power Usage	kW	8852.12	8729.80	1.38
FP Total Flow	ℓ/s	821.19	792.39	3.51
FP Evaporator Inlet Temp	°C	13.94	14.18	-1.68
FP Evaporator Outlet Temp	°C	4.13	4.14	-0.15
Chill Dam Temp	°C	5.04	5.06	-0.46
FP Average COP	0	5.17	5.04	-2.59
Condenser Flow	ℓ/s	2040.10	1999.04	2.01
Condenser Inlet	°C	25.71	25.84	0.53
Condenser Outlet	°C	30.40	30.60	0.63
BAC Total Water Flow	ℓ/s	398.99	374.18	6.22
BAC Outlet Air Temp WB	°C	11.19	11.48	-2.46
BAC Outlet Water	°C	10.81	10.87	0.56
Chilled Water Recycled	ℓ/s	52.22	48.21	92.32

Table 38 depicts the output values, which were not affected by the BAC water flow control. The average BAC outlet WB air temperature achieved with an evaporator water setpoint of 4℃ was 11.20℃. The BAC outlet air WB temperature was set to 11.5℃ to maintain an acceptable underground working environment and increase the power savings. Figure 141 represents the power reduction with the implemented BAC flow control.

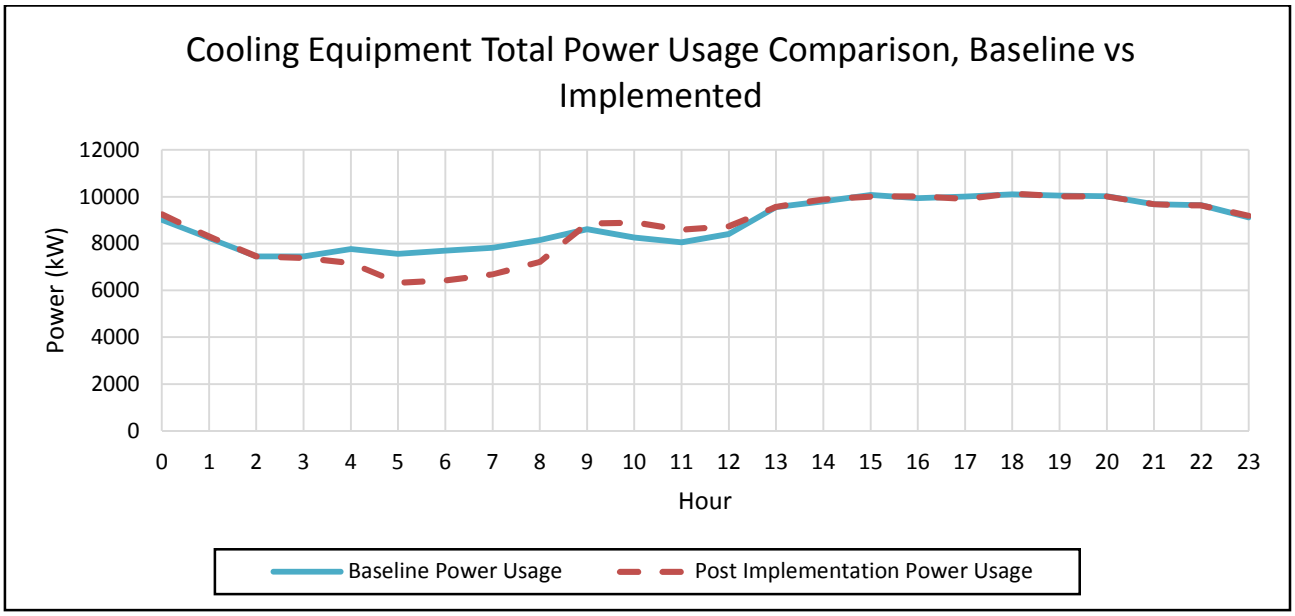

Figure 141: Cooling equipment total power usage comparison, baseline vs. implemented for a 4℃ setpoint

Figure 141 depicts the power usage, which was reduced between 04:00 and 09:00 when the ambient conditions allowed the BAC valves to reduce the cooling load. The lower ambient conditions allow the BAC valves to reduce the chill flow demand for the evaporator circuit. The reduced water demand allowed the mine to switch off one FP and its evaporator pumps during this period. The BAC valve control realised in an average power saving of 122.32 kW throughout the day. Figure 142 compares the FP evaporator water flow for the implemented simulation against the baseline simulation.

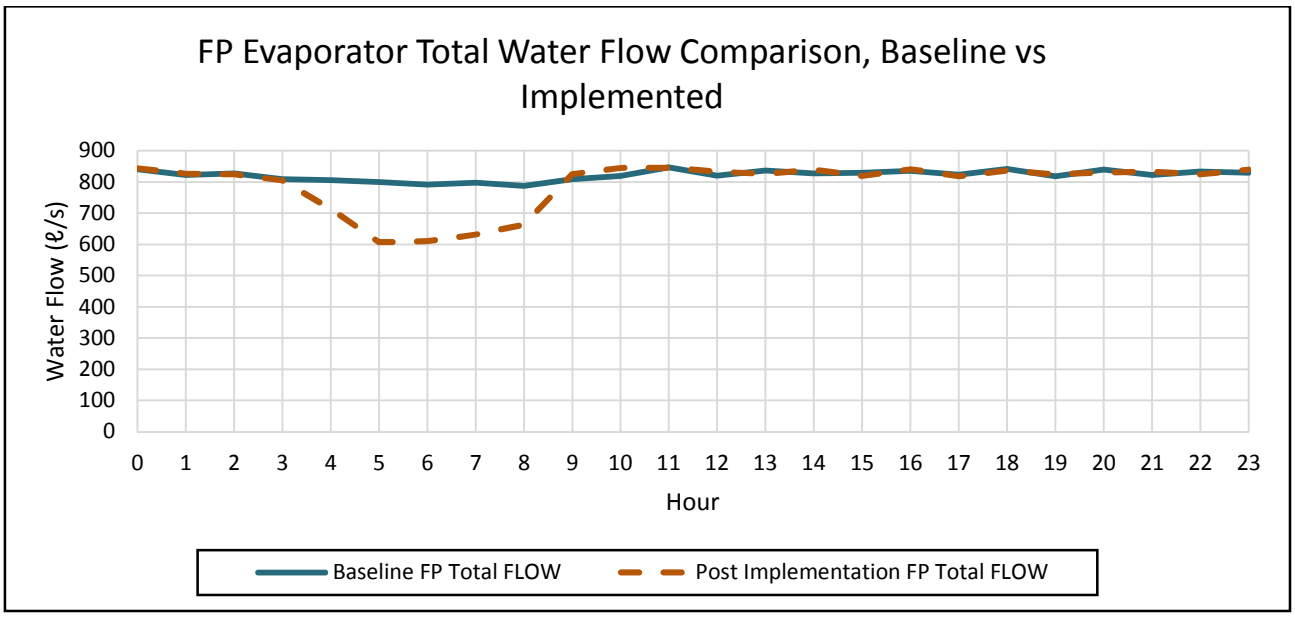

Figure 142: FP evaporator total water flow comparison, baseline vs. implemented for a 4℃ evaporator setpoint

Figure 142 depicts the water flow through the evaporator, which was reduced when the evaporator pumps were switched off between 04:00 and 09:00, due to the reduction in BAC chilled water demand. The lower water flow caused less water to be recycled, and led to an increased evaporator inlet temperature. Figure 143 represents the evaporator inlet and outlet water temperatures for the baseline and simulated simulations.

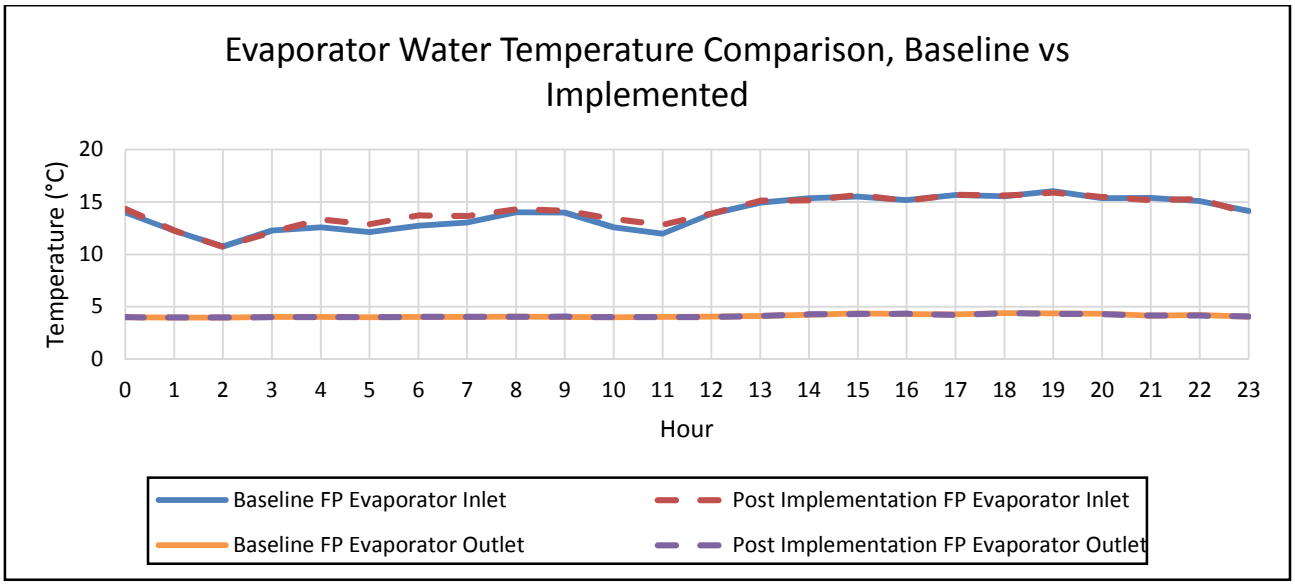

Figure 143: Evaporator water temperature comparison, baseline vs. implemented for a 4℃ evaporator setpoint

Figure 143 indicates that the FPs could maintain the same evaporator outlet temperature even though the evaporator inlet temperature increased slightly due to less chilled water being recycled. Figure 144 compares the BACs' total water flow for the baseline and implemented simulations.

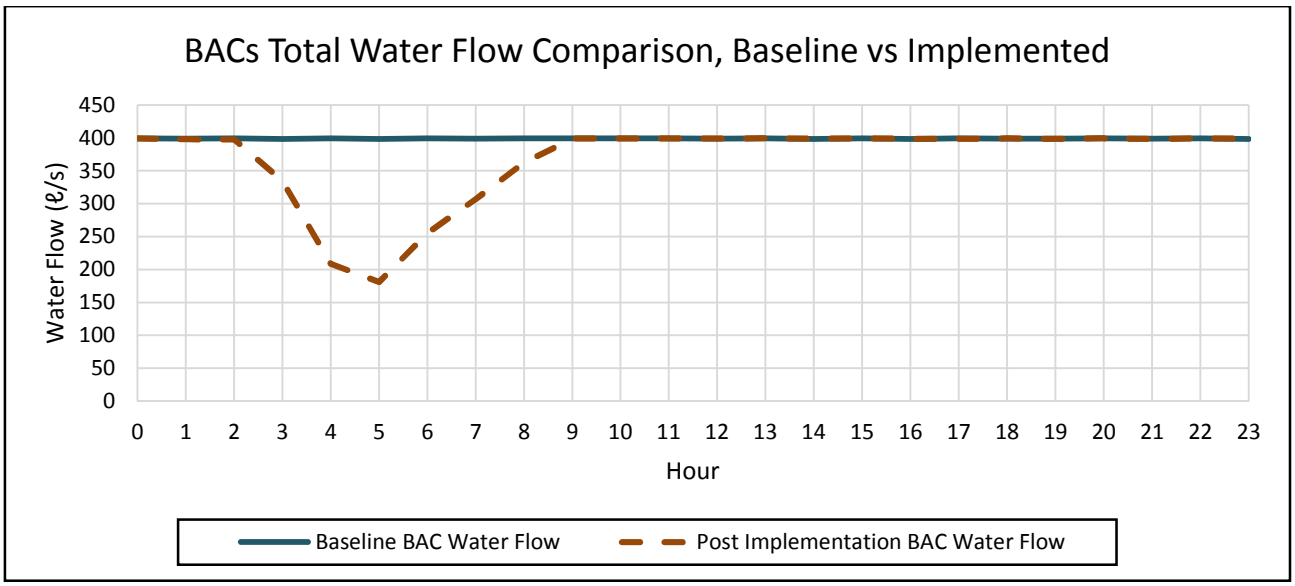

Figure 144: BAC water flow comparison, baseline vs. implemented for a 4℃ evaporator setpoint

Figure 144 depicts the BAC chilled water flow, which was decreased between 02:00 and 09:00 when the ambient temperatures allowed the BAC valves to reduce the chilled water

flow. The water flow was reduced to a minimum flow of 195 ℓ/s. Figure 145 depicts the BACs' inlet and outlet water temperature for the baseline and implemented simulation.

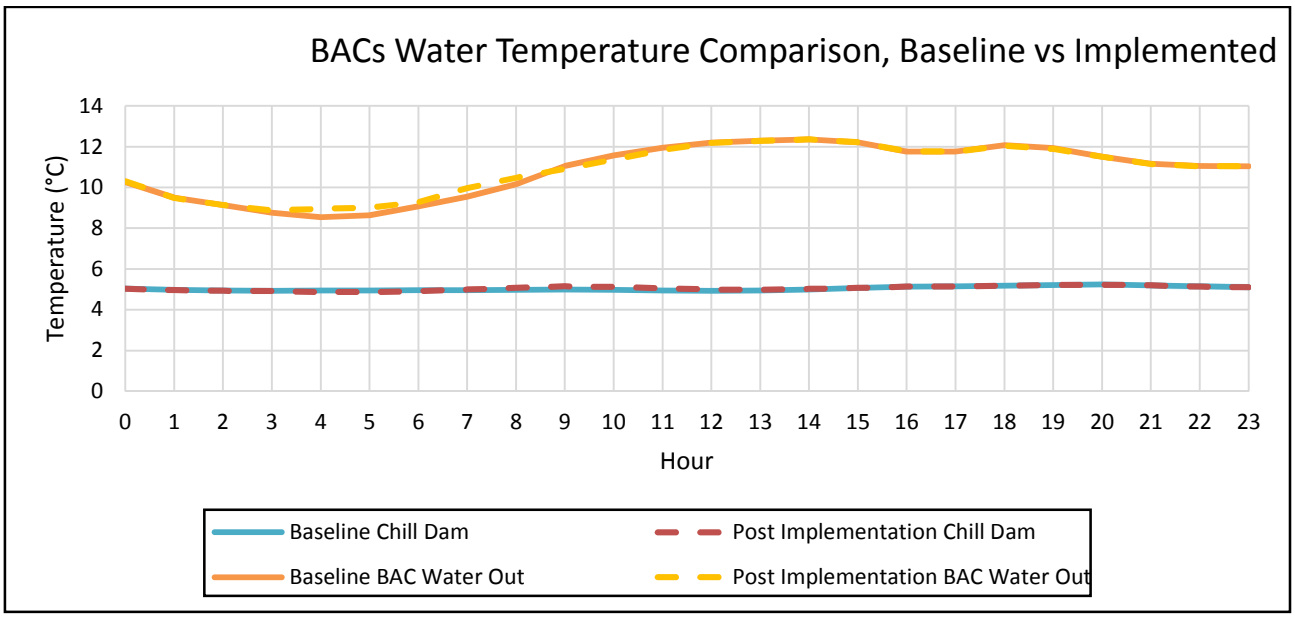

Figure 145: BACs water temperature comparison, baseline vs. implemented for a 4℃ evaporator setpoint

Figure 145 shows that the BACs outlet water temperature slightly increased between 03:00 and 06:00, since the chilled water flow through the BAC was reduced during this period. The lower volume chilled water extracted sufficient amounts of heat from the air to maintain the output WB temperature below the setpoint temperature. Figure 146 represents the inlet and outlet air temperatures for the BAC baseline and implemented simulations.

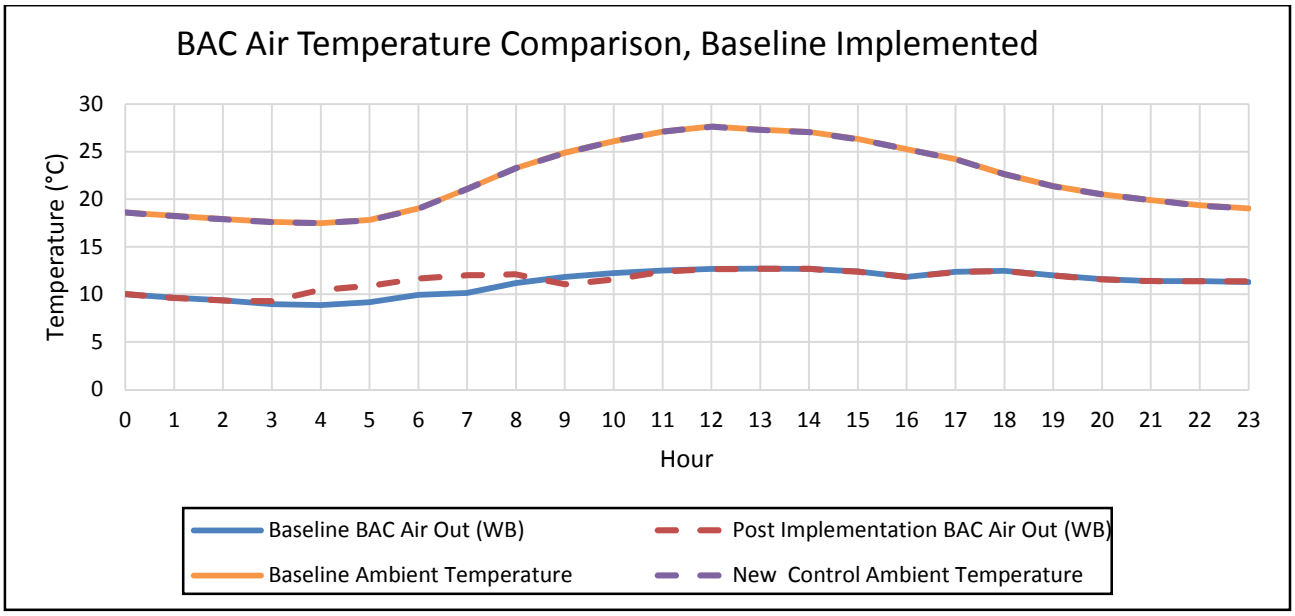

Figure 146: BACs air temperature comparison, baseline vs. implemented for a 4℃ setpoint

Figure 146 indicates that the same ambient temperature was utilised during the baseline and implemented simulations. The BACs' outlet WB temperature increased between 03:00 and 09:00 due to the BACs' valves throttling the chilled water flow through the BACs. However, the valves managed to maintain the BAC outlet temperature below the maximum temperature experienced during the baseline simulation with a daily average temperature increase of 0.28℃.

3℃ Evaporator outlet water temperature setpoint:

The evaporator outlet water temperature setpoint was set to 3℃ to determine what effect the BAC reconfiguration will have on the power usage, should the mine opt for maximum service delivery. Table 39 summarises the output temperatures and flows of the baseline and BAC reconfigured simulations.

Table 39: Baseline and implemented simulation output values BAC reconfiguration for energy saving, 3℃ setpoint

Outputs	Unit	Average Baseline	Average Implemented	Percentage (%) Deviation
Power Usage	kW	9300.38	9240.54	0.64
FP Total Flow	ℓ/s	820.74	804.36	2.00
FP Evaporator Inlet Temp	°C	13.71	13.90	-1.33
FP Evaporator Outlet Temp	°C	3.38	3.42	-1.26
Chill Dam Temp	°C	4.30	4.37	-1.50
FP Average COP	0	5.15	5.04	-2.16
Condenser Flow	ℓ/s	2087.86	2054.40	1.60
Condenser Inlet	°C	26.03	26.12	0.35
Condenser Outlet	°C	30.88	31.03	0.49
BAC Total Water Flow	ℓ/s	398.99	392.10	1.73
BAC Outlet Air Temp WB	°C	10.95	11.10	-1.37
BAC Outlet Water	°C	10.44	10.47	0.34
Chilled Water Recycled	ℓ/s	51.76	42.26	81.64

From Table 39 it is evident the BAC valve reconfiguration had no major effect on the FPs' outputs. The BAC's daily average output WB air temperature for the baseline simulation was 10.95℃. Therefore, the BAC valve control was set to maintain a BAC outlet WB air temperature of 11℃. The most important variables will be discussed from Figure 147 up to Figure 152. Figure 10 compares the baseline and implemented simulation's power profiles.

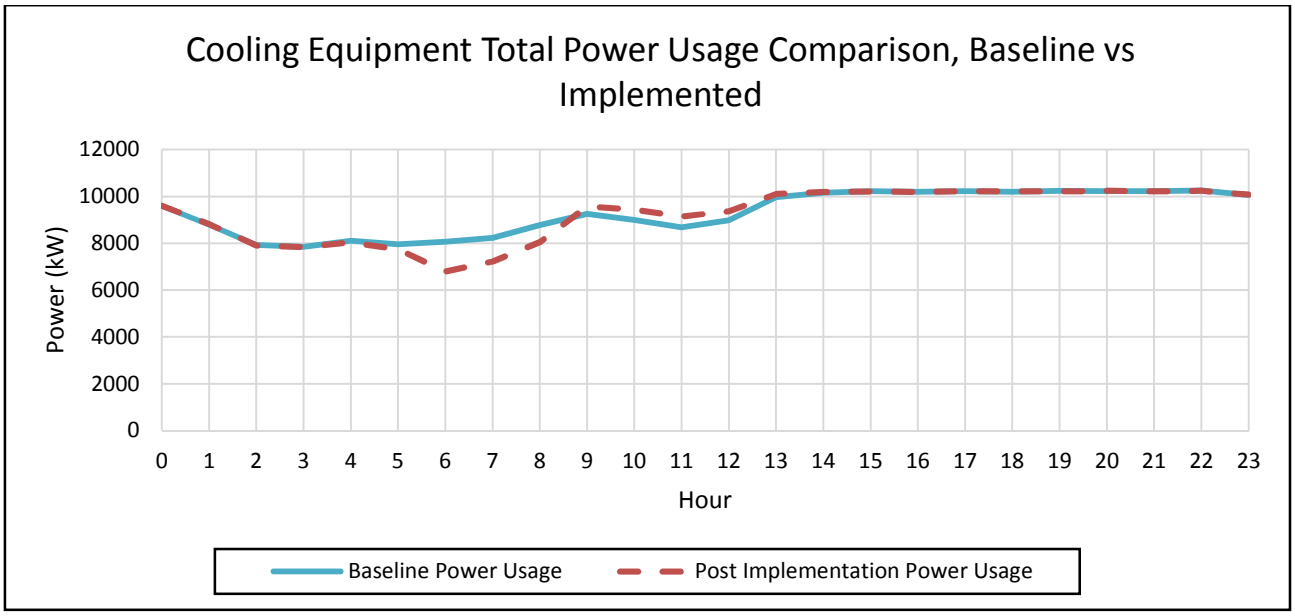

Figure 147: Cooling equipment total power usage comparison, baseline vs. implemented for a 3℃ setpoint

Figure 10 indicates there is a power reduction between 05:00 and 08:00, due to the cooling load reduced during this period. The reduced cooling load allowed one FP and its pumps to be swithced off during this period which resulted in a daily average power saving of 59.84 kW. Figure 148 represents the evaporator water flow through the FPs.

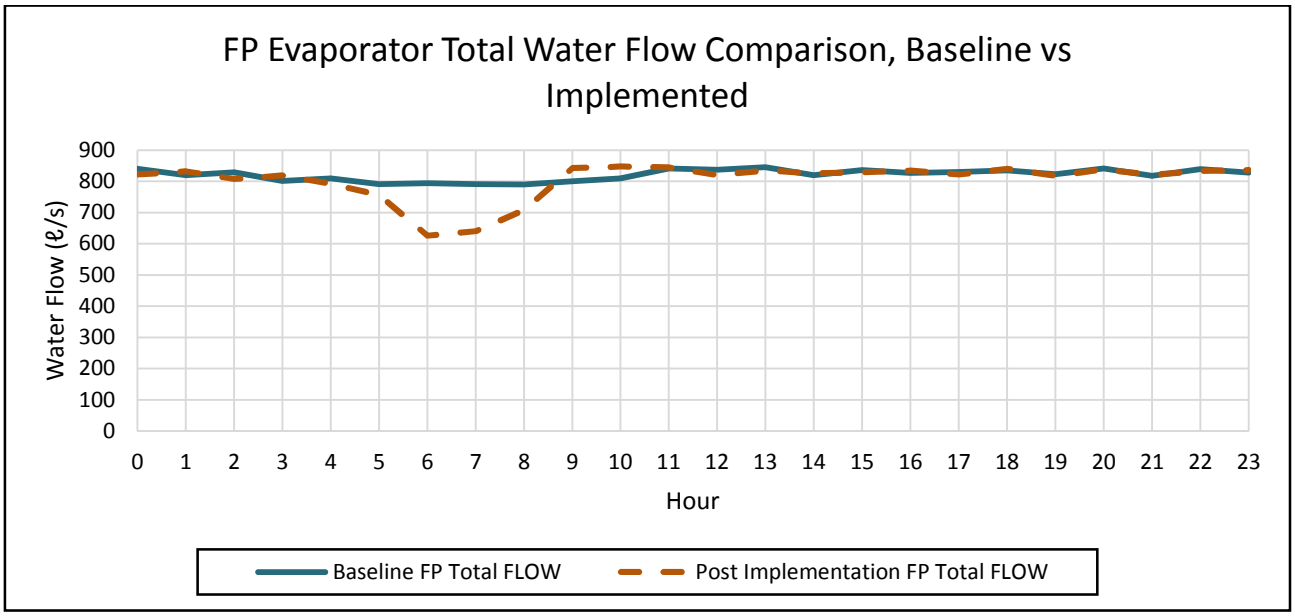

Figure 148: FP evaporator total water flow comparison, baseline vs. implemented for a 3℃ evaporator setpoint

Figure 148 depicts a water flow reduction between 05:00 and 09:00, due to the FP and pumps being switched off from a reduced chilled water demand. The reduced chilled water demand caused a reduction in the amount of chilled water being recycled. Figure 149 compares the evaporator inlet and outlet water temperature for the baseline and implemented simulations.

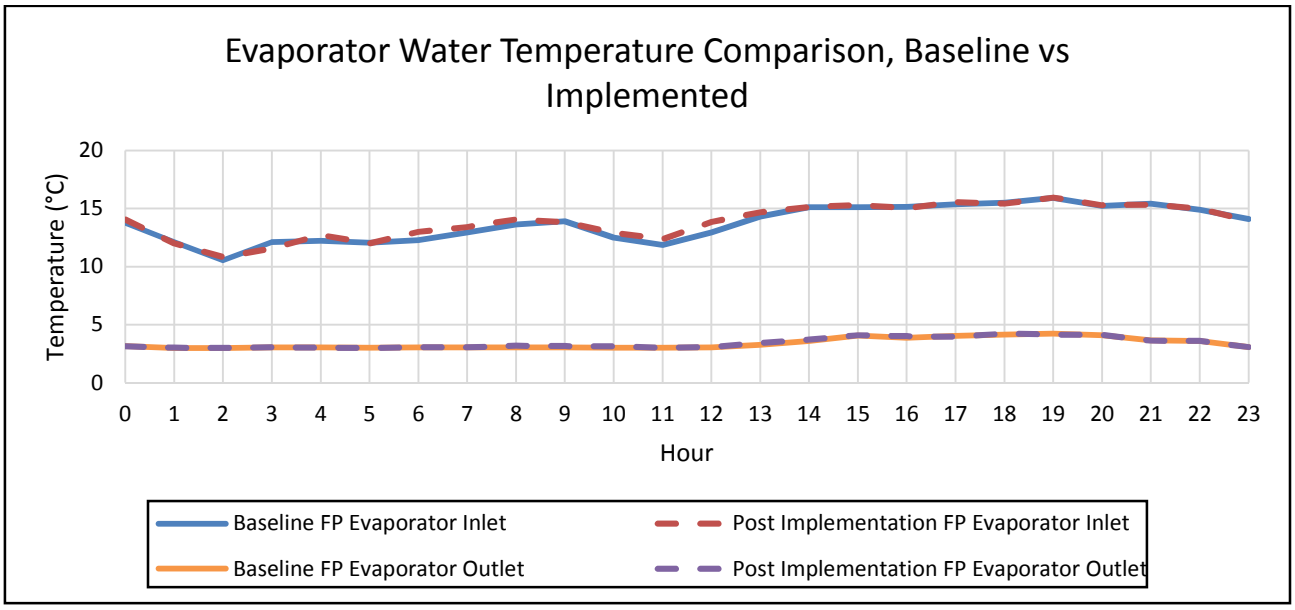

Figure 149: Evaporator water temperature comparison, baseline vs. implemented for a 3℃ evaporator setpoint

From Figure 149 it is evident that the FP's evaporator temperature was not affected by the new control philosophy. However, the inlet temperature increased between 06:00 and 13:00, due to a reduction in recycled chilled water. The FPs still manage to maintain the same evaporator outlet water temperature with the higher inlet temperature. Figure 150 represents the BAC total water flow for the baseline and new BAC valve control simulations.

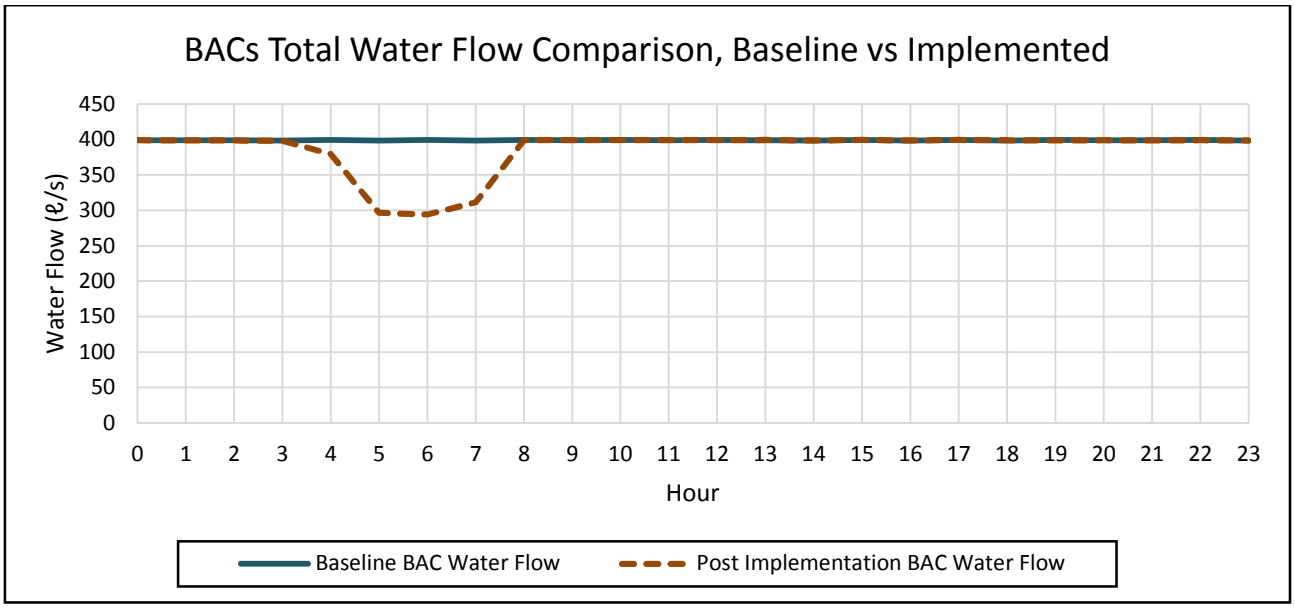

Figure 150: BAC water flow comparison, baseline vs. implemented for a 3℃ setpoint

Figure 150 indicates that the BAC water decreased between 04:00 and 08:00 which allowed the cooling load to be decreased for power savings. The BAC water flow was reduced to a minimum of 299.89 ℓ/s. The BAC chilled water flow is restored when the ambient temperature increases. Figure 151 represents the BACs inlet and outlet water temperature for the baseline and implemented simulations.

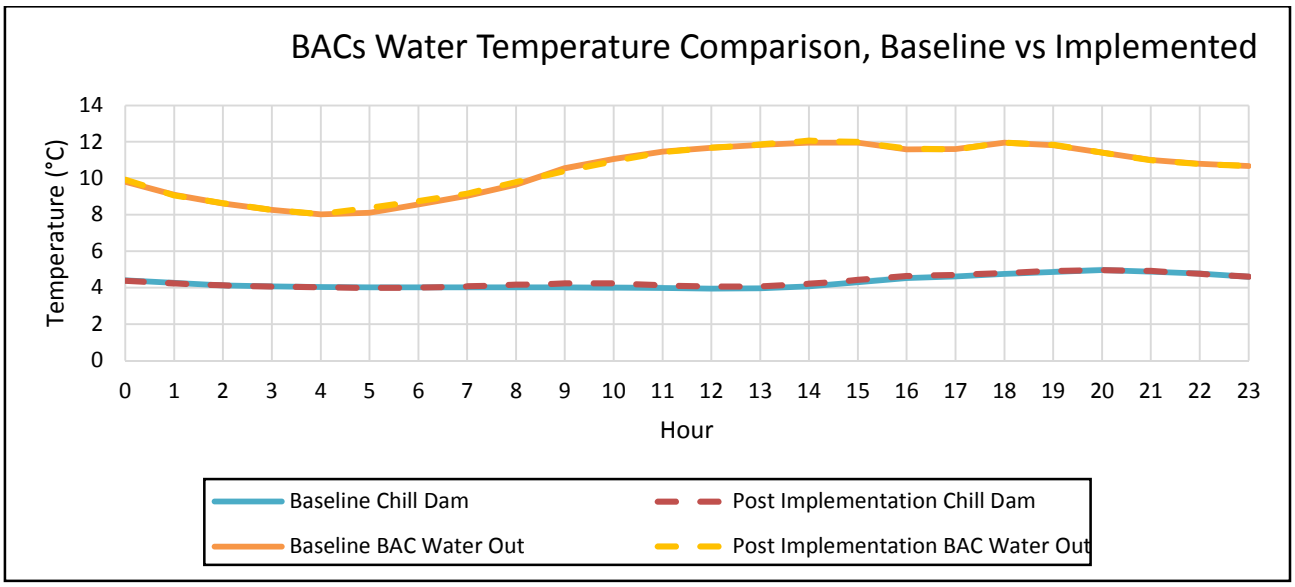

Figure 151: BACs water temperature comparison, baseline vs. implemented for a 3℃ evaporator setpoint

Figure 151 depicts the BAC inlet valve control, which had no effect on the BAC inlet and outlet water temperatures. Figure 152: BACs air temperature comparison, baseline vs

implemented for a 3℃ setpoint, represents the BAC air temperatures for the baseline and implemented simulations.

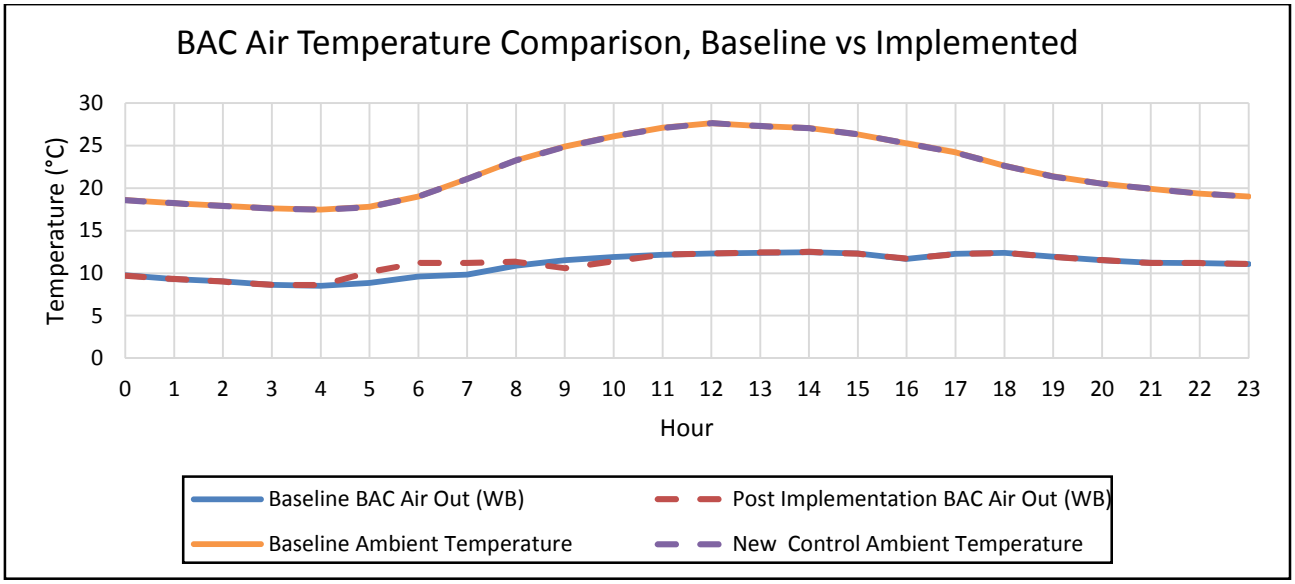

Figure 152: BACs air temperature comparison, baseline vs implemented for a 3℃ setpoint

Figure 110 depits the BAC inlet ambient air temperature, which was not changed during the simulations. However, the BAC outlet WB air temperature increased slightly during the morning period when the chilled water through the BACs was throttled due to the decreased ambient temperature. The outlet WB air temperature did not increase above the maximum temperature experienced during the baseline simulation. The daily average BAC oulet WB air temperature increased with 0.15℃.

Service delivery:

As described in a preceding section the BAC chilled water flow will be increased to the maximum of 150 ℓ/s. The valves will reduce the flow if the ambient air temperature allows it. The FPs' evaporator will be set to 5℃, 4℃ and 3℃ to determine the effect the increased water flow has on the BAC's service delivery with the different chilled water temperatures. The simulation will first be simulated with the BAC outlet air WB temperature set to 9℃ to determine the maximum service delivery of the system with the specific chilled water temperature. The BACs will then be controlled to the daily achievable average WB air temperature of the BACs. This will ensure the valves will reduce the chilled water flow when the ambient conditions are lower and will prevent cooling from being wasted unnecessarily.

5℃ Evaporator outlet water temperature setpoint:

The evaporator output water temperature setpoint was set to 5℃. Table 39 represents the average output values of the baseline and the implemented simulation. The BAC outlet WB temperature setpoint was set to 11℃. Table 39 also depicts the percentage deviation between the two average values.

Table 40: Baseline and implemented simulation output values BAC reconfiguration for maximum service delivery, 5℃ setpoint

Outputs	Unit	Average Baseline	Average Implemented	Percentage (%) Deviation
Power Usage	kW	8363.48	8535.20	-2.01
FP Total Flow	ℓ/s	822.94	835.41	-1.49
FP Evaporator Inlet Temp	°C	14.19	14.34	-1.07
FP Evaporator Outlet Temp	°C	5.04	5.07	-0.54
Chill Dam Temp	°C	5.94	6.06	-1.88
FP Average COP	0	5.18	5.21	0.59
Condenser Flow	ℓ/s	2019.32	2030.91	0.57
Condenser Inlet	°C	25.25	25.42	0.69
Condenser Outlet	°C	29.62	29.91	0.96
BAC Total Water Flow	ℓ/s	398.99	447.95	10.93
BAC Outlet Air Temp WB	°C	11.51	11.09	3.63
BAC Outlet Water	°C	11.26	11.14	-1.01
Chilled Water Recycled	ℓ/s	53.98	17.46	32.35

From Table 39 it is evident that the average daily values were not drastically affected by the increased water flow through the BAC. However, the power usage increased with 2.01% due to the increased chilled water demand from the BACs. Figure 153 compares the power utilised by the cooling equipment for the baseline and implemented simulations.

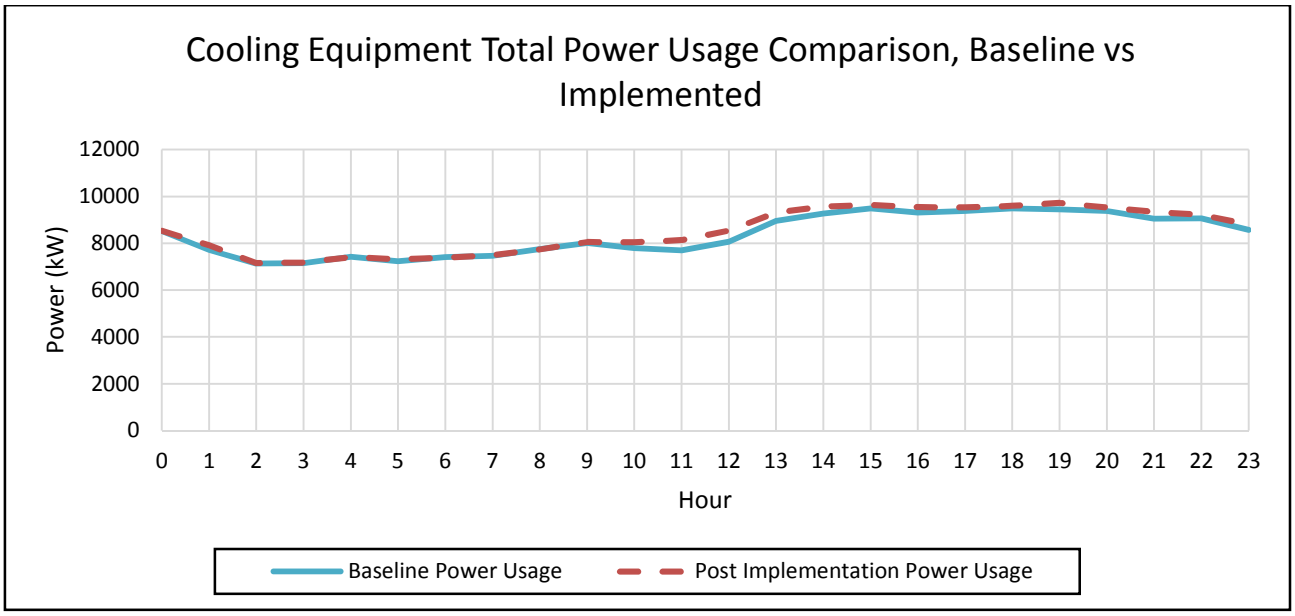

Figure 153: Cooling equipment total power usage comparison, baseline vs. implemented for a 5℃ setpoint

From Figure 153 it is evident that the power consumption increased due to an increased chilled water demand. More water had to be cooled by the FPs. The increased water demand caused an average daily power increase of 171.72 kW. Figure 154 compares the FP evaporator flow of the baseline and implemented simulations.

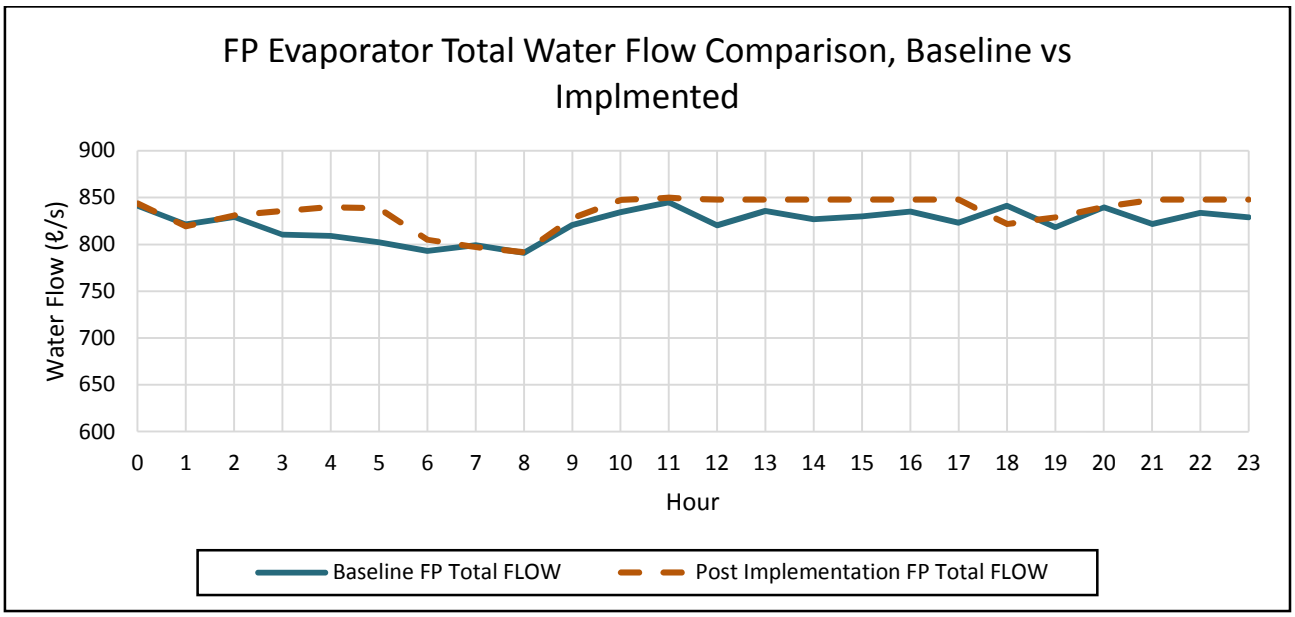

Figure 154: FP evaporator total water flow comparison, baseline vs. implemented for a 5℃ evaporator setpoint

Figure 154 depicts the evaporator flow, which increased throughout the majority of the day, due to the chilled water demand increasing. The increased chilled water demand also resulted in a 32.35% average reduction in the recycled chilled water. Figure 155 represents the evaporator inlet and outlet water temperatures for the baseline and implemented simulations.

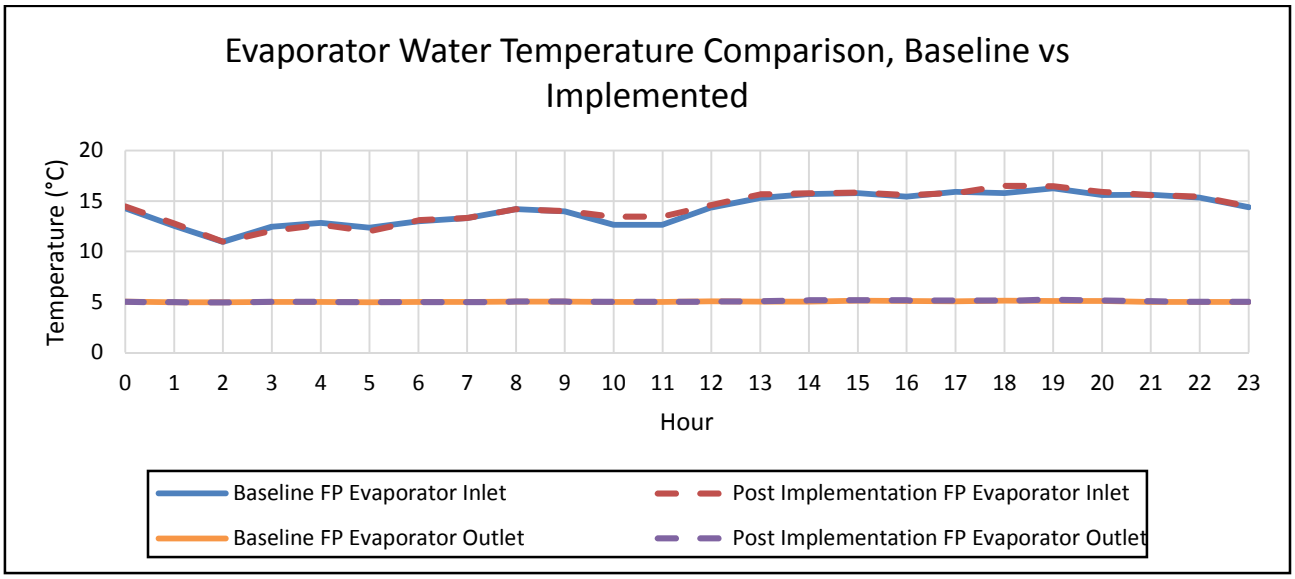

Figure 155: Evaporator water temperature comparison, baseline vs. implemented for a 5℃ evaporator setpoint

Figure 155 depicts the evaporator water inlet temperature increase during certain periods of the day. This is due to the reduction in recycled chilled water. The increased warmer water from the increased water flow through the BAC also caused the inlet water temperature to increase. However, the FPs still managed to maintain the same evaporator outlet temperature. Figure 156 compares the total water flow through the BAC of the baseline and implemented simulation.

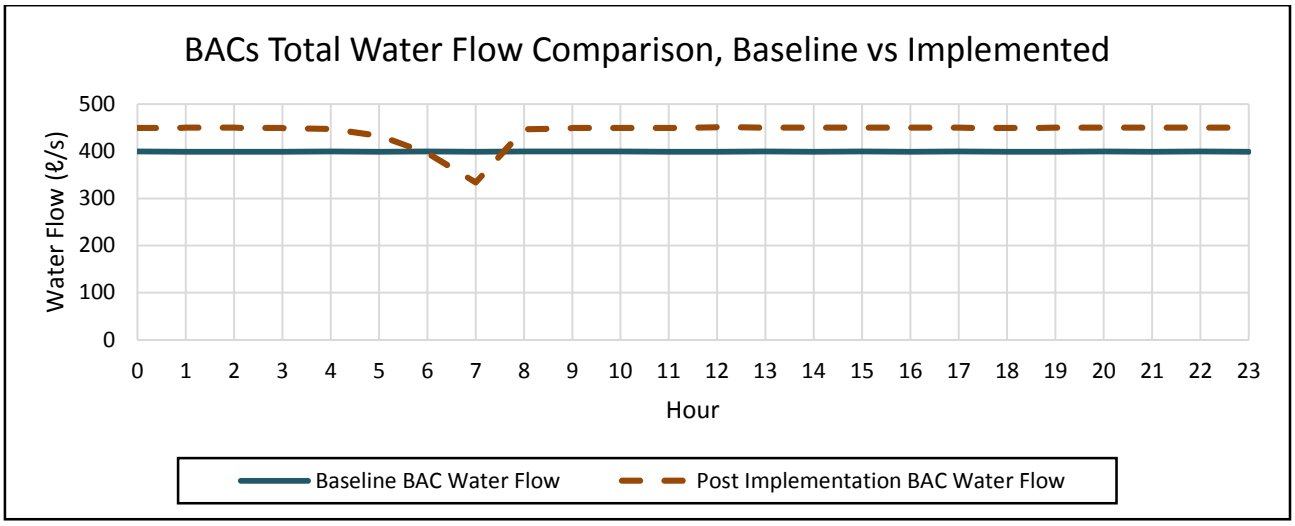

Figure 156: BAC water flow comparison, baseline vs. implemented for a 5℃ setpoint

Figure 156 depicts the total chilled water flow through the BACs, which were increased to 450 ℓ/s. The BAC water flow control valves reduced the chilled water flow between 05:00 and 08:00 as the ambient temperature lowered during this period. Figure 157 represents the BAC water temperatures of the baseline and implemented simulations.

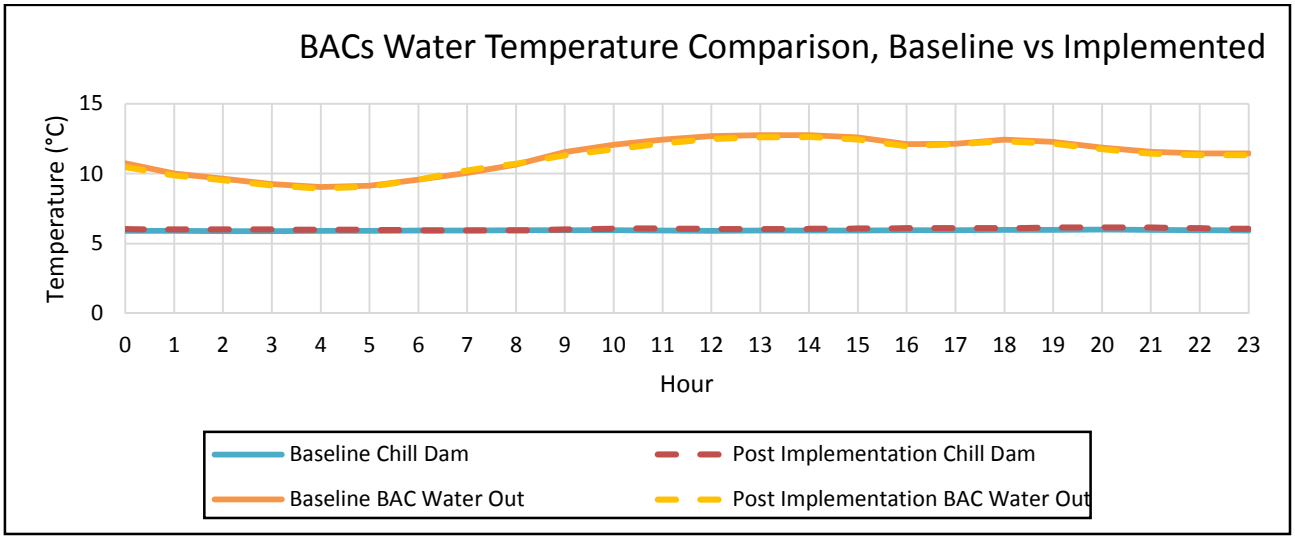

Figure 157: BACs water temperature comparison, baseline vs. implemented for a 5℃ evaporator setpoint

Figure 157 indicates that the water inlet was not affected by the increased water flow through the BAC. The outlet water temperature decreased slightly between 09:00 and 13:00. This is due to the setpoint being too low and the BAC cannot utilise all the cooling that is provided. In effect, a small amount of cooling is lost during this period. Figure 158 compares the BAC air temperatures of the baseline and implemented simulations.

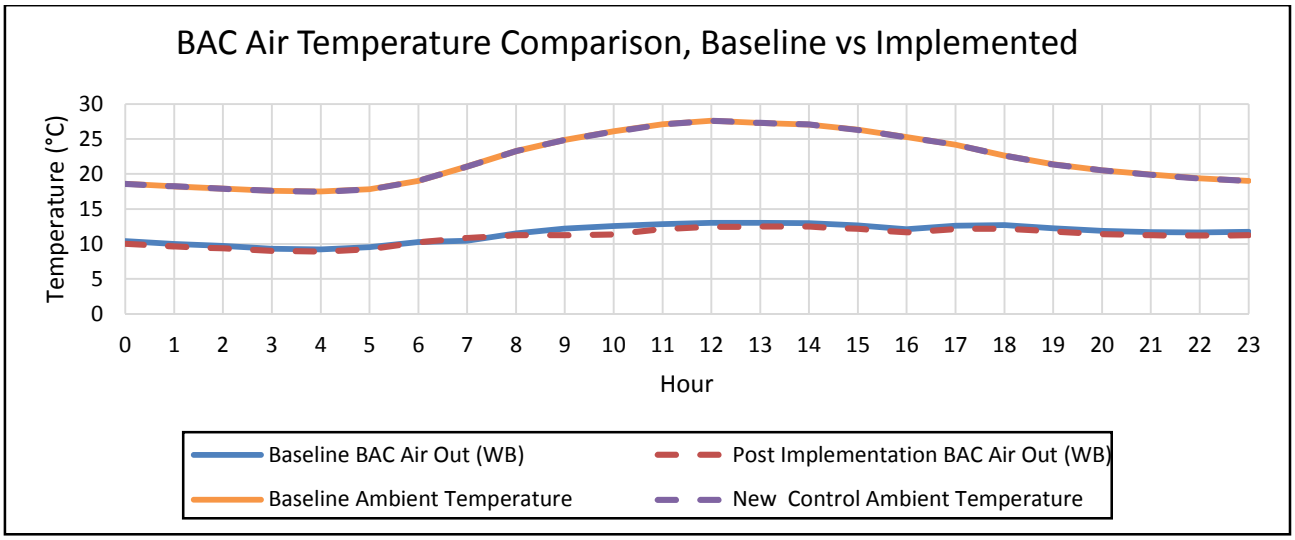

Figure 158: BACs air temperature comparison, baseline vs. implemented for a 5℃ setpoint

Figure 158 depicts the ambient temperatures, which remained the same throughout both simulations. The average BAC outlet WB temperature reduced with 0.42℃ throughout the day.

4℃ Evaporator outlet water temperature setpoint:

The evaporator output temperature was set to 4℃. The minimum achievable output WB air temperature of the BAC was determined and the BAC output WB air temperature was set to 11℃. Table 41 summarises the outputs of the baseline and implemented simulations. Table 41 also depicts the percentage deviation between the baseline and implemented simulation values.

Table 41: Baseline and implemented simulation output values BAC reconfiguration for maximum service delivery, 4℃ setpoint

Outputs	Unit	Average Baseline	Average Implemented	Percentage (%) Deviation
Power Usage	kW	8852.12	8941.01	-0.99
FP Total Flow	ℓ/s	821.19	810.78	-1.27
FP Evaporator Inlet Temp	°C	13.94	14.26	-2.24
FP Evaporator Outlet Temp	°C	4.13	4.20	-1.62
Chill Dam Temp	°C	5.04	5.20	-3.08
FP Average COP	0	5.17	5.08	-1.78
Condenser Flow	ℓ/s	2040.10	2031.33	0.43
Condenser Inlet	°C	25.71	25.90	0.76
Condenser Outlet	°C	30.40	30.69	0.95

BAC Total Water Flow	ℓ/s	398.99	424.87	6.09
BAC Outlet Air Temp WB	°C	11.19	11.00	1.76
BAC Outlet Water	°C	10.81	10.73	-0.74
Chilled Water Recycled	ℓ/s	52.22	15.92	30.48

From Table 41 it is evident that the increase in BAC chilled water flow did not affect the output values drastically. The total daily power consumed increased with 0.99% due to the increased cooling demand from the BACs. Figure 159 depicts the total power consumed of all the cooling equipment for the baseline and implemented simulations.

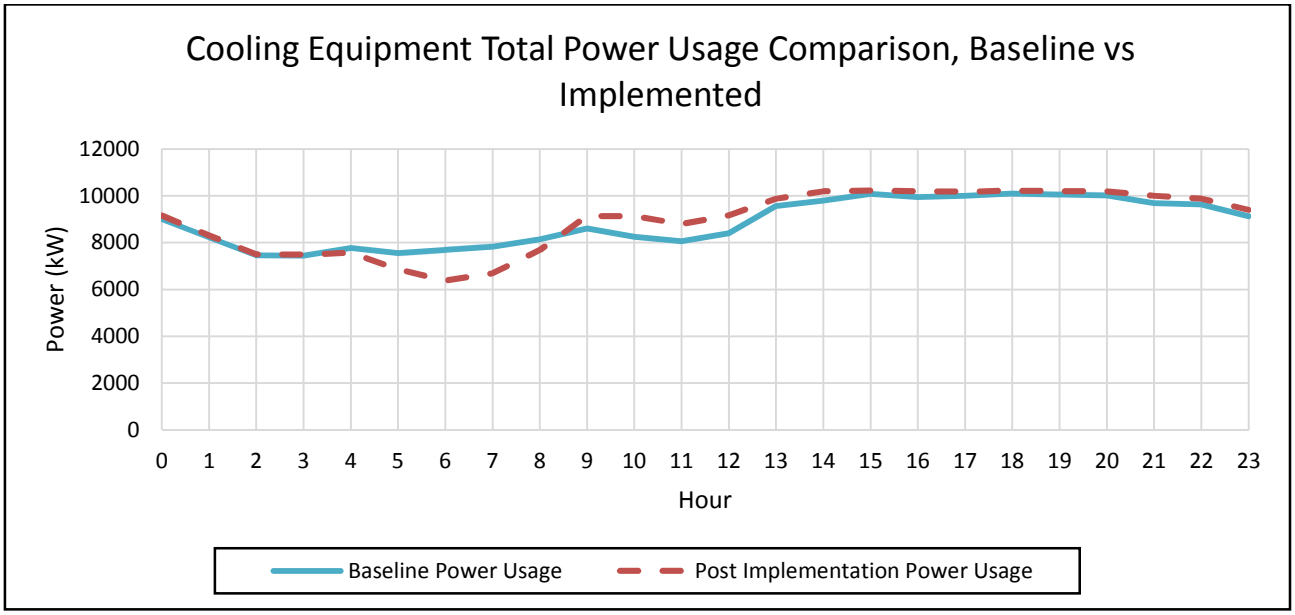

Figure 159: Cooling equipment total power usage comparison, baseline vs implemented for a 4℃ setpoint

From Figure 159 it is evident that there is a power reduction between 04:00 and 08: 00 from the reduced load caused by lower ambient conditions. However, the daily power increased with 88.89 kW throughout the day. Figure 160 compares the total evaporator water flow of both the baseline and implemented simulations.

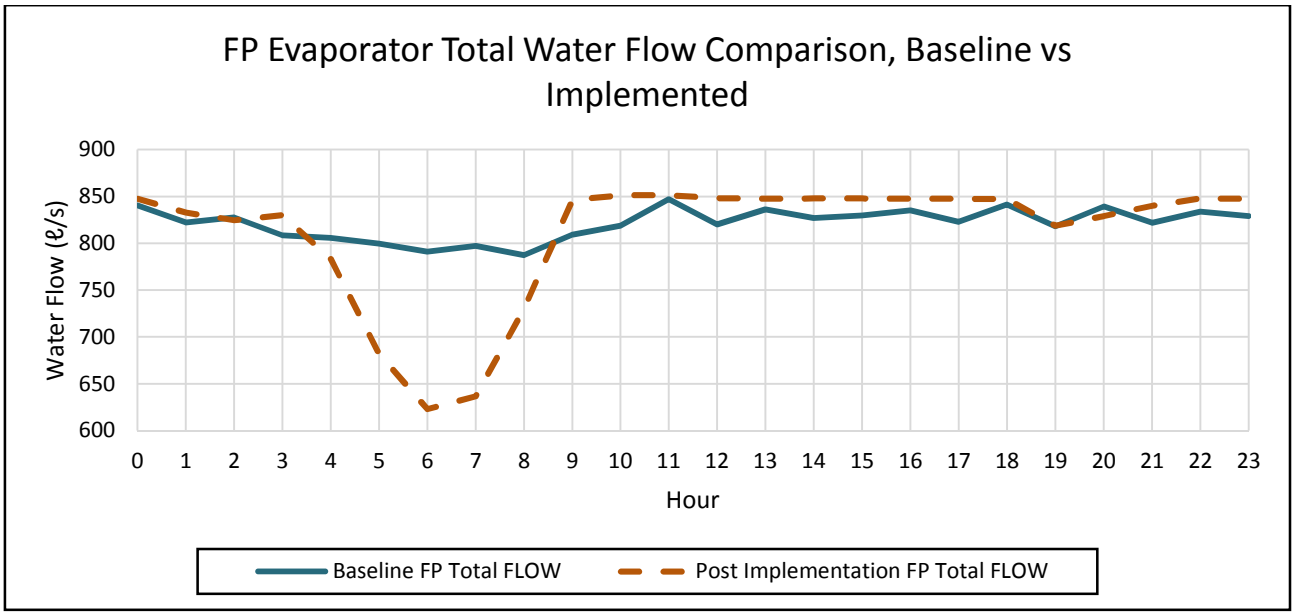

Figure 160: FP evaporator total water flow comparison, baseline vs. implemented for a 4℃ evaporator setpoint

Figure 160 depicts an evaporator water flow decrease between 04:00 and 08:00, due to a reduction in the cooling load from the lowered ambient temperature. The evaporator flow is increased during the rest of the day from the increased chilled water demand of the BACs. Figure 161 represents the evaporator water temperature of the baseline and implemented simulations.

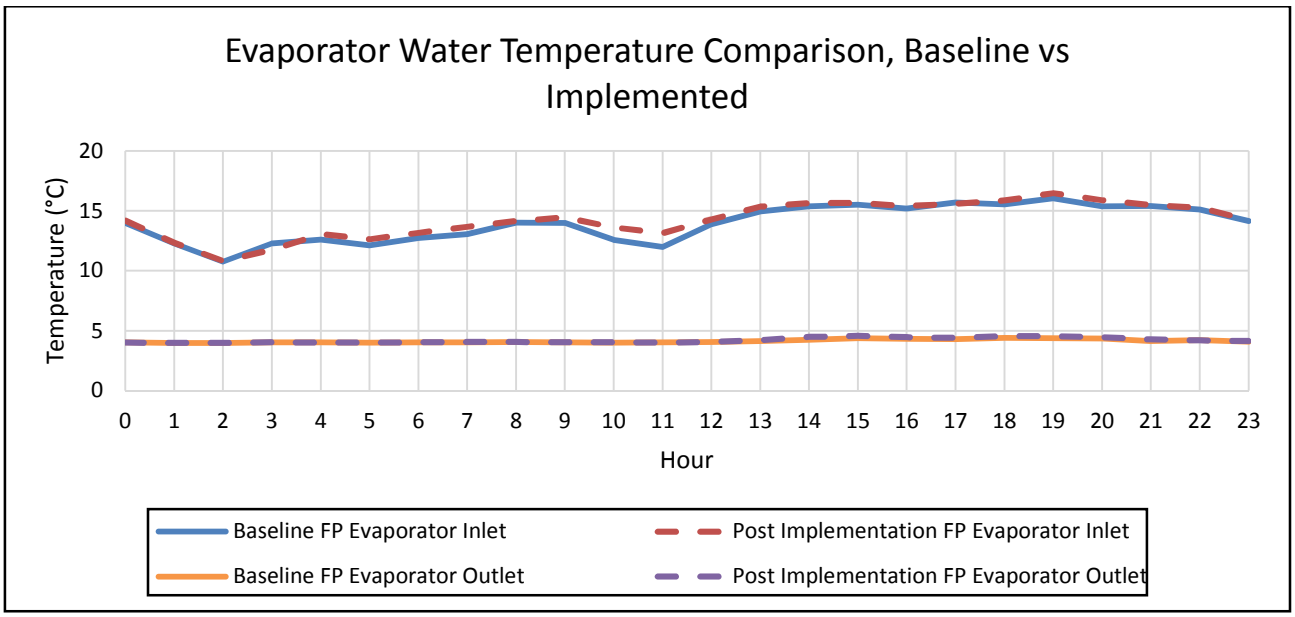

Figure 161: Evaporator water temperature comparison, baseline vs. implemented for a 4℃ evaporator setpoint

Figure 161 depicts the evaporator inlet temperature, which increased throughout the majority of the day. The average inlet temperature increased with 2.24% due to a reduction in recycled chilled water. The increased volume return water from the BACs also resulted in an increased evaporator inlet water temperature. However, the FPs still managed to maintain the same evaporator outlet temperature. Figure 162 represents the chilled water flow through the BACs of the baseline and implemented simulations.

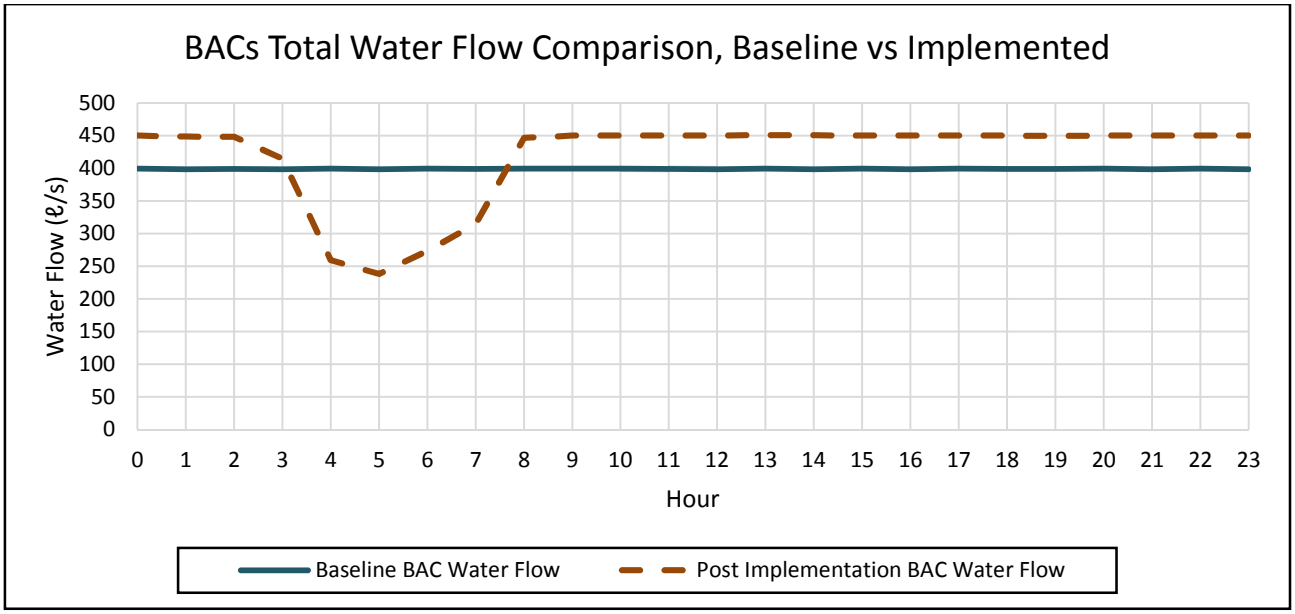

Figure 162: BAC water flow comparison, baseline vs. implemented for a 4℃ setpoint

From Figure 162 it is evident that the BAC maximum water flow was increased to 450 ℓ/s. The ambient temperature lowers between 03:00 and 08:00 to allow the BAC water flow to reduce to flow during this period to 248 ℓ/s, whilst maintaining the BAC outlet WB air temperature below the desired setpoint. Figure 163 compares the BAC water temperatures of the baseline and implemented simulations.

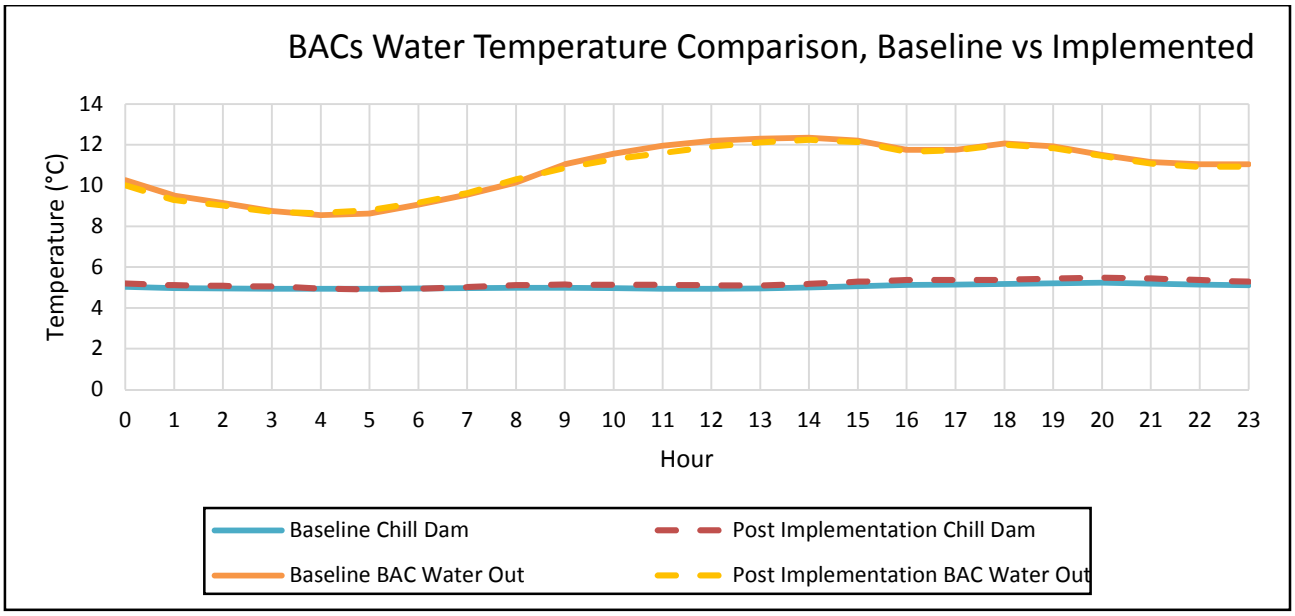

Figure 163: BACs water temperature comparison, baseline vs. implemented for a 4℃ evaporator setpoint

Figure 163 depicts the water temperature in and out of the BAC, which was not affected by the increased water flow through the BAC. Figure 164 compares the BAC air temperatures for the baseline and the implemented simulations.

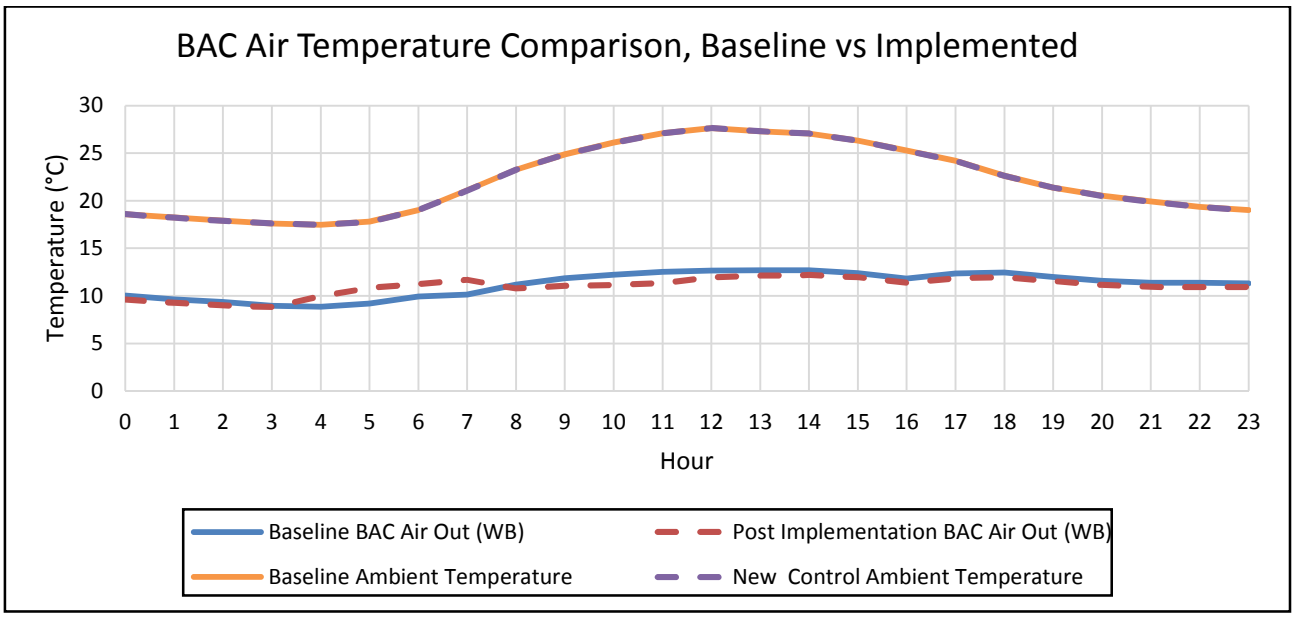

Figure 164: BACs air temperature comparison, baseline vs. implemented for a 4℃ setpoint

From Figure 164 it is evident that the ambient temperature was not changed during the simulations. The BAC outlet WB air temperature increased between 03:00 and 08:00 due

to the valves reducing the chilled water flow to maintain an outlet temperature below the setpoint temperature. The BAC outlet temperature is, however, lower during the rest of the day with an average temperature decrease of 0.19℃ throughout the day.

3℃ Evaporator outlet water temperature setpoint:

The evaporator output water temperature setpoint was set to 3℃. Table 42 represents the average output values of the baseline and the implemented simulation. The BAC outlet WB temperature setpoint was set to 10.5℃. Table 39 also depicts the percentage deviation between the two average values.

Table 42: Baseline and implemented simulation output values BAC reconfiguration for maximum service delivery, 3℃ setpoint

Outputs	Unit	Average Baseline	Average Implemented	Percentage (%) Deviation
Power Usage	kW	9300.38	9381.75	-0.87
FP Total Flow	ℓ/s	820.74	824.12	-0.41
FP Evaporator Inlet Temp	°C	13.71	14.01	-2.11
FP Evaporator Outlet Temp	°C	3.38	3.59	-5.75
Chill Dam Temp	°C	4.30	4.58	-6.20
FP Average COP	0	5.15	5.10	-1.00
Condenser Flow	ℓ/s	2087.86	2073.88	0.67
Condenser Inlet	°C	26.03	26.20	0.66
Condenser Outlet	°C	30.88	31.15	0.88
BAC Total Water Flow	ℓ/s	398.99	439.28	9.17
BAC Outlet Air Temp WB	°C	10.95	10.66	2.63
BAC Outlet Water	°C	10.44	10.38	-0.56
Chilled Water Recycled	ℓ/s	51.76	14.85	28.68

Table 42 depicts the increased flow through the BAC with an evaporator setpoint of 3℃, which did not affect the output values drastically. The power consumed by the cooling equipment increased with 0.87% to provide the improved service delivery of the BAC outlet WB air temperature. Figure 165 compares the cooling equipment power of the baseline and implemented simulations.

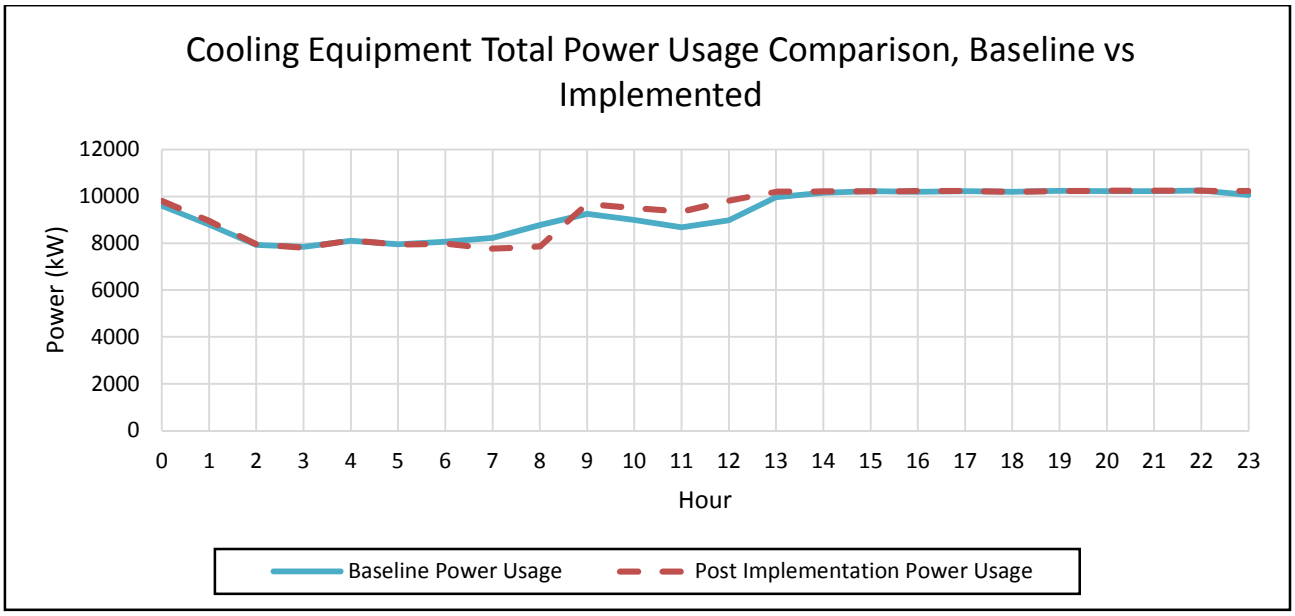

Figure 165: Cooling equipment total power usage comparison, baseline vs implemented for a 3℃ setpoint

Figure 165 depicts the power consumed by the cooling equipment, which decreased between 06:00 and 09:00 due to a reduced cooling load from the improved BAC flow control. The power increased between 09:00 and 13:00 due to the increased water demand from the BACs for an improved service delivery. During the rest of the day the power usage was at its maximum as with the baseline simulation. However, the average power consumption increased with 81.35 kW throughout the day. Figure 166 represents the water flow through the evaporator cycle of the baseline and implemented simulations.

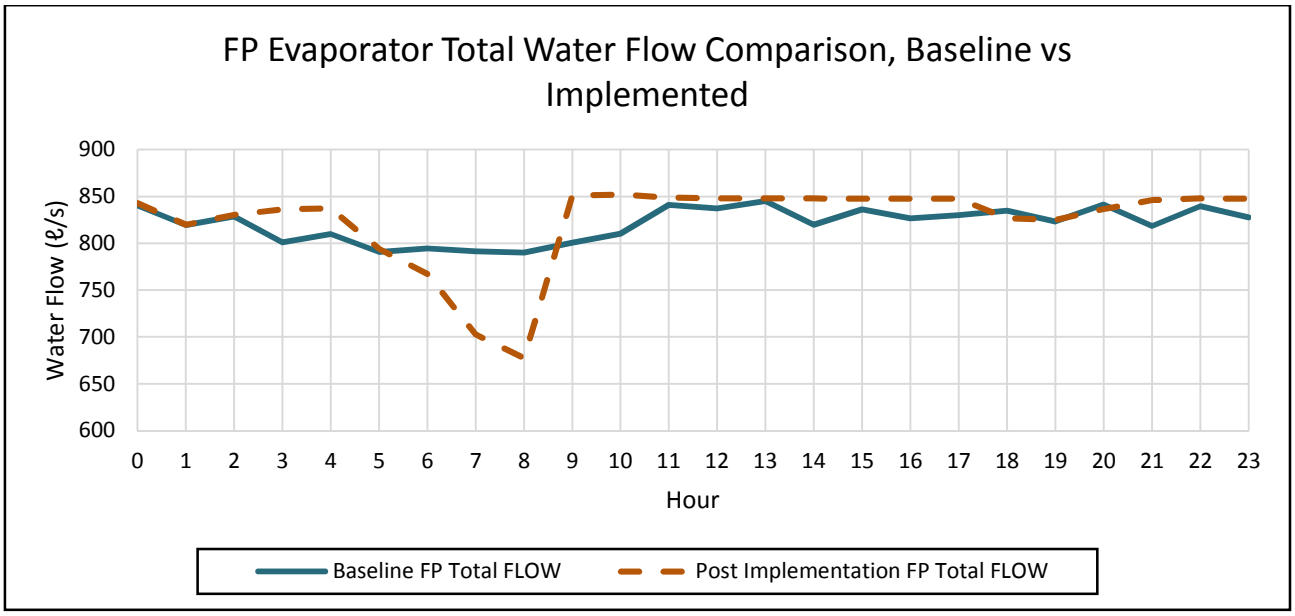

Figure 166: FP evaporator total water flow comparison, baseline vs. implemented for a 3℃ evaporator setpoint

From Figure 166 it is evident that the water flow through the evaporator cycle decreased between 05:00 and 09:00 as the chilled water demand decreased during this period. The water flow increased during the rest of the day as the BACs' chilled water demand increased to maintain the output WB air temperature setpoint. Figure 167 compares the evaporator water temperature of the baseline and simulated simulations.

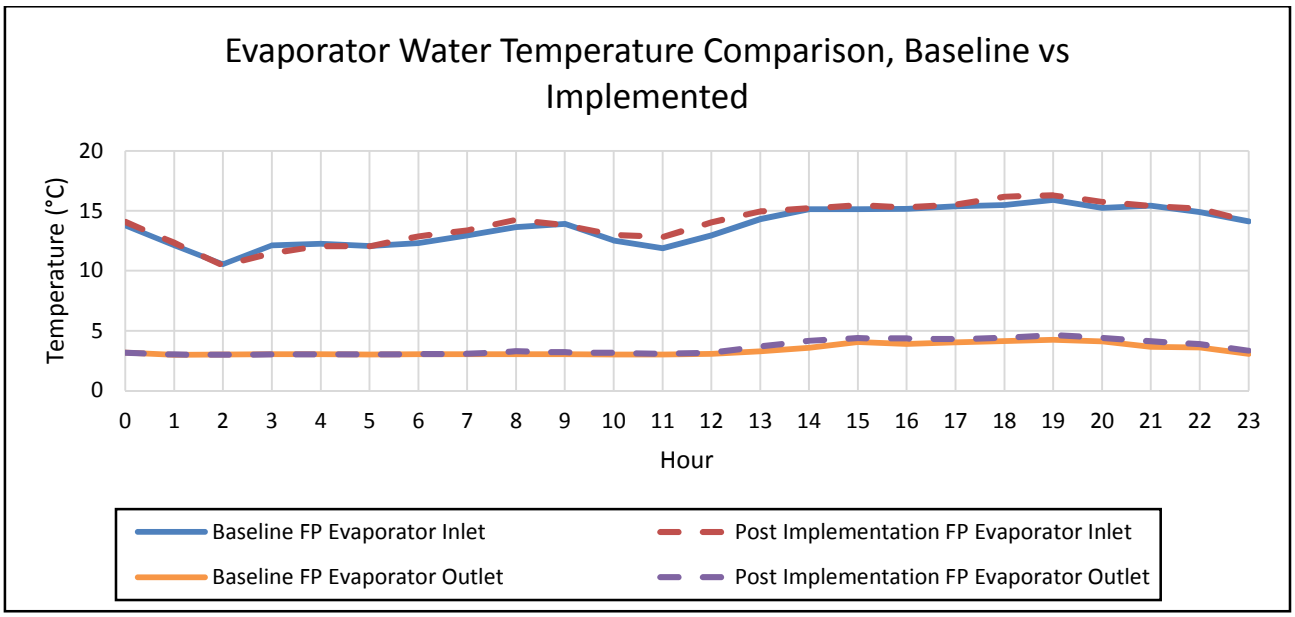

Figure 167: Evaporator water temperature comparison, baseline vs. implemented for a 3℃ evaporator setpoint

Figure 167 depicts the evaporator inlet water temperature, which increased during the day as the chilled water demand increased, resulting in a reduced recycled chilled water. The FPs fairly managed to maintain the evaporator outlet temperature with a slight increase of 0.21℃. Figure 168 represents the BAC water flow of the baseline and implemented simulations.

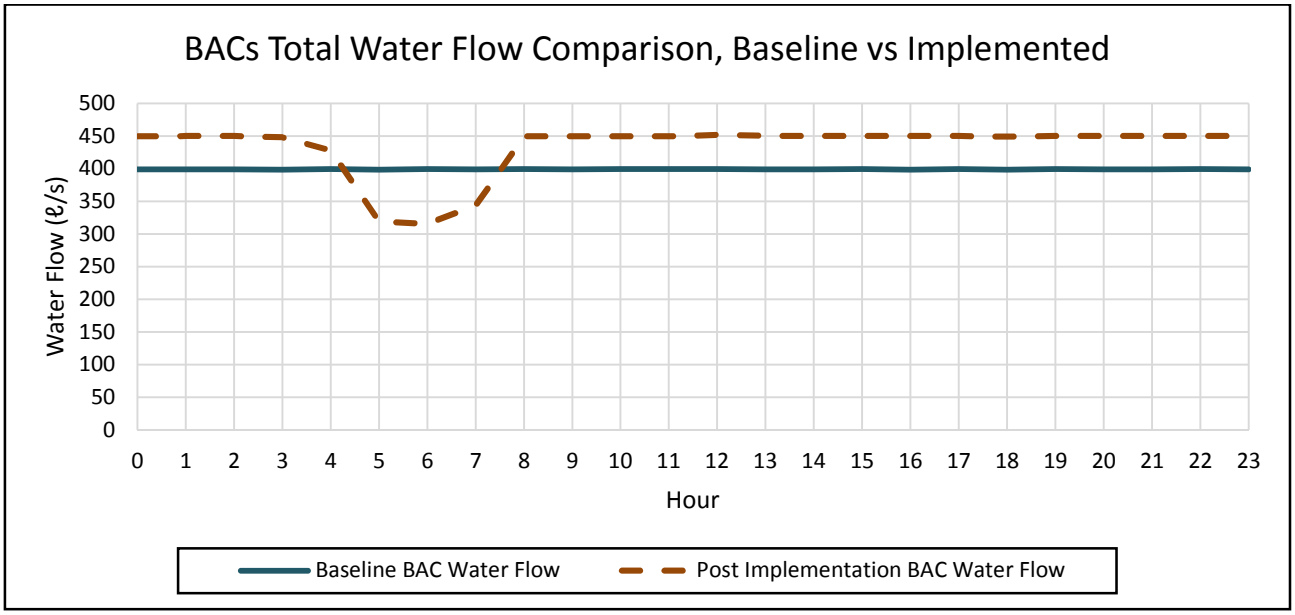

Figure 168: BAC water flow comparison, baseline vs. implemented for a 3℃ setpoint

From Figure 168 it is evident that the BAC maximum chilled water flow was increased to 450 ℓ/s to increase the service delivery of the BAC's outlet WB air temperature. The lowered ambient air temperature between 04:00 and 08:00 allowed the BAC valves to reduce the chilled water flow to 315 ℓ/s to prevent wastage of cooling. Figure 169 compares the BAC water temperatures of the baseline and implemented simulations.

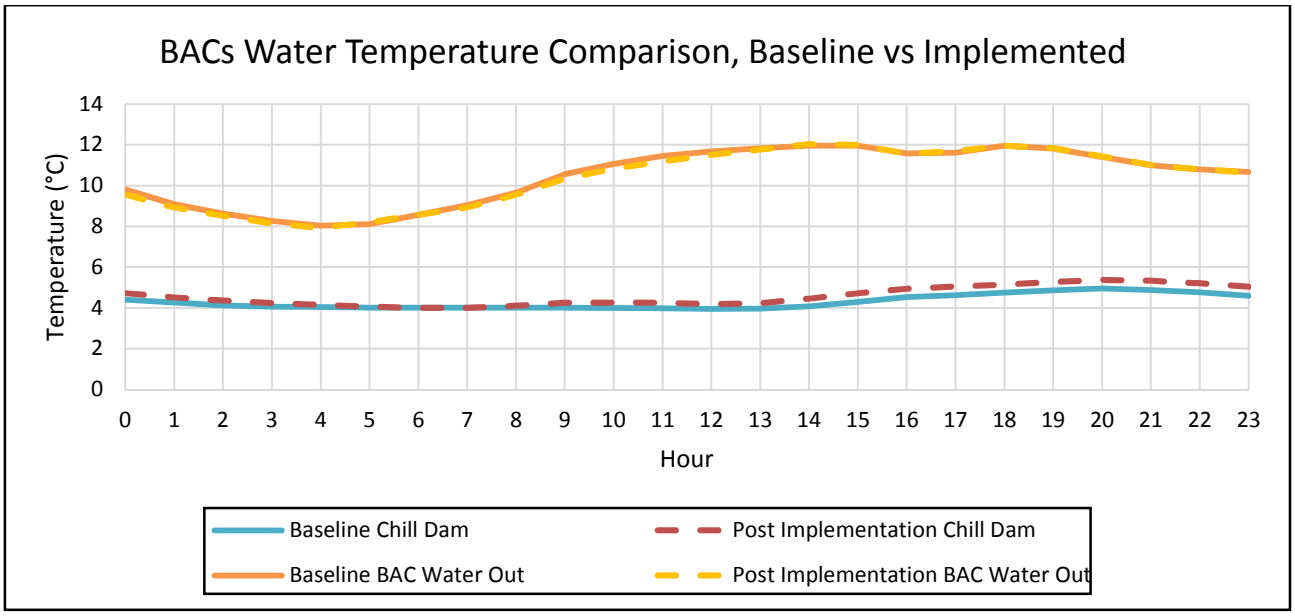

Figure 169: BACs water temperature comparison, baseline vs. implemented for a 3℃ evaporator setpoint

Figure 169 depicts an increase in the BAC inlet water temperature. However, BAC outlet WB air temperature decreased and the outlet water temperature remained the same. The increased water flow allowed warmer inlet water to extract sufficient heat from the air to maintain the BAC outlet air WB setpoint temperature. Figure 170 compares the BAC air temperatures of the baseline and the implemented simulations.

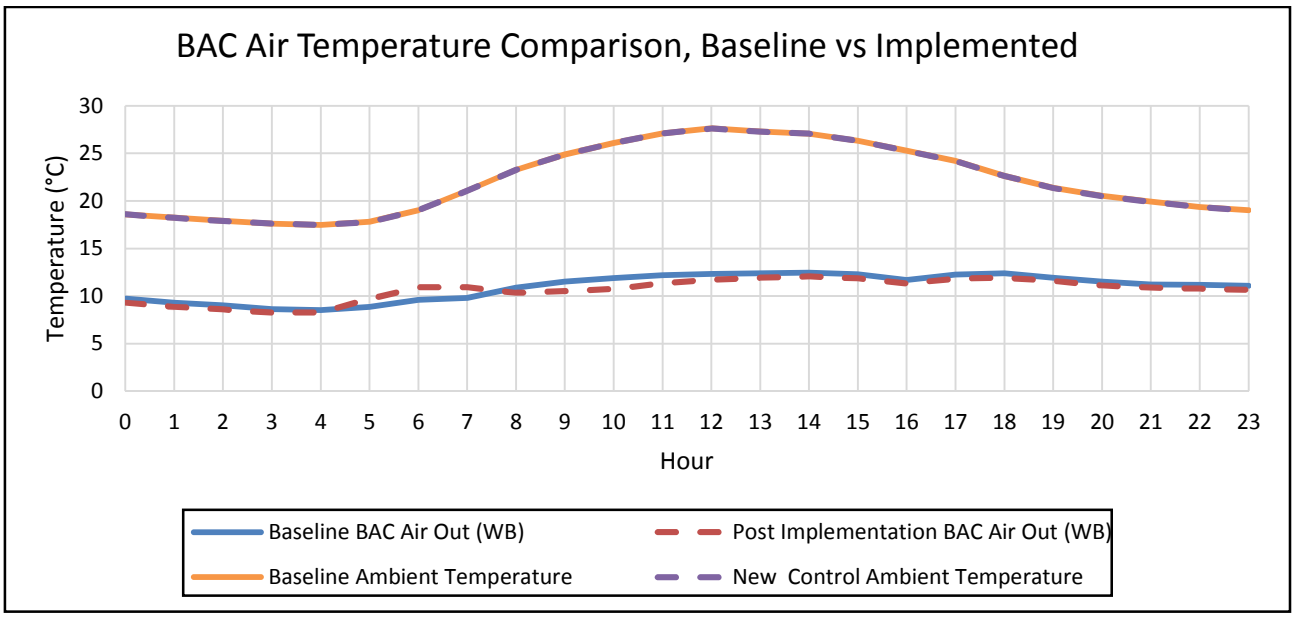

Figure 170: BACs air temperature comparison, baseline vs. implemented for a 3℃ setpoint

From Figure 170 it is evident that the ambient temperature was not changed during the simulations. The BAC outlet WB air temperature increased between 05:00 and 07:00 due to the valves reducing the chilled water flow to maintain an outlet temperature below the setpoint temperature. The BAC outlet temperature is, however, lower during the rest of the day with an average temperature decrease of 0.29℃ throughout the day.

Appendix F – RECONFIGURING OF MINE A'S PRE-COOLING TOWERS

5℃ Evaporator outlet water temperature setpoint:

The evaporator output water temperature was set to 5℃ to determine the maximum power saving that could realise from reconfiguring the pre-cooling towers whilst meeting mine A's minimum cooling demand. Table 43 compares the implemented pre-cooling tower reconfiguration simulation with the pump reconfigured simulation which can be considered as the baseline simulation. The table also depicts the percentage deviation between the two values.

Table 43: Baseline and implemented simulation output values for reconfiguring of Pre-cooling towers, 5℃ evaporator setpoint

Outputs	Unit	Average Baseline	Average Implemented	Percentage (%) Deviation
Power Usage	kW	8363.48	8076.08	3.44
FP Total Flow	ℓ/s	822.94	827.48	-0.55
FP Evaporator Inlet Temp	°C	14.19	14.55	-2.02
FP Evaporator Outlet Temp	°C	5.04	5.02	0.40
Chill Dam Temp	°C	5.94	5.91	0.49
FP Average COP	-	5.18	5.21	0.44
Condenser Flow	ℓ/s	2019.32	2013.77	0.27
Condenser Inlet	°C	25.25	25.17	0.32
Condenser Outlet	°C	29.62	29.48	0.48
BAC Total Water Flow	ℓ/s	398.99	399.00	0.00
BAC Outlet Air Temp WB	°C	11.51	11.50	0.06
BAC Outlet Water	°C	11.26	11.26	0.02
Chilled Water Recycled	ℓ/s	53.98	58.48	-7.70
Water From UG	°C	26.03	26.03	0.00
Pre-Cool 1 Water Out	°C	19.34	25.64	-24.60
Pre-Cool 2 Water Out	°C	17.09	17.95	-4.76
Pre-Cool 2 Dam	°C	13.60	13.95	-2.55

From Table 43 it is evident that the reconfirmation of the pre-cooling towers did not affect the entire cooling system. However, the pre-cooling water temperatures were affected as expected and will be discussed. Figure 171 compares the cooling equipment power consumed during the implemented simulation against the baseline simulation.

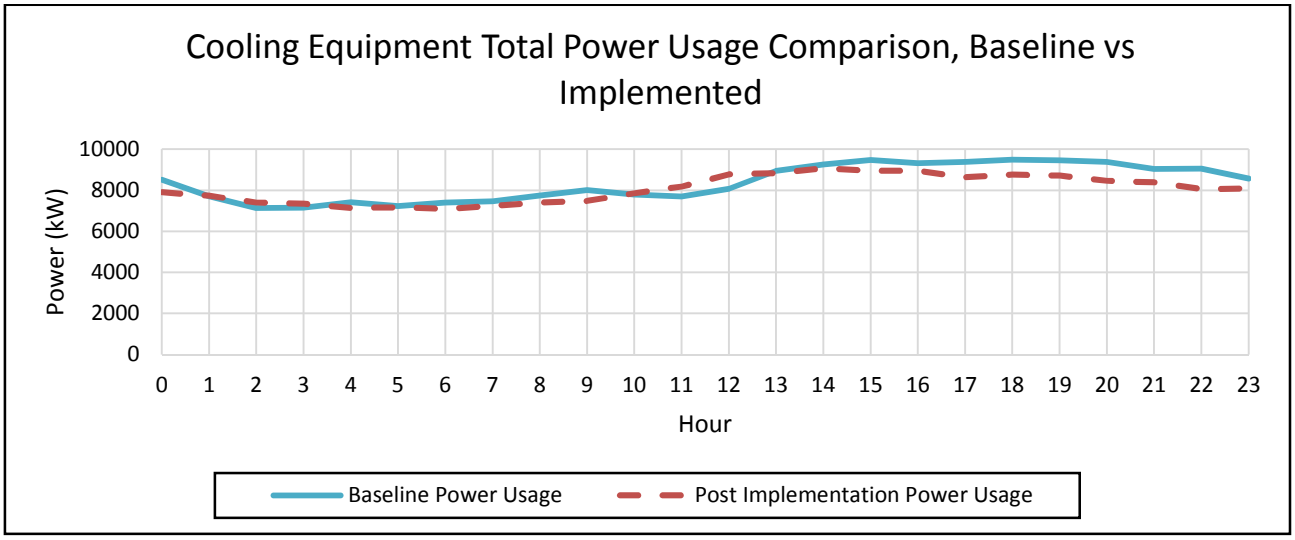

Figure 171: Cooling equipment total power usage comparison, baseline vs. implemented for a 5℃ setpoint

Figure 171 depicts the reconfiguration of the pre-cooling towers, which will reduce the total power consumed by the cooling system's equipment. The reconfiguration realised in a daily average power saving of 287.41 kW. Figure 172 represents the evaporator water flow through the FPs of the baseline and the implemented simulations.

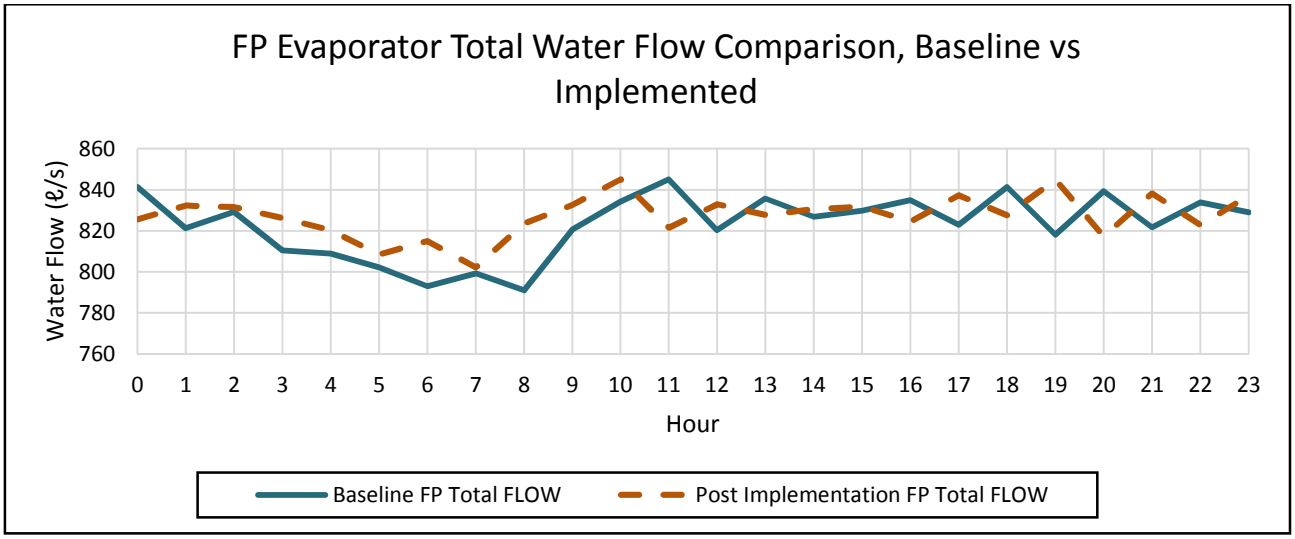

Figure 172: FP evaporator total water flow comparison, baseline vs. implemented for a 5℃ evaporator setpoint

Figure 172 depicts the evaporator flow varied throughout the day. The hourly average evaporator water flow increased with 0.55 ℓ/s, because the recycled water increased with 7.70%. The recycled water increased to maintain an evaporator inlet temperature close to

14℃. Figure 173 compares the evaporator water temperatures of the implemented simulation with the baseline simulation.

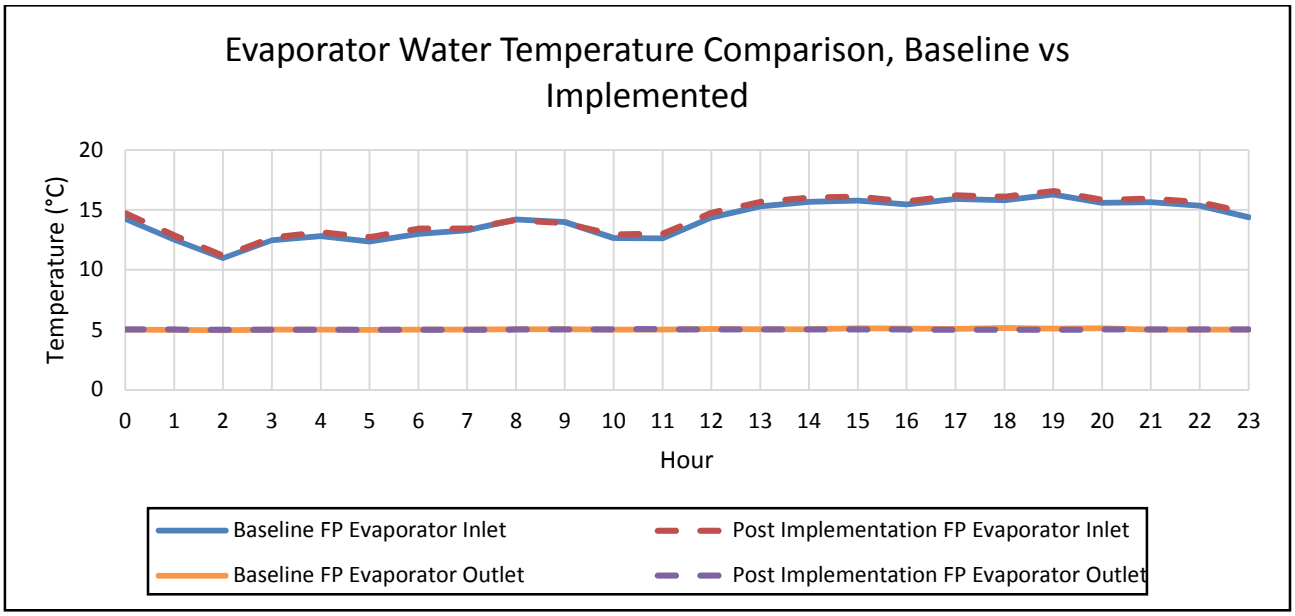

Figure 173: Evaporator water temperature comparison, baseline vs. implemented for a 5℃ evaporator setpoint

Figure 173 depicts the evaporator inlet water temperature, which is slightly warmer during the day. On average the evaporator inlet water temperature is 0.36℃ warmer during the day. However, the FPs still manage to reduce the evaporator outlet water temperature to 5.02℃; 0.02℃ lower than the baseline simulation. Figure 174 represents the pre-cool water temperatures of the baseline and implemented simulation.

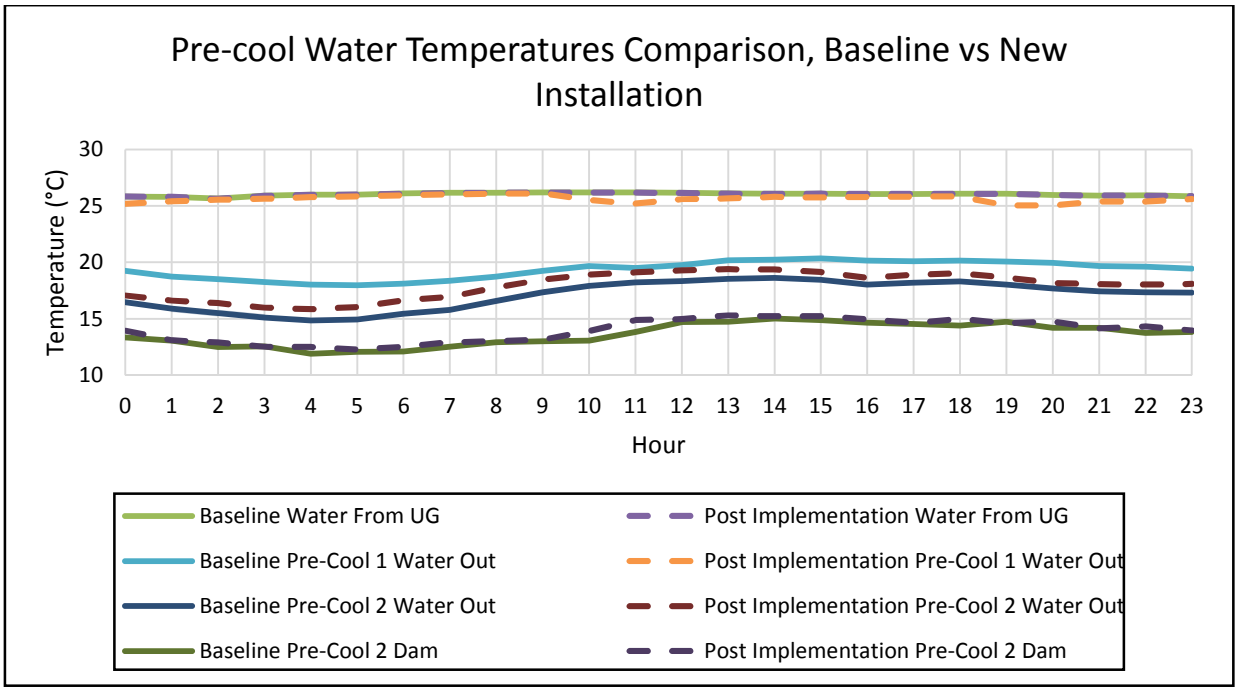

Figure 174: Pre-cool towers' water temperatures with a 5℃ evaporator setpoint temperature

Figure 174 depicts the water temperature from underground, which remained constant for both the baseline and implemented simulations. The first stage pre-cooling towers managed to reduce the water temperature with 0.39℃ with all the fans switched off. The second stage new pre-cooling towers managed to reduce the outlet water temperature to 0.86℃ above the baseline simulation outlet temperature. However, the pre-cool dam two's water temperature remained unchanged as the recycle chilled water flow was increased. Figure 175 compares the waterside efficiencies of the implemented and baseline simulations with each other.

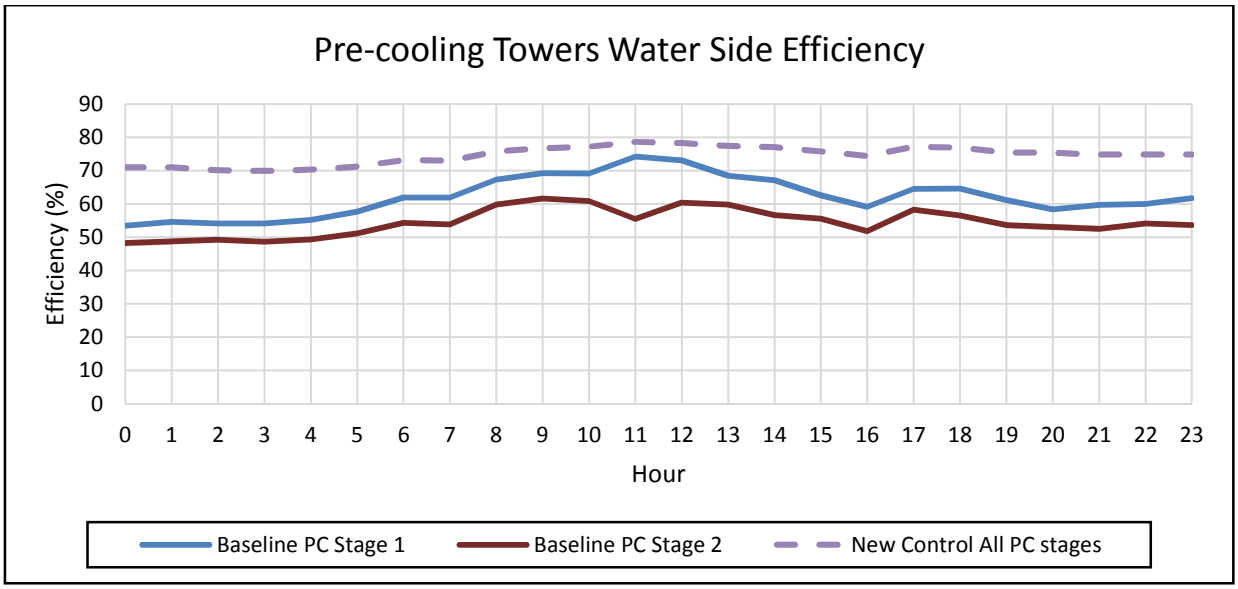

Figure 175: Pre-cool towers' water side efficiency with a 5℃ evaporator setpoint temperature

Figure 175 depicts the new pre-cooling towers' water side efficiency, which improved with 12% on average. The old pre-cooling towers had a cooling efficiency of 62.24% and 54.48% for the first and second stage respectively. With the new second stage pre-cooling towers and the first stage pre-cooling tower fans switched off, the water side efficiency from underground to the second stage outlet water temperature improved to 74.65%. This is a realistic service delivery and efficiency from the pre-cooling towers as a water side efficiency of 78% has been recorded for the same amount of pre-cooling towers at mine F [21].

4℃ Evaporator outlet water temperature setpoint:

Currently mine A's evaporator outlet water temperature is set at 4℃. Therefore, the effect that reconfiguring of the pre-cooling has on the cooling system was tested with the evaporator outlet water temperature setpoint set at 4℃. This will determine the amount of power saving realised from reconfiguring the pre-cooling towers with the mine's current operations. Table 44 summarises the baseline and implemented simulations output values and depicts the percentage deviation between the two values.

Table 44: Baseline and implemented simulation output values for reconfiguring of Pre-cooling towers, 4℃ evaporator setpoint

Outputs	Unit	Average Baseline	Average Implemented	Percentage (%) Deviation
Power Usage	kW	8852.12	8565.04	3.24
FP Total Flow	ℓ/s	821.19	825.27	-0.49
FP Evaporator Inlet Temp	°C	13.94	14.29	2.03
FP Evaporator Outlet Temp	°C	4.13	4.07	1.40
Chill Dam Temp	°C	5.04	4.97	1.33
FP Average COP	0	5.17	5.22	0.90
Condenser Flow	ℓ/s	2040.10	2056.35	0.79
Condenser Inlet	°C	25.71	25.60	0.42
Condenser Outlet	°C	30.40	30.18	0.75
BAC Total Water Flow	ℓ/s	398.99	398.99	0.00
BAC Outlet Air Temp WB	°C	11.19	11.18	0.14
BAC Outlet Water	°C	10.81	10.79	0.21
Chilled Water Recycled	ℓ/s	52.22	56.30	-7.24
Water From UG	°C	26.03	26.03	0.00
Pre-Cool 1 Water Out	°C	19.33	25.65	-24.65
Pre-Cool 2 Water Out	°C	17.09	17.96	-4.82
Pre-Cool 2 Dam	°C	13.34	13.69	-2.53

From Table 44 it is evident that the output values were not affected drastically by reconfiguration of the pre-cooling towers. The first stage pre-cooling outlet water temperature was affected due to the fans switched off. The recycled chilled water increased as well to maintain the evaporator inlet water temperature as close to the setpoint as possible. Figure 176 compares the baseline simulation power usage of the cooling equipment against the implemented simulation power usage.

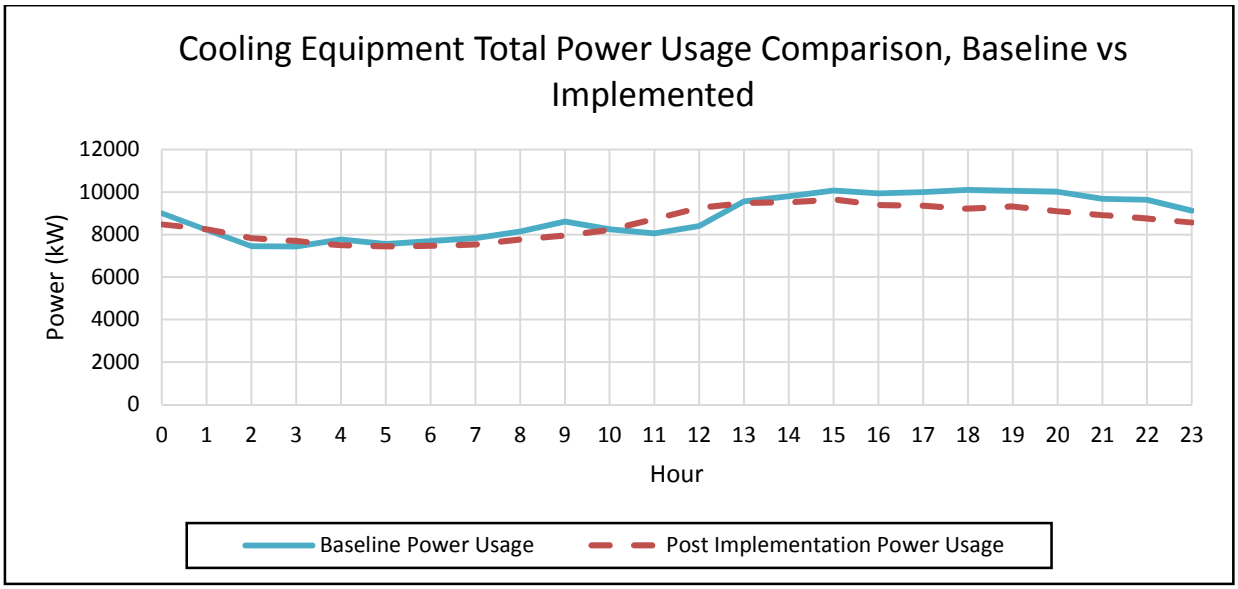

Figure 176: Cooling equipment total power usage comparison, baseline vs. implemented for a 4℃ setpoint

Figure 176 depicts the power usage, which reduced during the majority of the day, realising in a daily average power saving of 287.08 kW. Figure 177 represents the total evaporator water flow through the FPs for the baseline and implemented simulations.

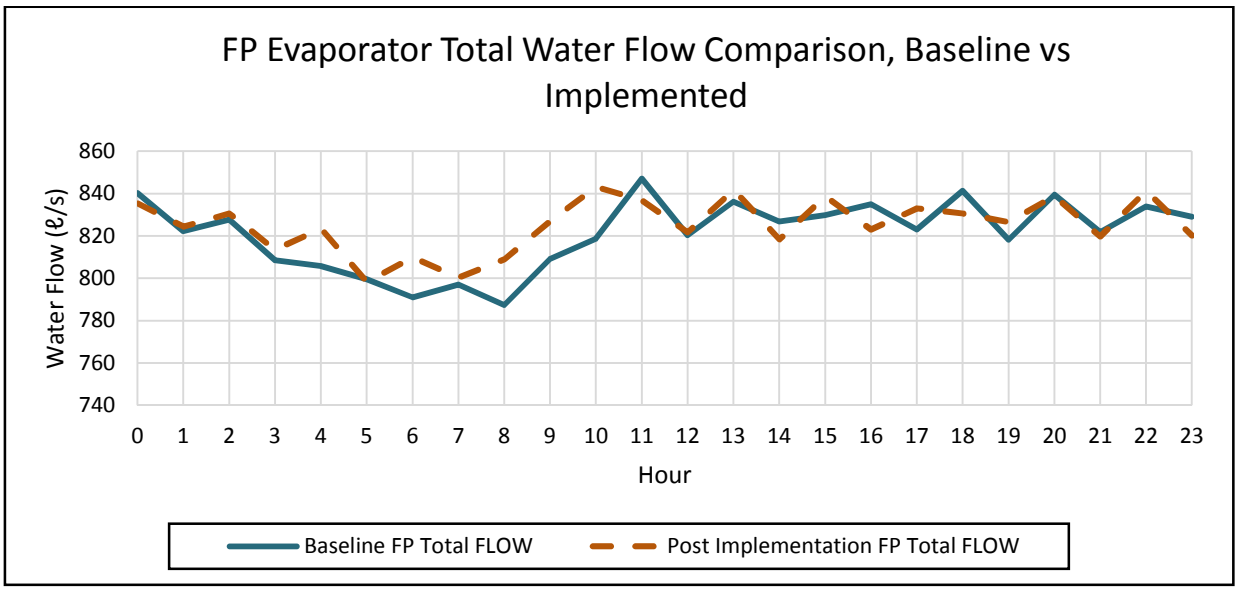

Figure 177: FP evaporator total water flow comparison, baseline vs. implemented for a 4℃ evaporator setpoint

From Figure 177 it is evident the evaporator flow increases during certain periods of the day. On average the evaporator flow increased with 0.49% due to the increase of 7.24% in recycled chilled water. The recycled chilled water increased to lower the FP's evaporator inlet temperature. The average evaporator inlet temperature increased with 0.35℃ throughout the day. Figure 178 compares the evaporator water temperature of the baseline simulation with the implemented simulation.

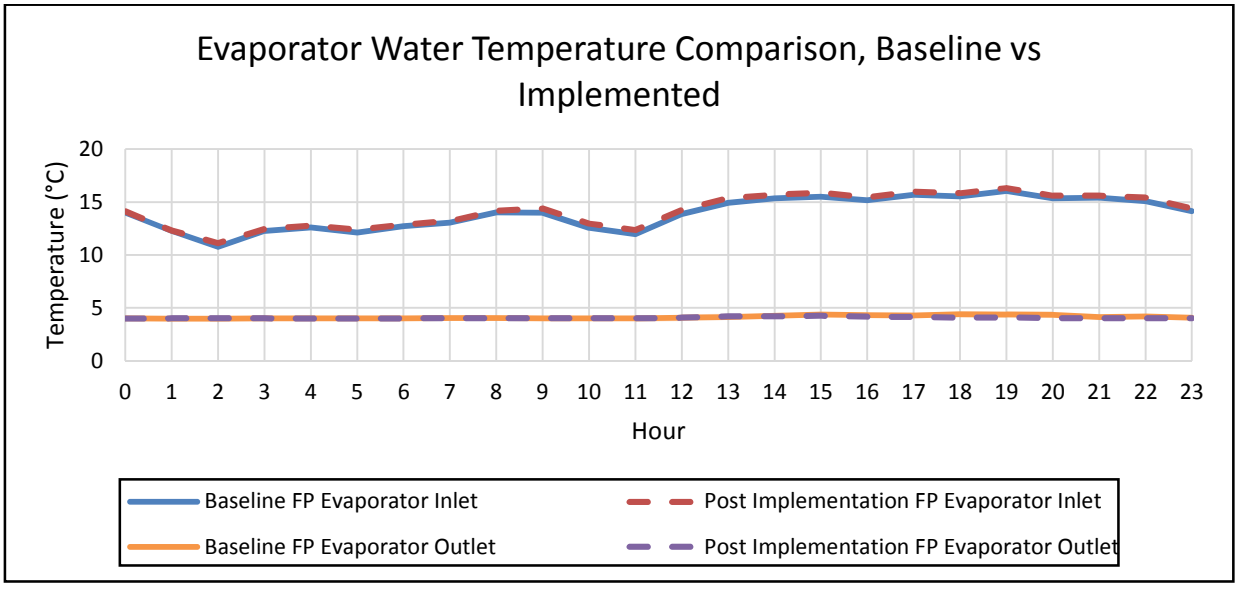

Figure 178: Evaporator water temperature comparison, baseline vs. implemented for a 4℃ evaporator setpoint

Figure 178 indicates that there is a slight increase in the evaporator inlet temperature. However, the FPs manage to maintain an average evaporator outlet water temperature of 4.07℃. Figure 179 represents the evaporator water temperatures of the baseline and implemented simulations.

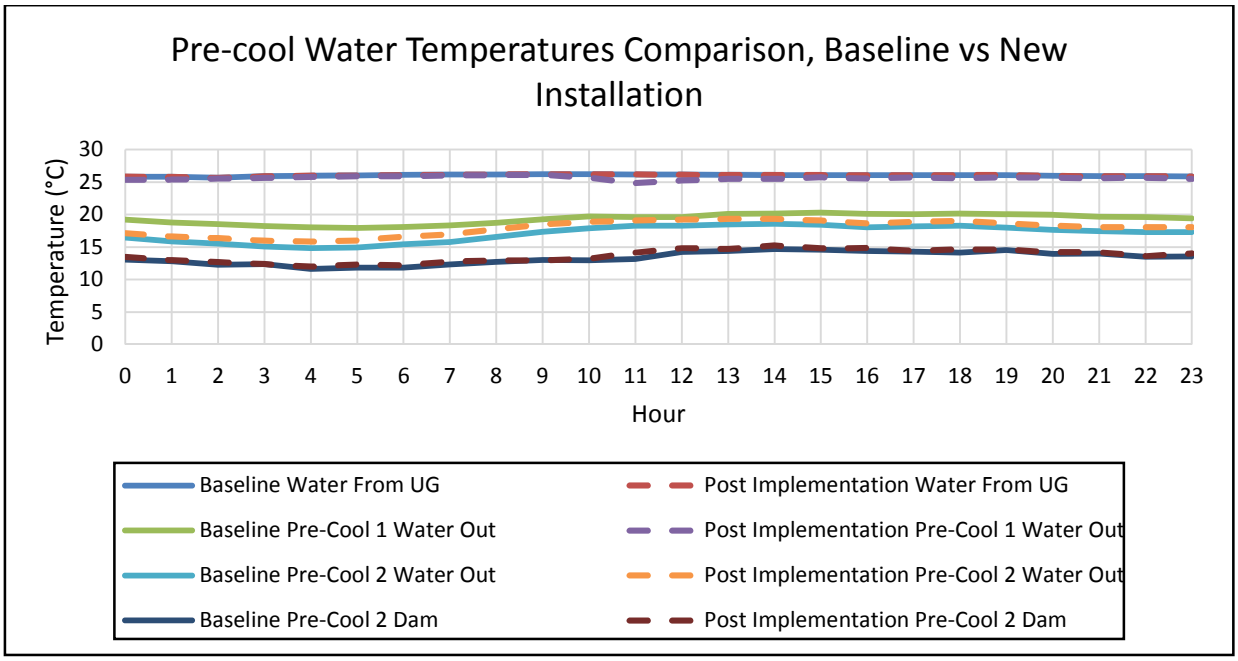

Figure 179: Pre-cool towers' water temperatures with a 4℃ evaporator setpoint temperature

Figure 179 depicts the water temperature from underground, which remained the same for both simulations. The first stage pre-cooling towers reduced the water temperature on average with 0.38℃. The second stage, with the replaced pre-cooling towers, managed to reduce the water temperature to 17.96℃, which is 0.87℃ warmer than the second stage pre-cooling tower outlet temperature of the baseline simulation. The recycled chilled water was increased to 7.24% to maintain an evaporator inlet water temperature of 14.29℃, 2.14% above the baseline inlet temperature. Figure 180 summarises the pre-cooling towers' water efficiencies of the baseline and implemented simulations.

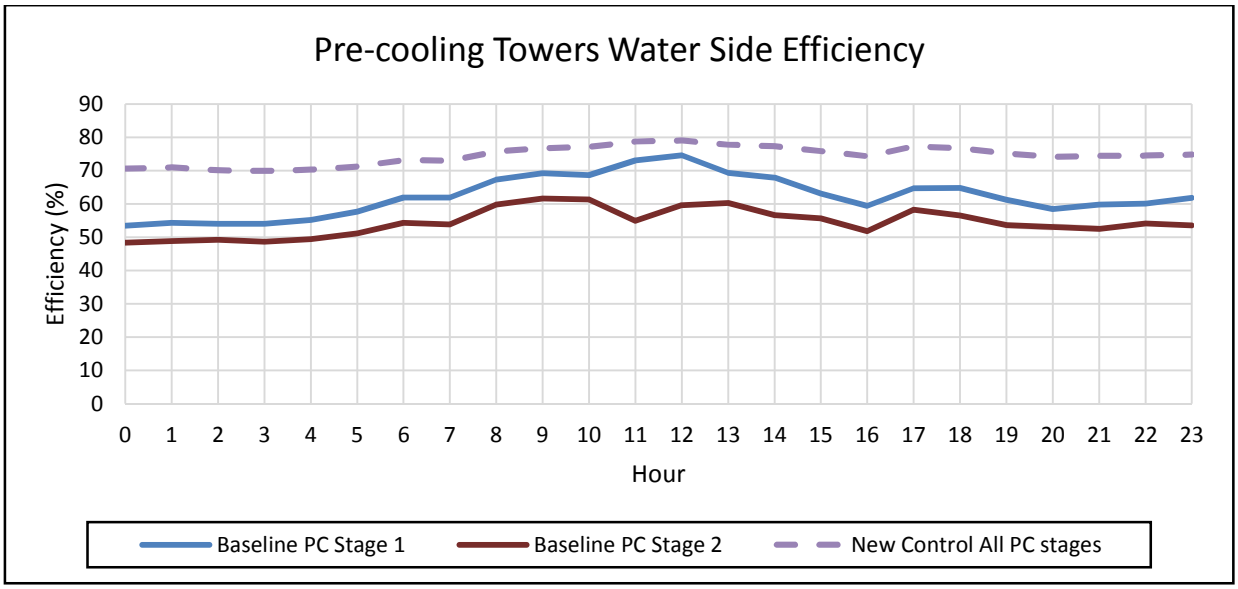

Figure 180: Pre-cool towers' water side efficiency

Figure 180 depicts the baseline water side efficiency for both pre-cooling stages, which are less than the implemented water side efficiency. The baseline simulation had an average water side efficiency of 62.34% and 54.49% for the first and second stage pre-cooling towers respectively. The implemented simulation realised in a water side efficiency of 74.59%. The efficiency is calculated from the water from underground temperature to the second stage pre-cooling tower outlet water temperature as the first stage pre-cooling tower's fans were switched off. This is a realistic service delivery and efficiency from the pre-cooling towers as a water side efficiency of 78% had been recorded for the same amount of pre-cooling towers at mine F [21].

3℃ Evaporator outlet water temperature setpoint:

The design maximum service delivery of mine A's FPs is 3℃. Therefore, reconfiguring of the mine's pre-cooling towers was simulated with an evaporator setpoint of 3℃. Table 45 summarises the simulated outputs of the baseline and implemented simulations.

Table 45: Baseline and implemented simulation output values for reconfiguring of Pre-cooling towers, 3℃ evaporator setpoint

Outputs	Unit	Average Baseline	Average Implemented	Percentage (%) Deviation
Power Usage	kW	9300.38	9114.56	2.00
FP Total Flow	ℓ/s	820.74	823.00	-0.28
FP Evaporator Inlet Temp	°C	13.71	14.44	-5.05
FP Evaporator Outlet Temp	°C	3.38	3.20	5.33
Chill Dam Temp	°C	4.30	4.11	4.49
FP Average COP	0	5.15	5.16	0.21
Condenser Flow	ℓ/s	2087.86	2105.70	0.85
Condenser Inlet	°C	26.03	25.97	0.20
Condenser Outlet	°C	30.88	30.78	0.32
BAC Total Water Flow	ℓ/s	398.99	398.99	0.00
BAC Outlet Air Temp WB	°C	10.95	10.89	0.54
BAC Outlet Water	°C	10.44	10.34	0.91
Chilled Water Recycled	ℓ/s	51.76	54.04	-4.21
Water From UG	°C	26.03	26.03	0.00
Pre-Cool 1 Water Out	°C	19.33	25.65	-24.65
Pre-Cool 2 Water Out	°C	17.09	17.95	-4.81
Pre-Cool 2 Dam	°C	13.12	13.44	-2.43

Table 45 depicts the reconfiguration of the pre-cooling towers, which did not drastically affect the outputs of the cooling system. The outlet water temperature of the first stage pre-cooling towers was affected and increased with 24.65% as their fans were switched off. Figure 181 represents a comparison between the implemented cooling equipment's total power usages against the baseline simulation.

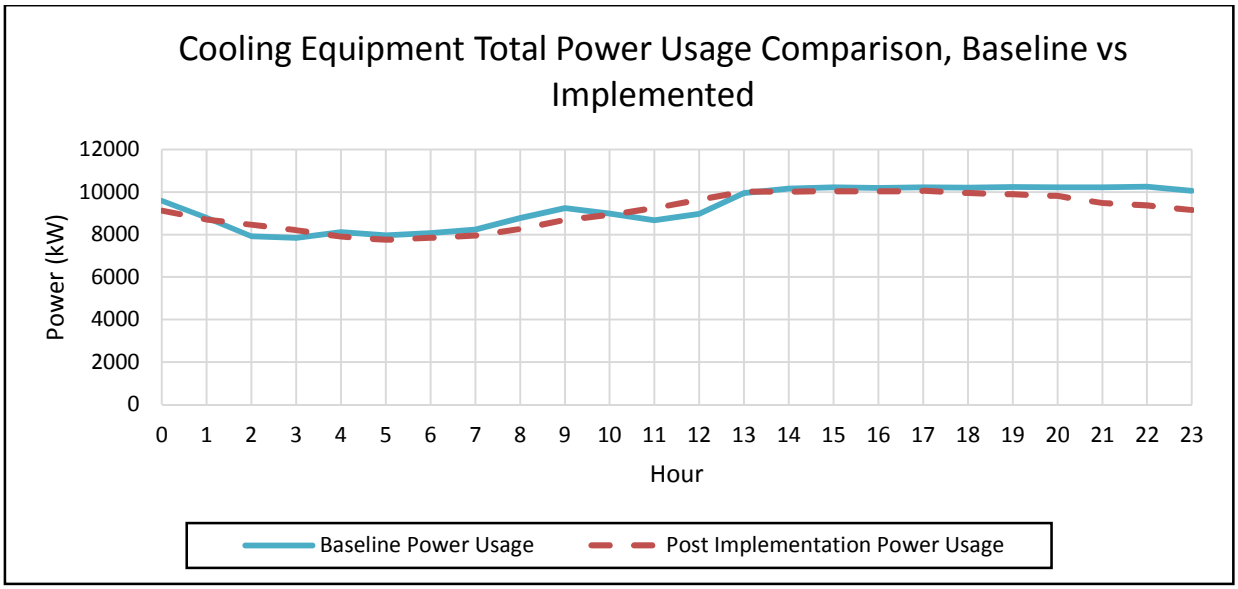

Figure 181: Cooling equipment total power usage comparison, baseline vs. implemented for a 3℃ setpoint

Figure 181 depicts a power reduction throughout the majority of the day, which will realise from reconfiguring the pre-cooling towers. The reconfiguration of mine A's precooling towers will realise in an average power saving of 185.82 kW throughout the day with an evaporator water output temperature setpoint of 3℃. Figure 182 compares the total water flow through the FP's evaporator cycle of the implemented simulation against the baseline simulation.

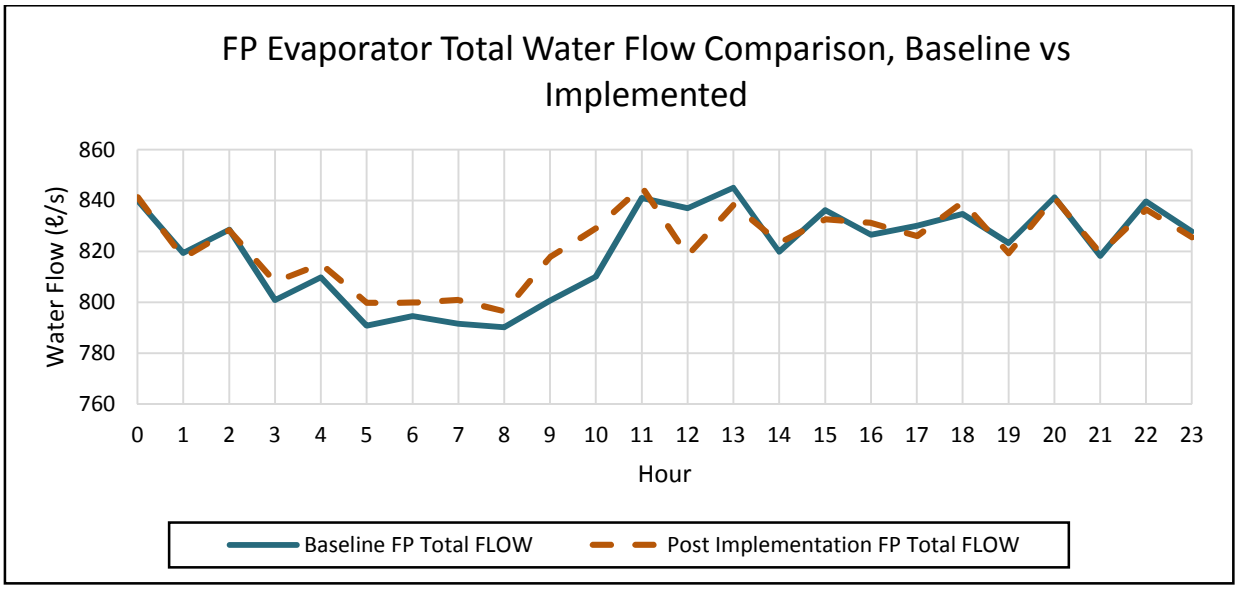

Figure 182: FP evaporator total water flow comparison, baseline vs. implemented for a 3℃ evaporator setpoint

Figure 182 depicts the evaporator water flow, which increased slightly during certain periods throughout the day. The evaporator water flow increased with 0.28% on average due to an increased recycle chilled water demand of 4.21% to maintain the evaporator inlet water temperature as close to 14℃. Figure 183 represents the evaporator water temperatures for the baseline and implemented simulations.

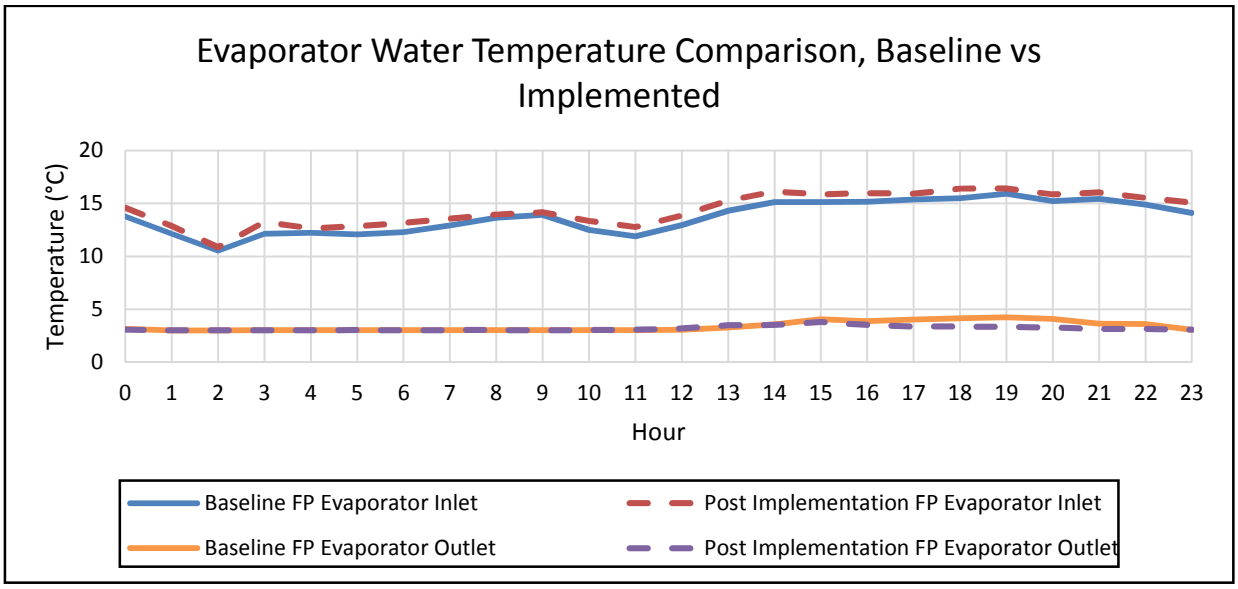

Figure 183: Evaporator water temperature comparison, baseline vs. implemented for a 3℃ evaporator setpoint

Figure 183 depicts the evaporator inlet water temperature, which increased throughout the day. The FPs managed to maintain an evaporator outlet temperature of 3.20℃. Figure 184 summarises the pre-cooling towers' water temperature for the baseline and implemented simulations.

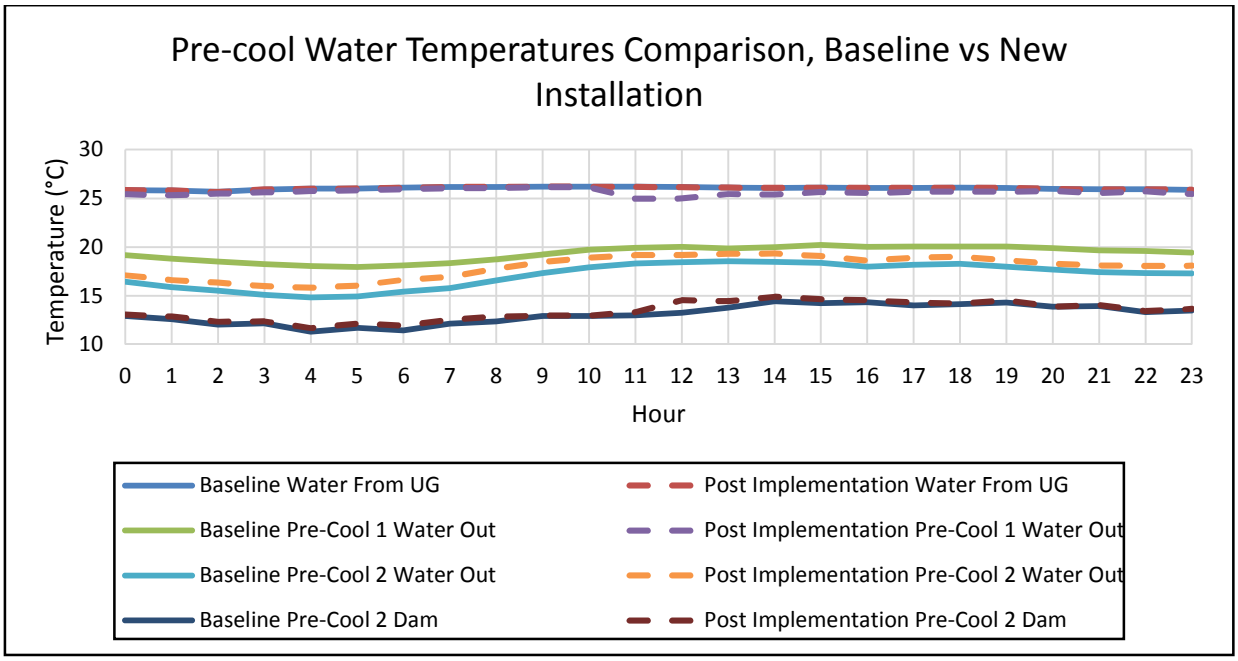

Figure 184: Pre-cool towers' water temperatures with an evaporator outlet water temperature setpoint of 3℃

Figure 184 depicts the water temperature, which remained constant through the baseline and implemented simulations. The first stage pre-cooling towers reduced the water temperature by 0.39℃ with the fans being switched off. The more efficient second stage pre-cooling towers managed to reduce the second stage outlet water temperature to 17.95℃; 0.86 C, warmer than the baseline simulation second stage output water temperature. However, the increased volume recycled chilled water managed to reduce the second stage pre-cool dam water temperature to 13.44℃; 2.43% warmer than the baseline simulation dam temperature. Figure 185 represents the water side efficiency of the pre-cooling towers for both the baseline and implemented simulations.

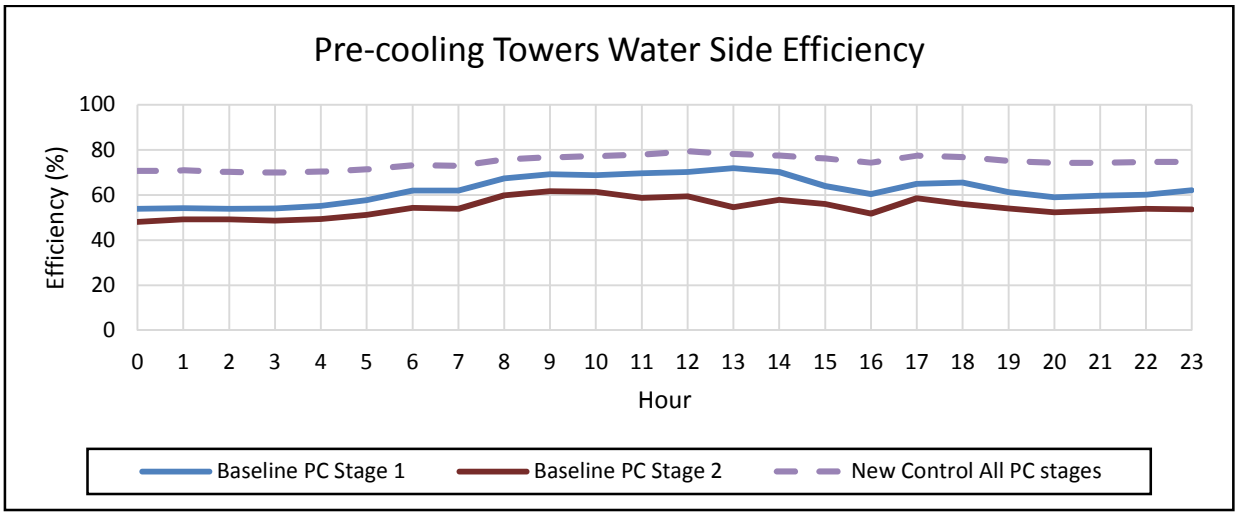

Figure 185: Pre-cool towers' water side efficiency

Figure 185 indicates that the new pre-cooling towers have an improved water side efficiency over the old baseline cooling towers' efficiencies. The baseline's first and second stage pre-cooling towers had a water side efficiency of 62.36% and 54.45% respectively. The new improved pre-cooling towers managed to obtain a water side efficiency of 74.61%. The water side efficiency was calculated over the water from underground to the second stage pre-cooling towers' outlet water temperature as the first stage pre-cooling towers were switched off. This is a realistic service delivery and efficiency from the pre-cooling towers as a water side efficiency of 78% had been recorded for the same amount of pre-cooling towers at mine F [21].